UNIVERSITY
of
LIMERICK
OLLSCOIL LUIMNIGH

An investigation into the general characterisation of bauxite residue and its potential for use as a low-cost adsorbent for the removal and re-use of phosphorus from forest run-off and an agricultural wastewater

by

Patricia B. Cusack

Academic Supervisors:

Dr. Ronan Courtney, Department of Biological Sciences, University of Limerick

Dr. Mark G. Healy, Civil Engineering, NUI Galway

This thesis is submitted to the University of Limerick, in fulfilment of the requirements for the Degree of Doctor of Philosophy.

December 2018

Abstract

Alumina production by the Bayer process generates bauxite residue at a global rate of approximately 150 Mt per annum. An estimated 3 Bt has been produced worldwide to date, which is either landfilled or collected in land storage facilities. Depending on the refinery, bauxite residue may undergo a separation technique in which the coarse fraction is separated from the fine fraction (<100 µm). The coarse fraction is often used in the construction of roadways around the bauxite residue disposal area, in which the fine fraction is stored. European Union policy advocates the re-use of materials in order to establish a more 'circular economy' and concurrent to this, there is emphasis on Europe maintaining a steady supply of critical raw materials (CRMs) such as gallium, phosphate rock and phosphorus, which are of high economic value due to their supply risk. Consequently, there is a focus on finding suitable secondary sources of CRMs. Bauxite residue has been identified as one possible source. In addition, due to its high abundance of iron and aluminium oxides, which are desirable for phosphorus (P) retention, it may be re-used as a low-cost adsorbent of P in the treatment of forest run-off and agricultural wastewater, which are two key attributors to poor water quality in Ireland. Therefore, the aim of this study was to investigate, for the first time, fine fraction (<100 µm) bauxite residue as a low-cost adsorbent in the removal and re-use of P from wastewater.

Bauxite residue samples representing twelve years of disposal were characterised for their mineralogical, elemental and physico-chemical properties. Changes in these properties may affect the potential for the re-use of bauxite, but no study has examined this to date. The general composition did not vary greatly, with the exception of pH and electrical conductivity, which ranged from 10 ± 0.1 to 12.0 ± 0.02 and from 0.4 ± 0.01 to 3.3 ± 0.2 mS cm^{-1}, respectively. The main mineralogical composition comprised iron and aluminium oxides, which were estimated to range from 40.1 ± 1.4 to $47.5\pm2\%$ and from 14.8 ± 1.5 to $17.8\pm0.73\%$, respectively. One notable high value CRM found in the bauxite residue was gallium (107 ± 7.3 mg kg^{-1}).

To determine the P adsorbent potential of bauxite residue, batch studies were performed using synthetic P water. Fresh samples of bauxite residue were obtained from two European alumina refineries and then treated with either gypsum or seawater, to determine if the treatments enhance its P adsorption capacity. Untreated and treated samples were placed in 50 mL capacity containers and overlain with water made up to concentrations ranging from 0 to 150 mg P L^{-1}. They were then placed on a reciprocating shaker for 24 hr, before being allowed to settle and the supernatant water tested for its P concentration. Langmuir adsorption isotherms were then used to model the data. The study found that bauxite residue has an adsorption capacity varying between 0.345 to 2.73 mg P g^{-1}, and that seawater and gypsum enhances the P adsorption capacity. Following the batch studies, a column study was used in order to assess the true P adsorbent capacity of the bauxite residue using real wastewater. Fine fraction bauxite residue was placed in small-scale columns and loaded with forest run-off and dairy soiled water (DSW) over a period of 24 to 36 hr. Data obtained were modelled to predict breakthrough curves and longevity of the bauxite. The longevity of the bauxite residue was estimated to be 1.08 min g^{-1} for the forest run-off and 0.28 min g^{-1} for DSW.

The efficacy of P-saturated bauxite residue from the column study as a fertiliser replacement was compared to a conventional superphosphate fertiliser in the growth of *Lolium perenne* L. in a P-deficient soil. The bauxite residue was comparable to the superphosphate fertiliser in terms of the biomass yield and there was no evidence to suggest phytotoxic effects on the growth of ryegrass, nor any effects on the *E. fetida* L. present in the soil.

The findings of this study highlight the potential re-use of bauxite residue as both a low-cost adsorbent and also as a potential resource/nutrient source for P supply.

Declaration

"I declare that this is entirely my own work, with the exception of where reference has been made to the work of others. This thesis has not been previously submitted for any other qualification. Where material from other sources has been used, it has been referenced in full".

Signed: _____ Date: _____

Patricia B. Cusack

Acknowledgements

I would like to begin by saying a huge thank you to my supervisor Dr. Ronan Courtney for everything over the past three years. Thank you for always being so supportive, kind and most of all patient throughout this experience. It has been an absolute privilege to get to work with you!

I would also like to say a huge thank you to my co-supervisor Dr. Mark G. Healy (NUIG). I am very grateful for all your guidance, support and patience over the past two years and it has been such a privilege to work with you and to get to experience working within another university setting!

A very special thank you to Dr. Oisín Callery for all the help and advice with the adsorption study and to Dr. Éva Ujaczki for the support and training with the aqua regia digestion and ICP analysis. I wish you both the best of luck in your research and academic careers!

I would like to thank all my colleagues here in the Department of Biological Sciences and the Bernal Institute, particularly Professor Seán Arkins, Dr. Ken Byrne, Samantha Prior, Mary Burton and Stephanie Brosnan for all the support and kindness over the past few years. Thank you also to Dr. Lisa O' Donoghue, all on the Alsource project and to the EPA for financing the project. Thanks also to Dr. Wynette Redington and Ms. Paula Olsthoorn for the training I received on the various material science equipment.

It would have been a very lonely experience without all the chats and cups of tea over the past three years and it was great getting to know the UL gang, Éva, Samantha, Ronan L, Elisa, Gemma and Chinnam and not forgetting Mary, Jose and Collette in NUIG. Thank you to Cora, Cheryl, Helen, Mary and Teresa, even though you never knew what I was really doing, thanks for always being there for the chats and for the support!

To my parents, Seán and Angela, sister Karen, and brother in law Kieran, thanks for always being there, no matter what! Ye are the best and I am blessed to have such a great family!

Finally, to possibly the most patient person in existence, Karl. Thanks for putting up with me over the past few years and for all the support and encouragement, not forgetting your assistance (and Baxter's!) on our adventures to collect seawater and forest run-off!

Table of Contents

List of Tables

List of Figures

List of Appendices

List of Abbreviations

A	A is a constant of proportionality (mg L^{-1})
Al	aluminium
Al^{3+}	aluminate ions
AlO(OH)	boehmite
$Al(OH)_3$	aluminium hydroxide hydrate
Al_2O_3	aluminium oxide
AMD	acid mine drainage
ANC	acid neutralising capacity (mol H^+ kg^{-1})
As	arsenic
B	is a model constant
BD	bulk density (g cm^{-3})
BR	bauxite residue
BRDA(s)	bauxite residue disposal area(s)
Bt	billion tonne
Ca	calcium
$CaCO_3$	calcium carbonate; calcite
CaO	calcium oxide
$Ca(OH)_2$	slaked lime
$CaTiO_3$	perovskite
Cd	cadmium
Ce	cerium
C_e	effluent concentration (mg L^{-1})
$C_{e,i}$	effluent contaminant concentration in the ith container (mg L^{-1})
Co	cobalt
C_o	influent contaminant concentration (mg L^{-1})
CO_2	carbon dioxide
CO_3^{2-}	carbonate ions
CRM(s)	critical raw material(s) (mg kg^{-1})
Cr	chromium
Cu	copper
DRP	dissolved reactive phosphorus (mg L^{-1})

DSC	differential scanning calorimetry (mW)
DSW	dairy soiled water
Dy	dysprodium
EBPR	enhanced biological phosphorus removal
EC	European Commission
EC	electrical conductivity (mS cm^{-1})
EDS	energy-dispersive x-ray spectroscopy (weight %)
Er	erbium
ESP	exchangeable sodium percentage (%)
Eu	europium
EU	European Union
$\sum Vi$	total volume of effluent collected (L)
Fe	iron
FeO(OH)	goethite
Fe$_2$O$_3$	iron oxide
Fl	fluoride
FT-IR	Fourier transform infrared
Ga	gallium
Gd	gadolinium
HCl	hydrochloric acid
HNO$_3$	nitric acid
Hg	mercury
Ho	holmium
H$_2$SO$_4$	sulphuric acid
ICP-OES	inductively coupled plasma optical emission spectrometer
In	indium
Kα	k alpha
kV	kilovolt
La	lanthanum
Lu	lutetium
1M	1 molar
m	mass of filter media contained in the filter column (g)
mA	milliamp
Mg	magnesium

$Mg(OH)_2$	brucite
Mn	manganese
Mo	molybdenum
MPa	megapascal
Mt	million tonne
N	nitrogen
n	the number of containers in which the total volume of effluent is collected
Na	sodium
NaOH	sodium hydroxide
Na_2SO_4	sodium sulphate
Nd	neodymium
Ni	nickel
OH^-	hydroxide ion
P	phosphorus
Pb	lead
ρb	bulk density (g cm^{-3})
PGM	platinum group metals
PVDF	polyvinylidene difluoride
pH	pH (pH unit)
Pr	praseodymium
PSA	particle size analysis (µm and in % of the total particle distribution)
PZC	point of zero charge
PZCpH	pH at which the point of zero charge occurs
q_e	cumulative mass of contaminant adsorbed per g of filter media (mg g^{-1})
RDA	residue disposal area
REE(s)	rare earth element(s) (mg kg^{-1})
REO(s)	rare earth oxide(s)
RSSCT(s)	rapid small-scale column test(s)
SAR	sodium adsorption ration, expressed in mEq L^{-1}
Sc	scandium
Se	selenium
SEM	scanning electron microscope (µm)
Si	silicon
SiO2	silicon oxide

Sm	samarium
SSA	specific surface area ($m^2\,g^{-1}$)
t	empty bed contct time of the column filter bed (min)
Tb	terbium
TGA	thermogravimetric analysis (mg)
Ti	titanium
TiO2	titanium oxide
Tm	thulium
Tn	terbium
TN	total N ($mg\,kg^{-1}$)
TP	total P ($mg\,kg^{-1}$)
TTD	thickened tailings disposal
V	vanadium
V	volume of the influent loaded onto the filter (L)
V_B	number of empty bed volumes of influent/solution filtered
WWTP	wastewater treatment plant
XRD	x-ray diffraction (°2Ө)
XRF	x-ray fluorescence (%)
Y	yttrium
Yb	ytterbium
Zn	zinc

Chapter 1

Introduction

Overview of Project

This PhD study was part of an EPA Funded Research Project, "Alsource" (2014-RE-MS-1) at the University of Limerick, coordinated by principal investigators Dr. Ronan Courtney and Dr. Lisa M. T. O' Donoghue. Alsource which was composed of two PhD studies, aimed to illustrate the value content in Irish Bauxite Residue via both re-use and recovery techniques, therefore turning bauxite residue into a resource for phosphorus and rare earth metals. The first PhD study, supervised by Dr. Ronan Courtney and Dr. Mark G. Healy (NUIG) which investigated the use of bauxite residue in the recovery and re-use of phosphorus from wastewater was undertaken by Patricia B. Cusack, whilst the second study, which investigated the potential recovery of rare earth metals from bauxite residue was carried out by Dr. Éva Ujaczki under the supervision of Dr. Lisa M. O' Donoghue and Dr. Ronan Courtney.

1.1 Background to Study

Alumina production by the Bayer Process generates bauxite residue (red mud) at a global rate of approximately 150 Mt per annum (Evans 2016). An estimated 3 Bt has been produced world-wide to date (Evans 2016), and despite multiple attempts to utilize bauxite residues in the construction, environmental, mining and agronomic industries, only 2 to 3% of this material is currently re-used or further processed (Evans 2016; Klauber et al., 2011; Ujaczki et al., 2018), with ~ 98 % of the bauxite residue (<100 μm) being either landfilled or collected in land storage facilities (Kong et al., 2017). This highlights a major storage issue for refineries, as well as the associated expense in the management required to maintain residue storage areas (Tsakiridis et al., 2004). In addition, there are potential environmental risks associated with bauxite residue if incorrectly managed (Higgins et al., 2017).

As a result of the Bayer Process, bauxite residue is highly alkaline in nature (which can be reduced through the use of treatments such as seawater or gypsum), composed of very fine particles, and can comprise various trace metals (Wang et al., 2015). However, bauxite residue has many desirable properties, such as a high specific surface area (SSA) and iron and aluminium oxide content, which results in it having a high phosphorus (P) adsorption capacity (Grace et al., 2015). Recently focus has been placed on the utilisation of using by-products such as bauxite residue, steel slag and fly ash particularly as low-cost P adsorbents for water treatment, promoting a more "circular economy" (Grace et al., 2016) and also in the recycling of P from wastewaters as it is one of the key nutrients causing the eutrophication of water bodies (Kok et al., 2018; Nättorp et al., 2017). Ironically, both phosphorus and phosphate rock (the main source of phosphorus for fertilisers) are non-renewable resources (Achat et al., 2014) and with an increasing population, further demand is being placed on these resources in order to maintain food supply (Achat et al., 2014). Both of these issues have been referred to as the *P paradox* (Baker et al., 2015; Sharpley 2015). In addition to its P adsorption capacity, bauxite residue may also contain critical raw materials (CRMs) such as the rare earth elements (REEs), which suggests that it may serve as a potential secondary source for these materials (Liu and Naidu 2014).

The overall aim of this study was to examine both treated and untreated fine fraction bauxite residue as a low-cost adsorbent for the removal of P and also as a potential source/nutrient source of P. This study examined the efficacy of alternative, environmentally friendly treatments (gypsum and seawater) as opposed to the more commonly used treatments involving heat and acids (Liu et al., 2007; Xue et al., 2016), which require large capital inputs and operational costs for the alumina industry. By using treatments such as seawater and gypsum, improvement of the physico-chemcial, mineralogical and elemental composition of bauxite residue also allowed the possibility to consider using the bauxite residue adsorbent media as a potential growth media/fertiliser, once fully saturated with P. This may promote the potential re-use of bauxite residue as both a medium for P removal and also as a source of P.

1.2 Knowledge Gaps Identified and Targeted

The following research gaps have been identified from the literature and will be addressed in this study:

1. Approximately 98% of the bauxite residue generated in the alumina industry is placed in specially built impoundments, bauxite residue disposal areas (BRDAs), constructed in close proximity to the alumina refineries (Burke et al., 2013). Previous studies have highlighted the potential of bauxite residue as a secondary source for CRMs and have noted their variation due to factors such as the type of bauxite ore used. However, no study has examined the potential variation in composition or CRM content of bauxite residue in a BRDA over time, which could affect its potential for re-use.

2. Several studies have investigated the use of bauxite residue as an adsorbent for P, using high cost and energy intensive treatments such as heat or acid to enhance the adsorption capacity of the bauxite residue (Liu et al., 2007; Xue et al., 2016). Depending on the refinery, bauxite residue may undergo a separation process in which the coarse and fine fractions are separated (Evans 2016; IAI 2015). The coarse fraction is predominantly used in the roadways to the BRDAs within close proximity to the refinery; however, the fine fraction is underused and commonly placed in the BRDA. No study has investigated the separate P adsorption capacity of both the coarse and fine fractions of bauxite residue, nor conducted a detailed characterisation of the coarse and fine fractions of bauxite residue in terms of its mineralogical, elemental and physico-chemical composition following treatment with gypsum or seawater.

3. The majority of P adsorption studies with bauxite residue focus on using batch studies with synthetic P aqueous solutions. No study has investigated the P adsorption capacity of the fine fraction bauxite residue as a sorbing material in the active treatment of actual agricultural wastewaters or forest run-off, which would contain other contaminants in addition to P.

4. The final gap that was identified was the potential recycling of P from P-saturated fine fraction bauxite residue following treatment of wastewater and its potential as a nutrient source/fertiliser to plants.

1.3 Research Aim and Objectives

The aim of this study was to investigate the potential for bauxite residue as a adsorbent for P from contaminated water, as well as studying the variation of CRM content while

stored in BRDAs, which may affect its use as a potential secondary source of CRM. To meet this aim, the objectives of this study were:

1. evaluate the general composition and critical raw material content of the dominant fraction (fine fraction) bauxite residue in storage over a twelve-year period, and to determine if there is any variation while in storage, which could affect options for its possible re-use.
2. quantify the impact of amendments with seawater or gypsum on the P adsorbent capacity of coarse and fine fractions of bauxite residue using synthetic P solutions.
3. determine the efficiency of bauxite residue as a low-cost adsorbent in the removal of P from agricultural water and forest run-off, as well as characterising changes in its mineralogical and physico-chemical content before and after use as an adsorbent.
4. investigate the effects of P-saturated bauxite residue compared to conventional P fertiliser on plant growth and P uptake in *Lolium perenne* L. (perennial ryegrass), and on soil physico-chemical properties.

1.4 Experimental Design and Procedures

A literature review was conducted which examined the generation of bauxite residue, its general composition, and potential re-use options, particularly as a potential secondary source of CRMs, and as a potential adsorbent for the removal of P from aqueous solutions and wastewaters.

Bauxite residue, which is commonly located in close proximity to the refinery in which it is produced, is generally similar in composition; however, some properties may vary between refineries because of the type of bauxite ore used and the parameters used within the Bayer Process. Therefore, in order to identify any potential variation in bauxite residue because of its time in storage, which may hinder potential re-use, bauxite residue in storage over a twelve-year period was characterised in terms of its mineralogical, elemental and physico-chemical properties (**Objective 1**).

Batch studies using synthetic P solutions were carried out on the main size fractions of bauxite residue, in its raw state and amended with gypsum and seawater, to identify which

4

size fraction had the greatest P adsorption capacity (**Objective 2**) before carrying out an adsorption study using two types of wastewater – forest runoff and dairy soiled water (DSW) (**Objective 3**). Forest run-off was used as a low P concentration wastewater, while DSW was chosen as a high P concentration wastewater. The bauxite residue was then packed into small-scale columns and a P adsorption study was carried out using forest run-off and an agricultural wastewater, highlighting the potential use of bauxite residue in a permeable reactive barrier if were to be upscaled in future research.

Following the rapid small-scale column tests (RSSCTs), the final part of the laboratory study examined the potential of P recycling from the P saturated bauxite residue column media as a potential nutrient source/fertiliser for *Lolium perenne* L. (perennial ryegrass) (**Objective 4**). This was carried using the RHIZOtest™ procedure (ISO 16198), which also allowed for the monitoring of any potential trace metal uptake within the plant biomass.

1.5 Structure of Thesis

A flowchart of the thesis is presented in Figure 1.1. Chapter 2, the literature review, reviews the process of bauxite residue generation, along with the main mineralogical, elemental and physico-chemical properties of the bauxite residue. Important considerations and implications that arise for both the management and potential re-use of bauxite residue as a result of its general composition are also discussed, as well as techniques and storage methods that mitigate any potential adverse effects associated with its re-use.

Chapter 3 evaluates the general composition and CRM content of bauxite residue in a storage area over a twelve-year period (**Objective 1**). Bauxite residue samples were examined from one specific storage area in order to identify any potential variation in mineralogical, elemental or physico-chemical composition over time, in addition to any variation in CRM content, which may affect its re-use potential.

Chapter 4 investigates the enhancement of separate fractions and sources of bauxite residue as a low-cost adsorbent for P in synthetic solutions, using seawater and gypsum treatments (**Objective 2**). This chapter also identifies which of the treatments enhances the P adsorption capacity of the bauxite residue.

5

Chapter 5 uses RSSCTs to determine the efficiency of bauxite residue as a low-cost adsorbent in the removal of dissolved reactive phosphorus (DRP) from an agricultural wastewater and forest run-off **(Objective 3)**. This chapter also uses the performance data from the RSSCTs to predict the longevity of the bauxite residue.

Chapter 6 investigates plant P uptake in *Lolium perenne* L. (perennial ryegrass) using recycled P from spent bauxite residue column media **(Objective 4)**. This chapter examines the potential application of the bauxite residue as both an adsorbent for P, as well as establishing a further re-use for the spent adsorbent by using it as a potential fertiliser for *Lolium perenne* L. (perennial ryegrass) by comparing it to a conventional superphosphate fertiliser in terms of biomass yield, and effects on main soil properties and potential toxicological effects on fauna and establishment of vegetation.

Chapter 7 summarises the main conclusions from this study, along with recommendations for future research.
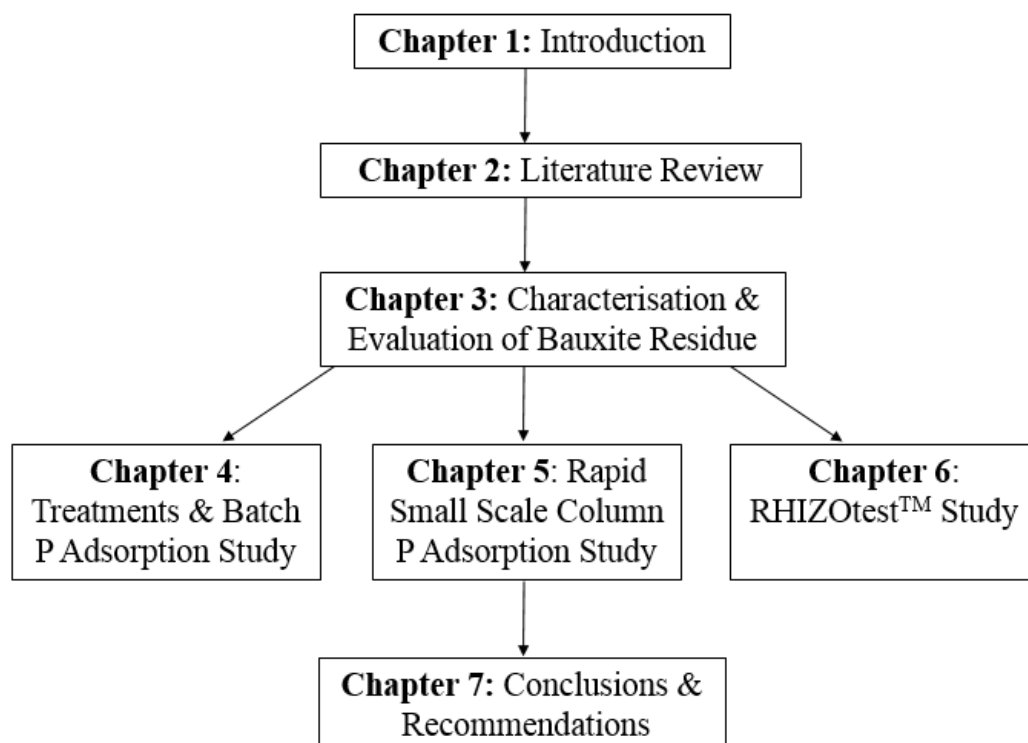
Figure 1.1 Flow chart of the thesis.

1.6 Contribution to Existing Knowledge and Research Outputs

1.6.1 Journal Papers (Published)

Cusack, P.B., Healy, M.G., Ryan, P.C., Burke, I.T., O'Donoghue, L.M., Ujaczki, É. and Courtney, R. (2018). Enhancement of bauxite residue as a low-cost adsorbent for phosphorus in aqueous solution, using seawater and gypsum treatments. *Journal of Cleaner Production*, 179, pp.217-224.

Cusack, P.B., Courtney, R., Healy, M.G., O'Donoghue, L.M. and Ujaczki, É. (2019). An evaluation of the general composition and critical raw material content of bauxite residue in a storage area over a twelve-year period. *Journal of Cleaner Production*, 208, pp. 393-401.

Cusack, P.B., Callery, O., Courtney, R., Ujaczki, É., O'Donoghue, L.M. and Healy, M.G. (2019). The use of rapid, small-scale column tests to determine the efficiency of bauxite residue as a low-cost adsorbent in the removal of dissolved reactive phosphorus from agricultural waters. *Journal of Environmental Management,* 241, pp.273-283.

Ujaczki, É., Feigl, V., Molnár, M., Cusack, P., Curtin, T., Courtney, R., O'Donoghue, L., Davris, P., Hugi, C., Evangelou, M.W. and Balomenos, E. (2018). Re-using bauxite residues: benefits beyond (critical raw) material recovery. *Journal of Chemical Technology & Biotechnology*, 93(9), pp.2498-2510.

1.6.2 Journal Paper (In Preparation)

Cusack, P. B., Healy, M. G., Ujaczki, É., O' Donoghue, L. M. T. and Courtney, R. (2019). An investigation into the Growth of *Lolium perenne* L. and Soil Properties such as Phosphorus Availability, pH and Electrical Conductivity following the use of Spent Bauxite Residue Column Media as a Nutrient Source.

1.6.3 Conference Presentations

Cusack, P., Healy, M.G., Ujaczki, É., O' Donoghue, L., Courtney, R. (2017) The use of Bauxite Residue for Phosphorus recovery in wastewater. Department of Biological Sciences Post Graduate Research Day, December 13th, 2017, Radisson Blu Hotel & Spa,

Limerick, Ireland. (Oral Presentation)

Cusack, P., Healy, M. G., Ujaczki, É., O′ Donoghue, L., Curtin, T., Courtney, R. (2017) The use of Bauxite Residue for Phosphorus (P) recovery in wastewater. 27th Irish Environmental Researchers Colloquium, April 10−12, 2017, Athlone, Ireland. (Oral Presentation)

Cusack, P., Healy, M.G., Callery, O., Ujaczki, É., O′ Donoghue, L., Courtney, R. (2016) Phosphorus removal, recovery and re-use in wastewater using Bauxite Residue. Ryan Institute Annual Research Day 2016, December 9th, 2016, National University of Ireland, Galway, Ireland. (Poster Presentation)

Cusack, P., Healy, M.G., Callery, O., Ujaczki, É., O′ Donoghue, L., Courtney, R. (2016) Phosphorus removal, recovery and re-use in wastewater using Bauxite Residue. Poster Presentation, Red Mud Summer School ″From Bauxite to Aluminium″ 2016 Katholieke Universiteit, Leuven, August 29th−31st, 2016, Leuven, Belgium. (Poster Presentation)

Cusack, P., Ujaczki, É., O′ Donoghue, L., Courtney, R. (2016) The use of Bauxite Residue for Phosphorus recovery in wastewater. Oral Presentation, Department of Life Sciences Post Graduate Research Day, May 3, 2016, Radisson Blu Hotel & Spa, Limerick, Ireland. (Oral Presentation)

Cusack, P., Ujaczki, É., O′ Donoghue, L., Courtney, R. (2016) The use of Bauxite Residue for Phosphorus recovery in wastewater. Oral Presentation, 26th Irish Environmental Researchers Colloquium, March 22−24, 2016, Limerick, Ireland. (Oral Presentation)

The published journal papers may be found in Appendix A.

1.7 References

Achat, D.L., Sperandio, M., Daumer, M.L., Santellani, A.C., Prud'Homme, L., Akhtar, M. and Morel, C., 2014. Plant-availability of phosphorus recycled from pig manures and dairy effluents as assessed by isotopic labeling techniques. *Geoderma*. *232*, pp.24-33.

Baker, A., Ceasar, S.A., Palmer, A.J., Paterson, J.B., Qi, W., Muench, S.P. and Baldwin, S.A., 2015. Replace, re-use, recycle: improving the sustainable use of phosphorus by plants. *J. Experiment. Botany. 66*(12), pp.3523-3540.

Burke, I.T., Peacock, C.L., Lockwood, C.L., Stewart, D.I., Mortimer, R.J., Ward, M.B., Renforth, P., Gruiz, K. and Mayes, W.M., 2013. Behavior of aluminum, arsenic, and vanadium during the neutralization of red mud leachate by HCl, gypsum, or seawater. *Environ. Sci. Technol*. 47, 6527-6535.

Evans, K., 2016. The history, challenges, and new developments in the management and use of bauxite residue. *J. Sustain. Metallurgy.* 2, 316-331.

Grace, M.A., Clifford, E., Healy, M.G., 2016. The potential for the use of waste products from a variety of sectors in water treatment processes. *J. Clean. Prod*. 137, 788-802.

Higgins, D., Curtin, T. and Courtney, R., 2017. Effectiveness of a constructed wetland for treating alkaline bauxite residue leachate: a 1-year field study. *Environ. Sci. Poll. Res.* 24, 8516-8524.

IAI, 2015. Bauxite Residue Management: Best Practice. http://www.world-aluminium.org/media/filer_public/2015/10/15/bauxite_residue_management_-_best_practice_english_oct15edit.pdf. (accessed 14.10.2017).

Klauber, C., Gräfe, M. and Power, G., 2011. Bauxite residue issues: II. options for residue utilization. *Hydrometallurgy.* 108(1-2), pp.11-32.

Kok, D.J.D., Pande, S., Lier, J.B.V., Ortigara, A.R., Savenije, H. and Uhlenbrook, S., 2018. Global phosphorus recovery from wastewater for agricultural re-use. *Hydrol. Earth. Syst. Sc*. 22(11), pp.5781-5799.

Kong, X., Guo, Y., Xue, S., Hartley, W., Wu, C., Ye, Y. and Cheng, Q., 2017. Natural evolution of alkaline characteristics in bauxite residue. *J. Clean. Prod.* 143, 224-230.

Liu, Y. and Naidu, R., 2014. Hidden values in bauxite residue (red mud): recovery of metals. *Waste. Manage.* 34(12), pp.2662-2673.

Liu Y, Lin C and Wu Y., 2007. Characterization of red mud derived from a combined Bayer process and bauxite calcination method. *J. Hazard. Mater.* 146:255–261.

Nättorp, A., Remmen, K. and Remy, C., 2017. Cost assessment of different routes for phosphorus recovery from wastewater using data from pilot and production plants. *Water. Sci. Technol.* 76(2), pp.413-424.

Sharpley, A.N., 2015. The Phosphorus Paradox: Productive Agricultural and Water Quality. Available: https://scholar.uwindsor.ca/cgi/viewcontent.cgi?article=1018&context=icei2015 [accessed 08.08.2018].

Tsakiridis, P.E., Agatzini-Leonardou, S. and Oustadakis, P., 2004. Red mud addition in the raw meal for the production of Portland cement clinker. *J. Hazard. Mater.* 116, 103-110.

Chapter 2

Literature Review

Overview

With the European Commission (EC) advocating for the creation of a more 'circular economy' in order to establish a 'zero waste' society (European Commission 2015), emphasis is being placed on the utilisation of waste and/or by-products produced within industry and their potential re-use as low-cost adsorbents for the treatment of wastewater (Grace et al., 2016). One such by-product that has been examined for its adsorbent potential, particularly in the removal of phosphorus (P), is bauxite residue (Zhou and Haynes 2010; Liu et al., 2011).

Bauxite residue is the by-product generated in the extraction of alumina (Manfroi et al., 2014) and is being produced globally at an annual rate of approximately 150 Mt, adding to the already 3 Bt in storage worldwide (Evans 2016). Over the past number of decades, emphasis has been placed on finding suitable re-use for bauxite residue. However, numerous limitations and barriers, such has high alkalinity, potential leaching of trace metals, and low solid content have prevented this (Klauber et al., 2011; Evans 2016). This chapter discusses the generation of bauxite residue and its mineralogical, elemental and physico-chemical properties, with a focus on its potential for re-use as a low-cost adsorbent in the removal of P from aqueous solutions.

2.1 Bauxite Ore and Generation of Bauxite Residue

2.1.1 Bauxite Ore

The production of aluminium metal involves three stages: (1) the mining of bauxite ore (2) extraction of alumina from bauxite ore, and (3) the transformation of alumina to aluminium (Rai et al., 2012). On average, four tonnes of bauxite ore is required in order to produce two tonnes of alumina (Lumley 2010).

Bauxite ore, which is generally enriched in aluminium (Al) and titanium (Ti) but low in soluble elements such as potassium (K), calcium (Ca), sodium (Na) and magnesium (Mg) (Maynard 2012), is formed in deposits in tropical or sub-tropical regions, with up to 80% found in shallow open pit mines (Gow and Lozej 1993). Factors affecting the formation of bauxite ore include climate, parent rock and topography (Wang et al., 2011), and depending on the type of bedrock on which the bauxite ore is deposited, is classified as one of three types: karstic (found on limestone and dolomite, and composed of aluminosilicate residues), lateritic (lying on alumosilicate rocks) or Tikhvin-type, which is layered on aluminosilicate rock but has no derivation from them (Bárdossy, 1982).

Of the three main types (lateritic, karstic and Tikhvin), particular interest is placed on the karstic type as they are known to contain high levels of rare earth elements (REEs) (Deady et al., 2016; Mordberg 1993). The main regions in which karstic bauxite ore is located are Austria, Bulgaria, France, Greece, Iran, Italy, Jamaica, Romania, Spain, USA, USSR, the Socialist Republic of Vietnam and Yugoslavia, while lateritic bauxite ore is found in regions in Brazil, Guinean Republic and India (Bárdossy 2013).

The presence of aluminium-hydroxide minerals such as gibbsite (which is dominant in lateritic bauxite ore) (Rai et al., 2012), boehmite and/or diaspore (also dominant in karstic bauxite ore) (Rai et al., 2012) means that alumina may be extracted from bauxite ore under alkaline conditions using lime (Lime Sinter Process) (Goldberg et al., 1970), sodium carbonate (Deville Pechiney Process), high temperatures in a reducing environment in the presence of coke and nitrogen (N) (Serpeck Process) (Reddy 2001), or through alkalinisation by the use of sodium hydroxide (NaOH) (Bayer Process) (Rai et al., 2012). The Bayer Process is the most widely used, with up to 85 % the alumina produced via the Bayer Process (Xue et al., 2016).

2.1.2 Generation of Bauxite Residue

Bauxite residue (commonly referred to as red mud), Bayer process tailings, or bauxite process tailings (Gräfe et al., 2011; Kirwan et al., 2013; Liu et al., 2014; Manfroi et al., 2014) is the slurry by-product generated from the Bayer Process (Gräfe et al., 2011). Bauxite residue typically has a distinctive red colour due to an abundance of iron oxide in its composition (Rai et al., 2012). For every 1 tonne of alumina formed through the Bayer Process, between 1 and 1.5 tonnes of bauxite residue is generated (Evans, 2016).

However, this may be lower depending on the alumina refinery and the type of ore used, with values reported to be as low as 0.3 tonnes of bauxite residue produced per tonne of alumina (IAI 2015). Currently, the global inventory for bauxite residue is approximately 3 billion tonnes, with an estimated annual production rate of 150 million tonnes (Evans, 2016; Mayes et al., 2016).

The Bayer Process may be broken up into five different stages as seen in Figure 2.1, which include (1) the grinding of bauxite ore (2) digestion of the bauxite ore (3) liquor clarification (4) precipitation of alumina hydrate, and (5) calcination to alumina (Jones and Haynes 2011). The overall extraction of alumina from the bauxite ore is generated from the precipitation of gibbsite in its crystalline form from alkaline solutions containing aluminates (Hind et al., 1999).
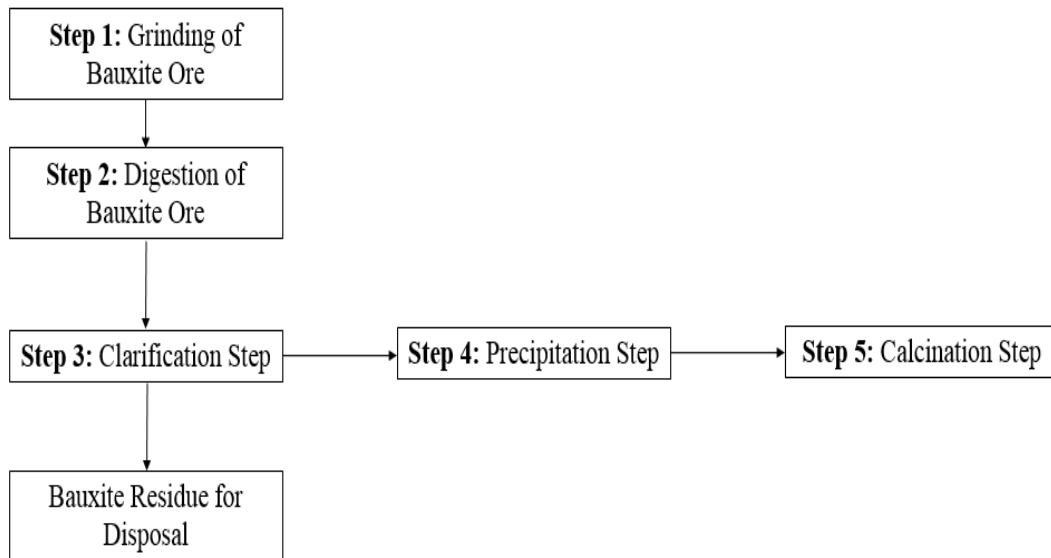
Figure 2.1 Diagrammatical representation of the main steps in the Bayer Process.

2.1.2.1 Grinding of the Bauxite Ore

Once mined, Bauxite ore is washed and then crushed, resulting in an increase in the surface area of the materials (Power et al., 2011). The bauxite ore is then mixed with a high temperature caustic liquor forming a slurry mixture (Gräfe et al., 2011). Under the action of a pump mechanism, the slurry is transported to holding tanks before moving onto the digestion units where the mixture undergoes a predesilication phase, which involves the removal of silica (Jones and Haynes 2011).

2.1.2.2 Digestion

The digestion step in the Bayer Process involves the bauxite ore being digested in a concentrated caustic solution, NaOH, under high temperature and pressure (Bray et al., 2017). The temperature used will vary due to the composition of the bauxite ore; approximately 150°C for the gibbsite bauxites and 250°C for boehmite and diaspore bauxite ores (Whittington 1996). The high temperature and pressure environment results in the removal of hydrate alumina from insoluble oxides due to a reaction with the NaOH present in the caustic mixture (Jones and Haynes 2011) as shown in Eqn. 1 (Hind et al., 1999).

Extraction:

$$Al(OH)_{3(s)} + NaOH_{(aq)} \rightarrow Na^+ Al(OH)^-_{4(aq)}$$
and,
$$AlO(OH)_{(s)} + NaOH_{(aq)} + H_2O \rightarrow Na^+ Al(OH)^-_{4(aq)} \qquad \text{Eqn. 1}$$
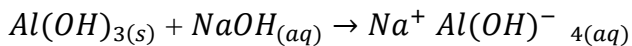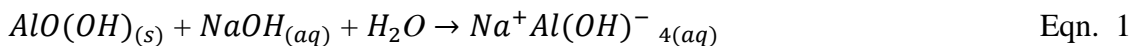
2.1.2.3 Liquor Clarification

In this stage, the bauxite residue solids are removed from the green liquor formed, which is mainly composed of sodium aluminate dissolved in the caustic mixture (Power et al., 2011). In the first part of this separation process, the coarse fraction (>100µm, known as bauxite process sand) is separated under the influence of gravity, which is then repeatedly washed in order to recover NaOH before the bauxite process sand is then transported to the residue disposal area (RDA) (Jones and Haynes 2011). However, this process is not carried out in every alumina refinery (Evans 2016). Following the removal of the coarse fraction, the finer fraction of bauxite residue left behind in the green liquor is removed using thickener vessels, which involves the use of flocculants, and once separated the finer fraction (<150µm) of bauxite residue undergoes repeated washing in what is known as a *Countercurrent Washing Train*, which allows in the recovery of NaOH and which may be re-used in the Bayer Process once more (Gräfe et al., 2011). At the half-way stage of the washing process, the overflow stream is heated and mixed with lime slurry, a process known as *Causticisation*. This allows the hydrated lime to react with the sodium carbonate, which causes the regeneration of NaOH and the precipitation of calcium carbonate ($CaCO_3$) (Jones and Haynes 2011) as noted in Eqn. 2 (Hind et al., 1999):

Precipitation:

$$Na^+ Al(OH)^-_{4(aq)} \rightarrow Al(OH)_{3(s)} + NaOH_{(aq)} \qquad \text{Eqn. 2}$$
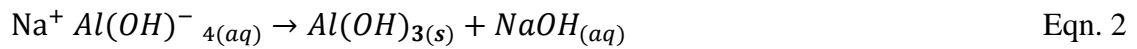
Once the clarification stage is complete, the purified liquor is allowed to cool to a temperature of 50-75 °C and then pumped on to allow for the fourth stage to begin - precipitation (Jones and Haynes 2011).

2.1.2.4 Precipitation of Alumina Hydrate

In this step, the cooled green liquor is seeded with aluminium trihydrate crystals, which enhance the precipitation process (Xue et al., 2016). Once again there is a separation process within this stage, which separates the slurry into coarse and fine fractions. The coarse fraction is then sent onto the final stage, the calcination stage, while the fine fraction is returned for re-use in the seeding process (Jones and Haynes 2011). The caustic solution is re-concentrated, heated and recycled back to the digesters (Gräfe et al., 2011).

2.1.2.5 Calcination to Alumina

The calcination step involves the alumina hydrate being washed and dried using temperatures up to 1200 °C in order to fully maximise the removal of any water molecules, leaving behind a dry white powder, alumina (Al_2O_3), which is then transferred from the alumina refinery to an aluminium smelter (Jones and Haynes 2011), as seen in Eqn. 3 (Hind et al., 1999).

$$2Al(OH)_{3(s)} \rightarrow Al_2O_{3(s)} + 3H_2O \qquad \text{Eqn. 3}$$

2.2 Mineralogical, Elemental and Physico-chemical Composition of Bauxite Residue

The use of bauxite ores from various locations around the world, as well as refineries using different parameters within the Bayer Process, results in a variation of physical, mineralogical and chemical properties (Liu et al., 2007; Menzies et al., 2004).

The relative amounts of the main elements found in bauxite residue are iron (Fe) > Al > silicon (Si) ~ Ti > Ca > Na (Wang et al., 2008). This is reflected in the mineralogical composition of bauxite residue which mainly comprises iron oxides such as hematite (Fe_2O_3), goethite (FeO(OH)) and boehmite (γ-AlO(OH)) (Hanahan et al., 2004), in addition to aluminium hydroxides and calcium and titanium oxides (Binnemans et al., 2015). The vast abundance of oxides results in bauxite residue having many hydroxyl groups on its surface (Zhang et al., 2008). The percentage range of the chemical composition of bauxite residue is shown in Table 2.1 (Evans 2016). Bauxite residue is typically low in elements such as N, P, K, Ca, manganese (Mn), copper (Cu) and zinc (Zn) (Xue et al., 2016). Depending on the type of bauxite ore used the critical raw material (CRM) content may vary within the bauxite residue (Ujaczki et al., 2018). Bauxite residue generated from the karstic type bauxite ore are recognised for their higher concentration of CRMs, particularly the REEs (Binnemans et al., 2015).

Table 2.1 The main chemical composition of bauxite residue[*], expressed as oxides (Evans 2016).

Component	Typical range (weight %)[*]
Fe_2O_3	5–60
Al_2O_3	5–30
TiO_2	0.3–15
CaO	2–14
SiO_2	3–50
Na_2O	1–10

[*]The typical range (weight %) is the average chemical composition range as determined for all bauxite residue generated from the three main bauxite ore types. Therefore, the wide variation in composition is a reflection of the main composition of the type of bauxite ore used.

The physico-chemical properties (Table 2.2) of bauxite residue have an average particle size ranging from 2 to 2000µm, and as a result may be described as being "silt to fine sand" (Gee et al., 1986). As a result of the fine particle size, the specific surface area (SSA) of bauxite residue is on average $32.7 \pm 12.2 m^2\,g^{-1}$, whilst the bulk density has been reported to be on average 2.5 g cm^3.

Following the Bayer Process and depending on the method of disposal, the solid content of bauxite residue is relatively low at ~ 20%, but can be increased to ~ 80%, depending

on the method of disposal used. Alkalinity is high due to residual sodium (Na), normally a mixture of sodium aluminate and sodium carbonate (Evans 2016), resulting in an average pH value of 11.3 (Table 2.2). In addition to high alkalinity, bauxite residue is also highly sodic (exchangeable sodium percentage (ESP) of 50–90%; Jones and Haynes 2011), which is linked with poor ability to form an aggregate structure. The elevated concentration of Na ions also affects the EC, which is on average 7.4 mS cm^{-1} (Gräfe et al., 2011).

Table 2.2 Selection of chemical and physical characteristics of bauxite residue (Gräfe et al., 2011).

Parameter	Average	Std. Dev.	Max	Min	n
pH	11.3	1.0	12.8	9.7	44
EC (mS)[a]	7.4	6.0	28.4	1.4	46
[Na$^+$][b] (mmol$^+$ L^{-1})	101.4	81.6	225.8	8.9	9
SAR[c]	307.2	233.1	673	31.5	10
ESP[d]	68.9	19.6	91	32.1	10
ANC, 7.0[e]	0.94	0.3	1.64	0.68	13
ANC, 5.5[f]	4.56	-	-	-	1
PZC (pH)[g]	6.9	1.0	8.25	5.1	11
BD (g cm^{-3})[h]	2.5	0.7	3.5	1.6	13
SSA (m^2 g^{-1})[i]	32.7	12.2	58.0	15.0	30

[a]EC (mS) = electrical conductivity, expressed in mS.

[b][Na$^+$] = sodium concentration, expressed in mmol$^+$ L^{-1}.

[c]SAR = sodium adsorption ratio, expressed in mEq L^{-1}.

[d]ESP = exchangeable sodium percentage, expressed as a percentage.

[e]ANC, 7.0 = acid neutralization capacity normalized to the weight of the residue to a given pH endpoint of pH 7, expressed as mol H$^+$ kg^{-1}.

[f]ANC, 5.5 = acid neutralization capacity normalized to the weight of the residue to a given pH endpoint of pH 5.5, expressed as mol H$^+$ kg^{-1}.

[g]PZCpH = the pH at which the point of zero charge is occurring.

[h]BD = bulk density, expressed as g cm^{-3}.

[i]SSA = specific surface area, expressed in m^2 g^{-1}.

The point of zero charge (PZC) is an important property, as it is related to the phenomenon of adsorption (Lyklema 1984) and relates to the stage when the surface charges on the surface are zero. The average pH at which PZC occurs in bauxite residue is pH 6.9 (Table 2.2) (Gräfe et al., 2011).

2.3 Current Disposal and Re-use Pathways of Bauxite Residue

2.3.1 Disposal Pathways

Approximately 2 % of the bauxite residue generated is currently reutilised (Ujaczki et al., 2018), with the remaining ~ 98 % adding to the already to 3 Bt in storage worldwide, the majority of which are in containments referred to as RDAs or bauxite residue disposal areas (BRDAs) (Burke et al., 2013). The cost of managing such storage areas has been estimated to be 5 % of the overall production cost of alumina (Kumar et al., 2006). Nguyen and Boger (1998) calculated that the treatment (practiced by some alumina refineries prior to disposal) and disposal of the bauxite residue may be as high as 30 to 50 % of the total expenditure for the alumina refinery. The choice of disposal methods used by the alumina refinery will vary and is based on several factors such as storage space availability, climate, and governmental and environmental regulations (Jones and Haynes 2011).

Up until the 1970s, the main method of disposing of bauxite residue was through wet disposal directly to sea and storage in lagoons (Power et al., 2011). However, current best practice management advocates the use of techniques that increase the solids content such as dry stacking (Evans 2016) and dry cake disposal (IAI 2015) to protect the surrounding environment from risks (Higgins et al., 2017; Kong et al., 2017) such as dust pollution, run-off of alkaline leachate and potential leaching of trace elements (Kong et al., 2017; Wang et al., 2015).

The dry stacking or thickened tailings disposal (TTD) technique involves the thickening of the bauxite residue slurry from the washing stage to a paste by using vacuum filtration or a filter press to achieve a solid concentration of ~ 58%, before being diluted and piped to the BRDA (Figure 2.2 (a)) in 400 mm deep layers (300 mm following mud farming) (Clohessy 2015; McMahon 2017). Due to the solid content of the residue layers, conventional farm machinery cannot travel on the residue and therefore further dewatering and compaction is necessary. This is carried out by Amphirolls, amphibious

vehicles which travel using scrolls over the residue, creating furrows, allowing water to be "squeezed" and drained from the residue (Evans 2016) along the sloping stack to the cell perimeter wall and into the perimeter channel (Figure 2.2 (b)). Once the residue is compacted to > 70 % solids (Power et al., 2011) by multiple passes of the Amphiroll, the surface is then graded by a bulldozer to level the surface and generate a constant gradient from the discharge (high point) to the perimeter wall (low point). This then makes the residue suitable for conventional agricultural machinery to travel and operate on its surface.

Atmospheric carbonation of the residue by the Amphiroll and agricultural machinery allows for exposure of the residue to carbon dioxide (CO_2) in the air, a technique known as mud farming. Sufficient exposure and carbonation reduces the causticity below 30 % and reduces the residue pH to below 11.5 (McMahon 2017). Measurements of pH are used to identify the completion of carbonation. At this point, the area is re-graded using a bulldozer to remove any depressions. The cell is then ready for the subsequent layer of bauxite residue (McMahon 2017). The BRDA operates as an upstream system, whereby each raised terraced area sits several metres in from the perimeter of the underlying raise. Access to these raised terraced areas allows for the collection of bauxite residue representing different years of deposition. The design of the BRDA includes sprinklers in the case of preventing any fugitive dust, whilst all run-off from the BRDA enters the underlying drainage and returned to the alumina refinery where it is recycled (Figure 2.2 (a)). The use of dry stacking helps to reduce the storage space required by a refinery, while also reducing the risk of alkaline leachate coming into contact with the surrounding environment (Xue et al., 2016).
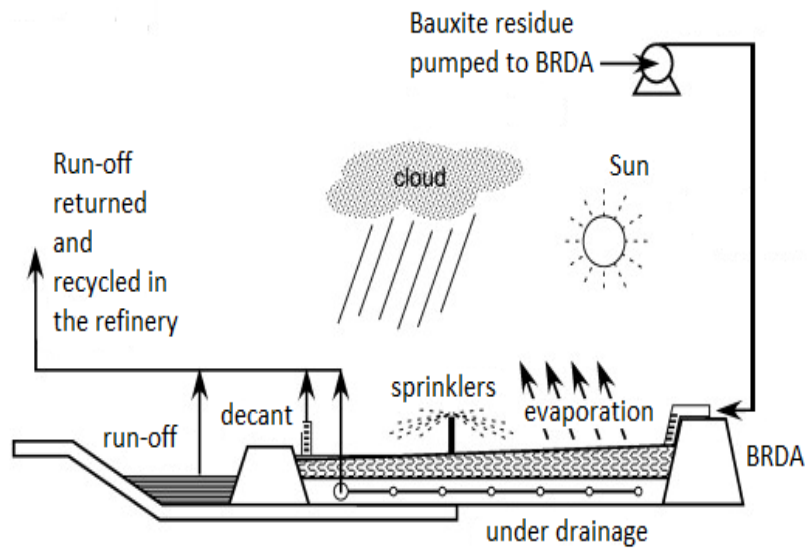
Figure 2.2 (a) Schematic of a BRDA, which incorporates the dry stacking or TTD technique for storage of bauxite residue, adapted from Alcoa (2005) **(b)** Image of an Amphiroll machine, which aids in the dewatering and atmospheric carbonation of bauxite residue (IAI 2015).

Dry cake disposal, a newer method of disposal, involves achieving a solid content of > 65 % for the bauxite residue before moving into the BRDA (Nikraz et al., 2007). This process involves the removal of water via a mechanical mechanism to achieve this high solid content. As a result, it is not pumpable and must be transported to the BRDA using trucks or conveyor belts (Power et al., 2011).

To further improve the state of the bauxite residue in storage and minimise the risk to the surrounding environment, neutralisation techniques such as through the addition of seawater (Hanahan et al., 2004), mineral acids such as sulphuric acid application (McConchie et al., 2002), carbon dioxide (Cooling et al., 2002), sulphur dioxide application (Fois et al., 2007), gypsum application (Courtney and Kirwan 2012) and even microbial addition (Krishna et al., 2005) are sometimes employed. However, this is not practiced by all alumina refineries.

2.3.2 Neutralisation of Bauxite Residue

Following the Bayer Process, bauxite residue remains highly alkaline as a result of the residual NaOH still present, giving the bauxite residue a pH value in the range of 10 to 12 (Jones and Haynes 2011). High alkalinity is one of the key issues posed by bauxite residue in storage, which if incorrectly managed, can cause risk to the surrounding environment (Xue et al., 2016) and also hinders establishment of vegetative cover on bauxite residue (Jones and Haynes 2011). Depending on the alumina refinery, bauxite residue may be treated using various neutralisation techniques in order to reduce the alkalinity prior to its deposition in the BRDA (Power et al., 2011). The choice of neutralisation technique employed by the alumina refinery (if any) is determined by cost and location (Xue et al., 2016). For example, seawater neutralisation is a popular choice of neutralisation treatment, but only if the alumina refinery is in close proximity to a seawater source (Xue et al., 2016). Similarly, gypsum is typically added to the bauxite residue when trying to establish vegetative cover (Courtney et al., 2009).

2.3.2.1 Seawater Neutralisation

When seawater is added to bauxite residue, a reaction occurs where hydroxide ions (OH^-), carbonate ions (CO_3^{2-}) and aluminate ions (Al^{3+}) (Palmer and Frost 2009) are eliminated due to a reaction predominantly involving Mg^{2+} (from the seawater), as seen in Eqn. 4 (Kirwan et al., 2013) and also Ca^{2+} ions present in the seawater. This results in the

formation of solids of an alkaline nature such as brucite ($Mg(OH)_2$) or hydrotalcite ($Mg_5Al_2(OH)_{16}.MgCO_3.4H_2$) (Eqn. 4) or calcite ($CaCO_3$). Following this reaction, there is a buffering effect, which is reflected in a new pH, usually in the range of 8 to 9 (Power et al., 2011).

$$6Mg^{2+} + 8OH^- + 2Al(OH)_{4^-} + CO_{3^{2-}} \leftrightarrow Mg_5Al_2(OH)_{16}.MgCO_{3}.4H_2O \text{ (hydrotalcite)}$$

Eqn. 4
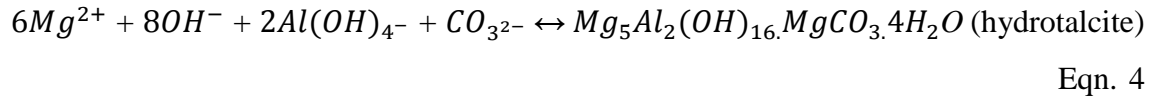
2.3.2.2 Gypsum Neutralisation

The use of gypsum ($CaSO_4.2H_2O$), a grey/white mineral composed of hydrated calcium sulphate, in the remediation of bauxite residue is another well-known method of neutralisation (Courtney et al., 2009) and when added to bauxite residue, a similar effect occurs with the precipitation of OH^-, CO_3^{2-} and Al^{3+} ions (Eqn. 5 and 6; Lehoux et al., 2013). This causes a reduction in pH to approximately 8.6 by the buffering effect of $CaCO_3$ (Gräfe et al., 2011). In addition to this drop in pH, an increase in the EC is also noted in the bauxite residue due to the formation of sodium sulphate (Na_2SO_4) (Gräfe et al., 2011).

$$OH^-{}_{(aq)} + CO_{2(aq)} \rightarrow HCO_{3(aq)}^-$$

Eqn. 5

$$2OH^-{}_{(aq)} + CaSO_4 . 2H_2O_{(s)} + 2CO_2$$
$$\leftrightarrow CaCO_{3(s)} + SO_{4(aq)}^{2-} + 2H_2O_{(l)} + H_2CO_{3(aq)}$$

Eqn. 6
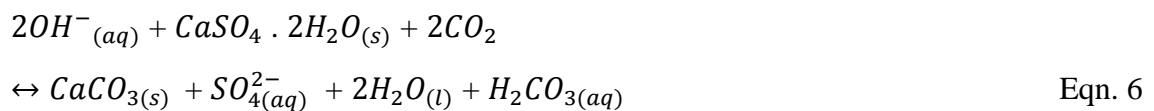
2.3.2.3 Atmospheric Carbonation and Carbon dioxide

Atmospheric carbonation, also known as mud farming, of bauxite residue is carried out by the use of Amphirols and agricultural machinery within BRDAs, which allows for exposure of the bauxite residue to carbon dioxide (CO_2) in the air. Sufficient exposure and carbonation reduces the causticity below 30% and reduces the residue pH to below 11.5. The completion of the carbonation/neutralisation is evidenced by pH measurements of bauxite residue samples from within the BRDA (McMahon 2017).

Another technique which may be implemented by alumina refineries using CO_2 is direct carbonation. The addition of CO_2 gas to the bauxite residue results in the rapid

neutralisation through a series of reactions (Eqns. 7 to 9) in which carbonic acid (H_2CO_3) is formed and dissociates into bicarbonate (HCO_3^-) and carbonate (CO_3^{2-}) ions, resulting in the release of a hydrogen ion (H^+) which ultimately leads to a reduction in pH (Dilmore et al., 2007). The pH may be reduce to approximately pH 8.5 using direct carbonation (Power et al., 2011).

$$CO_{2(g)} + H_2O \rightarrow H_2CO_{3(aq)}^- \qquad\qquad \text{Eqn. 7}$$

$$H_2CO_{(aq)} = HCO_{3(aq)}^- + H_{(aq)}^+ \qquad\qquad \text{Eqn. 8}$$

$$HCO_{3(aq)}^- = CO_{3(aq)}^- + H_{(aq)}^+ \qquad\qquad \text{Eqn. 9}$$

2.3.4 Re-use Pathways of Bauxite Residue

Approximately 2 to 3.5 Mt of bauxite residue that is produced per annum is utilised in several ways within industry (Table 2.3), but this can vary due to changes in the economy (Evans 2016). The majority of bauxite residue is utilised is in construction, with 500,000 – 1,500,000 tonnes being used as an additive to cement (Table 2.3). The iron and steel industry, in addition to roads and soil amelioration, are the other key areas in which bauxite residue used, with roughly 100,000 tonnes (Table 2.3) of bauxite residue being used as an adsorbent and in acid mine drainage (AMD).

Table 2.3 Table showing the approximate values in tonne of the areas in which bauxite residue utilisation is occurring (Evans 2016).

Area of utilisation	Amounts utilised (tonne)
Cement	500,000 – 1,500,000
Raw material in iron and steel production	400,000 – 1, 500, 000
Landfill capping/roads/soil amelioration	200,000 - 500,000
Construction materials	100,000 – 300,000
Other (refractory, adsorbent, AMD, catalyst etc.)	100,000

2.4 Opportunities for Re-use

2.4.1 P Adsorbent

Bauxite residue has been identified as a potential adsorbent for the removal of P from aqueous solutions (Grace et al., 2016; Ye et al., 2016) due to it having a high surface reactivity potential as a result of the presence of particles of silica, Al, Fe, Ca and Ti

oxides and hydroxides (Santona et al., 2006). In general, it is titanium oxide and iron oxide that are the two main active components required in order for adsorption of pollutants to occur (Liu et al., 2007). However, when focussing on the removal of P, it is both Fe and Al oxides that are key requirements which aid in the removal of P (Jacukowicz-Sobala et al., 2015). Bauxite residue is typically comprised of a high composition of both Fe and Al oxides, with values reported to be between 5 to 60 % and 5 to 30 %, respectively (Evan 2016). It has been shown that bauxite residue has a high capability to adsorb and retain P onto the Fe and Al oxides at a neutral pH of approximately 8 (Klauber et al., 2011). One knowledge gap identified, questions the potential differences in P adsorption capacity within the different fractions of bauxite residue (fine and coarse fraction) which may be separated depending on the refinery as previously mentioned and of which the fine fraction is currently underutilised and placed in the BRDAs.

The typical mechanism in which P is removed with Fe and Al oxides can be described as being specific and non-specific (Stumm 1992; Cornell and Schwertmann 2003). *Specific adsorption* involves the process of ligand exchange (Jacukowicz-Sobala et al., 2015) and involves the exchanging of a phosphate ion with one or more hydroxyl groups, resulting in the release of a (hydroxide) OH_2 and/or a hydroxyl group (OH^-) back into the surrounding aqueous solution, which contributes to an increase in the alkalinity of the surrounding environment (Cornell and Schwertmann 2003). This can be seen in Eqn. 10 and 11:

$$\equiv FeOH + An^- \leftrightarrow\ FeAn \equiv +OH^-$$

Eqn. 10

$$Fe(OH)_2 + An^- \leftrightarrow\ \equiv Fe_2 + An^+ + 2OH^-$$

Eqn. 11
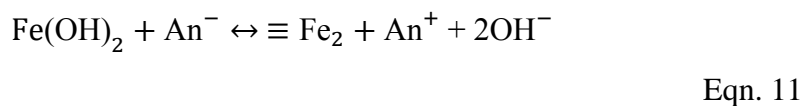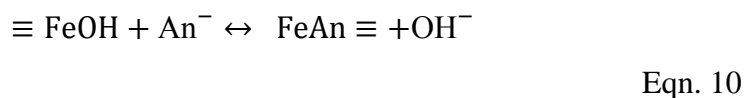
Non-specific adsorption involves electrostatic interactions between the surface of the adsorbent (which has an electric charge) and the phosphate ion (Jacukowicz-Sobala et al., 2015). This mechanism is greatly influenced by the pH of the aqueous solution, with solutions with a high pH resulting in a reduction in the number of positive charges present on the surface of the oxide involved (Jacukowicz-Sobala et al., 2015). Knowing the

PZCpH of the adsorbent material is essential in identifying how effective it will be in the removal of specific ions (Appel et al., 2003). If the pH is below the PZCpH for the adsorbent, then it will have an overall positive charge and therefore retain or adsorb more anions (which carry a negative charge) such as phosphate ions (Appel et al., 2003).

There are several factors which affect the adsorbance of P by iron and aluminium oxides; these include pH in the solution which influences the overall charge on the adsorbent (Weng et al., 2012), the presence of natural organic matter (NOM) which block positively charge adsorption sites for potential anions (Moshi et al., 1974) and solution ion composition which may influence competition for occupancy of adsorption sites on the adsorbent (Weng et al., 2012). One particular ion, Ca, which may be added through the use of gypsum application in the neutralisation process, influences the precipitation of phosphates at high concentrations, with sorption occurring at low P concentrations (Holten et al., 1988; Bastin et al., 1999).

The results of previous studies using bauxite residue in the adsorption of P are shown in Table 2.4. The majority of the research has been carried out at laboratory scale using batch studies and have investigated the impact of pH, initial concentration of P, and contact time. However, batch studies have some disadvantages, such as failing to replicate the often passive nature of the adsorption process which exists on site, as well as sometimes using unrealistic ratios of adsorbent to solution, shaking of the samples and fail to realistically replicate any incidental releases of contaminants, which may occur when some materials are placed in filters (ÁdÁm et al., 2007; Søvik and Kløve, 2005). In order to determine the full potential and longevity of an adsorbent, larger scale "column" studies are necessary (Pratt et al., 2012). One notable gap in the literature highlights the absence of studies using the fine fraction bauxite residue in column studies to treat actual wastewaters, with the exception of Penn et al., (2011) and Herron et al., (2016) who carried out studies using bauxite residue as a sorbing material to prevent P run-off. Enhancement of bauxite residue using various treatments such as heat, acid and seawater application has also been carried out and shown to enhance the P adsorption capacity of the bauxite residue examined (Table 2.4).

Treatments such as the application of high temperature results in mineral phase transitions within the mineralogical composition of the bauxite residue and leads to an overall

increase in the SSA of the bauxite residue and also removes water molecules from the surface of the bauxite residue (Ha et al., 2011; Tong et al., 2013). Similarly, the application of acid treatments such as the addition of HCl, result in a noticeable increase in the SSA of the bauxite residue and thus the overall adsorption capacity as a result of the acid increasing the positive charge on the surface of the bauxite residue and also allowing for the exposure or "cleansing" of more OH^- groups (Altundogan et al., 2002). Applications of seawater or gypsum result in reducing alkalinity and also introduction cations such as Ca^{2+}, which promotes precipitation of phosphate from solution and have been shown as effective treatments in the enhancement of the bauxite residues adsorption capacity (Despland et al., 2011; Lopez et al., 1998).

Bauxite residue may also contribute to the removal of other contaminants such as Ni(II) (Hannachi et al., 2010), Cu(II) (Agrawal et al., 2004), Cd(II) (Zhu et al., 2007), Zn(II) (Lopez et al., 1998) and Pb(II) (Apak et al., 1998) due to the wide range of minerals such as Fe oxides like hematite and Al oxides like gibbsite (which have individual PZCpH values; 8.7 to 9.8 for hematite and 5 for gibbsite) (Power et al., 2011). As a result, two products, Redmedite™ and Bauxsol™, have been developed from modified bauxite residue for the removal of several contaminants in wastewater treatment (Evans 2016).

Table 2.4 Reported adsorption behaviour of bauxite residue using various pre-treatment methods.

Country	P Recovery Technique	Factors Investigated	Type of media	Initial P concentration of the water	P Recovery Efficiency per g media	Reference
Untreated bauxite residue						
Ireland	Batch adsorption experiment	Kinetics, pH and temperature	Synthetic water	5–100 mg P L^{-1}	0.2 mg P g^{-1}	Grace et al., 2015
Gypsum treated bauxite residue						
Spain	Batch adsorption experiment Column filtration set up	Contact time (3, 6, 24, 48 hr) Percolation	Synthetic water	20-400 mg P L^{-1}	7 mg P g^{-1}	Lopez et al., 1998
Brine treated bauxite residue (Bauxsol™*)						
Australia	Batch adsorption experiment	pH, ionic strength, time	Synthetic water	0.5-2 mg P L^{-1}	6.5-14.97 mg P g^{-1}	Akhurst et al., 2006
Acid treated bauxite residue						
Australia	Batch adsorption experiment	Acid type, pH	Synthetic water	1 mg P L^{-1}	0.6 mg P g^{-1}	Huang et al., 2008
Acid and heat treated bauxite residue						
China	Batch adsorption experiment	Time, pH and initial concentration	Synthetic water	155 mg P L^{-1}	202.9 mg P g^{-1}	Liu et al., 2007

*Bauxsol™ = neutralised bauxite residue produced using the Basecon™ procedure, which uses brines high in Ca2+ and Mg2+ (McConchie et al., 2001)

2.4.2 Elements that are CRM

The 'Raw Materials Initiative' as set out by the European Union (EU), aims to secure and sustain an affordable supply of CRMs which have been identified as materials as having high economic importance and listed with their potential supply risk (Figure 2.3) (COM/2017/0490). The list of CRMs contains 27 materials (Figure 2.3) which are inclusive of the platinum group metals (PGM) and REEs which can be broken down into light REE [lanthanum (La), cerium (Ce), praseodymium (Pr), neodymium (Nd), samarium (Sm), europium (Eu)] and heavy REE [gadolinium (Gd), terbium (Tb), dysprodium (Dy), holmium (Ho), erbium (Er), thulium (Tm), ytterbium (Yb), lutetium (Lu), including yttrium (Y)] (Xu et al., 2017), phosphate rock, and scandium (Sc) (Binnemans et al., 2018) which was added in 2017. Phosphorus was also added to the list of CRMs in 2017 (COM/2017/0490).

Figure 2.3 The list of 27 critical raw materials (CRMs) as listed by the Raw Materials Initiative is seen here in the shaded box. The non-critical raw materials are noted in the non-shaded box ((COM/2017/0490)).

CRMs have many industrial uses. For example, V is required in the manufacture of electrodes (Morel et al., 2016), whilst Ga is necessary in the production of catalysts (Qin and Schneider 2016). Research in recent years has focussed on the use of various industrial by-products such as phosphogypsum, mine tailings, slags and bauxite residue as potential secondary sources for CRM supply (Binnemans et al., 2015). Of these industrial by-products, bauxite residue has been studied as a potential secondary source for CRMs in several studies (Borra et al., 2015; Mohaptra et al., 2012; Qu et al., 2013).

Bauxite residue, in particular the residue generated from karstic type bauxite ore, has been identified as having high concentrations of various CRMs such the REEs in particular such La and Ce etc. (Table 2.5), as these have the greatest supply risk and associated economic value to Europe (Binnemans et al., 2015). The accumulation of the REEs occurs during the processing of the bauxite ore during the Bayer Process and is associated with Fe and titanium (Ti) minerals, of which bauxite ore is mainly composed (Derevyankin et al., 1981). An additional factor which has not currently been reported in the literature and which may have an impact on the CRM content of bauxite residue is the time spent in a BRDA and therefore is a key consideration to include in the potential use of bauxite residue as a potential secondary source for these CRMs.

In order to extract and recover CRMs from by-products such as bauxite residue, large amounts of chemical and energy inputs are required, and are generally unfeasible from a financial point of view (Ujaczki et al., 2018). The typical recovery of CRMs may involve direct leaching using mineral acids such as sulphuric (H_2SO_4), hyrdrochloric (HCl) or nitric acids (HNO_3), leaching following pyrometallurgical/mechanical operations, or indirect hydrometallurgical leaching (Binnemans et al., 2013). However, it may be argued that the capital investment required in the extraction and recovery of CRMs from bauxite residue could be offset against the overall benefits of using bauxite residue as a potential secondary source of CRMs such as the reduced costs associated with bauxite residue disposal, reduction in the loss of fertile land that would be required for the storage of bauxite residue, as well as the financial value of the recovered CRMs (Ujaczki et al., 2018), particularly Sc which is valued at 4,600,000 US $ t^{-1} (USGS 2016).

Table 2.5 Average concentrations of REEs in Greek bauxite residue, expressed in $g\ t^{-1}$. Amended table taken from Ochsenkühn-Petropoulou et al., (1994).

Element	Concentration ($g\ t^{-1}$)
La	149
Ce	418
Pr	25.8
Nd	115
Sm	28.9
Eu	5
Gd	23.3
Tb	N.D.[*]
Dy	12.8
Ho	4.3
Er	17.2
Tm	N.D.[*]
Yb	15.6
Lu	2.4
Y	93.9
Sc	127.9

*N.D. = not detectable

2.4.2.1 Phosphorus and Phosphate Rock

Phosphorus (P), a non-metal element found in the N group which is fundamental to life, with some of its main functions in the human body inclusive of helping in the formation of strong healthy bones and teeth, helping to produce energy, and assisting in the moving of muscles (Karl 2000; Desmidt et al., 2015). Phosphorus is also required in the growing of crops and plants (Cordell and White 2011) and is therefore crucial in the production and supply of food (Cooper et al., 2011). As phosphorus cannot be produced synthetically, it is a non-renewable resource (Neset and Cordell 2012), the majority of which is sourced from phosphate rock (Cooper et al., 2011).

Phosphate rock accounts for up to 60% of P available to humans for use in fertilisers, which are applied to soil (Cordell, 2011). The remaining P is recycled through the use of manures, crop residuals and human excreta (Cooper et al., 2011). In recent years, with

both increases in the global population and the increase demand on food supply, emphasis has been placed on the estimated phosphate rock reserves , with reserves likely to be used up in the next 50 to 100 (Gunther 2005). As a result, both P and phosphate rock have been listed as CRMs within a European context (EU COM/2017/0490). Phosphate rock, also known as phosphorite (Desmidt et al., 2015), is found deposited at different locations throughout the world (Figure 2.4) and is commonly found as sedimentary phosphate rock deposits or igneous phosphate rock deposits (Aydin et al., 2009). Sedimentary phosphate rock deposits are found in much lower quantities than igneous forms, and are therefore more expensive. As a result, igneous phosphate rock sources account for 80% or more for production on a global scale (Desmidt et al., 2015).
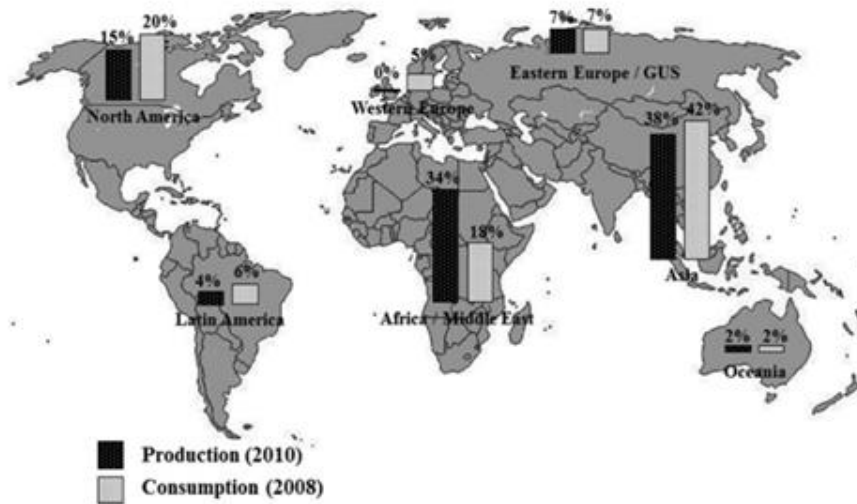
Figure 2.4 Global map (as taken from Desmidt et al., 2015) showing both production and consumption of phosphorus (data from U.S. Geological Survey, 2012).

The distribution of phosphate rock can be observed in Figure 2.4, which shows the volume (%) of phosphate rock associated with each continent. The sedimentary type is predominantly found in North Africa, China, the Middle East and USA with the igneous found in Brazil, Canada, Russia and South Africa (Desmidt et al., 2015).

On an annual basis, 180 to 190 Mt of phosphate rock are mined across the world, with China, USA and Morocco (Figure 2.4) being the main areas (U.S. Geological Survey 2012; Desmidt et al., 2015). Increasing the price of fertilisers is one way in which the issue of declining supply of phosphate is being dealt with (Cordell et al., 2009), with 2008 seeing an 800% increase in the price of phosphate rock and its fertilisers (Cordell and

White 2011). Cordell et al. (2009) state that there is "no quick fix" to finding a replacement for fertilisers from phosphate rock, but that there are numerous ways to recover and recycle P, particularly from wastewater (Hukarie et al., 2016).

2.4.2.1.1 Soil P and Water Quality

Phosphorus is present within soil in organic and inorganic forms (Battini et al., 2017), with only a minute amount (<1 %) readily available for uptake by vegetation (Richardson et al., 2005). Soil P uptake greatly influenced by pH, with the most plant available between pH 6.3 to 7 (Plunkett et al., 2019). The soil P cycle includes inputs through the process of weathering, decomposed plants, application of inorganic and organic fertilisers and animal wastes and includes many processes within the soil such as sorption, desorption, immobilisation, mineralisation, precipitation and dissolution reactions (Kruse et al., 2015). Outputs of phosphorus from soil include uptake by vegetation, and P that is lost through erosion and leaching (Kruse et al., 2015).

Within Ireland and the larger European setting, grass is the main source of nutrition for cattle within the dairy and beef industry and therefore vital for the sustenance of the agriculture sector (Peeters, 2015). In recent years with the expansion of the dairy sector, there is increased pressure to ensure adequate grass supply (Chen and Holden, 2018). There, greater emphasis has been placed on ensuring that soils have sufficient P in order to maximise high quality grass growth (Plunkett et al., 2019). The approach taken is to build and manage P content within soil through the use of regular soil testing (recommended every 3-4 years) and thereby applying the correct volume of P to the soil in order to achieve and maintain "good" soil P status (Plunkett et al., 2019).

The amount of P within soil determines its P status and is quantified through the use of soil test phosphorus (STP) methods which vary from region to region and include methods such as Morgan's P test (Plunkett et al., 2019). From an Irish context, the STP method used is Morgan's P test and following the determination of the soil P content, the soil is then given a P index value (Lalor and Culleton, 2009). The P index values range from one to four, with one being the very deficient in P (0.0 – 3.0 mg L^{-1}) and four (> 8 mg L^{-1}) having a very high soil P concentration (Lalor and Culleton, 2009), with the approximate time frame to move up one soil P index roughly four years (Plunkett et al., 2019). Under article 16(5) of the Good Agricultural Practice for Protection of Waters

Regulations (S.I. No 605/2017), effective from 1 January 2018, grassland farmers now have the option of using increased P build-up levels to rectify soil phosphorus deficiency (S.I. No 605/2017).

However, soil P (and N) may become problematic over time following build-up or over application through the intensification of agriculture and making, its way into surrounding water bodies (Withers and Haygarth, 2007). The movement of P from soil to water bodies is predominantly in the form of particulate or dissolved reactive P (DRP) (Brennan et al., 2014). Particulate P is not 100% bioavailable, as it has to enter solution before becoming bioavailable; however, DRP is 100% available for aquatic biota and, therefore, has an immediate effect on the surrounding ecosystems, leading to eutrophication (Penn et al., 2014). Eutrophication arises when excess phosphates and nitrates enter water bodies. This causes the dissolved oxygen to become depleted by the excessive growth of algal blooms (Anderson et al., 2002), and can be described as the "over-enrichment" of a water body with minerals (Correll 1998). As a result of the intensification of agriculture which is the largest land using sector in Ireland, the degradation of the water of quality, particularly in rivers is as a result of agriculture (Figure 2.5) (EPA, 2017), which accounts for 53% followed by municipal sources which account for the degradation of 34 % of water bodies (EPA, 2017). The source of P loss and other nutrients such as N can be classified as being point, which includes drains or outlets from infrastructure housing livestock and non-point sources which include run-off from land (Yang et al., 2017). This is mainly attributed to P loss from run-off as a result of over application of P fertiliser, soil type (poorly drained and peaty have poor P retention due to the lack of Fe and Al) and/or close proximity to water bodies (Daly et al., 2001). In addition, dairy soiled water (DSW) which is composed of milk parlour washings composed of cow faeces and urine, milk and detergents (Minogue et al., 2015) is one area for concern for dairy farmers as several studies have shown that the over application of these effluents lead to N and P loss to ground and surface waters and the move to improving on-farm nutrient management (Murnane et al., 2016).
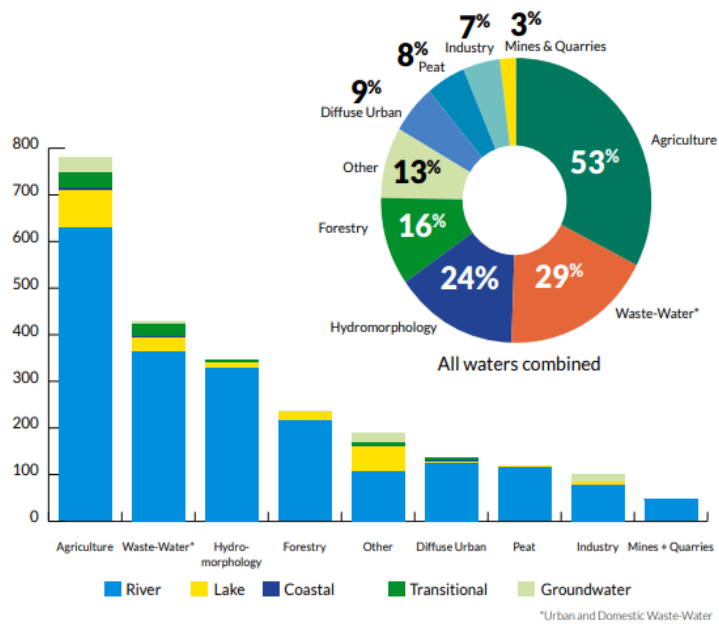
Figure 2.5 Breakdown of the main contributors to poor water quality status in Irish water bodies (EPA, 2017).

The Water Framework Directive (WFD) is an EU Directive (EC, 2000), which has an overall aim to improve water quality and is applicable to rivers, lakes, groundwater, estuaries and coastal waters, in which Ireland has been set the target to achieve a 'good status'. Since 2006, there has been focus on reducing water pollution caused by P and N within agriculture under the Nitrates Directive (EC, 1991). Overall, little net change has been observed in the status of our water bodies, even though 398 bodies have improved this has been offset with 515 that have disimproved (EPA, 2017). Due to little improvement in the status over the past 2-3 decades, the Irish Government has adopted a new strategy The River Basin Management Plan for improving water quality between 2018 and 2021 (River Basin Management Plan 2018) along with the inclusion of the Agricultural Sustainability Support and Advice Programme (ASSAP), a new advisory service to liase with farmers in order to achieve the aim of improving water quality and focusses on the agricultural pressures (Teagasc 2017).

One other source of the degradation of Irish water quality, which accounts for 16 %, is forestry (Figure 2.5). Approximately 10.5 % of land use in Ireland, is forest, of which 44 % are planted on peatland (National Forest Inventory, 2012). It is widely reported that highly organic soils and peats, lack both Al and Fe, which result in these soil types having poor P retention capacity, which is a major environmental issues once felling

34

and harvesting occurs due to the P loss and its potential to run-off into surrounding water bodies (Finnegan et al., 2014). However, key steps and best practice management is to incorporate the use of riparian strips as a preventive measure to prevent P run-off into water bodies (Forest Service, 2000).

In wastewater treatment, techniques for the removal and recovery of P include chemical precipitation, biological removal of P, crystallisation methods, novel chemical precipitation and sludge methods (Morse et al., 1998). Chemical precipitation involves metal salts such chlorides or sulphates being added to the wastewater, which result in the precipitation of insoluble metal phosphate (Desmidt et al., 2015). Enhanced Biological Phosphorus Removal (EBPR) involves the activation of sludge, which may result in as much as 97% of total phosphorus (TP) being removed (Clark et al., 1997).

2.4.2.2 Recycling of Phosphorus from Wastewater

In recent years, the EU has focused on the implementation of a Circular Economy, which move towards a "zero waste" approach (European Parliament, 2015). This is set out in an action plan titled "Closing the Loop" which focusses on the move from waste to resources with the aim of increasing the potential market for the use of secondary raw materials and water reuse. In particular, one category of great importance is the recycled nutrients category, which would reduce the need for mineral-based fertilisers, which is dependent on phosphate rock, a finite resource and is a lead cause in affecting the environment (European Parliament 2015).

Emphasis has been placed on the removal of P from both municipal and industrial wastewaters (Kok et al., 2018; Nättorp et al., 2017) highlighting an untapped source of P which would help in the achievement of P sustainability (Koppelaar and Weikard 2013). Interest has been shown on the potential re-use of by-products such as bauxite residue, steel slag and fly ash particularly as low-cost P adsorbents for water treatment (Grace et al., 2016). Studies carried out by Penn et al., (2011) and Herron et al., (2016) highlighted the potential of such by-products in the treatment of agricultural wastewater, particularly bauxite residue in the removal of P within a farm practice. However, there is a gap within the literature as to how they may perform in terms of potential fertiliser replacements, particularly in an agricultural setting.

There has been significant progress within the wastewater treatment process, with numerous P removal techniques have been established for application in various stages of the wastewater treatment process such as (1) liquid phase (2) sludge phase, and (3) mono-incerated sludge ash, which occurs when sludge is incinerated separately from other wastes (Cornel and Schaum 2009). On average, up to 90% of P present in wastewater may be removed in sewage sludge (Egle et al., 2016), while 40 to 50% of P may be removed from the liquid phase (Cornel and Schaum 2009). Recently, focus has shifted from P removal from wastewater (which aims for P free effluent) to P recovery, which aims to find re-use in either an agricultural setting or within industry for the P recovered from wastewater (Desmidt et al,. 2015). This offers a potential P nutrient source, which in some countries such as Ireland is being practiced with up to 80% of treated sludge being applied to land (Healy et al., 2017).

Another mechanism for potential P recovery from wastewater is through the incorporation of a crystallisation process in the waste water treatment plant (WWTP), which facilitates the precipitation and recovery of P in the form of calcium phosphates (Ca-P) or struvite (magnesium-ammonium-phosphate/$MgNH_4PO4.6H_2O$; Desmidt et al., 2015; Hukari et al., 2016). Calcium phosphate is the main component in phosphate rock (the main source of P for the production of fertilisers) and following its recovery, may be utilised within the phosphate industry (Desmidt et al., 2015). Struvite, which accumulates in the pipelines within WWTP, is of particular interest as a potential source of fertiliser replacement (Talboys et al., 2016) due to its solubility in aqueous and soil solutions, which means that it may be a source of P, N and magnesium (Mg) for plants (Ryu et al., 2012).

Within an EU context, several technologies involving struvite crystallisation processes such as Pearl, AirPrex and NuReSys have been implemented full scale (Hukari et al., 2016); however, issues still arise in the total implementation of P recovery within the EU due to the need for revisions in current legislation such as the Fertilisers Regulation which would allow for the inclusion of recycled fertilisers (Hukari et al., 2016).

2.4.2.3 European Legislation on Phosphorus Recycling from Wastewater
Several barriers for the recovery and recycling of P have been identified within the current EU legislation and regulations together with the limitations within the emerging

recovery and recycling sectors (ERRS) (Hukari et al., 2016).   The central legislation, which controls recovery and recycling installations in for example a wastewater treatment plant (WWTP), includes the Environmental Impact Assessment Directive (EIA) (Dir. 2011/92/EU (European Parliament, 2011)) and the Directive on Industrial Emissions (IED) (Dir. 2010/75/EU (European Parliament, 2010)). In the event that a WWTP is aiming to produce a fertiliser product from the recycled P, it is required to declare itself as a "fertiliser producer" which involves the need for EIA and IED-permits. The origin of the input waste to undergo the recycling or recovery process is also a key factor for consideration, and if originating outside the country where the WWTP is located, then another piece of legislation applies, the Shipment of Waste Regulation (Reg. 1013/2006 EC (European Parliament, 2006a)).

The P recovered and recycled is identified as waste unless the WWTP recycler is successful in achieving the criteria as set out by the The End-Of-Waste (EoW) criteria of the Waste Framework directive (Article 6(1) and (2) of the WFD/EC Directive 2008/98/EC; European Parliament, 2008a) which stipulates that, instead of waste-related obligations, product legislation can be applied for materials recovered from waste. Once product legislation is met the "product" needs to achieve the criteria as set out by the European Chemicals Regulation (REACH; Reg. 1907/2006 EC (European Parliament, 2006b)) and the Classification, Labelling and Packaging of Substances and Mixtures Legislation (CLP; Reg. 1272/2008 EC (European Parliament, 2008b)) in order to be permitted for production and sale of the product. One stipulation that is set out by REACH is that chemical substances (inclusive of fertilizers and ashes) that are either manufactured in or imported into Europe in quantities greater than 1 tonne per year must be registered with the European Chemicals Agency (ECHA) which requires full safety data sheets (SDSs) which provide all information on the chemical substance, its preparation and any potential hazards. For the product to be fully recognised as a fertiliser, it must meet all criteria set out by the Fertilisers Regulation (Reg. EC 2003/2003 (European Parliament, 2003)). The current process and various pieces of legislation highlights the need for more harmonious approach to allow for the successful recovery and recycling of P (Hukari et al., 2016).

2.5 Limitations and Barriers for the General Re-use of Bauxite Residue

There are several barriers and potential implications in the general re-use of bauxite residue, particlulary as a P adsorbent due its general composition (Klauber et al., 2011b). Depending on its pH and origin, the potential leaching of metals and pollution swapping from bauxite residue is one key concern (Cornelis et al., 2008). Metals such as chromium (Cr) and arsenic (As) are the two of greatest concern, due to their potential for uptake in plant vegetation (Evans 2016). This is also a key issue for other by-products such as fly ash (Chou et al., 2009) and ground granular blast furnace slag (Grace et al., 2016) which have been investigated as potential P adsorbents. Similarly and depending on the location of the bauxite ore from which the bauxite residue is generated, radioactivity emittance from the bauxite residue may be also be an issue because of the presence of uranium (^{238}Ur) and thorium (^{232}Th) (Kovács et al., 2013).

Other key barriers and limitations for the re-use of bauxite residue include the issue of high alkalinity, sodicity and salinity associated with bauxite residue (Johnston et al., 2010; Jones and Haynes 2011). However, this can be greatly reduced using various amendments such as with gypsum application or neutralisation techniques such as with seawater (Kirwan et al., 2013) but this will have implications such as equipment necessary to carry out such treatments. For a refinery, the cost of neutralisation techniques is an obvious consideration when deciding which technique(s) to use. The use of seawater as a neutralisation technique would be a cheap and feasible option for a refinery that is close to the sea. The establishment of a pipeline (if not already in place) would be the dominant capital cost. Gypsum may be a more expensive option, requiring machinery such as Amphirolls and agricultural machinery such as tractors. Depending on the refinery's location, waste gypsum from construction sites or fossil fuel powered power stations may be used (Jones and Haynes, 2011). However, the overall cost implications of implementing such measures to amend/treat the bauxite residue for use as a P adsorbent may be offset by the further re-use potential of the bauxite residue as a possible nutrient source/fertiliser, particularly with the current focus on phosphate rock depletion (Desmidt et al., 2015). The low solid content that is present in bauxite residue is also an issue and source of high costs in the potential transport of the bauxite residue within/from the alumina refinery in order to be processed for potential re-use (Evans 2016). Overall, for any potential re-use outlet for bauxite residue, it must be cost effective, low risk, perform well and incorporate high volumes of the bauxite residue (Klauber et al., 2011b).

2.6 Summary

The generation of bauxite residue is increasing by an estimated 150 Mt annually. The management of this by-product is a big concern both from an environmental and policy point of view, due to its composition and the high management costs involved. The lack of utilisation of this by-product is something that the alumina refineries, environmental and governmental agencies need to consider. As it has a high adsorption capacity for P, due to its high Fe and Al oxide content, there are potential options for its re-use in wastewater and water treatment, particularly in the removal of P, which has recently been identified as a CRM. In addition, phosphate rock, the source of P for the production of P fertiliser, is also listed as a CRM. Bauxite residue has also been recognised as a potential secondary source for other CRM such as V, Sc and Ga. However, the general composition and CRM content of bauxite residue varies because of the bauxite ore used and the parameters used within the Bayer Process. In addition, variation may also be present within the BRDA of an alumina refinery due to factors such as neutralisation techniques implemented by the refinery prior to disposal, residue management and disposal strategies, and weathering of deposited residue.

Using bauxite residue as an adsorbent for P removal from wastewater is one potential option in the recovery and recycling of P from wastewater. From the various studies using bauxite residue (Table 2.4), it is clear that compounds high in Fe and Al oxides, containing a high SSA and have a PZC in the range of pH 8 to 9, have high adsorption capacities for P. In order to achieve the maximum adsorption capacity possible, modification of the bauxite residue is necessary in order to lower the pH to the optimum PZC (pH 8 to 9) for the highest adsorption of P. The preferred methods of modifying the bauxite residue in order to lower the pH are seawater and gypsum treatments, as these are more cost effective and logistically easier than modification using acids. Further re-use of the bauxite residue following the P adsorption process could involve the use of the bauxite residue as a potential nutrient source.

2.7 References

ÁdÁm, K., Sovik, A.K., Krogstad, T. and Heistad, A., 2007. Phosphorous removal by the filter materials light-weight aggregates and shellsand-a review of processes and experimental set-ups for improved design of filter systems for wastewater treatment. *Vatten. 63*(3), p.245.

Alliance for the Great Lakes, 2010. Available at: https://greatlakes.org/2017/10/rescuing-lake-erie-assessment-progress/ [accessed 24.11.2018].

Agrawal, A., Sahu, K.K. and Pandey, B.D., 2004. A comparative adsorption study of copper on various industrial solid wastes. *AIChE journal*. 50(10), pp.2430-2438.

Akhurst, D.J., Jones, G.B., Clark, M., McConchie, D., 2006. Phosphate removal from aqueous solutions using neutralised bauxite refinery residues (Bauxsol™). *Environ. Chem.* 3, 65-74.

Alcoa Kwinana Refinery Long Term Residue Management Strategy, 2005. Sinclair Knight Merz, Perth. Available: https://www.alcoa.com/australia/en/sustainability/reports-publications.asp [accessed 23.04.2019].

Altundoğan, H.S., Altundoğan, S., Tümen, F. and Bildik, M., 2002. Arsenic adsorption from aqueous solutions by activated red mud. *Waste Manage.* 22(3), pp.357-363.

Anderson, D.M., Glibert, P.M. and Burkholder, J.M., 2002. Harmful algal blooms and eutrophication: nutrient sources, composition, and consequences. *Estuaries.* 25(4), pp.704-726.

Apak, R., Tütem, E., Hügül, M. and Hizal, J., 1998. Heavy metal cation retention by unconventional sorbents (red muds and fly ashes). *Water. Res.* 32(2), pp.430-440.

Appel, C., Ma, L.Q., Rhue, R.D. and Kennelley, E., 2003. Point of zero charge determination in soils and minerals via traditional methods and detection of electroacoustic mobility. *Geoderma.* 113(1-2), pp.77-93.

Aydin, I., Imamoglu, S., Aydin, F., Saydut, A. and Hamamci, C., 2009. Determination of mineral phosphate species in sedimentary phosphate rock in Mardin, SE Anatolia, Turkey by sequential extraction. *Microchem. J.* 91(1), pp.63-69.

Bardossy, G., 1982. Karst Bauxites (Bauxite deposits on carbonate rocks) Budapest. Hungary.

Bárdossy, G., 2013. Karst bauxites (Vol. 14). Elsevier.

Bastin, O., Janssens, F., Dufey, J. and Peeters, A., 1999. Phosphorus removal by a synthetic iron oxide–gypsum compound. *Ecol. Eng.* 12(3), pp.339-351.

Battini, F., Grønlund, M., Agnolucci, M., Giovannetti, M. and Jakobsen, I., 2017. Facilitation of phosphorus uptake in maize plants by mycorrhizosphere bacteria. *Scientific Reports.* 7(1), p.4686.

Binnemans, K., Jones, P.T., Blanpain, B., Van Gerven, T., Yang, Y., Walton, A. and Buchert, M., 2013. Recycling of rare earths: a critical review. *J. Clean. Prod.* 51, pp.1-22.

Binnemans, K., Jones, P.T., Blanpain, B., Van Gerven, T. and Pontikes, Y., 2015. Towards zero-waste valorisation of rare-earth-containing industrial process residues: a critical review. *J. Clean. Prod.* 99, 17-38.

Binnemans, K., Jones, P.T., Müller, T. and Yurramendi, L., 2018. Rare earths and the balance problem: How to deal with changing markets? *J. Sustain. Metall.* 4(1), pp.1-21.

Borra CR, Pontikes Y, Binnemans K and Van Gerven T, 2015. Leaching of rare earths from bauxite residue (red mud). *Miner. Eng.* 76:20–27.

Bray, A.W., Stewart, D.I., Courtney, R., Rout, S.P., Humphreys, P.N., Mayes, W.M. and Burke, I.T., 2017. Sustained bauxite residue rehabilitation with gypsum and organic matter 16 years after initial treatment. *Environ. Sci. Technol.* 52(1), pp.152-161.

Brennan, R.B., Wall, D., Fenton, O., Grant, J., Sharpley, A.N. and Healy, M.G., 2014. The impact of chemical amendment of dairy cattle slurry before land application on soil phosphorus dynamics. *Commun. Soil Sci. Plant Anal.* 45(16), 2215 – 2233.

Burke, I.T., Peacock, C.L., Lockwood, C.L., Stewart, D.I., Mortimer, R.J., Ward, M.B., Renforth, P., Gruiz, K. and Mayes, W.M., 2013. Behavior of aluminum, arsenic, and vanadium during the neutralization of red mud leachate by HCl, gypsum, or seawater. *Environ. Sci. Technol.* 47, 6527-6535.

Chen, W. and Holden, N.M., 2018. Bridging environmental and financial cost of dairy production: A case study of Irish agricultural policy. *Sci. Total. Environ.* 615, pp.597-607.

Chou, J.D., Wey, M.Y., Liang, H.H. and Chang, S.H., 2009. Biotoxicity evaluation of fly ash and bottom ash from different municipal solid waste incinerators. *J. Haz. Mat.* 168(1), pp.197-202.

Clark, T., Stephenson, T. and Pearce, P.A., 1997. Phosphorus removal by chemical precipitation in a biological aerated filter. *Water. Res.* 31(10), pp.2557-2563.

Clohessy, J., 2015. Closure and rehabilitation of Rusal Aughinish BRDA, presented at the Residue Closure and Rehabilitation Workshop. In 10th Alumina Quality Workshop, Perth, Western Australia (http://aqw.com.au/2015papers.html) [accessed 18.04.2018].

Cooling, D.J., Hay, P.S. and Guilfoyle, L., 2002, September. Carbonation of bauxite residue. In Proceedings of the 6th international alumina quality workshop (pp. 185-190). AQW Inc.: Brisbane.

Cooper, J., Lombardi, R., Boardman, D. and Carliell-Marquet, C., 2011. The future distribution and production of global phosphate rock reserves. *Resourc. Conserv. Recycl.* 57, pp.78-86.

Cordell, D., Drangert, J.O. and White, S., 2009. The story of phosphorus: global food security and food for thought. *Global. Environ. Chang.* 19(2), pp.292-305.

Cordell, D. and White, S., 2011. Peak phosphorus: clarifying the key issues of a vigorous debate about long-term phosphorus security. *Sustain.* 3(10), pp.2027-2049

Cornelis, G., Johnson, C.A., Van Gerven, T. and Vandecasteele, C., 2008. Leaching mechanisms of oxyanionic metalloid and metal species in alkaline solid wastes: a review. *Appl. Geochem.* 23(5), pp.955-976.

Cornell RM and Schwertmann U., 2003. The Iron Oxides. Weinheim, Germany: Wiley-VCH Verlag.

Cornel, P. and Schaum, C., 2009. Phosphorus recovery from wastewater: needs, technologies and costs. *Water. Sci. Technol.* 59(6).

Correll, D.L., 1998. The role of phosphorus in the eutrophication of receiving waters: A review. *J. Environ. Qual.* 27(2), pp.261-266.

Courtney, R.G., Jordan, S.N., Harrington, T., 2009. Physico-chemical changes in bauxite residue following application of spent mushroom compost and gypsum. *Land. Degrad. Dev.* 20, 572-581.

Courtney, R. and Kirwan, L., 2012. Gypsum amendment of alkaline bauxite residue–plant available aluminium and implications for grassland restoration. *Ecol. Eng.* 42, pp.279-282.

Daly, K., Jeffrey, D. and Tunney, H., 2001. The effect of soil type on phosphorus sorption capacity and desorption dynamics in Irish grassland soils. *Soil. Use. Manage.* 17(1), pp.12-20.

Daniel, T.C., Sharpley, A.N. and Lemunyon, J.L., 1998. Agricultural phosphorus and eutrophication: A symposium overview. *J. Environ. Qual.* 27(2), pp.251-257.

Deady, É.A., Mouchos, E., Goodenough, K., Williamson, B.J. and Wall, F., 2016. A review of the potential for rare-earth element resources from European red muds: examples from Seydişehir, Turkey and Parnassus-Giona, Greece. *Mineral. Mag.* 80(1), pp.43-61.

Derevyankin, V., 1981. A Study of Lanthanum- and Scandium-Containing Phases of Aluminocalcium Slags. Izv. V. U. Z. Tsvetn. *Met.* (5), pp.84-85.

Desmidt, E., Ghyselbrecht, K., Zhang, Y., Pinoy, L., Van der Bruggen, B., Verstraete, W., Rabaey, K. and Meesschaert, B., 2015. Global phosphorus scarcity and full-scale P-recovery techniques: a review. *Crit. Rev. Env. Sci. Technol.* 45(4), pp.336-384.

Despland, L.M., Clark, M.W., Vancov, T., Erler, D. and Aragno, M., 2011. Nutrient and trace-metal removal by Bauxsol pellets in wastewater treatment. *Env. Sci. Technol.* 45(13), 5746-5753.

Dilmore, R., Lu, P., Allen, D., Soong, Y., Hedges, S., Fu, J.K., Dobbs, C.L., Degalbo, A. and Zhu, C., 2007. Sequestration of CO2 in mixtures of bauxite residue and saline wastewater. *Energ. Fuel.* 22(1), pp.343-353.

ECHA, 2010 ECHA Guidance on waste and recovered substances. Available: https://echa.europa.eu/view-article/-/journal_content/title/echa-publishes-new-guidance-on-waste-and-recovered-substances [accessed 09.04.2019].

Egle, L., Rechberger, H., Krampe, J. and Zessner, M., 2016. Phosphorus recovery from municipal wastewater: An integrated comparative technological, environmental and economic assessment of P recovery technologies. *Sci. Total. Environ.* 571, pp.522-542.

EPA, 2017. Water Quality in 2017, An Indicators Report. Available: https://www.epa.ie/pubs/reports/water/waterqua/Water%20Quality%20in%202017%20-%20an%20indicators%20report.pdf [accessed 23.04.2019].

European Commission, 1991. The Nitrates Directive. Available: http://ec.europa.eu/environment/water/water-nitrates/index_en.html [accessed 23.04.2019].

European Commission, 2000. EU Water Framework Directive. Available: http://ec.europa.eu/environment/water/water-framework/info/intro_en.htm [accessed 23.04.2019].

European Commission, 2015. COM(2015) 614 Communication from the commission to the European Parliament, the Council, the European Economic and Social Committee and the Committee of the regions - Closing the loop – An EU action plan for the circular economy. Brussels. Available: https://eur-lex.europa.eu/resource.html?uri=cellar:8a8ef5e8-99a0-11e5-b3b7-01aa75ed71a1.0012.02/DOC_1&format=PDF [accessed 02.12.2018].

European Commission, 2017. Study on the review of the list of critical raw materials. Critical raw materials factsheets. Catalogue number ET-04-15-307-EN-N. Available: https://publications.europa.eu/en/publication-detail/-/publication/7345e3e8-98fc-11e7-b92d-01aa75ed71a1/language-en [accessed 15.05.2018].

European Parliament, 2003. Regulation (EC) no 2003/2003 of the European Parliament and of the Council of 13 October 2003 relating to fertilisers
European Parliament, Brussels (2003). Available: https://eur-lex.europa.eu/legal-content/EN/TXT/?uri=CELEX%3A32003R2003 [accessed 09.04.2019].

European Parliament, 2006a. Regulation (EC) no 1013/2006 of the European Parliament and of the Council of 14 June 2006 on shipments of waste
European Parliament, Brussels (2006). Available: https://eur-lex.europa.eu/legal-content/en/ALL/?uri=CELEX%3A32006R1013 [accessed 09.04.2019].

European Parliament, 2006b. Regulation (EC) no 1907/2006 of the European Parliament and of the Council of 18 December 2006 concerning the registration, evaluation, authorisation and restriction of chemicals (REACH), establishing a European chemicals agency, amending directive 1999/4. European Parliament, Brussels (2006). Available: https://eur-lex.europa.eu/legal-content/EN/TXT/?uri=CELEX%3A02006R1907-20140410 [accessed 09.04.2019].

European Parliament, 2008a. Directive 2008/98/EC of the European Parliament and of the Council of 19 November 2008 on waste and repealing certain directives. European Parliament, Brussels (2008). Available: http://ec.europa.eu/environment/waste/framework/ [accessed 09.04.2019].

European Parliament, 2008b. Regulation (EC) no 1272/2008 of the European Parliament and of the Council of 16 December 2008 on classification, labelling and packaging of substances and mixtures, amending and repealing directives 67/548/EEC and 1999/45/EC, and amending regulation (EC). European Parliament, Brussels (2008). Available: https://eur-lex.europa.eu/legal-content/en/TXT/?uri=CELEX%3A32008R1272 [accessed 09.04.2019].

European Parliament, 2010. Directive 2010/75/EU of the European Parliament and of the Council of 24 November 2010 on industrial emissions (integrated pollution prevention and control) text with EEA relevance
European Parliament, Brussels (2010). Available: https://eur-lex.europa.eu/legal-content/EN/TXT/?uri=celex%3A32010L0075 [accessed 09.04.2019].

European Parliament, 2011. Directive 2011/92/EU of the European Parliament and of the council of 13 December 2011 on the assessment of the effects of certain public and private projects on the environment. Available: https://eur-lex.europa.eu/LexUriServ/LexUriServ.do?uri=OJ:L:2012:026:0001:0021:En:PDF [accessed 09.04.2019].

European Parliament (2015) COMMUNICATION FROM THE COMMISSION TO THE EUROPEAN PARLIAMENT, THE COUNCIL, THE EUROPEAN ECONOMIC AND SOCIAL COMMITTEE AND THE COMMITTEE OF THE REGIONS Closing the loop - An EU action plan for the Circular Economy

COM/2015/0614 final Available: https://eur-lex.europa.eu/resource.html?uri=cellar:8a8ef5e8-99a0-11e5-b3b7-01aa75ed71a1.0012.02/DOC_1&format=PDF [accessed 09.04.2019].

Evans, K., 2016. The history, challenges, and new developments in the management and use of bauxite residue. *J. Sustain. Metallurgy.* 2, 316-331.

Finnegan, J., Regan, J.T., O'Connor, M., Wilson, P. and Healy, M.G., 2014. Implications of applied best management practice for peatland forest harvesting. *Eco. Eng.* 63, pp.12-26.

Fois, E., Lallai, A. and Mura, G., 2007. Sulfur dioxide absorption in a bubbling reactor with suspensions of Bayer red mud. *Ind. Eng. Chem. Res.* 46(21), pp.6770-6776.

Forest Service, 2000. Code of Best Forest Practice Available: http://www.agriculture.gov.ie/forestservice/publications/codeofbestforestpractice/ [accessed 23.04.2019].

Goldberg DC, Gray AG, Hamaker JC, Raudebaugh RJ, Ridge JD, Runk RJ., 1970. Processes for extracting Alumina from nonbauxite ores. Alkaline Processes for low grade bauxites and clays, No. NMAB-278. National Academy of Sciences-National Academy of Engineering, Washington, D.C.

Gow, N.N. and Lozej, G.P., 1993. Bauxite. Geoscience Canada, 20(1).

Grace, M.A., Healy, M.G., Clifford, E., 2015. Use of industrial by-products and natural media to adsorb nutrients, metals and organic carbon from drinking water. *Sci. Total. Environ.* 518, 491-497.

Grace, M.A., Clifford, E., Healy, M.G., 2016. The potential for the use of waste products from a variety of sectors in water treatment processes. *J. Clean. Prod.*137, 788-802.

Gräfe, M., Power, G. and Klauber, C., 2011. Bauxite residue issues: III. Alkalinity and associated chemistry. *Hydrometallurgy.* 108(1-2), pp.60-79.

Gunther, F., 2005. A solution to the heap problem: the doubly balanced agriculture: integration with population. Available: http://www.holon.se/folke/kurs/Distans/ Ekofys/Recirk/Eng/balanced.shtml [accessed 09.03.2016].

Ha, H.K.P., Mai, T.T.N. and Le Truc, N., 2011. A study on activation process of red mud to use as an arsenic adsorbent. *ASEAN Engineering Journal.* 4, pp.66-72.

Hanahan, C., McConchie, D., Pohl, H.,, Creelman, R., Clark, M., Stocksiek C., 2004. Chemistry of seawater neutralization of bauxite refinery residues (red mud). *Environ. Eng. Sci.* 21,125–138

Hannachi, Y., Shapovalov, N.A. and Hannachi, A., 2010. Adsorption of nickel from aqueous solution by the use of low-cost adsorbents. *Kor. J. Chem. Eng.* 27(1), pp.152-158.

Healy, M.G., Fenton, O., Cormican, M., Peyton, D.P., Ordsmith, N., Kimber, K., Morrison, L., 2017. Antimicrobial compounds (triclosan and triclocarban) in sewage sludges, and their presence in runoff following land application. *Ecotox. Environ. Safe.* 142: 448 – 453.

Herron, S.L., Sharpley, A.N., Brye, K.R. and Miller, D.M., 2016. Optimizing Hydraulic and Chemical Properties of Iron and Aluminum Byproducts for Use in On-Farm Containment Structures for Phosphorus Removal. *J. Environ. Protection.* 7(12), p.1835.

Higgins, D., Curtin, T. and Courtney, R., 2017. Effectiveness of a constructed wetland for treating alkaline bauxite residue leachate: a 1-year field study. *Environ. Sci. Poll. Res.* 24, 8516-8524.

Hind, A.R., Bhargava, S.K. and Grocott, S.C., 1999. The surface chemistry of Bayer process solids: a review. *Colloid. Surface. A.* 146(1-3), pp.359-374.

Holtan, H., Kamp-Nielsen, L. and Stuanes, A.O., 1988. Phosphorus in soil, water and sediment: an overview. *In Phosphorus in Freshwater Ecosystems.* pp. 19-34.

Huang, W., Wang, S., Zhu, Z., Li, L., Yao, X., Rudolph, V. and Haghseresht, F., 2008. Phosphate removal from wastewater using red mud. *J. Hazard. Mat.* 158(1), pp.35-42.

Hukari, S., Hermann, L. and Nättorp, A., 2016. From wastewater to fertilisers—technical overview and critical review of European legislation governing phosphorus recycling. *Sci. Total. Environ.* 542, pp.1127-1135.

IAI, 2015. Bauxite Residue Management: Best Practice. http://www.world-aluminium.org/media/filer_public/2015/10/15/bauxite_residue_management_-_best_practice_english_oct15edit.pdf. (accessed 14.10.2017).

Jacukowicz-Sobala, I., Ociński, D. and Kociołek-Balawejder, E., 2015. Iron and aluminium oxides containing industrial wastes as adsorbents of heavy metals: application possibilities and limitations. *Waste Manage. Res.* 33(7), 612-629.

Johnston, M., Clark, M.W., McMahon, P. and Ward, N., 2010. Alkalinity conversion of bauxite refinery residues by neutralization. *J. Hazard. Mat.* 182(1-3), pp.710-715.

Jones, B.E. and Haynes, R.J., 2011. Bauxite processing residue: a critical review of its formation, properties, storage, and revegetation. *Crit. Rev. Env. Sci. Tec.* 41(3), pp.271-315.

Karl, D.M., 2000. Aquatic ecology: Phosphorus, the staff of life. *Nature*. 406(6791), pp.31-33.

Kirwan, L.J., Hartshorn, A., McMonagle, J.B., Fleming, L. and Funnell, D., 2013. Chemistry of bauxite residue neutralisation and aspects to implementation. *Int. J. Miner. Process.* 119, pp.40-50.

Klauber, C., Gräfe, M. and Power, G., 2011. Bauxite residue issues: II. options for residue utilization. *Hydrometallurgy.* 108(1-2), pp.11-32.

Kok, D.J.D., Pande, S., Lier, J.B.V., Ortigara, A.R., Savenije, H. and Uhlenbrook, S., 2018. Global phosphorus recovery from wastewater for agricultural re-use. *Hydrol. Earth. Syst. Sc*. 22(11), pp.5781-5799.

Kong, X., Guo, Y., Xue, S., Hartley, W., Wu, C., Ye, Y. and Cheng, Q., 2017. Natural evolution of alkaline characteristics in bauxite residue. *J. Clean. Prod.* 143, 224-230.

Koppelaar, R.H.E.M. and Weikard, H.P., 2013. Assessing phosphate rock depletion and phosphorus recycling options. *Glob. Environ. Chang.* 23(6), pp.1454-1466.

Kovács, T., Sas, Z., Jobbágy, V., Csordás, A., Szeiler, G. and Somlai, J., 2013. Radiological aspects of red mud disaster in Hungary. *Acta Geophysica.* 61(4), pp.1026-1037.

Krishna, P., Reddy, M.S. and Patnaik, S.K., 2005. Aspergillus tubingensis reduces the pH of the bauxite residue (red mud) amended soils. *Water. Air. Soil. Poll.* 167(1-4), pp.201-209.

Kruse, J., Abraham, M., Amelung, W., Baum, C., Bol, R., Kühn, O., Lewandowski, H., Niederberger, J., Oelmann, Y., Rüger, C. and Santner, J., 2015. Innovative methods in soil phosphorus research: A review. *J. Plant. Nutr. Soil. Sci.* 178(1), pp.43-88.

Kumar, S., Kumar, R., and Bandopadhyay, A., 2006. Innovative methodologies for the utilization of wastes from metallurgical and allied industries. *Resour. Conserv. Recy*. 48, 301–314.

Lalor, S. and Culleton, N., 2000. Managing Soil Phosphorus Levels on Intensive Dairy Farms.   Available: https://www.teagasc.ie/media/website/publications/2000/managing_soil_phosphorus_le vels.pdf [accessed 23.04.2019].

Lehoux, A.P., Lockwood, C.L., Mayes, W.M., Stewart, D.I., Mortimer, R.J., Gruiz, K. and Burke, I.T., 2013. Gypsum addition to soils contaminated by red mud: implications

for aluminium, arsenic, molybdenum and vanadium solubility. *Environ. Geochem. Hlth*. 35(5), pp.643-656.

Li, Y., Liu, C., Luan, Z., Peng, X., Zhu, C., Chen, Z., Zhang, Z., Fan, J. and Jia, Z., 2006. Phosphate removal from aqueous solutions using raw and activated red mud and fly ash. *J. Hazard. Mater.* 137(1), pp.374-383.

Liu Y, Lin C and Wu Y., (2007) Characterization of red mud derived from a combined Bayer process and bauxite calcination method. *J. Hazard. Mater.* 146:255–261.

Liu, X., Wang, Q., Deng, J., Zhang, Q., Sun, S. and Meng, J., 2010. Mineralogical and geochemical investigations of the Dajia Salento-type bauxite deposits, western Guangxi, China. *J. Geochem. Explor.* 105(3), pp.137-152.

Liu, Y., Naidu, R. and Ming, H., 2011. Red mud as an amendment for pollutants in solid and liquid phases. *Geoderma,* 163(1-2), pp.1-12.

Liu, W., Chen, X., Li, W., Yu, Y., Yan, K., 2014. Environmental assessment, management and utilization of red mud in China. *J. Clean. Prod.* 84, 606-610.

Lopez, E., Soto, B., Arias, M., Nunez, A., Rubinos, D. and Barral, M.T., 1998. Adsorbent properties of red mud and its use for wastewater treatment. *Water. Res.* 32(4), pp.1314-1322.

Lumley, R. ed., 2010. Fundamentals of aluminium metallurgy: production, processing and applications. Elsevier.

Lyklema, J., 1984. Points of zero charge in the presence of specific adsorption. *J. Colloid. Interf. Sci.* 99(1), pp.109-117.

McMahon, K., 2017 'Bauxite Residue Disposal Area Rehabilitation', ISCOBA conference November 2017, Hamburg, 02-05 Oct, Hamburg, Germany, available: http://icsoba.org/sites/default/files/2017papers/Bauxite%20Residue%20Papers/BR01%2

0-%20Bauxite%20Residue%20Disposal%20Area%20Rehabilitation.pdf   [accessed: 21.02.2018].

Manfroi, E.P., Cheriaf, M. and Rocha, J.C., 2014. Microstructure, mineralogy and environmental evaluation of cementitious composites produced with red mud waste. *Construct. Build. Mater.* 67, pp.29-36.

Martinez, J., Dabert, P., Barrington, S. and Burton, C., 2009. Livestock waste treatment systems for environmental quality, food safety, and sustainability. *Bioresource. Technol*. 100(22), pp.5527-5536.

Mayes, W.M., Burke, I.T., Gomes, H.I., Anton, A.D., Molnár, M., Feigl, V., Ujaczki, É., 2016. Advances in understanding environmental risks of red mud after the Ajka spill, Hungary. J. *Sustain. Metallurgy*. 2, 332-343.

Menzies, N.W., Fulton, I.M., Morrell, W.J., 2004. Seawater neutralization of alkaline bauxite residue and implications for revegetation. *J. Environ. Qual*. 33, 1877-1884.

McConchie, D., Clark, M. and Davies-McConchie, F., 2002, September. New strategies for the management of bauxite refinery residues (red mud). In Proceedings of the 6th international alumina quality workshop (Vol. 1, pp. 327-332).

McMahon, K., 2017. Bauxite Residue Disposal Area Rehabilitation, ISCOBA conference November 2017, Hamburg, 02-05 Oct, Hamburg, Germany.   Available: http://icsoba.org/sites/default/files/2017papers/Bauxite%20Residue%20Papers/BR01%2 0-%20Bauxite%20Residue%20Disposal%20Area%20Rehabilitation.pdf   [accessed: 21.02.2018].

Maynard, J.B., 2012. Geochemistry of sedimentary ore deposits. Springer Science & Business   Media.   Available: https://books.google.ie/books?hl=en&lr=&id=C04yBwAAQBAJ&oi=fnd&pg=PT11&d q=Maynard,+J.B.,+2012.+Geochemistry+of+sedimentary+ore+deposits.+Springer+Scie nce+%26+Business+Media.&ots=2Y95a0qX66&sig=er8mJG5IMuDIRPOZIn6ur_- AzJc&redir_esc=y#v=onepage&q=Maynard%2C%20J.B.%2C%202012.%20Geochemi

stry%20of%20sedimentary%20ore%20deposits.%20Springer%20Science%20%26%20
Business%20Media.&f=false [accessed 26.07.2018].

Minogue, D., French, P., Bolger, T. and Murphy, P.N.C., 2015. Characterisation of dairy soiled water in a survey of 60 Irish dairy farms. *Irish J. Agricultural and Food Res.* 54(1), 1-16.

Mohapatra BK, Mishra BK and Mishra CR, Studies on Metal Flow from Khondalite to Bauxite to Alumina and Rejects from an Alumina Refinery, India, in Light Metals 2012, ed. by Suarez CE. Springer, Cham, Switzerland (2012).

Mordberg, L.E., 1993. Patterns of distribution and behaviour of trace elements in bauxites. *Chem. Geol.* 107(3-4), pp.241-244.

Morel, A., Borjon-Piron, Y., Porto, R.L., Brousse, T. and Bélanger, D., 2016. Suitable conditions for the use of vanadium nitride as an electrode for electrochemical capacitor. J. *Electrochem. Soc*. 163, A1077-A1082.

Morse, G.K., Brett, S.W., Guy, J.A. and Lester, J.N., 1998. Review: phosphorus removal and recovery technologies. *Sci. Total. Environ.* 212(1), pp.69-81.

Moshi, A.O., Wild, A. and Greenland, D.J., 1974. Effect of organic matter on the charge and phosphate adsorption characteristics of Kikuyu red clay from Kenya. *Geoderma.* 11(4), pp.275-285.

Murnane, J.G., Brennan, R.B., Healy, M.G. and Fenton, O., 2016. Assessment of intermittently loaded woodchip and sand filters to treat dairy soiled water. *Water. Res.* 103, pp.408-415.

National Forest Inventory, 2012. National Forest Inventory. Available: https://www.agriculture.gov.ie/nfi/nfisecondcycle2012/nationalforestinventorypublications2012/ [accessed 23.04.2019].

Nättorp, A., Remmen, K. and Remy, C., 2017. Cost assessment of different routes for phosphorus recovery from wastewater using data from pilot and production plants. *Water. Sci. Technol.* 76(2), pp.413-424.

Neset, T.S.S. and Cordell, D., 2012. Global phosphorus scarcity: identifying synergies for a sustainable future. *J. Sci. Food. Agri.* 92(1), pp.2-6.

Nguyen QD, Boger DV, 1998. Application of rheology to solving tailings disposal problems. *Int. J. Miner. Process.* 54:217–233

Nikraz HR, Bodley AJ, Cooling DJ, Kong PYL, Soomro M., 2007. Comparison of physical properties between treated and untreated bauxite residue mud. *J. Mater. Civ. Eng.* 19:2–9.

Ochsenkühn-Petropulu, M., Lyberopulu, T. and Parissakis, G., 1994. Direct determination of landthanides, yttrium and scandium in bauxites and red mud from alumina production. *Anal. Chim. Acta.* 296(3), pp.305-313.

Palmer, S.J. and Frost, R.L., 2009. Characterisation of bauxite and seawater neutralised bauxite residue using XRD and vibrational spectroscopic techniques. *J. Mat. Sci.* 44(1), pp.55-63.

Peeters, A., 2015. Environmental impacts and future challenges of grasslands and grassland-based livestock production systems in Europe. Grasslands: A Global Resource Perspective. Army Printing Press, Lucknow, India, pp.365-390.

Penn, C.J., Bryant, R.B., Callahan, M.P. and McGrath, J.M., 2011. Use of industrial by-products to sorb and retain phosphorus. *Comm. Soil. Sci. Plant. Analysis.* 42(6), pp.633-644.

Penn, C., McGrath, J., Bowen, J. and Wilson, S., 2014. Phosphorus removal structures: A management option for legacy phosphorus. *J. Soil Water Conserv.* 69(2), 51A-56A.

Plunkett, M., Wall, D., Sheil, T. and Bolger, J., 2019. The Efficient Use of Phosphorus in Agricultural Soils. Available: https://www.teagasc.ie/media/website/crops/soil-and-soil-fertility/Efficient-Use-of-Phosphorus-In-Agriculture-Tech-Bulletin-No.-4.pdf [accessed 23.04.2019].

Poulin, É., Blais, J.F. and Mercier, G., 2008. Transformation of red mud from aluminium industry into a coagulant for wastewater treatment. *Hydrometallurgy.* 92(1), pp.16-25.

Power, G., Gräfe, M. and Klauber, C., 2011. Bauxite residue issues: I. Current management, disposal and storage practices. *Hydrometallurgy.* 108(1-2), pp.33-45.

Pratt, C., Parsons, S.A., Soares, A. and Martin, B.D., 2012. Biologically and chemically mediated adsorption and precipitation of phosphorus from wastewater. *Current. Opinion. Biotechnol. 23*(6), pp.890-896.

Qin, B. and Schneider, U., 2016. Catalytic use of elemental gallium for carbon–carbon bond formation. *J. Am. Chem. Soc* 138, 13119-13122.

Qu, Y., Li, H., Tian, W., Wang, X., Wang, X., Jia, X., Shi, B., Song, G. and Tang, Y., 2015. Leaching of valuable metals from red mud via batch and continuous processes by using fungi. *Min. Eng.* 81, pp.1-4.

Rai, S., Wasewar, K., Mukhopadhyay, J., Yoo, C.K. and Uslu, H., 2012. Neutralization and utilization of red mud for its better waste management. *World.* 6, p.5410.

Reddy KL., 2001. Principles of Engineering Metallurgy. Extraction of non-ferrousmetals. KK Gupta (Ed) ISBN: 81-224-0952-0, New Age International (P) Ltd., Daryaganj, New Delhi, India: Sarasgraphics, New Delhi, 3-35.

Richardson, A.E., 2005. Utilization of soil organic phosphorus by higher plants. *Organic Phosphorus in the Environment*, pp.165-184.

The River Basin Management Plan 2018-2021. Available: https://www.housing.gov.ie/sites/default/files/publications/files/rbmp_report_english_web_version_final_0.pdf [accessed 23.04.2014].

Ryu, H.D., Lim, C.S., Kang, M.K. and Lee, S.I., 2012. Evaluation of struvite obtained from semiconductor wastewater as a fertilizer in cultivating Chinese cabbage. *J. Hazard. Mater.* 221, pp.248-255.

Santona, L., Castaldi, P. and Melis, P., 2006. Evaluation of the interaction mechanisms between red muds and heavy metals. *J. Hazard. Mater.* 136(2), pp.324-329.

Statutory Instruments, 2017. European Union (Good Agricultural Practice for Protection of Waters) Regulations 2017. Available: http://www.irishstatutebook.ie/eli/2017/si/605/made/en/print [accessed 23.04.2019].

Stumm, W., 1992. Chemistry of the solid-water interface: processes at the mineral-water and particle-water interface in natural systems. John Wiley & Son Inc..

Talboys, P.J., Heppell, J., Roose, T., Healey, J.R., Jones, D.L. and Withers, P.J., 2016. Struvite: a slow-release fertiliser for sustainable phosphorus management?. *Plant. Soil.* 401(1-2), pp.109-123.

Teagasc, 2017. Agricultural Sustainability Support and Advisory Programme – ASSAP. Available: https://www.teagasc.ie/media/website/publications/2018/Agricultural-Sustainability-Support-Advisory-Programme-.pdf [accessed 23.04.2019].

Tong, W., Zhang, Y., Zhen, Z., Yu, L., An, Q., Zhang, Z., Lv, F. and Chu, P.K., 2013. Effects of surface properties of red mud on interactions with Escherichia coli. *J. Mater. Res.* 28(17), pp.2332-2338.

Ujaczki, É., Feigl, V., Molnár, M., Cusack, P., Curtin, T., Courtney, R., O'Donoghue, L., Davris, P., Hugi, C., Evangelou, M.W. and Balomenos, E., 2018. Re-using bauxite residues: benefits beyond (critical raw) material recovery. *J. Chem. Technol. Biotechnol.* 93(9), pp.2498-2510.

U.S. Geological Survey., 2012. Mineral commodity summaries January 2012, Phosphorus, [online], available: http://minerals.usgs.gov/minerals/pubs/commodity/phosphate rock/ [accessed 02.03.2016].

United States Geological Survey Website (USGS). Commodity Statisctics and Information (2016). Available: http://minerals.usgs.gov/minerals/pubs/commodity/ [accessed 30.01.2018].

Wang S, Ang HM and Tadé MO., (2008). Novel applications of red mud as coagulant, adsorbent and catalyst for environmentally benign processes. *Chemosphere.* 72:1621–1635.

Wang, Q., Deng, J., Zhang, Q., Liu, H., Liu, X., Wan, L., Li, N., Wang, Y., Jiang, C. and Feng, Y., 2011. Orebody vertical structure and implications for ore-forming processes in the Xinxu bauxite deposit, Western Guangxi, China. *Ore Geology Reviews.* 39(4), pp.230-244.

Wang, B., Lehmann, J., Hanley, K., Hestrin, R., Enders, A., 2015. Adsorption and desorption of ammonium by maple wood biochar as a function of oxidation and pH. *Chemosphere.* 138,120-126.

Weng, L., Van Riemsdijk, W.H. and Hiemstra, T., 2012. Factors controlling phosphate interaction with iron oxides. *J. Environ. Qual.* 41(3), pp.628-635.

Whittington, B.I., 1996. The chemistry of CaO and Ca (OH) 2 relating to the Bayer process. *Hydrometallurgy.* 43(1-3), pp.13-35.

Withers, P.J.A. and Haygarth, P.M., 2007. Agriculture, phosphorus and eutrophication: a European perspective. *Soil. Use. Manage.* 23, pp.1-4.

Xue, S., Zhu, F., Kong, X., Wu, C., Huang, L., Huang, N. and Hartley, W., 2016. A review of the characterization and revegetation of bauxite residues (Red mud). *Environ. Sci. Poll. Res.* 23(2), pp.1120-1132.

Xu, C., Kynický, J., Smith, M.P., Kopriva, A., Brtnický, M., Urubek, T., Yang, Y., Zhao, Z., He, C. and Song, W., 2017. Origin of heavy rare earth mineralization in South China. *Nature Communications.* 8, p.14598.

Xue, S., Zhu, F., Kong, X., Wu, C., Huang, L., Huang, N. and Hartley, W., 2016. A review of the characterization and revegetation of bauxite residues (Red mud). *Environ. Sci. Poll. Res.* 23(2), pp.1120-1132.

Yang, B., Huang, K., Sun, D. and Zhang, Y., 2017. Mapping the scientific research on non-point source pollution: a bibliometric analysis. *Environ. Sci. Poll. Res.* 24(5), pp.4352-4366.

Ye, J., Cong, X., Zhang, P., Zeng, G., Hoffmann, E., Liu, Y., Wu, Y., Zhang, H., Fang, W. and Hahn, H.H., 2016. Application of acid-activated Bauxsol for wastewater treatment with high phosphate concentration: Characterization, adsorption optimization, and desorption behaviours. *J. Environ. Manage.* 167, pp.1-7.

Zhang, K.Y., Hu, H.P., Zhang, L.J. and Chen, Q.Y., 2008. Surface charge properties of red mud particles generated from Chinese diaspore bauxite. *Transactions. Nonferrous. Metals. Society. China.* 18(5), pp.1285-1289.

Zhao, Y., Wang, J., Luan, Z., Peng, X., Liang, Z. and Shi, L., 2009. Removal of phosphate from aqueous solution by red mud using a factorial design. *J. Hazard. Mater.* 165(1), pp.1193-1199.

Zhou, Y.F. and Haynes, R.J., 2010. Sorption of heavy metals by inorganic and organic components of solid wastes: significance to use of wastes as low-cost adsorbents and immobilizing agents. *Critical. Reviews. Environ. Sci. Technol.* 40(11), pp.909-977.

Zhu, C., Luan, Z., Wang, Y. and Shan, X., 2007. Removal of cadmium from aqueous solutions by adsorption on granular red mud (GRM). *Separation. Purification. Technol.* 57(1), pp.161-169.

Chapter 3

An Evaluation of the General Composition and Critical Raw Material Content of Bauxite Residue in a Storage Area over a Twelve-year Period

Overview

The aim of this chapter was to investigate the general composition of fine fraction bauxite residue samples in storage over a twelve-year period in terms of its physico-chemical, elemental and mineralogical composition. This would allow for the determination of any possible variation within the bauxite residue whilst in storage, which could affect potential re-use as a secondary source of critical raw materials or use as an adsorbent for the removal of phosphorus.

This study has been published in the Journal of Cleaner Production (Cusack, P.B., Courtney, R., Healy, M.G., O'Donoghue, L.M. and Ujaczki, É., 2019. An evaluation of the general composition and critical raw material content of bauxite residue in a storage area over a twelve-year period. Journal of Cleaner Production, 208, pp.393-401. DOI Link: https://doi.org/10.1016/j.jclepro.2018.10.083). Due to the complexity and associated risks of obtaining the bauxite residue samples over a twelve-year period from the main refinery, samples were taken by workers at the alumina refinery and provided to Patricia B. Cusack and Dr. Éva Ujaczki who shared in the characterisation and determination of critical raw material content of these samples. Patricia B. Cusack is the primary author main contributor to the experimental design and set-up of this study and publication. Dr. Ronan Courtney and Dr. Mark G. Healy were the main contributors to editing of this manuscript and also contributed to the experimental design and set-up, with inputs also from Dr. Éva Ujaczki. Dr. Lisa M. O' Donoghue was also listed as an author on this publication as this study was part of the overall Alsource project. The published paper is included in Appendix A.

3.1 Introduction

Bauxite residue (red mud) is the by-product generated during the extraction of alumina from bauxite ore using the Bayer Process (Kirwan et al., 2013), and is currently being produced at a global rate of 150 Mt per annum, adding to the 3 Bt already in storage worldwide (Evans 2016). Currently, less than 2 % of the bauxite residue generated annually is being re-used (Ujaczki et al., 2018), with the remaining ~ 98 % going into bauxite residue disposal areas (BRDAs) (Burke et al., 2013). The average cost of disposing and managing of bauxite residue in storage is 1-2 % of the alumina price for the alumina refinery (Tsakiridis et al., 2004).

Current best practice guidelines for the storage of bauxite residue is to use dry-stacking, a method which involves the thickening of the bauxite residue slurry from the Bayer process, using a filter press or vacuum filtration (depending on the refinery), before being spread in layers in the BRDA (Power et al., 2011; Evans 2016). Depending on the nature of the bauxite ore used, some refineries operate a separation technique (Evans 2016), which allows the bauxite residue to be separated into two main size fractions: a fine fraction (particle size <100 µm) and a coarse fraction (particle size > 150 µm) (IAI 2015; Jones et al., 2012). Bauxite residue is typically characterised as being highly alkaline, saline and composed of mainly fine particles comprised of a wide range of metal(loid)s and minerals (Gräfe et al., 2009). This poses challenges in the long-term management of BRDAs in terms of protecting the surrounding environment (Higgins et al., 2017; Kong et al., 2017), due to the high alkalinity, increased risk of dust pollution (due to the fine particles), and leaching of trace elements (Wang et al., 2015; Kong et al., 2017). The disposal conditions and management of residue in a BRDA is dependent on many factors such as location, climate, engagement with local communities and stakeholders (IAI 2015) and involves licencing permits from regulatory authorities (such as the Environmental Protection Agency). For example, European operators must meet the requirements according to the European List of Waste and Directive (EU Communities 1999, 2002). As a result of this, some refineries implement neutralisation techniques prior to disposal, such as carbon dioxide (CO_2) sparging of residues (Cooling 2007) or post disposal through the use of atmospheric carbonation (mud farming) with amphirolling (Evans 2016) in the BRDA, which helps in the neutralisation, dewatering and compaction of the bauxite residue (Evans 2016; Gomes et al., 2016; Higgins et al.,

2016; Zhu et al., 2016), reducing both alkalinity and moisture content, which are two limitations to the re-use of bauxite (Evans 2016).

Traditionally, the re-use of bauxite residue has focussed on construction applications such as cementitious application (Pontikes and Angelopoulos 2013; Nikbin et al., 2018). Some other re-use options for bauxite residue have included polymers (Hertel et al., 2016), ceramics (Pontikes et al., 2009) and catalysts (Wang et al., 2008); adsorbents for wastewater treatment (Bhatnagar et al., 2011), particularly for the removal of arsenic (As) (Arco-Lázaro et al., 2018), chromium (Cr) (Dursun et al., 2008), nickel (Ni) (Hannachi et al., 2010), copper (Cu) (Atasoy and Bilgic 2018), cadmium (Cd) (Ha et al., 2017) and phosphorus (P) (Cusack et al., 2018), as well as applications as potential soil ameliorants (Ujaczki et al., 2015). More recently and due to the demand of critical raw materials (CRMs), particularly the rare earth elements (REEs), studies have examined the potential of bauxite residue as a secondary source of these materials and their potential economic value (Gomes et al., 2016; Xue et al., 2016; Ujaczki et al., 2017).

Within the European Union (EU), the 'Raw Materials Initiative' ensures that Europe secures and sustains an affordable supply of CRMs which are identified as being of high economic importance and having a risk to their supply (EU COM/2017/0490). The list of 27 CRMs features elemental groups and single elements, including platinum group metals (PGM) and REEs (EU COM/2017/0490). The REEs are divided into light REE [lanthanum (La), cerium (Ce), praseodymium (Pr), neodymium (Nd), samarium (Sm), europium (Eu)] and heavy REE [gadolinium (Gd), terbium (Tb), dysprodium (Dy), holmium (Ho), erbium (Er), thulium (Tm), ytterbium (Yb), lutetium (Lu), including yttrium (Y)] (Xu et al., 2017) plus scandium (Sc) (Binnemans et al., 2018). Depending on the origin of the bauxite residue generated, it may be a potentially valuable source of CRM and other elements e.g. REEs, Sc, V, Ga, and titanium (Ti) (Liu and Naidu 2014). Also included in the 2017 CRM list is P and phosphate rock, which are also of particular interest, as bauxite residue has been previously identified as having a high P retention capacity (Grace et al., 2015, 2016; Cusack et al., 2018) due to its high aluminium (Al) and iron (Fe) oxide content (IAI 2015), making it a possible resource in the removal and recovery of P from aqueous solutions (Grace et al., 2015; Cusack et al., 2018).

Although bauxite residues are typically similar in composition, properties can vary between refineries and this is attributed to the type of ore used, as well as different process parameters, such as temperature, pressure and concentrations of caustic soda (NaOH), slaked lime ($Ca(OH)_2$) and other additives used in the Bayer process (Gräfe et al., 2009; Gräfe et al., 2011). This indicates that re-use options should be refinery-specific (Balomenos et al., 2017). A further potential limitation, is that bauxite residue composition, such as pH and bulk density, may change over time in storage (Kong et al., 2017a; Zhu et al., (2016a,b), which greatly influences the possibility of reusing bauxite residue.

To date, no study has investigated the CRM content variability in bauxite residue stored within one specific BRDA. Therefore, the objectives of this study were to: (1) characterise the physico-chemical, elemental and mineralogical composition of the dominant fraction (fine fraction) bauxite residue in storage over a twelve-year period, and to determine if there is any variation over the time spent in storage, which could affect possible re-use of the bauxite residue (2) create an inventory of economically interesting elements in bauxite residue over the storage period, and (3) calculate the financial value of economically interesting elements present in the bauxite residue.

3.2 Materials and Methods

3.2.1 Site Description and Sample Collection

Bauxite residue was obtained from a European refinery, who operated a separation technique to isolate the fine (particle sizes <100 µm) and coarse (particle sizes >150 µm) fractions of bauxite residue before disposal (IAI 2015), in an approximate ratio of 9:1 (fine: coarse). Bauxite residue was sampled to a depth of 30 cm and the bulk samples were stored in 1 L containers, returned to the laboratory, and dried at 105°C for 24 hr. Once dry, the samples were pulverised using a mortar and pestle and sieved to a particle size < 2 mm. In this paper, the age of the samples will be described (Table 3.1) relative to the sample collection time (2016).

Table 3.1 Sample information regarding the year of production for each of the bauxite residue samples over a twelve-year period. The sample code for each bauxite residue sample is also included in the table.

Sample Code	Sample Description	Year of Disposal
BR 12	Bauxite Residue	2004
BR 11	Bauxite Residue	2005
BR 10	Bauxite Residue	2006
BR 9	Bauxite Residue	2007
BR 8	Bauxite Residue	2008
BR 7	Bauxite Residue	2009
BR 6	Bauxite Residue	2010
BR 5	Bauxite Residue	2011
BR 4	Bauxite Residue	2012
BR 3	Bauxite Residue	2013
BR 2	Bauxite Residue	2014
BR 1	Bauxite Residue	2015

3.2.2 Characterisation Study

3.2.2.1 Physico-Chemical Composition

The bauxite residue samples were characterised (n=3) for their physical, chemical, elemental and mineralogical properties (Figure 3.1). The pH and electrical conductivity (EC) were measured using a 5 g sample in an aqueous extract, using a 1:5 ratio (solid: liquid) (Courtney and Harrington, 2010). The bulk density (ρ_b) was determined after Blake (1965), the effective particle size analysis (PSA) was determined on particle sizes < 53 µm using optical laser diffraction on a Malvern Zetasizer 3000HS® (Malvern, United Kingdom) with online autotitrator and a Horiba LA-920, and reported at specific cumulative % (10, 50 and 90 %).
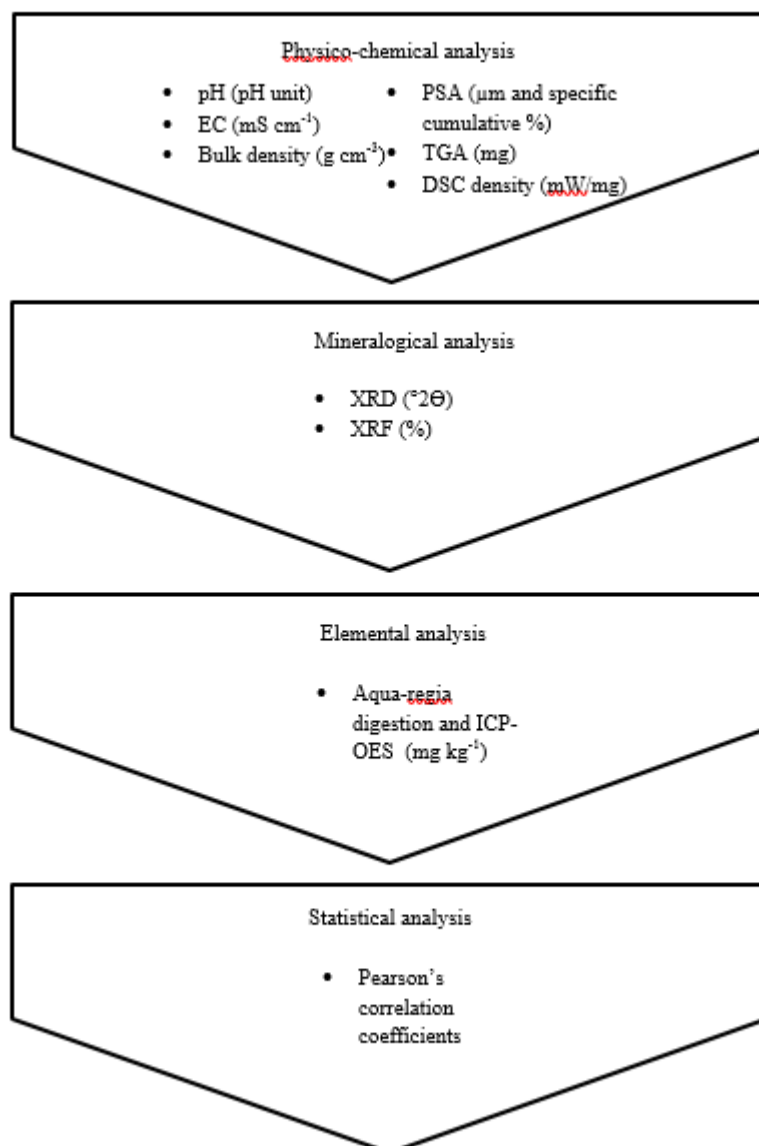
Figure 3.1 Flow chart illustrating the experimental analysis carried out on the bauxite residue samples obtained. Once obtained from the BRDA, the bauxite residue was analysed for its main physico-chemical analysis (pH, EC, bulk density, PSA, TGA and DSC), mineralogical analysis (XRD and XRF), and elemental analysis (measure using ICP-OES following aqua-regia digestion). Once all data was obtained, statistical analysis was carried out using Pearson's correlation coefficients.

Thermogravimetric analysis (TGA) was carried out to identify any change in mass over time with temperature, and change in heat flow over time with temperature was analysed using differential scanning calorimetry (DSC). TGA and DSC were carried performed using a Labsys TG (DSC/TGA 1600) in a nitrogen (N) atmosphere at a temperature range

of 30 °C to 1000 °C at a heating rate of 10 °C min^{-1} (Borra et al., 2015). Due to cost limitations, only six samples were analysed (BR12, BR10, BR8, BR6, BR4 and BR2).

3.2.2.2 Mineralogical Composition

Mineralogical detection was carried out on 1 g powdered samples using X-ray diffraction (XRD) on a Philips X'Pert PRO MPD® (California, USA) at 40 kV, 40 mA, 25 °C by Cu X-ray tube (Kα-radiation). The patterns were collected in the angular range from 5 to 80 ° (2ɵ) with a step-size of 0.008 ° (2ɵ) (Castaldi et al., 2011), whilst surface morphology and elemental detection were carried out using scanning electron microscopy (SEM) and energy-dispersive X-ray spectroscopy (EDS) on a Hitachi SU-70 (Berkshire, UK). X-ray fluorescence (XRF) analysis was carried out onsite at the refinery using a Panalytical Axios XRF (Malvern, UK).

3.2.2.3 Elemental Composition

Chemical analysis of minor elements was performed after aqua regia digestion (HCl: HNO_3) with a solid to liquid ration of 1:10 in a Multiwave 3000 (Rotor 8XF100) type microwave digestion system at 200 °C 1.25 MPa. After digestion, the solutions were filtered through 0.45 μm PVDF syringe filters and diluted in 1 M HNO_3 for the analysis (Ujaczki et al., 2017). The metal analysis was carried out using an Agilent Technologies 5100 inductively coupled plasma optical emission spectrometer (ICP-OES). The calibration curve was constructed using standard solutions of 100, 50, 10, 5 and 1 g L^{-1} multi-element standard (Inorganic Ventures, Ireland) and 5, 2.5, 0.5, 0.25 and 0.05 g L^{-1} REE standard (Inorganic Ventures, Ireland). The 1M HNO_3 solution was also used for the dilutions of the standard solutions and as a calibration blank. For the ICP-OES analysis, the following analytical lines (in nm) were used for the calculations of each of the elements: Ce 418.659, 446.021; cobalt (Co) 228.615, 230.786; Dy 353.171; Er 349.910, 369.265; Eu 397.197, 412.972, 420.504; Ga 294.363; Gd 335.048, 336.224; Ho 339.895, 345.600, 389.094; indium (In) 230.606, 352.609; La 333.749, 379.477, 408.671; Lu 261.541, 307.760; molybdenum (Mo) 202.032, 203.846, 204.598; Nd 401.224, 406.108, 410.945; Pr 390.843, 417.939; Sc 335.372, 361.383, 363.074; Sm 359.259, 360.949; Tb 350.914,367.636; Tm 313.125, 342.508; Y 360.074, 371.029, 377.433; Yb 289.138, 328.937, 369.419; V 268.796, 292.401, 311.070 (Bridger and Knowles, 2000).

3.2.3 Statistical Analysis

Pearson's correlation coefficients were used to determine any relationships between age of sample and sample properties (pH, EC, bulk density, particle size, mineralogical composition and elemental composition), using IBM SPSS Statistics 24.

3.3 Results
3.3.1 Physico-Chemical Composition

The pH of the bauxite residue (Table 3.2) ranged from 10.0 ± 0.1 to 12.0 ± 0.02 over the twelve-year period, with the ten-year-old sample (BR10) having the highest value. The EC (Table 3.2) of the bauxite residue ranged from 0.4 ± 0.01 to 3.3 ± 0.2 mS cm^{-1}, with again, the highest being for BR10. Small variation in the moisture content (Table 3.2) for the each of the bauxite residues was recorded. The bulk density (Table 3.2) for the bauxite residue ranged from 1.2 ± 0.1 to 1.5 ± 0.02 g cm^{-3}.

The bauxite residue had a high composition of fine particles, which ranged from 0.6 ± 0.01 to 12.7 ± 2.3 µm (Table 3.2). There was some agglomerate formation evident in all samples, as seen in the accumulation of finer particles in the images captured by SEM (Figure B1, B2, B3 in Appendix B). The medium value, d_{50}, of the particle size distribution for bauxite residues ranged from 2.2 ± 0.1µm (BR1) to 4.3 ± 0.4 µm (BR9). Ninety percent of the distribution (d_{90}) was under 12.7 ± 2.7 µm and 10 % (d_{10}) was under 0.5 ± 0.01 µm (Table 3.2). Iron, Al, sodium (Na), calcium (Ca), titanium (Ti), and silicon (Si) were the main elements present in all the bauxite residue samples (Figure B4). TGA curves showed weight loss between 300 and 975 °C for all the bauxite residues (Figures 3.2 and B5). However, sample BR12 (from 2014) had a larger temperature range over which weight loss occurred (between 150 and 975 °C).

Table 3.2 Physico-chemical composition of the bauxite residue mud over a twelve-year storage period, inclusive of pH, EC, moisture content, bulk density and particle size distribution.

Sample	pH	EC (mS cm^{-1})	Moisture content (%)	Bulk density (g cm^{-3})	d_{10} (μm)[a]	d_{50} (μm)[b]	d_{90} (μm)[c]
BR 12	11.6 ± 0.02	1.0 ± 0.01	26.8 ± 0.7	1.4 ± 0.04	0.7 ± 0.1	2.6 ± 0.1	7.0 ± 1.2
BR 11	10.8 ± 0.1	0.4 ± 0.02	28.2 ± 0.7	1.3 ± 0.03	0.9 ± 0.1	3.5 ± 0.5	9.6 ± 0.5
BR 10	12.0 ± 0.02	3.3 ± 0.2	26.8 ± 0.1	1.4 ± 0.1	1.4 ± 0.1	4.0 ± 0.3	12.3 ± 1.6
BR 9	10.0 ± 0.1	0.4 ± 0.01	24.3 ± 0.3	1.1 ± 0.1	1.0 ± 0.1	4.3 ± 0.4	12.4 ± 1.0
BR 8	11.4 ± 0.1	1.0 ± 0.1	27.2 ± 0.3	1.4 ± 0.1	0.8 ± 0.1	2.6 ± 0.1	6.8 ± 0.2
BR 7	10.4 ± 0.02	0.5 ± 0.01	22.3 ± 0.6	1.4 ± 0.04	0.9 ± 0.2	3.2 ± 0.5	12.7 ± 2.7
BR 6	10.7 ± 0.03	0.5 ± 0.03	25.8 ± 1.0	1.3 ± 0.04	0.7 ± 0.1	2.6 ± 0.01	6.7 ± 0.2
BR 5	10.3 ± 0.1	0.4 ± 0.03	22.0 ± 0.5	1.2 ± 0.1	0.6 ± 0.01	2.4 ± 0.04	7.9 ± 1.1
BR 4	11.5 ± 0.1	0.9 ± 0.02	31.1 ± 0.5	1.3 ± 0.1	1.2 ± 0.1	3.8 ± 0.6	12.70 ± 2.3
BR 3	10.6 ± 0.02	0.5 ± 0.01	23.8 ± 0.3	1.3 ± 0.03	0.8 ± 0.2	2.6 ± 0.3	8.3 ± 1.6
BR 2	11.2 ± 0.01	0.9 ± 0.02	28.1 ± 1.9	1.3 ± 0.1	1.1 ± 0.02	3.2 ± 0.02	9.7 ± 0.9
BR 1	10.3 ± 0.1	0.7 ± 0.03	25.0 ± 2.7	1.5 ± 0.02	0.5 ± 0.01	2.2 ± 0.1	6.7 ± 0.6

[a]d_{10} (μm) = the size of particles at 10% of the total particle distribution.

[b]d_{50} (μm) = the median; the size of particles at 50% of the total particle distribution.

[c]d_{90} (μm) = the size of particles at 90% of the total particle distribution.

Figure 3.2 TGA (descending) / DSC (ascending) curve obtained for bauxite residue (a) BR12 (2004) and (b) BR2 (2014). Remaining TGA / DSC graphs found in Figure B5 in Appendix B. The TGA curves showed weight loss between 300 and 975 °C for all the bauxite residues examined.

3.3.2 Mineralogical Composition

The main mineralogical composition of the bauxite residue detected by XRD included haematite (Fe_2O_3), goethite ($FeO(OH)$), perovskite ($CaTiO_3$), rutile (TiO_2), gibbsite $Al(OH)_3$, sodalite ($Na_8(Al_6Si_6O_{24})Cl_2$) and cancrinite ($Na_6Ca_2(CO_3)$) (Figure B6 and B7). Sample BR9 had an extra rutile peak at position 27.459 °2Θ and no sodalite peak at position 14 °2Θ; samples BR1 to BR6 had similar patterns, but with less intense peaks and sodalite peaks at position 14 °2Θ (Figure B6). Sample BR1 had one peak of boehmite ($AlO(OH)$) at position 13.9 °2Θ and gibbsite at position 18.5 °2Θ (Figure B6). Sample BR1 also had an unidentified peak at position 47 °2Θ (Figure B6).

XRF analysis carried out on the bauxite residue samples (Table 3.3) reflected the main mineralogical composition detected by XRD analysis. The dominant oxides found were Fe_2O (ranging from 40.1 ± 1.40 to 47.5 ± 2.0 %) and Al_2O_3 (14.8 ± 1.5 to 17.8 ± 0.73 %). SiO_2 (7.20 ± 1.0 to 10.9 ± 0.47 %), TiO_2 (8.62 ± 0.71 to 10.3 ± 0.95 %) and CaO (5.70 ± 0.66 to 6.1 ± 1.0%) were also present (Table 3.3).

Table 3.3 Main mineralogical composition (%) of the bauxite residue samples taken from the BRDA ranging from one to eleven[*] years old, as determined by XRF.

Code	Al_2O_3	Fe_2O	SiO_2	TiO_2	CaO
BR 11	17.0±0.61	42.0±1.20	9.82±0.32	9.41±0.34	6.03±0.79
BR 10	17.1±0.4	41.5±0.96	10.2±0.56	9.52±0.6	6.03±0.49
BR 9	17.8±0.73	40.1±1.40	10.9±0.47	8.97±0.51	6.04±0.4
BR 8	16.8±0.58	41.8±1.40	9.89±0.39	9.41±0.61	5.97±0.49
BR 7	14.8±1.5	47.5±2.0	7.20±1.0	10.3±0.95	6.1±1.0
BR 6	16.2±0.54	45.9±2.10	8.0±0.57	9.54±0.78	5.70±0.66
BR 5	16.2±0.66	44.4±1.30	9.35±0.60	8.62±0.71	5.75±0.53
BR 4	16.5±0.65	43.3±1.20	9.38±0.53	8.91±0.53	6.21±0.35
BR 3	15.8±0.45	44.3±1.90	8.85±0.47	9.18±0.62	6.34±0.35
BR 2	16.0±0.71	46.6±1.80	8.95±0.70	8.21±0.38	5.0±0.40
BR 1	16.2±0.6	46.8±1.61	8.76±0.48	8.33±0.56	4.69±0.43

[*]XRF data was not obtained from the alumina refinery for the twelve-year-old sample, BR12.

3.3.3 Elements of Economic Importance in Bauxite Residue

An extensive inventory of CRMs and further elements of economic importance were developed using microwave-assisted aqua regia digestion, with subsequent ICP-OES analysis (Table 3.4). Overall, no trend was noted in the elemental content between the oldest and newest bauxite residue in the BRDA. However, In, Mo, Ce, Nd, Dy and Er were present in smaller amounts in the oldest samples compared to the fresh sample. Terbium (Tb), Tm and Ho were not detected in the bauxite residue.

Table 3.4 CRM composition (in mg kg^{-1}) of the eleven[*] bauxite residue samples, taken from the BRDA, as detected on ICP-OES following aqua regia digestion.

Element	BR 12	BR 11	BR 10	BR 9	BR 8	BR 7	BR 6	BR 5	BR 4	BR 3	BR 2
Dy	3.6 ± 0.02	5.4 ± 0.01	7.19 ± 0.01	5.39 ± 0.001	5.4 ± 0.04	5.39 ± 0.01	5.4 ± 0.01	5.38 ± 0.02	4.51 ± 1.3	7.2 ± 0.002	5.4 ± 0.02
Er	4.8 ± 0.5	5.4 ± 0.01	5.7 ± 0.5	4.94 ± 0.6	5.4 ± 0.04	5.39 ± 0.01	4.49 ± 0.01	5.38 ± 0.01	4.05± 0.6	5.4 ± 0.001	5.4 ± 0.02
Lu	8.39 ± 0.5	7.8 ± 0.5	8.09 ± 0.01	7.49 ± 0.5	8.1 ± 0.05	7.63 ± 0.6	8.1 ± 0.02	8.37 ± 0.5	7.66±0.7	8.1 ± 0.002	8.09 ± 0.03
Y	35.6 ± 3.2	39.8 ± 1.2	44.4 ± 1.5	41.9 ± 1.5	42 ± 0.4	39.5 ± 0.04	33.4 ± 0.4	41 ± 2.0	36.9± 1.4	47.4 ± 1.2	39.3 ± 0.5
Yb	8.39 ± 0.6	8.8 ± 0.3	9.39 ± 0.3	8.79 ± 0.7	9.4 ± 0.3	8.68 ± 0.4	8.2 ± 0.4	8.97 ± 0.9	8.11± 0.4	9.6 ± 0.002	8.71 ± 0.4
Ce	126 ± 10.1	126 ± 3.5	156 ± 2.2	136 ± 7.6	157 ± 2.2	128 ± 3.3	146 ± 6.7	200 ± 8.4	102± 3.5	147 ± 4.2	139 ± 6.8
Eu	2.40 ± 0.01	2.40 ± 0.01	2.40 ± 0.005	2.40 ± 0.01	2.40 ± 0.02	2.39 ± 0.003	2.40 ± 0.01	3.59 ± 0.01	2.40± 0.01	2.40 ± 0.001	2.40 ± 0.005
Gd	6.75 ± 0.6	6.60 ± 0.5	7.64 ± 0.6	7.63 ± 0.6	9.30 ± 0.6	7.18 ± 1.3	6.75 ± 0.6	8.98 ± 0.02	5.41± 0.02	9 ± 0.002	6.73 ± 0.6
La	91.3 ± 8.6	88.2 ± 3.2	108 ± 2.3	94.1 ± 2.7	106.4 ±1.0	89.2 ± 0.9	104 ± 3.5	134 ± 4.4	68.8± 4.0	98.2 ± 2.1	91± 2.4
Nd	80.1 ± 7.4	77.2 ± 5.3	93.9 ± 6.5	84.7 ± 1.3	98 ± 5.3	85.6 ± 8.6	88.9 ± 8.6	118 ± 4.4	64.6± 4.0	93 ± 2.2	94.3 ± 11.3
Pr	41.1 ± 3.5	42.9 ± 4.2	47.7 ± 3.3	42.5 ± 3.1	50.1 ± 1.6	40.8 ± 1.9	45 ± 2.7	56.2 ± 5.3	34.7± 3.3	45 ± 0.9	42.3 ± 1.1
Sc	50.2 ± 4.1	50.4 ± 1.6	60.2 ± 2.2	56.1 ± 2.7	54.2 ± 0.9	55.7 ± 1.3	45.4 ± 0.2	56 ± 4.2	42.9± 2.3	49 ± 1.3	45.6 ± 4.3
Sm	19.3 ± 0.7	20.7 ± 1.8	21 ± 2.2	21.6 ± 0.9	21.6 ± 0.8	18.4 ± 1.9	21.6 ± 0.9	25.1 ± 0.05	18± 1.2	21 ± 1.0	20.3 ± 2.0

Co	8.69 ± 0.5	7.64 ± 0.6	7.79 ± 0.5	6.73 ± 0.6	8.10 ± 0.05	7.63 ± 0.6	6.6 ± 0.5	8.67 ± 0.5	7.21 ± 0.02	8.4 ± 0.5	7.49 ± 0.6
Ga	107 ± 8.5	112 ± 2.3	102 ± 0.7	114 ± 5.2	98.6 ± 0.2	113 ± 3.8	106 ± 2.7	114 ± 5.1	99.5 ± 1.8	114 ± 1.9	94.4 ± 2.7
In	30.1 ± 1.8	34.6 ± 0.7	31.5 ± 1.5	32.1 ± 2.7	36.9 ± 0.9	30.5 ± 1.3	29.2 ± 2	33.6 ± 0.7	28.4 ± 0.7	34.5 ± 7.2	36.4 ± 4.3
Mo	3.14 ± 0.6	4.49 ± 0.01	4.04 ± 0.6	4.95 ± 0.6	4.48 ±0.004	4.95 ± 0.6	4.49 ± 0.01	4.48 ± 0.01	4.94 ± 1.9	4.8 ± 0.5	4.48± 0.01
V	593 ± 60.6	419 ± 8.2	596 ± 19.8	439 ± 41.1	491 ± 20.3	445 ± 41.2	484 ± 48.2	600 ± 24.3	401 ± 41.2	571 ± 13.3	573 ± 41.1

[*]The CRM composition was not determined for the fresh sample of bauxite residue, BR1.

3.4 Discussion

3.4.1 Characterisation of Bauxite Residue

Bauxite residue typically has a pH >10 (Goloran et al., 2013) and an EC ranging from 1.4 to 28.4 mS cm^{-1} (Gräfe et al., 2011). The high pH is attributed to the presence of alkaline anions such as hydroxides (OH$^-$), carbonate or bicarbonates (CO$_3^{2-}$ / HCO$_3^-$), aluminates or aluminium hydroxides (Al(OH)$_4^-$ / Al(OH)$_3$), and di/trihydrogen orthosilicates (H$_2$SiO$_4^{2-}$ / H$_3$SiO$_4^-$) introduced and formed during the Bayer process (Gräfe et al., 2011). At the end of the Bayer process, prior to disposal, residue undergoes a repeated washing stage. However, the bauxite residue remains highly alkaline due to the alkalinity being in the form of slow dissolving solid phases (Gräfe et al., 2011).

Depending on the refinery and the advances in residue management steps employed, the pH may be further reduced through practices such as atmospheric carbonation (mud farming) (Clohessy 2015; Evans 2016), seawater disposal (Menzies et al., 2009), application of spent acid (Kirwan et al., 2013), phosphogypsum (Xue et al., 2018), or by the addition of an acidic gas such as CO$_2$ or SO$_2$ (Xue et al., 2016). Consequently, surface pH values for residues may vary between refineries and within BRDAs.

The bauxite residue examined in this study showed variation in terms of both the pH and the EC ($p < 0.01$) (Table 3.2). Whilst the pH and EC did decrease across all the bauxite residue samples examined in this study (Table 3.2), this was attributed to different causes. The reduced pH value of the fresh bauxite residue examined (BR1) in this study (Table 3.2) is as a result of the atmospheric carbonation technique, mud farming, which can effectively decrease alkalinity (Clohessy 2015; McMahon 2017). This helps in removing the alkalinity limitation/barrier to the reutilisation of the bauxite residue (Evans 2016) and has been shown to successfully decrease the pH of fresh bauxite residue ($\sim$ 13.5) to below < 11.5 within seven days (Clohessy 2015). The mud farming technique sequesters CO$_2$ from the atmosphere, allowing for the accelerated carbonation of the bauxite residue (IAI 2015; Evans 2016). Due to this process, the free OH$^-$ present in the bauxite residue is neutralised due to the carbonation of the CO$_2$ present in the surrounding atmosphere (air), resulting in the formation of carbonates, therefore creating a buffering effect, which results in a drop in pH (Han et al., 2017).

Natural weathering processes may play an important role in the improvement of the physico-chemical composition of bauxite residue in storage (Zhu et al., 2018). The reduction observed in the pH of the older samples (Table 3.2) is as a result of the natural ageing and weathering of the bauxite residue in storage. Evidence of the natural weathering decreasing the pH was shown by Khaitan et al., (2010), who reported a pH of 10.5 for 14-year-old bauxite residue and 9.5 for 35-year-old bauxite residue, with the decreases attributed to the slow carbonation from atmospheric CO_2. Zhu et al., (2016a,b) also measured a decrease in residue pH from 10.98 to 9.45 in stored bauxite residue exposed to natural weathering processes. Similar to pH, EC usually decreases with time in the storage area due to weathering (Zhu et al., 2016a,b; Kong et al., 2017a). Rainfall events allow the soluble alkaline minerals such as sodalite and calcite, which result in a buffering effect for both pH and salinity (EC) (Santini and Fey, 2013).

The thermal analysis (TGA/DSC) indicated an overall weight loss occurring between 300 and 975 °C for all the bauxite residue samples examined. Previous work has shown weight loss between temperature ranges of 300 and 600 °C (attributed to the decomposition of hydroxides in different stages), 300 and 400 °C (as a result of the decomposition of diaspora), and between 600 and 800 °C (due to the decomposition of calcium carbonate) (Agatzini-Leonardou et al., 2008), all dominant minerals in bauxite residue. There were numerous endothermic peaks observed on the DSC curve for the six samples examined, particularly in the region above 800°C. Endothermic peaks above this temperature are indicative of the decomposition of sodalite phases and also the decomposition of quartz, which occurs between 550 to 1000°C (Atasoy 2005). Small endothermic peaks throughout the DSC curve may be attributed to loss of physically held water (Atasoy, 2005), which was notable in all the bauxite residue samples examined.

The mineralogical composition of bauxite residue typically comprises Al_2O_3 and Fe_2O_3 in the range of 20 to 45 % and 10 to 22 %, respectively (IAI 2015). This composition is reflected in the XRF and XRD analysis, which showed the dominant presence of Fe_2O_3, $FeO(OH)$, and $Al(OH)_3$. $CaTiO_3$, $AlO(OH)$ and TiO_2 were also detected in all samples, which is common amongst bauxite residue (Gräfe et al., 2011). Sodalite ($Na_8(Al_6Si_6O_{24})Cl_2$) was also present in the bauxite residue, and is one of the most common desilication products formed during the pre-desilication stage during the Bayer

process, along with $CaTiO_3$ which is often found as a result of the lime added (Gräfe et al., 2011).

3.4.2 Economic Value of Bauxite and Potential for Re-use

In recent years, several studies have been conducted to investigate the potential use of industrial residues such as phosphogypsum, mine tailings, slags and bauxite residue as a possible source for CRMs and REEs (Binnemans et al., 2015). Currently, the global production rate of REEs, which is typically expressed in tons of rare earth oxides (REOs) is 130,000 to 140,000 tons, of which 95% is produced in China (Binnemans et al., 2018). Five of the REEs (Nd, Eu, Tb, Dy, Y) are now described as being of a high supply risk within Europe, Japan and the USA (Binnemans et al., 2018). Such CRMs and REEs are necessary for the production of magnets, lighting, lasers, batteries, catalysts, and alloys in aerospace (Weng et al., 2015).

While this study did show differences in the bauxite residue over the twelve-year period, in terms of decreased pH and EC, there were no significant changes in the CRM content of the bauxite residue (Table 3.4). This indicates that some BRDAs may be a potential resource for the reprocessing and recovery of CRMs and REEs. However, this is not certain for all BRDAs, as variation can and does occur within BRDAs and refineries due to differences in bauxite ore type, parameters used within the Bayer Process, as well as varying disposal and neutralisation techniques.

The Sc, Ga and V content of the bauxite residue in the current study are of particular interest, due to their high economic value (Table 3.5) and supply risk. Scandium, a trace constituent of igneous rocks (European Commission, 2017), is used in the production of aluminium alloys (Ricketts and Duyvesteyn 2018), and V, present in minor amounts in the Earth's crust and seawater and the majority of which is sourced as a by-product of the steel industry (European Commission, 2017), is used in electrodes (Morel et al., 2016). Gallium is primarily sourced from bauxite ore and bauxite residue, as it found naturally as a trace element dispersed in minerals, which also includes coal (Qin et al., 2015), and is used in the production of catalysts (Qin and Schneider 2016). The Sc in this study (Table 3.4) was lower than values found in fresh Hungarian (Ujaczki et al., 2017), Greek (Borra et al., 2015), Russian (Petrakova et al., 2015) and Australian (Wang et al., 2013) bauxite residues. However, the Ga content (Table 3.4) was higher than that found by

Ujaczki et al., (2017) in Hungarian bauxite residue, as well as in Australian (Wang et al., 2013), Indian (Mohapatra et al., 2012) and Turkish (Abdulvaliyev et al., 2015) bauxite residues. Finally, the V content was present in higher amounts compared to Hungarian (Ujaczki et al., 2017), Indian (Mohapatra et al., 2012) and Turkish (Abdulvaliyev et al., 2015) bauxite residues. This is indicative of the variation of CRM content in residues between refineries.

In addition to Sc, Ga and V, there is now a focus on further valuable element extraction (Jowitt et al., 2018) and recovery of REE due to the overproduction of REEs such as La and Ce, which is leading to an imbalance in the supply of REEs produced and a demand for Nd and Dy (Binnemans and Jones 2015; Binnemans et al., 2018), both of which were found in the bauxite residue in this study.

The typical methods of CRM recovery from bauxite residue include direct leaching using mineral acids such as HNO_3, sulphuric acid (H_2SO_4) or hydrochloric acid (HCl), or leaching following pyrometallurgical applications such as roasting (Ujaczki et al., 2018). Although there are high recovery rates of CRMs from bauxite residue reported (Abdulvaliyev et al., 2015; Borra et al., 2015), so too are the associated costs for acids and energy required in these processes, which questions the justification of extracting CRMs from by-products such as bauxite residue. Recent studies have also highlighted the need to develop new technologies to optimise the efficiency of CRM recovery from bauxite residue to ensure cost-effectiveness (Gomes et al., 2016; Akcil et al., 2017). Ujaczki et al., (2018) in their review on the re-use of bauxite residue as a source of CRMs, highlighted the extent of the benefits following CRM recovery from a wider perspective in terms of the technological (development of more efficient technologies), social (such as improvements to health), economic (mainly reduction in refinery disposal costs), and environmental factors such as reduced emissions and loss of habitable land.

Table 3.5 Associated financial value of economically interesting elements in the bauxite residue (average over a twelve-year period, n = 11).

Element	Average aqua regia extracted content (mg kg^{-1})	Price[*] (US \$ t^{-1})	Economic value of the bauxite residue in this study[***] (US \$ t^{-1})
Ga	107±7.3	400,000	42.73
Sc	51.4±5.4	4,600,000	236.44
In	32.5±2.9	240,000	7.81
V	510±77.8	6,889	3.51
Nd	89.0±13.6	39,500	3.51
Dy	5.48±1.0	184,500	1.01
Pr	44.4±5.6	5,500[**]	0.24
Y	40.1±3.9	35,500	1.42
Ce	142±24.9	2,000	0.28
Sm	20.8±1.9	12,500[**]	0.26
Co	7.72±0.7	26,444	0.20
La	97.5±16.3	2,000	0.19
Eu	2.51±0.4	66,000	0.16
Yb	8.82±0.5	5,500[**]	0.04
Lu	7.99±0.3	5,500[**]	0.04
Gd	7.45±1.2	5,500[**]	0.04
Mo	4.48±0.5	14,500	0.06
Er	5.12±0.5	5,500[**]	0.03

[*]Values from USGS (2016)

[**]Average value for mischmetals of REE/expected higher individual prices

[***] Economic value of the bauxite residue in this study, determined using current price (US \$ t^{-1}) multiplied by the average content in the bauxite residue studied.

3.4.3 The Findings of this Study From an Industrial Perspective on Potential Re-use of Bauxite Residue

This study found that there was very little variation in the CRM content of bauxite residue in a BRDA over a twelve-year period. This shows promise for the potential re-use of bauxite residue as a secondary source of CRMs. Finding a suitable and long-term use for bauxite residue may be hampered by several barriers and limitations (Klauber et al., 2011; Evans 2016), such as high alkalinity and salinity which were shown by this study to be reduced by weathering and mud farming. However, limitations to the re-use of bauxite residue may be overcome through management strategies involving its partial neutralisation and increased solids content (Klauber et al., 2011).

3.5 Conclusions

This study showed that there was a reduction in both the pH and the EC ($p < 0.01$) of bauxite residue in a BRDA over a twelve-year period. There was little variation in the CRM content of the bauxite residue sampled. The CRMs of particular interest were V, Ga and Sc due their potential supply risk and associated economic value. The V, Ga and Sc content of the bauxite residue samples were 510 ± 77.8, 107 ± 7.3 and 51.4 ± 5.4 mg kg^{-1}, respectively, giving current economic values of 3.51, 42.73 and 236.44 US \$ t^{-1}. From a European and global context, this highlights a potential resource for CRMs in the event of a scarcity of these materials. However, the general composition and CRM content of bauxite residue varies greatly due to the bauxite ore and parameters used in the Bayer Process, as well as the disposal and neutralisation methods implemented by refineries. Depending on the history of the refinery and BRDA, there may be little variation over time, making BRDAs possible sources for the extraction of CRMs. There are currently high-costs associated with the extraction of CRMs from bauxite residue due to the large amount of reagent and/or energy required in the process, before purifying the CRMs recovered for re-use. However, these need to be set against the overall benefits of recovering CRMs in terms of the environmental, economic and social factors. Further research is necessary to investigate the cost and environmental implications and limitations of extraction of CRMs from BRDAs, as opposed to conventional extraction techniques from mines, in terms of emissions produced, machinery required, fuel needed and human resources required.

3.6 References

Abdulvaliyev, R.A., Akcil, A., Gladyshev, S.V., Tastanov, E.A., Beisembekova, K.O., Akhmadiyeva, N.K. and Deveci, H., 2015. Gallium and vanadium extraction from red mud of Turkish alumina refinery plant: Hydrogarnet process. *Hydrometallurgy* 157, 72-77.

Agatzini-Leonardou, S., Oustadakis, P., Tsakiridis, P.E. and Markopoulos, C., 2008. Titanium leaching from red mud by diluted sulfuric acid at atmospheric pressure. *J. Hazard. Mater.* 157, 579-586.

Akcil, A., Akhmadiyeva, N., Abdulvaliyev, R., Abhilash and Meshram, P., 2018. Overview on extraction and separation of rare earth elements from red mud: focus on scandium. *Mineral. Process. Extract. Metall. Rev.* 39,145-151.

Arco-Lázaro, E., Pardo, T., Clemente, R. and Bernal, M.P., 2018. Arsenic adsorption and plant availability in an agricultural soil irrigated with As-rich water: effects of Fe-rich amendments and organic and inorganic fertilisers. *J. Environ. Manage.* 209, 262-272.

Atasoy, A., 2005. An investigation on characterization and thermal analysis of the Aughinish red mud. *J. Therm. Anal. Calorim.* 81, 357-361.

Atasoy, A.D. and Bilgic, B., 2018. Adsorption of copper and zinc ions from aqueous solutions using montmorillonite and bauxite as low-cost adsorbents. *Mine Wat. Environ.* 37, 205-210.

Balomenos, E., Davris, P., Pontikes, Y. and Panias, D., 2017. Mud2Metal: Lessons learned on the path for complete utilization of bauxite residue through industrial symbiosis. *J. Sustain. Metall.* 3, 551-560.

Bhatnagar, A., Vilar, V.J., Botelho, C.M. and Boaventura, R.A., 2011. A review of the use of red mud as adsorbent for the removal of toxic pollutants from water and wastewater. *Environ. Technol.* 32, 231-249.

Binnemans, K. and Jones, P.T., 2015. Rare earths and the balance problem. *J. Sustain. Metall.* 1, 29-38.

Binnemans, K., Jones, P.T., Blanpain, B., Van Gerven, T. and Pontikes, Y., 2015. Towards zero-waste valorisation of rare-earth-containing industrial process residues: a critical review. *J. Clean. Prod.* 99, 17-38.

Binnemans, K., Jones, P.T., Müller, T. and Yurramendi, L., 2018. Rare earths and the balance problem: how to deal with changing markets? *J. Sustain. Metall.* 4, 1-21.

Blake, G.R., 1965. Bulk Density 1. Methods of soil analysis. Part 1. Physical and mineralogical properties, including statistics of measurement and sampling, (methodsofsoilana), 374-390. Available: https://dl.sciencesocieties.org/publications/books/tocs/agronomymonogra/methodsofsoilana [accessed 24.05.2018].

Borra, C.R., Pontikes, Y., Binnemans, K. and Van Gerven, T., 2015. Leaching of rare earths from bauxite residue (red mud). *Minerals Engin.* 76, 20-27.

Bridger, S. and Knowles, M., 2000. A complete method for environmental samples by simultaneous axially viewed ICP-AES following USEPA guidelines. Varian ICP-OES At Work (29). Available: https://www.agilent.com/cs/library/applications/ICPES-29.pdf [accessed 24.05.2018].

Burke, I.T., Peacock, C.L., Lockwood, C.L., Stewart, D.I., Mortimer, R.J., Ward, M.B., Renforth, P., Gruiz, K. and Mayes, W.M., 2013. Behavior of aluminum, arsenic, and vanadium during the neutralization of red mud leachate by HCl, gypsum, or seawater. *Environ. Sci. Technol.* 47, 6527-6535.

Castaldi, P., Silvetti, M., Enzo, S. and Deiana, S., 2011. X-ray diffraction and thermal analysis of bauxite ore-processing waste (red mud) exchanged with arsenate and phosphate. *Clays and Clay Min.* 59, 189-199.

Clohessy, J., 2015. Closure and rehabilitation of Rusal Aughinish BRDA, presented at the Residue Closure and Rehabilitation Workshop. In 10th Alumina Quality Workshop, Perth, Western Australia. Available: (http://aqw.com.au/2015papers.html) [accessed 18.04.2018].

Cooling, D.J., 2007. Improving the sustainability of residue management practices-Alcoa World Alumina Australia. Paste and thickened tailings: a guide, 316. Available: http://citeseerx.ist.psu.edu/viewdoc/download?doi=10.1.1.629.1067&rep=rep1&type=pdf [accessed 24.05.2018].

Courtney, R. and Harrington, T., 2010. Assessment of plant-available phosphorus in a fine textured sodic substrate. *Ecol. Engin.* 36, 542-547.

Communication from the commission to the European Parliament, the council, the European economic and social committee and the committee of the regions, 2017. Available: http://eur-lex.europa.eu/legal-content/EN/TXT/PDF/?uri=CELEX:52017DC0490&from=EN [accessed 26.02.2018].

Cusack, P.B., Healy, M.G., Ryan, P.C., Burke, I.T., O'Donoghue, L.M., Ujaczki, É. and Courtney, R., 2018. Enhancement of bauxite residue as a low-cost adsorbent for phosphorus in aqueous solution, using seawater and gypsum treatments. *J. Clean. Prod.* 179, 217-224.

Dursun, S., Guclu, D., Berktay, A. and Guner, T., 2008. Removal of chromate from aqueous system by activated red-mud. *Asian J. Chem.* 20, 6473–6478.

EU Communities Commission Decision 2000/532/EC, OJ L 226, 06.09.2000; pp. 3–24. Available online: http://eur-lex.europa.eu/legal-content/EN/TXT/PDF/?uri=CELEX:22002D0009&from=EN [accessed 27.09.2018].

EU Communities Council Directive 1999/31/EC on the landfill of waste, OJ L 182, 16.07.1999; pp. 1–19. Available online:http://eur-lex.europa.eu/legal-content/EN/TXT/PDF/?uri=CELEX:31999L0031&from=EN [accessed on 27.09.2018].

European Commission, 2017. Study on the review of the list of critical raw materials. Critical raw materials factsheets. Catalogue number ET-04-15-307-EN-N. Available: https://publications.europa.eu/en/publication-detail/-/publication/7345e3e8-98fc-11e7-b92d-01aa75ed71a1/language-en [accessed 15.05.2018].

Evans, K., 2016. The history, challenges, and new developments in the management and use of bauxite residue. *J. Sustain. Metall*. 2, 316-331.

Goloran, J.B., Chen, C.R., Phillips, I.R., Xu, Z.H. and Condron, L.M., 2013. Selecting a nitrogen availability index for understanding plant nutrient dynamics in rehabilitated bauxite-processing residue sand. *Ecol. Engin.* 58, 228-237.

Gomes, H.I., Jones, A., Rogerson, M., Burke, I.T. and Mayes, W.M., 2016. Vanadium removal and recovery from bauxite residue leachates by ion exchange. *Environ. Sci. Poll. Res.* 23, 23034-23042.

Grace, M.A., Healy, M.G. and Clifford, E., 2015. Use of industrial by-products and natural media to adsorb nutrients, metals and organic carbon from drinking water. *Sci. Tot. Environ.* 518, 491-497.

Grace, M.A., Clifford, E. and Healy, M.G., 2016. The potential for the use of waste products from a variety of sectors in water treatment processes. *J. Clean. Prod*. 137, 788-802.

Gräfe, M., Power, G. and Klauber, C., 2011. Bauxite residue issues: III. Alkalinity and associated chemistry. *Hydrometallurgy* 108, 60-79.

Ha, X.L., Hoang, N.H., Nguyen, T.T.N., Nguyen, T.T., Nguyen, T.H., Dang, V.T. and Nguyen, N.H., 2017, October. Removal of Cd (II) from aqueous solutions using red mud/graphene composite. In Congrès International de Géotechnique–Ouvrages–Structures (1044-1052). Springer, Singapore.

Han, Y.S., Ji, S., Lee, P.K. and Oh, C., 2017. Bauxite residue neutralization with simultaneous mineral carbonation using atmospheric CO2. *J. Hazard. Mater*. 326, 87-93.

Hannachi, Y., Shapovalov, N.A. and Hannachi, A., 2010. Adsorption of nickel from aqueous solution by the use of low-cost adsorbents. *Korean J. Chem. Engin*. 27, 152–158.

Hertel, T., Blanpain, B. and Pontikes, Y., 2016. A proposal for a 100% use of bauxite residue towards inorganic polymer mortar. *J. Sustain. Metall.* 2, 394-404.

Higgins, D., Curtin, T., Pawlett, M. and Courtney, R., 2016. The potential for constructed wetlands to treat alkaline bauxite-residue leachate: Phragmites australis growth. *Environ. Sci. Poll. Res.* 23, 24305-24315.

Higgins, D., Curtin, T. and Courtney, R., 2017. Effectiveness of a constructed wetland for treating alkaline bauxite residue leachate: a 1-year field study. *Environ. Sci. Poll. Res*. 24, 8516-8524.

IAI, 2015. Bauxite residue management: best practice. http://www.world-aluminium.org/media/filer_public/2015/10/15/bauxite_residue_management_-_best_practice_english_oct15edit.pdf. [accessed 14.10.2017].

Jones, B.E., Haynes, R.J. and Phillips, I.R., 2012. Addition of an organic amendment and/or residue mud to bauxite residue sand in order to improve its properties as a growth medium. *J. Environ. Manage.* 95, 29-38.

Jowitt, S.M., Werner, T.T., Weng, Z. and Mudd, G.M., 2018. Recycling of the rare Earth elements. Curr. *Opin. Green. Sustain. Chem* 13, 1-7.

Khaitan, S., Dzombak, D.A., Swallow, P., Schmidt, K., Fu, J. and Lowry, G.V., 2010. Field evaluation of bauxite residue neutralization by carbon dioxide, vegetation, and organic amendments. *J. Environ. Engin*. 136, 1045-1053.

Kirwan, L.J., Hartshorn, A., McMonagle, J.B., Fleming, L. and Funnell, D., 2013. Chemistry of bauxite residue neutralisation and aspects to implementation. *Int. J. Miner. Process*s., 119, 40-50.

Klauber, C., Gräfe, M. and Power, G., 2011. Bauxite residue issues: II. Options for residue utilization. *Hydrometallurgy.* 108, 11-32.

Kong, X., Guo, Y., Xue, S., Hartley, W., Wu, C., Ye, Y. and Cheng, Q., 2017a. Natural evolution of alkaline characteristics in bauxite residue. *J. Clean. Prod.* 143, 224-230.

Kong, X., Li, M., Xue, S., Hartley, W., Chen, C., Wu, C., Li, X. and Li, Y., 2017b. Acid transformation of bauxite residue: conversion of its alkaline characteristics. *J. Hazard. Mat.* 324, 382-390.

Kong, X., Tian, T., Xue, S., Hartley, W., Huang, L., Wu, C. and Li, C., 2018. Development of alkaline electrochemical characteristics demonstrates soil formation in bauxite residue undergoing natural rehabilitation. *Land. Degrad. Dev* 29, 58-67.

Liu, Y. and Naidu, R., 2014. Hidden values in bauxite residue (red mud): recovery of metals. *Waste Manage.* 34, 2662-2673.

Menzies, N.W., Fulton, I.M., Kopittke, R.A. and Kopittke, P.M., 2009. Fresh water leaching of alkaline bauxite residue after sea water neutralization. *J. Environ. Qual.* 38, 2050-2057.

McMahon, K., 2017. Bauxite Residue Disposal Area Rehabilitation, ISCOBA conference November 2017, Hamburg, 02-05 Oct, Hamburg, Germany. Available: http://icsoba.org/sites/default/files/2017papers/Bauxite%20Residue%20Papers/BR01%20-%20Bauxite%20Residue%20Disposal%20Area%20Rehabilitation.pdf [accessed 21.02.2018].

Mohapatra, B.K., Mishra, B.K. and Mishra, C.R., 2012. Studies on metal flow from khondalite to bauxite to alumina and rejects from an alumina refinery, India. In Light Metals 2012 (87-91). Springer, Cham.

Morel, A., Borjon-Piron, Y., Porto, R.L., Brousse, T. and Bélanger, D., 2016. Suitable conditions for the use of vanadium nitride as an electrode for electrochemical capacitor. *J. Electrochem. Soc.* 163, A1077-A1082.

Nikbin, I.M., Aliaghazadeh, M., Charkhtab, S. and Fathollahpour, A., 2018. Environmental impacts and mechanical properties of lightweight concrete containing bauxite residue (red mud). *J. Clean. Prod.* 172, 2683-2694.

Petrakova, O.V., Panov, A.V., Gorbachev, S.N., Klimentenok, G.N., Perestoronin, A.V., Vishnyakov, S.E. and Anashkin, V.S., 2015. Improved efficiency of red mud processing through scandium oxide recovery. In Light Metals 2015 (93-96). Springer, Cham.

Pontikes, Y., Rathossi, C., Nikolopoulos, P., Angelopoulos, G.N., Jayaseelan, D.D. and Lee, W.E., 2009. Effect of firing temperature and atmosphere on sintering of ceramics made from Bayer process bauxite residue. *Ceramics Internat.* 35, 401-407.

Pontikes, Y. and Angelopoulos, G.N., 2013. Bauxite residue in cement and cementitious applications: current status and a possible way forward. *Resourc. Conserv. Recycl.* 73, 53-63.

Power, G., Gräfe, M. and Klauber, C., 2011. Bauxite residue issues: I. current management, disposal and storage practices. *Hydrometallurgy* 108, 33-45.

Qin, S., Sun, Y., Li, Y., Wang, J., Zhao, C. and Gao, K., 2015. Coal deposits as promising alternative sources for gallium. *Earth-Science Reviews* 150, 95-101.

Qin, B. and Schneider, U., 2016. Catalytic use of elemental gallium for carbon–carbon bond formation. J. *Am. Chem. Soc.* 138, 13119-13122.

Ricketts, N.J. and Duyvesteyn, W.P., 2018, March. Scandium recovery from the Nyngan laterite project in NSW. In TMS Annual Meeting & Exhibition (1539-1543). Springer, Cham.

Santini, T.C. and Fey, M.V., 2013. Spontaneous vegetation encroachment upon bauxite residue (red mud) as an indicator and facilitator of in situ remediation processes. *Environ. Sci. Technol.* 47, 12089-12096.

Tsakiridis, P.E., Agatzini-Leonardou, S. and Oustadakis, P., 2004. Red mud addition in the raw meal for the production of Portland cement clinker. *J. Hazard. Mat.* 116, 103-110.

Ujaczki, É., Klebercz, O., Feigl, V., Molnár, M., Magyar, Á., Uzinger, N. and Gruiz, K., 2015. Environmental toxicity assessment of the spilled Ajka red mud in soil microcosms for its potential utilisation as soil ameliorant. Periodica Polytechnica. *Chem. Engin.* 59, 253.

Ujaczki, É., Zimmermann, Y., Gasser, C., Molnár, M., Feigl, V. and Lenz, M., 2017. Red mud as secondary source for critical raw materials–purification of rare earth elements by liquid/liquid extraction. *J. Chem. Technol. Biotech.* 92, 2835-2844.

Ujaczki, É., Feigl, V., Molnár, M., Cusack, P., Curtin, T., Courtney, R., O'Donoghue, L., Davris, P., Hugi, C., Evangelou, M.W. and Balomenos, E., 2018. Re-using bauxite residues: benefits beyond (critical raw) material recovery. *J. Chem. Technol. Biotech.* 93, 2498-2510.

United States Geological Survey Website (USGS). Commodity Statisctics and Information., 2016. Available: http://minerals.usgs.gov/minerals/pubs/commodity/ [accessed 30.01.2018].

Wang, S., Ang, H.M. and Tade, M.O., 2008. Novel applications of red mud as coagulant, adsorbent and catalyst for environmentally benign processes. *Chemosphere.* 72, 1621-1635.

Wang, W., Pranolo, Y. and Cheng, C.Y., 2013. Recovery of scandium from synthetic red mud leach solutions by solvent extraction with D2EHPA. *Sep. Purif. Technol.* 108, 96-102.

Wang, X., Zhang, Y., Lv, F., An, Q., Lu, R., Hu, P. and Jiang, S., 2015. Removal of alkali in the red mud by SO2 and simulated flue gas under mild conditions. *Environ. Prog. Sustain. Ener.* 34, 81-87.

Weng, Z., Jowitt, S.M., Mudd, G.M. and Haque, N., 2015. A detailed assessment of global rare earth element resources: opportunities and challenges. *Econ. Geol.* 110, 1925-1952.

Xu, C., Kynický, J., Smith, M.P., Kopriva, A., Brtnický, M., Urubek, T., Yang, Y., Zhao, Z., He, C. and Song, W., 2017. Origin of heavy rare earth mineralization in South China. *Nature Comm.* 8, 14598.

Xue, S., Kong, X., Zhu, F., Hartley, W., Li, X. and Li, Y., 2016. Proposal for management and alkalinity transformation of bauxite residue in China. *Environ. Sci. Poll. Res.* 23, 12822-12834.

Xue, S., Li, M., Jiang, J., Millar, G.J., Li, C. and Kong, X., 2018. Phosphogypsum stabilization of bauxite residue: conversion of its alkaline characteristics. *J. Environ. Sci.* 77, 1-10.

Zhu, F., Liao, J., Xue, S., Hartley, W., Zou, Q. and Wu, H., 2016. Evaluation of aggregate microstructures following natural regeneration in bauxite residue as characterized by synchrotron-based X-ray micro-computed tomography. *Sci. Tot. Environ.* 573, 155-163.

Zhu, F., Xue, S., Hartley, W., Huang, L., Wu, C. and Li, X., 2016. Novel predictors of soil genesis following natural weathering processes of bauxite residues. *Environ. Sci. Poll. Res.* 23, 2856-2863.

Zhu, F., Cheng, Q., Xue, S., Li, C., Hartley, W., Wu, C. and Tian, T., 2018. Influence of natural regeneration on fractal features of residue microaggregates in bauxite residue disposal areas. *Land Degrad. Dev.* 29, 138-149.

Chapter 4

Enhancement of Bauxite Residue as a Low-cost Adsorbent for Phosphorus in Aqueous Solution, using Seawater and Gypsum Treatments.

Overview

The aim of this chapter was to investigate the adsorption capacity of various fractions of bauxite residue in the removal of phosphorus (P) from synthetic P solutions. This study also involved the application and assessment of seawater and gypsum treatments to assess their impact on the P adsorption capacity of the bauxite residue.

This study has been published in Journal of Cleaner Production (Cusack, P.B., Healy, M.G., Ryan, P.C., Burke, I.T., O' Donoghue, L.M., Ujaczki, É. and Courtney, R., 2018. Enhancement of bauxite residue as a low-cost adsorbent for phosphorus in aqueous solution, using seawater and gypsum treatments. Journal of Cleaner Production, 179, pp.217-224. DOI Link: https://doi.org/10.1016/j.jclepro.2018.01.092). Patricia B. Cusack carried out all the experimental analysis and is the primary author of this publication. Dr. Ronan Courtney and Dr. Mark G. Healy contributed to the experimental design and set-up and were also the main contributors to editing of this manuscript, with inputs also from Dr. Paraic Ryan who carried out the statistical analysis on the data obtained from the study. Dr. Ian T. Burke carried out the XRF analysis on all samples. Dr. Éva Ujaczki and Dr. Lisa M. O' Donoghue were also listed as authors on this publication as this study was part of the overall Alsource project. The published paper is included in Appendix A.

4.1 Introduction

During the extraction of alumina from bauxite ore using the Bayer process, a by-product called bauxite residue (red mud) (Kirwan et al., 2013; Liu et al., 2014) is produced. The global inventory for bauxite residue is approximately 3 billion tonnes, with an estimated

annual production rate of 150 million tonnes (Evans, 2016; Mayes et al., 2016). Bauxite residue is highly alkaline (pH >10) (Goloran et al., 2013), with a high salinity and sodicity (Gräfe et al., 2009). Current best practice within this industry includes careful planning and management of highly engineered bauxite residue disposal areas (BRDAs), avoiding contamination of the surrounding environment (Prajapati et al., 2016). In addition, some refineries use neutralisation techniques for the bauxite residue before disposal into the BRDAs (Klauber et al., 2011; IAI, 2015; Evans 2016). These techniques include (1) direct carbonation, whereby the residue slurry is treated with either carbon dioxide, sulfur dioxide gas, or undergoes intensive mud farming using amphirollers (atmospheric carbonation) (Cooling, 2007; Fois et al., 2007; Dilmore et al., 2009; Evans, 2016) (2) addition of spent acids and/or gypsum ($CaSO_4.2H_2O$) (Kirwan et al., 2013), or (3) reaction of residues with seawater (Hanahan et al., 2004; Palmer and Frost, 2009; Couperthwaite et al., 2014).

Bauxite residues typically comprise very fine particles, ranging from 0.01 µm to 200 µm (Pradhan et al., 1996). Depending on the type of bauxite ore used, in some refineries the bauxite residue undergoes a separation technique during processing (Evans, 2016), which allows it to be separated into two main fractions: a fine fraction with a particle size <100 µm and a coarse fraction with a particle size >150 µm (Eastham et al., 2006; Jones et al., 2012). The coarse fraction mainly consists of quartz (SiO_2), whereas the fine fraction is dominated by iron (Fe) oxides (Snars and Gilkes, 2009). The ratio of the fine to coarse fraction produced is dependent on the bauxite ore used and the Bayer process employed (Li, 2001). Refineries which carry out the separation technique, have found use for the coarse fraction to create roadways to the BRDA and/or storage embankments (Evans, 2016). However, finding appropriate options for the re-use of the fine fraction bauxite residue remains elusive (Power et al., 2011; IAI, 2015).

Fine fraction bauxite residue comprises Fe oxides (20-45%) and aluminium (Al) oxides (10-22%) (IAI 2015), which make it suitable as a medium to adsorb phosphorus (P). The European Commission (EC) has identified waste management as an important aspect of the "circular economy" (EC, 2015), so in recent years, emphasis has been placed on investigating alternative methods of P recovery from wastewater (Grace et al., 2015, 2016). A move from the more conventional methods of P recovery such as biological removal and chemical precipitation (Wang et al., 2008), to the use of low-cost adsorbents

from industrial solid wastes, such as bauxite residue, have been examined. In comparison to standard P removal by sand, bauxite residue has a high P retention capacity (Vohla et al., 2007). However, its P removal potential is enhanced following treatment by heat, acid or gypsum (Table 4.1). Of the methods employed, acid and heat treatment have proved most successful in increasing the P adsorption capacity of the bauxite residue, with maximum adsorption capacities of up to 203 mg P g^{-1} bauxite being achieved (Liu et al., 2007) compared to untreated residue (0.20 mg P g^{-1}; Grace et al., 2015) (Table 4.1). However, whilst acid and heat treatments have proven to be very successful in increasing the adsorption capacity of bauxite residue, they are expensive, energy consuming (using high temperatures up to 700˚C) (Xue et al., 2016), and, without further treatment, do not allow for the easy re-use of the bauxite residue (e.g. as a possible media for plant growth) (Xue et al., 2016).

Treatments such as seawater or gypsum provide relatively inexpensive, alternative treatments, which may not only enhance the P adsorption capacity of the bauxite residue media, but may also help to improve its physicochemical characteristics. Seawater treatment improves bauxite's physical structure, due to the addition of magnesium (Mg) and calcium (Ca) which behave as flocculating agents, allowing many of the fine particles in bauxite residue to form more stable aggregates (Jones and Haynes, 2011), and a partial decrease in sodium (Na) due to ion exchange with Mg, Ca and potassium (K) (Hanahan et al., 2004). Seawater-treated bauxite residues also allow adsorbed P to become bio-available, unlike the metal cations which are unavailable, highlighting the P and metal retention capabilities (Fergusson, 2009). Revegetation of bauxite residue using gypsum has also improved plant growth by reducing its alkalinity and salinity, and improving the structure of the residue (Courtney et al., 2009; Courtney and Kirwan, 2012). In addition to this, modern alumina refineries are often located close to deep water ports, to allow for the bulk shipment of incoming bauxite (sometimes from multiple sources) to the refinery and/or for bulk shipment of alumina to aluminium smelters situated elsewhere. Therefore, there is ample scope for the increasing use of seawater neutralization technology for pre-treatment of residues in refineries not already employing treatments previously mentioned, prior to their deposition in the BRDA.

Table 4.1 Phosphorus (P) adsorption studies that have been carried out using bauxite residues, untreated and treated residues, and their recovery efficiencies.

	P recovery technique	Factors investigated	Type of water	Initial P concentration of the water	P recovered	Reference
Untreated bauxite residue	Batch adsorption experiment	Kinetics, pH and temperature	Synthetic water	5-100 mg P L^{-1}	0.2 mg P g^{-1}	Grace et al., 2015
Gypsum Treated	Batch adsorption experiment	Contact time (3, 6, 24, 48hr)	Synthetic water	20-400 mg P L^{-1}	7.0 mg P g^{-1}	Lopez et al., 1998
Brine treated bauxite residue (Bauxsol™*)	Batch adsorption experiment	pH, ionic strength, time	Synthetic water	0.5-2 mg P L^{-1}	6.5-14.9 mg P g^{-1}	Akhurst et al., 2006
Acid and brine treated bauxite residue (Bauxsol™*)	Batch adsorption experiment	Kinetics and isotherms	Synthetic water	200 mg P L^{-1}	55.7 mg P g^{-1}	Ye et al., 2014
Heat treated bauxite residue	Batch adsorption experiment	Time, pH and initial concentration	Synthetic water	155 mg P L^{-1}	155.2 mg P g^{-1}	Liu et al., 2007
Acid and heat treated bauxite residue	Batch adsorption experiment	Time, pH and initial concentration	Synthetic water	155 mg P L^{-1}	202.9 mg P g^{-1}	Liu et al., 2007
Acid treated bauxite residue	Batch adsorption experiment	Acid type, pH	Synthetic water	1 mg P L^{-1}	1.1 mg P g^{-1}	Huang et al., 2008

*Bauxsol™ = neutralised bauxite residue produced using the Basecon™ procedure, which uses brines high in Ca^{2+} and Mg^{2+} (McConchie et al. 2001).

To the best of the authors' knowledge, no study has previously compared the use of raw seawater or gypsum treatments on the separate fractions of bauxite residue as a method

of neutralisation and preparation for the re-use of bauxite residue in its separated and unseparated fractions as low-cost adsorbents and a potential source of P. The objectives of this study were to (1) characterise bauxite residue from two different sources, before and after treatment with seawater and gypsum, and to investigate their potential to release trace elements (2) investigate the effect of the treated bauxite residue on P adsorption (3) assess the impact of particle size, mineral and elemental (particularly Ca and Mg) composition of the bauxite residue on the adsorption of P.

4.2 Materials and Methods
4.2.1 Sample Preparation

A one kilogram, sample of fresh bauxite residue was obtained from Alteo Gardanne [Gardanne, France (43˚27'9"N, 5˚27'41" E)], who operate a co-disposal method (do not separate the bauxite residue into its separate fractions, i.e. fine and coarse fractions of bauxite). This sample will be referred to hereafter as UFR. One kilogram of mud-farmed bauxite residue samples (treated by atmospheric carbonation and therefore non-hazardous), were also obtained from Rusal Aughinish Alumina [Limerick, Ireland (52˚37'06"N, 9˚04'19"W)], who separate the fine (particle sizes <100 μm) and coarse (particle sizes >150 μm) fraction of bauxite residue before disposal (IAI 2015) in a ratio of 9:1 (fine: coarse). The fine and coarse fractions will be referred to hereafter as UF (untreated fine) and UC (untreated coarse).

Before any analysis or experiments were conducted, all bauxite residue samples were dried at 105˚C for 24 hr. Once dry, the samples were pulverised using a mortar and pestle and sieved to a particle size <2 mm. 0.3 kg of each sample were then treated with either seawater (S) or laboratory-grade gypsum (G) (Lennox, Ireland), so two treatments were applied to each source of bauxite residue. S or G, placed after the above abbreviations, indicates the treatment applied. Gypsum was applied to the 0.3 kg bauxite residue samples at a ratio of 8% (w/w) (Lopez et al., 1998) and leached for 72 hr in accordance with standard methods (BSI, 2002). Seawater amendment involved mixing with 0.3 kg bauxite at a ratio of 5:1 (v/w) (after Johnston et al., 2010), for 1 hr, followed by a 12 hr settlement period overnight. The bauxite residue and seawater mixture was then filtered through a 0.45 μm membrane using a vacuum pump. The treated bauxite residue samples were then oven dried for 24 hr, pulverised with a mortar and pestle, and sieved to <2 mm in size.

4.2.2 Characterisation Study

Untreated and treated bauxite samples were characterised (n=3) for their physical, chemical, elemental and mineralogical properties. Soil pH and electrical conductivity (EC) were measured in an aqueous extract, using 5 g of bauxite residue sample in a 1:5 ratio (solid: liquid) (Courtney and Harrington, 2010). The bulk density (ρ_b) was determined after Blake (1965) and the particle density (ρ_p) after Blake and Hartge (1986) using 10 g of bauxite residue samples. Total pore space (S_t) was calculated using the values obtained for the bulk and particle densities (Danielson and Sutherland, 1986). The effective particle size analysis (PSA) was determined on particle sizes <53 μm using optical laser diffraction on the Malvern Zetasizer 3000HS® (Malvern, United Kingdom) with online autotitrator and a Horiba LA-920, and reported at specific cumulative % (10, 50 and 90%). Mineralogical detection was carried out using X-ray diffraction (XRD) on 1 g samples using a Philips X'Pert PRO MPD® (California, USA), whilst surface morphology and elemental detection were carried out using scanning electron microscopy (SEM) and energy-dispersive X-ray spectroscopy (EDS) on a Hitachi SU-70 (Berkshire, UK), using approximately 1 g samples. Quantification of the elemental content was carried out on 1 g samples by Brookside Laboratories (OH, USA) after digestion (EPA, 1996) using Inductively Coupled Plasma Atomic Emission Spectroscopy (ICP-AES) and elemental composition quantified using X-ray fluorescence (XRF). Measurement of the point of zero charge (PZCpH) was after Vakros et al., (2002) using 1 g samples, and cation exchange capacity (CEC) was determined using the K saturation technique (Thomas, 1982), using 5 g samples. Brunauer-Emmett-Teller specific surface area (SSA) and pore volume analysis were conducted on 1 g samples, which were degassed at 120ºC for 3 hr prior to analysis carried out by Glantreo Laboratories (Cork, Ireland).

4.2.3 Phosphorus Adsorption Batch Study

The P adsorption capacity of nine bauxite samples (untreated and gypsum/seawater treated samples) were examined in a bench-scale experiment. To conduct a P adsorption isotherm test, ortho-phosphorus (PO_4^{3-}-P) solutions were made up to known concentrations using potassium dihydrogen phosphate (K_2HPO_4) in distilled water. One gram of each of the sieved media was placed into a series of 50 ml-capacity containers and was overlain with 25 ml of the solutions. Each sample was then shaken in a reciprocal shaker at 250 rpm for 24 hr. At t = 24 hr, the supernatant water from each sample container was filtered using 0.45μm filters and analysed immediately using a nutrient

analyser (Konelab 20, Thermo Clinical Labsystems, Finland). The data obtained from the P adsorption batch studies were modelled using the Langmuir adsorption isotherm (McBride, 2000), which assumes monolayer adsorption on adsorption sites and allows for the estimation of the maximum P adsorption capacity (q_{max}) of the media:

$$q_i = q_{max} \left(\frac{k_a C_e}{1 + k_a C_e} \right) \qquad (1)$$

where q_i is the quantity of the contaminant adsorbed per gram of media (g g^{-1}), C_e is the equilibrium contaminant concentration in the water (g m^{-3}), k_a is a measure of the affinity of the contaminant for the media (m^3 g^{-1}), and q_{max} is the maximum amount of the contaminant that can be adsorbed onto the media (g g^{-1}).

4.2.3.1. Mobilization of Metals

To determine whether the residue media released trace elements, 25 mL of water was mixed with 1 g of media for 24 hr and the supernatant was analysed by ICP-MS. The elements selected for detection were Al, arsenic (As), barium (Ba), beryllium (Be), boron (B), cadmium (Cd), Ca, chromium (Cr), copper (Cu), Fe, gallium (Ga), K, lead (Pb), Mg, manganese (Mn), mercury (Hg), molybdenum (Mo), Na, nickel (Ni), P, selenium (Se), silicon (Si), titanium (Ti), vanadium (V), and zinc (Zn).

4.2.4 Statistical Analysis

Linear regression analysis was utilised to examine the extent of correlation between the individual characteristic parameters of the bauxite residue samples and bauxite adsorption, using Minitab. A Pearson correlation coefficient and a correlation p-value were determined to quantify correlation. The p-value represents the probability that the correlation between the bauxite residue characteristic in question and the response variable (adsorption) is zero i.e. the probability that there is no relationship between the two.

4.3 Results and Discussion

4.3.1 Characterisation of Bauxite Residue

4.3.1.1 Effect of Treatments on Elemental and Mineralogical Composition

The mineral and total elemental composition of the three untreated bauxite residues [UF(untreated fine fraction), UC (untreated coarse fraction), and UFR (untreated co-disposed)] are shown in Tables 4.2 and 4.3. Bauxite residues are typically high in Fe and Al oxides (Liu et al., 2007), which was found to be the case in this study. The mineralogical composition present for all untreated samples was dominated by Fe_2O_3, Al_2O_3, SiO_2 and CaO. A decrease in Al_2O_3 was noted following treatment with the gypsum and the seawater in all samples, with an increase in CaO content noted in samples treated with gypsum.

Table 4.2 Mineralogical composition of the bauxite residues untreated and treated.

Parameter	Untreated Fine (UF)	Fine +gypsum (UFG)	Fine+ seawater (UFS)	Untreated Coarse (UC)	Coarse+ gypsum (UCG)	Coarse +seawater (UCS)	Untreated French (UFR)	French+ gypsum (UFRG)	French +seawater (UFRS)
Fe_2O_3 (%)	43.9±1.1	40.6±0.6	41.8±1.2	64.0±5.1	61.4±3.0	69.9±3.8	43.9±0.6	47.9±0.5	53.3±5.8
Al_2O_3 (%)	12.7±0.6	11.3±1.0	11.1±2.5	19.4±1.8	11.1±0.6	7.4±0.7	14.0±1.0	11.2±0.3	11.4±2.2
CaO (%)	5.9±0.2	8.2±0.5	4.4±0.3	1.1±0.2	7.6±0.4	1.2±0.1	5.6±0.1	7.7±0.3	3.2±0.5
MgO (%)	3.6±1.3	3.5±0.8	3.1±1.0	4.7±1.8	3.6±0.8	2.6±0.6	4.1±0.6	3.8±0.9	3.2±1.6
SiO_2 (%)	8.6±0.7	8.5±0.9	8.6±1.7	2.6±0.3	1.3±0.2	1.4±0.2	9.4±0.5	5.1±0.4	4.3±0.3
TiO_2 (%)	2.4±0.3	2.1±0.6	2.7±0.1	0.9±0.1	1.0±0.1	2.1±0.6	2.5±0.02	2.3±0.1	2.3±0.5
P_2O_5 (%)	0.6±0.04	0.4±0.02	0.4±0.1	0.3±0.02	0.2±0.02	0.2±0.06	0.5±0.01	0.5±0.02	0.5±0.01

Table 4.3 Elemental composition of the bauxite residues untreated and treated.

Parameter	Untreated Fine (UF)	Fine +gypsum (UFG)	Fine+ seawater (UFS)	Untreated Coarse (UC)	Coarse+ gypsum (UCG)	Coarse +seawater (UCS)	Untreated French (UFR)	French+ gypsum (UFRG)	French +seawater (UFRS)
B (mg kg⁻¹)	470±8.81	425±29	448±13	615±13.3	622±29	722±32.1	566±18.9	539±25	483.8±31
Al (mg kg⁻¹)	72538±1390	81095±1219	80608±3090	45854±2769	48851±2336	45917±2080	67295±3343	65389±1326	64189±595
As (mg kg⁻¹)	21.9±1.73	9.7±0.4	<LODˡ	<LODˡ	<LODˡ	<LODˡ	8.1±0.2	9.75±0.6	6.51±0.43
Ba (mg kg⁻¹)	43.8±1.19	29.4±5	33.3±0.7	13.9±1.01	18.3±3.4	12.7±2.8	45.7±1.5	41.4±1.4	49.4±3.8
Cd (mg kg⁻¹)	8.033±0.16	7.02±0.3	7.33±0.19	10.7±0.18	10.8±0.5	11.8±0.59	9.31±0.2	8.87±0.3	8.21±0.3
Cr (mg kg⁻¹)	1698±37.2	933±44	1170±12.9	880±3.8	817±13	803±21.3	1184±15.9	1090±9	1159±31.2
Fe (mg kg⁻¹)	338571±3057	289459±1859	298282±4937	434739±9980	460078±23043	471204±25753	353392±10003	328114±4498	332251±3435
Pb (mg kg⁻¹)	34.88±0.54	27.8±2.8	36.9±0.8	29.56±3.03	24.6±3	22.06±2.47	34.5±0.9	32.3±0.8	37.4±2.1
Mg (mg kg⁻¹)	122.28±4.96	163±37	1047±25.6	18.32±4.78	8.5±2.21	511.6±25.4	109±3.9	150±9	2203.8±134
Mn(mg kg⁻¹)	163±2.63	140±6.1	167±6.8	187±15.5	223±99	185±31.1	134±0.9	139±1.9	142.9±4.2
Ni (mg kg⁻¹)	18.6±0.89	<LODˡ	2.25±0.2	3.54±0.27	3.15±0.5	4.18±0.22	1.1±0.1	1.24±0.2	1.23±0.3
K (mg kg⁻¹)	391±13.68	454±29	1108±41	255±38	195±23	556.99±67.38	399±13	359±11	1048±63.2
Si (mg kg⁻¹)	223.5±46.1	256±92	245.7±35	213±6.6	234±34	194.46±10.58	276±20	285±34	258.5±11.7
Na (mg kg⁻¹)	28347±553	38180±352	41864±2012	8804±666	5935±114	11101.55±1121.8	25514±317	23703±499	31974±1087
Ti (mg kg⁻¹)	1395±196	1309±100	1265±22	<LODˡ	<LODˡ	<LODˡ	1382±38	1288±120	1233±46
V(mg kg⁻¹)	1050±21.6	781±29	777±8	786±23.6	731±20	731.04±23	1036±12	920±7	983±21
Zn (mg kg⁻¹)	50.7±0.71	40.6±1.2	42.6±1.3	86.7±1.7	82±5.4	84.68±4.2	55.8±0.5	55.6±1.17	57.3±0.9
Ga(mg kg⁻¹)	78.9±2.02	81.2±0.53	73.9±0.6	71.8±1.03	69.3±2.3	73.5±1.6	86.8±1.3	78.6±2	78.8±0.9

Ca(mg kg⁻¹)	46657±832	51641±485	17159±413	4152±490	12771±823	4089.42±588.32	15084±358	42703±2383	14820±926
P(mg kg⁻¹)	955±0.57	962±99	1018±15	1040±23	1011±59	1039.6±23	1298±26	1220±10	1320±53.8
Be(mg kg⁻¹)	<LOD[1]	<LOD[1]	<LOD[1]	<LOD[1]	<LOD[1]	<LOD[1]	<LOD[1]	<LOD[1]	<LOD[1]
Cu (mg kg⁻¹)	<LOD[1]	<LOD[1]	<LOD[1]	<LOD[1]	<LOD[1]	<LOD[1]	<LOD[1]	<LOD[1]	<LOD[1]
Hg (mg kg⁻¹)	<LOD[1]	<LOD[1]	<LOD[1]	<LOD[1]	<LOD[1]	<LOD[1]	<LOD[1]	<LOD[1]	<LOD[1]
Mo(mg kg⁻¹)	<LOD[1]	<LOD[1]	<LOD[1]	<LOD[1]	<LOD[1]	<LOD[1]	<LOD[1]	<LOD[1]	<LOD[1]
Se (mg kg⁻¹)	<LOD[1]	<LOD[1]	<LOD[1]	<LOD[1]	<LOD[1]	<LOD[1]	<LOD[1]	<LOD[1]	<LOD[1]

[1]<LOD = below the limits of detection.

XRD analysis showed that the main crystalline phases present in UF were haematite (Fe_2O_3), goethite ($FeO(OH)$), perovskite ($CaTiO_3$), boehmite ($AlO(OH)$), rutile (TiO_2), gibbsite $Al(OH)_3$ and sodalite $Na_8(Al_6Si_6O_{24})Cl_2$ (Figure C1 in Appendix C). Similarly, the main minerals in UFR were haematite (Fe_2O_3), goethite ($FeO(OH)$), boehmite ($AlO(OH)$), rutile (TiO_2), gibbsite $Al(OH)_3$ and sodalite $Na_8(Al_6Si_6O_{24})Cl_2$ (Figure C2). Boehmite ($AlO(OH)$), rutile (TiO_2), gibbsite $Al(OH)_3$ haematite (Fe_2O_3) were the predominant minerals present in UC (Figure C3). Following treatment with seawater and gypsum, a change in mineral phase in UFG, UFS, UFRS and UFRG occurred (Figure C4, C5, C6, C7). After treatment with gypsum, a higher presence of the calcium carbonate, calcite ($CaCO_3$), was detected in UFRG and UCG (Figure C7 and C8), and post seawater treatment, small peaks representing brucite ($Mg(OH)_2$ were detected in UFS and UCS (C5 and C9).

These findings are similar to previous studies that examined various neutralization techniques for bauxite residue (Gräfe et al., 2009). When seawater is added to bauxite residue, a reaction occurs where the hydroxide, carbonate and aluminate ions are eliminated due to a reaction involving Mg^{2+} and Ca^{2+} (from the seawater) (Gräfe et al., 2009; Palmer and Frost, 2009). This results in the formation of alkaline solids such as the calcium carbonates, calcite and brucite, which cause a buffering effect, evidenced in a shift of pH to between 8 and 9 (Power et al., 2011). The addition of gypsum ($CaSO_4$) results in a drop in the pH (approximately 8.6) due to the precipitation of excess hydroxides ($OH-$), aluminium hydroxides ($Al(OH)_4^-$), carbonates (CO_3^{2-}) to form calcium hydroxide/lime ($Ca(OH)$), tri-calcium aluminate (TCA), hydrocalumite and calcium carbonate ($CaCO_3$), which behave as buffers and maintain pH (Gräfe et al., 2009). The addition of Ca also flocculates and helps with the formation of more stable aggregates (Jones and Haynes, 2011).

An analysis of water samples (Table C1) to examine mobilisation of metals showed that As, Al and Cr were present in the leachate from the UFR sample, but decreased following gypsum and seawater treatments. Arsenic, Fe and Al were mobilised from the UF sample, but these concentrations were reduced following treatment with gypsum and seawater. Aluminium was mobilised from the UC. The reduction in Fe and Al following treatment with either gypsum or seawater is in line with previous studies, which have shown that water soluble Fe and Al decrease following gypsum application (Courtney and Timpson,

2005). Overall, Al still remained above the maximum allowable concentration (MAC) of 0.2 mg L^{-1} (200 µg L^{-1}) (EPA, 2014) for Al for drinking water. Sodium was still at a high level following gypsum and seawater treatments, ranging from 139.3±3.2 to 153±24.8 mg L^{-1} and 241.3±26 to 388.7±18.6 mg L^{-1}, respectively. The MAC for Na in drinking water is 200 mg L^{-1} (EPA, 2014).

4.3.1.2 Effect of Treatments on Physico-chemical Properties

The untreated bauxite residues had high pH (10.8±0.12 to 11.9±0.06) and EC (704±90.8 to 1184±48.8µS cm^{-1}) (Table 4.4). Following treatment with gypsum and seawater, pH decreased and EC increased. Changes for pH after treatment with either seawater or gypsum are due to precipitation of calcium carbonates such calcite, brucite and aragonite, which behave as buffers and maintain a reduced pH (Menzies et al., 2004), while the increase in EC is attributed to the introduction of excess Na$^+$ and Ca^{2+} (Gräfe et al., 2009). The pH of bauxite residue is normally within the range of 11 to 13 (Newson et al., 2006), but varies due to the type of bauxite ore, Bayer process, and neutralisation techniques used in the refinery. Both seawater (Menzies et al., 2004; Johnston et al., 2010) and gypsum applications (Jones and Haynes, 2011; Courtney and Kirwan, 2012; Lehoux et al., 2013) are recognised methods of reducing the alkalinity of bauxite residues.

No change was observed in the particle size or particle size density following the addition of the gypsum and seawater treatments to the various bauxite residue samples (Table 4.4). Similarly, the addition of gypsum or seawater did not have any impact on bulk density (Table 4.4).

The surface morphology of bauxite residues typically comprises 30% amorphous and 70% crystalline phase (Gräfe et al., 2009). However, in this study SEM imaging suggests that the bauxite residue samples were not present in strong crystalline form (Figure 4.1), in particular for samples UF and UFR, as no distinctive crystalline structure to the bauxite residue samples was observed. Liu et al., (2007) examined the effect of age on stored bauxite residue, and found that fresh bauxite residue particles are present in poorly formed crystallised or amorphous form in comparison to older bauxite residue (10 years), which has a stronger crystalline formation, indicating that crystallisation occurs in some of the minerals over time. As the bauxite residue used in this study was fresh, this would explain why there was not a strong distinction between amorphous or crystalline forms, similar

to the findings of Liu et al., (2007). The composition of fine particles and larger particles in the coarse fraction (UC) were noticeable from the SEM (Figure 4.1).

Table 4.4 Physical and chemical characterisation of the bauxite residues, untreated and treated.

Parameter	Untreated Fine (UF)	Fine +gypsum (UFG)	Fine+ seawater (UFS)	Untreated Coarse (UC)	Coarse+ gypsum (UCG)	Coarse +seawater (UCS)	Untreated French (UFR)	French+ gypsum (UFRG)	French +seawater (UFRS)
pH	10.8±0.12	8.7±0.04	9.02±0.07	11.4±0.29	6.79±0.08	7.95±0.16	11.9±0.06	9.17±0.02	9.49±0.01
EC (μS cm^{-1})	704±90.8	1338±3.5	3080±17.3	856±1.53	909±2	916±1.53	1184±48.8	1219±7.21	5323±172
% Water	23.5±0.65	28.9±0.6	32.1±1.72	0.39±0.2	0.82±0.18	3.13±0.72	28±0.54	35.3±1.32	36.5±0.16
d_{10} (μm)[a]	0.6±0.09	1.37±0.23	1.26±0.06	1.27±0.47	1.11±0.23	1.66±0.83	1.3±0.04	1.49±0.06	1.08±0.74
d_{50} (μm)[b]	2.43±0.29	3.56±0.59	3.52±0.11	5.13±0.63	3.69±0.49	3.68±0.4	3.7±0.12	4.11±0.39	3.47±0.98
d_{90} (μm)[c]	6.02±0.86	7.12±1.98	7.69±1.97	12.04±1.27	9.51±0.25	7.0±0.13	10.11±2.37	9.81±2.68	7.17±3.25
Total Pore Space (%)[d]	50.03±2.25	50.73±9.04	50.03±1.75	9.63±6.46	10.82±1.09	7.65±5.26	61.77±1.16	53.6±1.95	53.87±0.78
Bulk Density (g cm^{-3})[e]	1.5±0.02	1.5±0.01	1.49±0.01	2.53±0.01	2.48±0.03	2.55±0.01	1.31±0.03	1.32±0.03	1.31±0.02
Particle Size Density (g cm^{-3})[f]	2.99±0.1	3.11±0.5	2.94±0.12	2.81±0.21	2.65±0.4	2.7±0.14	3.41±0.07	2.85±0.08	2.85±0.07

PZCpH[g]	6.96±1.21	3.43±0.73	6.28±0.98	6.89±0.09	3.11±0.12	6.39±0.51	6.16±0.21	6.32±0.51	4.43±0.09
CEC (K)(cmol kg^{-1})[h]	63.3±2.56	64.1±3.41	60.1±2.96	N/A[k]	N/A[k]	N/A[k]	57.5±2.13	56.4±3.49	48.9±13.7
Total Pore Volume (cm^{-3} g^{-1})[i]	0.03	0.03	0.03	0.02	0.02	0.03	0.03	0.04	0.03
BET SSA (m^2 g^{-1})[j]	11.73	12.77	13.82	12.58	13.19	15.37	15.24	17.57	17.57

[a]d_{10} (µm) = the size of particles at 10% of the total particle distribution, expressed in µm.

[b]d_{50} (µm) = the median; the size of particles at 50% of the total particle distribution, expressed in µm.

[c]d_{90} (µm) = the size of particles at 90% of the total particle distribution, expressed in µm.

[d]Total Pore Space = the total pore space which may be calculated from particle density and bulk density.

[e]Bulk density = the mass of soil per unit volume, expressed as g cm^{-3}.

[f]Particle size density = the density of the solid particles, excluding pore spaces between them, expressed as g cm^{-3}.

[g]PZCpH = the pH at which the point of zero charge is occurring.

[h]CEC= the cation exchange capacity, expressed as cmol kg^{-1}.

[i]BET SSA = specific surface area analysed using Brunauer-Emmett-Teller isotherm and expressed as m^2 g^{-1}.

[j]Total Pore Volume = measurement of total pore volume expressed as cm^{-3} g^{-1}.

[k]N/A =not available

Improved aggregate formation was noticeable in the gypsum and seawater-treated bauxite residues (Figure 4.1), due to the addition of Ca^{2+}, which results in flocculation (Zhu et al., 2016). Changes in the surface morphology were also evident in the gypsum and seawater-treated residues in comparison to the untreated residues, which appeared to have a much smoother surface (Figure 4.1). This change in surface morphology following the treatments was attributed to the changes in mineral phase (Huang et al., 2008).

4.3.2 Phosphorus Adsorption Study

4.3.2.1 Effect of Seawater and Gypsum Treatment on P Adsorption

All nine bauxite residue samples in this study were successful in removing P from aqueous solution (Table 4.5). Bauxite residue has been shown in numerous P adsorption studies to have a high P retention capacity, particularly following treatment or modification (Ye et al., 2014; Grace et al., 2015). In this study, gypsum or seawater treatment had a positive impact on P removal, with the gypsum-treated bauxite residue performing best (Table 4.5).

Following seawater treatment, the P adsorption capacity of the bauxite residues increased to q_{max} values of 0.48, 0.66 and 1.92mg P g^{-1} media for UFS, UCS and UFRS, respectively. In previous studies, following treatment with seawater, bauxite residue had a higher adsorption capacity for P. Akhurst et al., (2006) reported a maximum adsorption of 6.5 mg P g^{-1} when using a bauxite residue treated with brine (Bauxsol™). This relatively high adsorption may be attributed to the higher concentrations of Ca^{2+} and Mg^{2+} in the brines (or products such as Bauxsol™, developed by Basecon™), in comparison to raw seawater (0.41, 1.29 and 10.77g kg^{-1} of Ca^{2+}, Na and Mg^{2+}, respectively) used in this study (Gräfe et al., 2009). The gypsum-treated bauxite residues had the highest q_{max} values − 2.46, 1.39 and 2.73mg P g^{-1} media for UFG, UCG and UFRG, respectively. However, these values were lower than a P adsorption study carried out by Lopez et al., (1998), who used the same application rate of gypsum to the bauxite residue samples and reported a q_{max} of 7.03 mg P g^{-1}. The lower rate observed in the current study may be attributed to the 72 hr leaching process that the gypsum-treated bauxite residue underwent before use in the adsorption study, which may have allowed for further exchange and removal of Ca^{2+} following the leaching process.
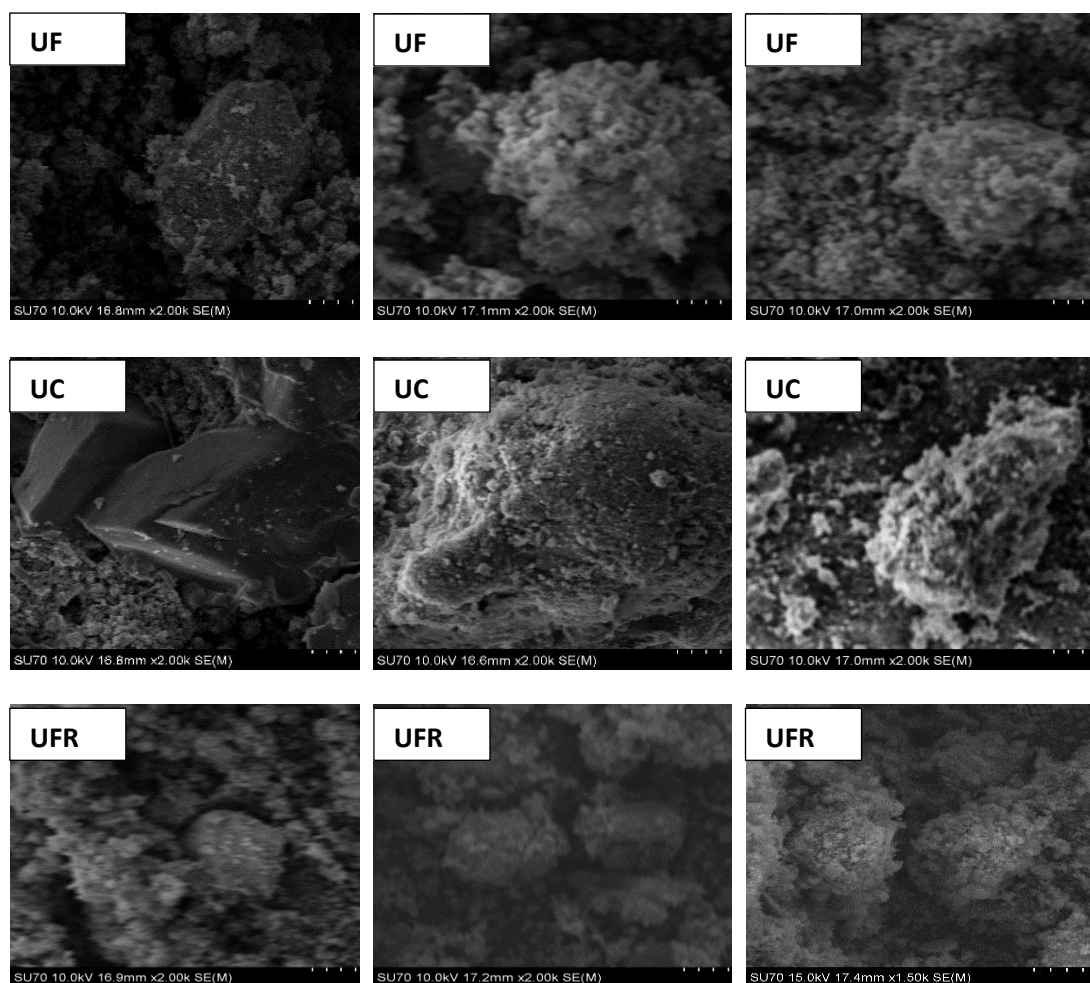
Untreated   **Gypsum Treated**   **Seawater Treated**

Figure 4.1. SEM (10kV; magnification x2,000; working distance 16.8mm) imaging for the three untreated bauxite residue pre and post treatment with either gypsum or seawater.

Table 4.5 Maximum adsorbency (mg P g^{-1} media) of P using each of the bauxite residue samples, untreated and treated (level of fit of the data, R^2, to Langmuir isotherm is included in brackets).

Media	Treatment method employed		
	Untreated	Gypsum	Seawater
	----------------------- mg P g^{-1} media ---------------------		
UFR	1 (0.99)	2.73 (0.99)	1.92 (0.99)
UF	0.38 (0.99)	2.46 (0.97)	0.48 (0.99)
UC	0.35(0.98)	1.39 (0.99)	0.66 (0.99)

Overall, the bauxite residue in the current study had a higher P adsorbency than in other studies for zeolite (0.01 mg P g^{-1}, Grace et al., 2015) and granular ceramics (0.9 mg g^{-1}; Chen et al., 2012), but lower than fly ash, granular blast furnace slag and pyritic fill (6.48, 3.61 and 0.88 mg P g^{-1}, respectively; Grace et al., 2015), crushed concrete (19.6 mg P g^{-1}; Egemose et al., 2012), untreated biochar (32 mg P g^{-1}; Wang et al., 2015), and NaOH-modified coconut shell powder (200 mg P g^{-1}; de Lima et al., 2012).

4.3.2.2 Factors Affecting P Adsorption

The adsorption of P onto media is influenced by many factors which include particle size, pH, component and surface characteristics (Wang et al., 2016). Numerous studies have investigated the effect of parameters such as kinetics of P adsorption (Akhurst et al., 2006; Liu et al., 2007; Ye et al., 2014; Grace et al., 2015), ionic solution (Akhurst et al., 2006), pH (Liu et al., 2007; Huang et al., 2008; Grace et al., 2015) on the adsorption of P from aqueous solution. While all bauxite residue samples in this study did remove P from aqueous solution, it is clear that the application of treatments, such as gypsum or seawater, has an effect on the adsorption capability, and that the rate of adsorption will vary as a result of the source of bauxite residue and treatments used (Wang et al., 2008).

The parameters which showed a statistically significant positive correlation of medium strength with P adsorption in this study were Ca (correlation coefficient = 0.47, p = 0.01, Degrees of Freedom (DoF) = 25) and CaO (correlation coefficient = 0.39, p = 0.04, DoF = 25). A statistically significant negative correlation of medium strength was also detected between pH and P adsorption (correlation coefficient = - 0.38, p = 0. 05, DoF = 25). pH was a contributing factor to the adsorption process with the amount of phosphate adsorbed increasing with a decrease in pH in the media following treatments, UFRG>UFRS>UFR, UFG>UFS>UF, UCG>UCS>UC. This was a similar finding to several studies carried out (Li et al., 2006; Liu et al., 2007; Huang et al., 2008; Grace et al., 2015). The Ca ions also influenced P adsorption. This is as a result of the high level of Ca^{2+} and Mg^{2+} present in the bauxite residue, particularly after seawater and gypsum treatments, when the majority of PO_4^{3-} is removed from solution due to the formation of magnesium phosphate ($Mg_3(PO_4)_2$) and calcium phosphate ($Ca_3(PO_4)_2$) (Akhurst et al., 2006).

The pH at which net charges are neutral on the surface of the adsorbent - the point of zero charge (PZC) - influences the rate of adsorption of P (Jacukowicz-Sobala et al., 2015). Where the pH is higher than the PZCpH, the surface of the adsorbent media becomes more negative (attracting more cations), as a result of the adsorption of OH^- from the surrounding solution (Prajapati et al., 2016). The PZCpH ranged from 6.16 ± 0.21 to 6.96 ± 1.21 (Table 4.4) in the three untreated samples. Following treatment with gypsum and seawater, there were notable changes, but no statistical relevance was detected between the PZCpH and P adsorption in this study. However, as bauxite residue is composed of numerous minerals, each with their own individual PZCpH (which, as noted in the literature, can range from anywhere between pH 2 to pH 9.8 (Gräfe et al., 2009)), this results in the bauxite residue being able to cater for a wide range of pH (Gräfe et al., 2009) and also having the capability of removing both cations and anions from solution.

The SSA analysis carried out on the bauxite residues show an increase in specific surface area in all samples following treatment with either the gypsum or the seawater (Table 4.4). There was also an increase in pore volume following the addition of either gypsum or seawater (Table 4.4). This is attributed to the formation of precipitates formed in the neutralisation process of both gypsum and seawater and the effect of the Ca acting as a flocculant with the finer particles present. This increase in surface area also contributes to the increase in P adsorption following treatments. Although particle size affects adsorption onto media, due to the availability of sites for P uptake, no significant correlation was observed in the current study.

4.3.3 Implications of the Findings of this Study

The use of gypsum and seawater treatments on bauxite residue improved the overall P adsorption capacity of the bauxite residue samples, but mixing the bauxite residue and treatments with actual wastewater will be necessary to fully understand the total adsorption behaviour of the bauxite residue. In addition to improving the P adsorption, alkalinity was significantly reduced following both treatments; however, the EC was increased. This may limit the growth of plants on the gypsum or seawater-treated bauxite residues; therefore, one option may be to increase the rinsing period of the bauxite residue following treatment to remove the excess Ca^{2+} and Na^+ ions in solution. Lowering the alkalinity, increasing the P, Ca^{2+} and Mg^{2+} content and improving the physical structure, provide the possible re-use option of using the treated bauxite residue as a growth media.

For a refinery, the cost of neutralisation techniques is an obvious consideration when deciding which technique(s) to use. The use of seawater as a neutralisation technique would be a cheap and feasible option for a refinery that is close to the sea. The establishment of a pipeline (if not already in place) would be the dominant capital cost. The use of a Nano filtration system to concentrate the Ca^{2+}, Mg^{2+} and Na^+ ions in the seawater (Couperthwaite et al., 2014) could allow for the reduction in volume of seawater necessary for the neutralisation process, but may add to the cost. Gypsum however may be a more expensive option, requiring machinery such as amphirolls for the mixing and spreading of the gypsum. However, depending on the refinery's location, waste gypsum from construction sites or fossil fuel powered power stations may be used (Jones and Haynes, 2011).

4.4 Conclusions

This study examined the impact of gypsum and seawater treatments on the mineral, elemental and physiochemical properties of bauxite residue. The untreated bauxite residues were high in Fe and Al oxides and their mineralogical composition was dominated by Fe_2O_3, Al_2O_3, SiO_2 and CaO. Following treatment with gypsum and seawater, the pH decreased and EC increased, but no change was observed in the particle size or density. The SSA and pore volume of the bauxite increased following both treatments, which contributed to increased P adsorbency. Although the P adsorbency measured in this study was not as high as measured in other studies using different media, it still indicates that re-use in water or wastewater treatment facilities may be an appropriate option for bauxite residue.

4.5 References

Akhurst, D.J., Jones, G.B., Clark, M., McConchie, D., 2006. Phosphate removal from aqueous solutions using neutralised bauxite refinery residues (Bauxsol™). *Environ. Chem.* 3, 65-74.

Blake, G.R., 1965. Bulk density, in: Black, C.A. (Ed), Methods of soil analysis. Part 1. Physical and mineralogical properties, including statistics of measurement and sampling. ASA, SSSA, Madison, WI, pp. 374 – 390.

Blake, G.R., Hartge, K.H., 1986. Particle density, in: Klute, A. (Ed), Methods of Soil Analysis: Part 1—Physical and Mineralogical Methods. SSSA, ASA, Madison, WI, pp. 377 – 382.

British Standard Institution, 2002. 12457-2. Characterisation of waste. Leaching. Compliance test for leaching of granular waste materials and sludges. One stage batch test at a liquid to solid ratio of 10 l/kg for materials with particle size below 4 mm (without or with size reduction).

Chen, N., Feng, C., Zhang, Z., Liu, R., Gao, Y., Li, M.,Sugiura, N., 2012. Preparation and characterization of lanthanum (III) loaded granular ceramic for phosphorus adsorption from aqueous solution. *J. Taiwan Instit. Chem. Eng.* 43, 783-789.

Cooling, D.J., 2007. Improving the sustainability of residue management practices-Alcoa World Alumina Australia. In: (A. Fouri and R.J. Jewell, Eds) Paste and Thickened Tailings: A Guide, 316. http://citeseerx.ist.psu.edu/viewdoc/download?doi=10.1.1.629.1067&rep=rep1&type=pdf. (accessed 31.10.17).

Couperthwaite, S.J., Johnstone, D.W., Mullett, M.E., Taylor, K.J., Millar, G.J., 2014. Minimization of bauxite residue neutralization products using nanofiltered seawater. *Ind. Eng. Chem. Res.* 53, 3787-3794.

Courtney, R.G., Timpson, J.P., 2005. Reclamation of fine fraction bauxite processing residue (red mud) amended with coarse fraction residue and gypsum. *Water Air Soil Poll.* 164(1-4), 91-102.

Courtney, R.G., Jordan, S.N., Harrington, T., 2009. Physico-chemical changes in bauxite residue following application of spent mushroom compost and gypsum. *Land. Degrad. Dev.* 20, 572-581.

Courtney, R., Harrington, T., 2010. Assessment of plant-available phosphorus in a fine textured sodic substrate. *Ecol. Eng.* 36, 542-547.

Courtney, R., Kirwan, L., 2012. Gypsum amendment of alkaline bauxite residue–plant available aluminium and implications for grassland restoration. *Ecol. Eng.* 42, 279-282.

Danielson, R.E., Sutherland, P.L., 1986. Porosity, in: Klute, A. (Ed), Methods of soil analysis. Part 1. Physical and Mineralogical Methods. SSSA, ASA, Madison, WI, pp. 443-461.

de Lima, A.C.A., Nascimento, R.F., de Sousa, F.F., Josue Filho, M., Oliveira, A.C., 2012. Modified coconut shell fibers: a green and economical sorbent for the removal of anions from aqueous solutions. *Chem. Eng. J.* 185, 274-284.

Dilmore, R.M., Howard, B.H., Soong, Y., Griffith, C., Hedges, S.W., DeGalbo, A.D., Morreale, B., Baltrus, J.P., Allen, D.E., Fu, J.K., 2009. Sequestration of CO2 in mixtures of caustic byproduct and saline waste water. *Environ. Eng. Sci.* 26, 1325-1333.

Eastham J, Morald T, Aylmore P., 2006. Effective nutrient sources for plant growth on bauxite residue. *Water Air Soil Poll.* 176(1–4),5–19

Egemose, S., Sønderup, M.J., Beinthin, M.V., Reitzel, K., Hoffmann, C.C., Flindt, M.R., 2012. Crushed concrete as a phosphate binding material: a potential new management tool. *J. Environ. Qual.* 41, 647-653.

EPA, 1996. EPA Method 3050B: Acid Digestion of Sediments, Sludges, and Soils. www.epa.gov/sites/production/files/2015-06/documents/epa-3050b.pdf [accessed 30.10.2017].

EPA, 2014. Drinking Water Parameters Microbiological, Chemical and Indicator Parameters in the 2014 Drinking Water Regulations. www.epa.ie/pubs/advice/drinkingwater/2015_04_21_ParametersStandaloneDoc.pdf [accessed 30.10.2017].

European Commission, 2015. COM 2015. 614 Communication from the commission to the European Parliament, the Council, the European Economic and Social Committee and the Committee of the regions - Closing the loop - An EU action plan for the circular economy. Brussels.

Evans, K., 2016. The history, challenges, and new developments in the management and use of bauxite residue. *J. Sustain. Metallurgy.* 2, 316-331.

Fergusson, L., 2009. Commercialisation of environmental technologies derived from alumina refinery residues: A ten-year case history of Virotec. http://citeseerx.ist.psu.edu/viewdoc/download?doi=10.1.1.458.2073&rep=rep1&type=pdf [accessed 08.12.17].

Fois, E., Lallai, A., Mura, G., 2007. Sulfur dioxide absorption in a bubbling reactor with suspensions of Bayer red mud. *Ind. Eng. Chem. Res.* 46, 6770-6776.

Grace, M.A., Healy, M.G., Clifford, E., 2015. Use of industrial by-products and natural media to adsorb nutrients, metals and organic carbon from drinking water. *Sci. Total. Environ.* 518, 491-497.

Grace, M.A., Clifford, E., Healy, M.G., 2016. The potential for the use of waste products from a variety of sectors in water treatment processes. *J. Clean. Prod.* 137, 788-802.

Goloran, J.B., Chen, C.R., Phillips, I.R., Xu, Z.H., Condron, L.M., 2013. Selecting a nitrogen availability index for understanding plant nutrient dynamics in rehabilitated bauxite-processing residue sand. *Ecol. Eng.* 58, 228-237.

Gräfe, M., Power, G., Klauber, C., 2009. Review of bauxite residue alkalinity and associated chemistry. CSIRO, Australia. http://enfo.agt.bme.hu/drupal/sites/default/files/vörösiszpa%20kémia%20és%20lúgossá g.pdf [accessed 12.12.17].

Hanahan, C., McConchie, D., Pohl, H.,, Creelman, R., Clark, M., Stocksiek C., 2004. Chemistry of seawater neutralization of bauxite refinery residues (red mud). *Environ. Eng. Sci.* 21, 125–138

Huang, W., Wang, S., Zhu, Z., Li, L., Yao, X., Rudolph, V., Haghseresht, F., 2008. Phosphate removal from wastewater using red mud. *J. Hazard. Mater.* 158, 35-42.

IAI, 2015. Bauxite residue management: best practice. http://www.world-aluminium.org/media/filer_public/2015/10/15/bauxite_residue_management_-_best_practice_english_oct15edit.pdf. [accessed 14.10.2017].

Jacukowicz-Sobala, I., Ociński, D., Kociołek-Balawejder, E., 2015. Iron and aluminium oxides containing industrial wastes as adsorbents of heavy metals: Application possibilities and limitations. *Waste. Manage. Res.* 33, 612-629.

Johnston, M., Clark, M.W., McMahon, P., Ward, N., 2010. Alkalinity conversion of bauxite refinery residues by neutralization. *J. Hazard. Mater.* 182, 710-715.

Jones, B.E., Haynes, R.J., 2011. Bauxite processing residue: a critical review of its formation, properties, storage, and revegetation. *Crit. Rev. in Env. Sci. Tec* 41, 271-315.

Jones, B.E., Haynes, R.J., Phillips, I.R., 2012. Addition of an organic amendment and/or residue mud to bauxite residue sand in order to improve its properties as a growth medium. *J. Environ. Manage.* 95, 29-38.

Kirwan, L.J., Hartshorn, A., McMonagle, J.B., Fleming, L., Funnell, D., 2013. Chemistry of bauxite residue neutralisation and aspects to implementation. *Int. J. Miner. Process.* 119, 40-50.

Klauber, C., Gräfe, M., Power, G., 2011. Bauxite residue issues: II. options for residue utilization. *Hydrometallurgy.* 108, 11-32.

Lehoux, A.P., Lockwood, C.L., Mayes, W.M., Stewart, D.I., Mortimer, R.J., Gruiz, K., Burke, I.T., 2013. Gypsum addition to soils contaminated by red mud: implications for aluminium, arsenic, molybdenum and vanadium solubility. *Environ. Geochem.* Hlth 35, 643-656.

Li, L.Y., 2001. A study of iron mineral transformation to reduce red mud tailings. *Waste Manage.* 21, 525-534.

Li, Y., Liu, C., Luan, Z., Peng, X., Zhu, C., Chen, Z., Zhang, Z., Fan, J., Jia, Z., 2006. Phosphate removal from aqueous solutions using raw and activated red mud and fly ash. *J. Hazard. Mater.* 137, 374-383.

Liu, Y., Lin, C., Wu, Y., 2007. Characterization of red mud derived from a combined Bayer Process and bauxite calcination method. *J. Hazard. Mater.* 146, 255-261.

Liu, W., Chen, X., Li, W., Yu, Y., Yan, K., 2014. Environmental assessment, management and utilization of red mud in China. *J. Clean. Prod.* 84, 606-610.

Lopez, E., Soto, B., Arias, M., Nunez, A., Rubinos, D., Barral, M.T., 1998. Adsorbent properties of red mud and its use for wastewater treatment. *Water. Res.* 32, 1314-1322.

Mayes, W.M., Burke, I.T., Gomes, H.I., Anton, A.D., Molnár, M., Feigl, V., Ujaczki, É., 2016. Advances in understanding environmental risks of red mud after the Ajka spill, Hungary. *J. Sustain. Metallurgy.* 2, 332-343.

Menzies, N.W., Fulton, I.M., Morrell, W.J., 2004. Seawater neutralization of alkaline bauxite residue and implications for revegetation. *J. Environ. Qual.* 33, 1877-1884.

McBride, M.B., 2000. Chemisorption and precipitation reactions. Handbook of Soil Science. CRC Press, Boca Raton, FL, B265-B302.

McConchie, D., Clark, M., Davies-McConchie, F., 2001. Processes and Compositions for Water Treatment, Neauveau Technology Investments, Australian, p. 28.

Newson, T., Dyer, T., Adam, C., Sharp, S., 2006. Effect of structure on the geotechnical properties of bauxite residue. *J. Geotech. Geoenviron.* 132, 143-151.

Palmer, S.J., Frost, R.L., 2009. Characterisation of bauxite and seawater neutralised bauxite residue using XRD and vibrational spectroscopic techniques. *J. Mater. Sci.* 44, 55-63.

Power, G., Gräfe, M., Klauber, C., 2011. Bauxite residue issues: I. Current management, disposal and storage practices. *Hydrometallurgy.* 108, 33-45.

Pradhan, J., Das, S.N., Das, J., Rao, S.B., Thakur, R.S., 1996. Characterization of Indian red muds and recovery of their metal values. Annual meeting and exhibition of the minerals, metals and materials society, Anaheim, CA, 4 – 8 February 1996.

Prajapati, S.S., Najar, P.A., Tangde, V.M., 2016. Removal of Phosphate Using Red Mud: An Environmentally Hazardous Waste By-Product of Alumina Industry. Adv. Phy. Chemistry, 2016.

Snars, K., Gilkes, R.J., 2009. Evaluation of bauxite residues (red muds) of different origins for environmental applications. *Appl. Clay. Sci.* 46, 13-20.

Thomas, G.W., 1982. Exchangeable cations. Methods of soil analysis. Part 2. Chemical and microbiological properties, (methodsofsoilan2), 159-165.

Vakros, J., Kordulis, C., Lycourghiotis, A., 2002. Potentiometric mass titrations: a quick scan for determining the point of zero charge. *Chem. Commun.* 17, 1980-1981.

Vohla, C., Alas, R., Nurk, K., Baatz, S., Mander, Ü., 2007. Dynamics of phosphorus, nitrogen and carbon removal in a horizontal subsurface flow constructed wetland. *Sci. Tot. Environ.* 380, 66-74.

Wang, S., Ang, HM., Tadé, M.O., 2008. Novel applications of red mud as coagulant, adsorbent and catalyst for environmentally benign processes. *Chemosphere.* 72, 1621–1635

Wang, B., Lehmann, J., Hanley, K., Hestrin, R., Enders, A., 2015. Adsorption and desorption of ammonium by maple wood biochar as a function of oxidation and pH. *Chemosphere.* 138, 120-126.

Wang, Z., Shen, D., Shen, F., Li, T., 2016. Phosphate adsorption on lanthanum loaded biochar. *Chemosphere.* 150, 1-7.

Xue, S., Zhu, F., Kong, X., Wu, C., Huang, L., Huang, N., Hartley, W., 2016. A review of the characterization and revegetation of bauxite residues (Red mud). *Environ. Sci. Poll. Res.* 23, 1120-1132.

Ye, J., Zhang, P., Hoffmann, E., Zeng, G., Tang, Y., Dresely, J., Liu, Y., 2014. Comparison of response surface methodology and artificial neural network in optimization and prediction of acid activation of Bauxsol for phosphorus adsorption. *Water Air Soil Poll.* 225(12), 2225.

Zhu, F., Li, Y., Xue, S., Hartley, W., Wu, H., 2016. Effects of iron-aluminium oxides and organic carbon on aggregate stability of bauxite residues. *Environ. Sci. Pollut. Res.* 23, 9073-9081.

Chapter 5

The use of rapid small-scale column tests to determine the efficiency of bauxite residue as a low-cost adsorbent in the removal of dissolved reactive phosphorus from agricultural waters.

Overview

The aim of this chapter was to determine the efficiency of fine fraction bauxite residue as a low-cost adsorbent in the removal of phosphorus (P) from both low and high P concentrated wastewater types. The bauxite residue media was also characterised before and after use as a P adsorbent. It was fully intended to use the gypsum treated fine fraction bauxite residue identified from the previous study (Chapter 4) which was identified as having an increased phosphorus adsorption capacity following treatment with gypsum. However, clogging arose when using the gypsum treated fine fraction bauxite residue when carrying out preliminary continuous flow experiments as a result of the low permeability associated with the fine fraction bauxite residue. Following the trialling the mixing the gypsum treated fine fraction bauxite residue with sand and Puraflo, clogging issues still arose. Finally, a technique developed by Dr. Oisín Callery (patent pending) was applied to the fine fraction bauxite residue and resulted in an increase in the permeability and also reduced the pH of the fine fraction bauxite residue.

This study has been published in the Journal of Environmental Management. (Cusack, P. B., Callery, O., Courtney, R., Ujaczki, É., O'Donoghue, L.M. and Healy, M.G., 2019. The use of rapid small-scale column tests to determine the efficiency of bauxite residue as a low-cost adsorbent in the removal of dissolved reactive phosphorus from agricultural waters. Journal of Environmental Management, 241, pp.273-283. DOI Link: https://doi.org/10.1016/j.jenvman.2019.04.042). Patricia B. Cusack carried out all the experimental analysis and is the primary author of this publication. Dr. Oisín Callery developed the design and model of the rapid small-scale column tests. Dr. Ronan

Courtney and Dr. Mark G. Healy also contributed to the experimental design and set-up and were the main contributors to the editing of this manuscript, with inputs also from Dr. Oisín Callery regarding the modelled data. Dr. Éva Ujaczki and Dr. Lisa M. O' Donoghue were also listed as authors on this publication as this study was part of the overall Alsource project.

5.1 Introduction

Phosphorus (P) is an essential component of all plant and animal life (Desmidt et al., 2015; Weissert and Kehr, 2018), and is critical in the production and maintenance of food supply (Cordell and White 2011; Pretty and Bharucha, 2014). Phosphorus is also identified as one of the key nutrients that leads to the eutrophication of water bodies, in which there is an excess production of algal blooms, resulting in detrimental effects to the aquatic life of the water body (Pan et al., 2018; Schindler et al., 2016). Agricultural practices, such as the application of slurry and fertiliser, may result in the transport of nutrients in surface runoff (Murnane et al., 2016a; Pan et al., 2018) and subsurface flow (O' Flynn et al., 2018; Zhou et al., 2016) to a water body, and have been identified as a major cause of eutrophication (Sharpley, 2016).

The movement of P from soil to water bodies is predominantly in the form of particulate or dissolved reactive P (DRP) (Brennan et al., 2014), the latter being 100% available for aquatic biota and which, therefore, has an immediate effect on the surrounding ecosystems (Penn et al., 2014). Conventional methods of P removal from water have involved the use of enhanced biological removal systems such as polyphosphate accumulating organisms (PAOs) (Ge et al., 2015) and algal biofilms (Sukačová et al., 2015), precipitation methods using hydrous ferric oxides (Hauduc et al., 2015) or struvite (Zhou et al., 2015), the use of adsorbents (Grace et al., 2015; Callery et al., 2016; Callery and Healy, 2017), ion exchange (Acelas et al., 2015), and reverse osmosis (Wang et al., 2016). In recent years, to address the concept of a 'circular economy' (United Nations, 2015), emphasis has been placed on the utilisation of industrial wastes as low-cost adsorbents (De et al., 2018; De Gisi et al., 2016; Grace et al., 2016). Materials that have been utilised include fly ash (Nowak et al., 2013; Vohla et al., 2011), steel slags (Barca et al., 2012; Claveau-Mallet et al., 2013) and chemical amendments (Callery et al., 2015). Particular focus has been placed on bauxite residue (red mud), the by-product generated in the Bayer Process during the extraction of alumina, as a potential low-cost P adsorbent

in aqueous solutions. It is currently being produced at a global rate of 150 Mt per annum (Evans 2016), but only approximately 2 % of the bauxite residue produced is currently re-used (Ujaczki et al., 2018), with the remaining ~ 98% being disposed of into bauxite residue disposal areas (BRDAs) (Burke et al., 2013; Kong et al., 2017). The general composition of bauxite residue comprises high amounts of iron (Fe) and aluminium (Al) oxides (Zhu et al., 2016), which are good adsorbents of P. In addition, bauxite residue has a high specific surface area (Gräfe et al., 2011) and therefore has numerous potential adsorption sites, giving it increased capacity for P retention. Previous laboratory studies have shown that bauxite residue has high P adsorption capacity (Table 5.1).

Table 5.1 Phosphorus (P) adsorption studies that have been carried out using bauxite residue, untreated and treated residues, and their recovery efficiencies (adapted from Cusack et al., 2018).

	P recovery technique	Factors investigated	Type of water	Initial P concentration of the water	P recovered	Reference
Untreated bauxite residue	Batch adsorption experiment	Kinetics, pH and temperature	Synthetic water	5-100 mg P L^{-1}	0.20 mg P g^{-1}	Grace et al., 2015
Untreated bauxite residue	Column study	Initial concentration, particle size	Synthetic water	60-1000 mg P L^{-1}	25 mg P g^{-1*}	Herron et al., 2016
Untreated bauxite residue	Batch adsorption experiment	Initial concentration, pH, particle size	Synthetic water	10-150 mg P L^{-1}	0.345-1 mg P g^{-1}	Cusack et al., 2018
Gypsum Treated	Batch adsorption experiment	Contact time	Synthetic water	20-400 mg P L^{-1}	7.03 mg P g^{-1}	Lopez et al., 1998

Gypsum Treated	Batch adsorption experiment	Initial concentration, pH, particle size	Synthetic water	10-150 mg P L^{-1}	1.39-2.73 mg P g^{-1}	Cusack et al., 2018
Seawater Treated	Batch adsorption experiment	Initial concentration, pH, particle size	Synthetic water	10-150 mg P L^{-1}	0.48-1.92 mg P g^{-1}	Cusack et al., 2018
Brine treated bauxite residue (Bauxsol™)**	Batch adsorption experiment	pH, ionic strength, time	Synthetic water	0.5-2 mg P L^{-1}	6.5-14.9 mg P g^{-1}	Akhurst et al., 2006
Brine treated bauxite residue (Bauxsol™)**	Column study	Kinetics, particle size	Secondary treated effluent	3-9.2 mg P L^{-1}	2.85-8.74 mg P g^{-1}	Despland et al., 2011
Acid and brine treated bauxite residue (Bauxsol™)**	Batch adsorption experiment	Kinetics and isotherms	Synthetic water	200 mg P L^{-1}	55.72 mg P g^{-1}	Ye et al., 2014

Heat treated bauxite residue	Batch adsorption experiment	Time, pH and initial concentration	Synthetic water	155 mg P L^{-1}	155.2 mg P g^{-1}	Liu et al., 2007
Acid and heat treated bauxite residue	Batch adsorption experiment	Time, pH and initial concentration	Synthetic water	155 mg P L^{-1}	202.9 mg P g^{-1}	Liu et al., 2007
Acid treated bauxite residue	Batch adsorption experiment	Acid type, pH	Synthetic water	1 mg P L^{-1}	1.1 mg P g^{-1}	Huang et al., 2008

*P_{max} value given i.e. Maximum amount of P adsorbed per g of media, as determined using the Langmuir adsorption isotherm.

**Bauxsol™ = neutralised bauxite residue produced using the Basecon™ procedure, which uses brines high in Ca^{2+} and Mg^{2+} (McConchie et al., 2001).

Traditionally, bench-scale "batch" studies are conducted to evaluate the effectiveness of a material to adsorb P (Table 5.1). These studies involve placing the material in small containers, overlaying it with solutions of known concentrations, mixing for a period usually of between 24 to 48 hr, and then fitting the results obtained to an adsorption isotherm such as the Freundlich or Langmuir, in order to quantify its adsorption potential (Cusack et al., 2018; Grace et al., 2015). However, batch studies have some disadvantages, such as failing to replicate the often passive nature of the adsorption process which exists on site, as well as sometimes using unrealistic ratios of adsorbent to solution, and shaking of the samples (ÁdÁm et al., 2007; Søvik and Kløve, 2005). In addition, concerns have been raised about their accuracy in replicating the actual performance when the adsorbent material is placed in a filter and operated on site (Fenton et al., 2009). Due to the nature of the batch experiment, they also fail to realistically replicate any incidental releases of contaminants, which may occur when some materials are placed in filters. This may be particularly pertinent in the evaluation of the feasibility of bauxite residue, which contains metals (Cusack et al., 2018). In order to determine the full potential and longevity of an adsorbent, larger scale "column" studies are necessary (Pratt et al., 2012). In these studies, the material is placed in a column, usually operated at laboratory-scale, and water of a known concentration is passed through the material until the effluent concentration is the same as the influent concentration. These continuous flow column studies require vast amounts of influent water, which depending on the type of water utilised, is often difficult to source in the laboratory (Callery and Healy 2017). On account of this, rapid, small-scale column studies which utilise smaller volumes of media and wastewater have been gaining in popularity, and have been used to successfully model the adsorbancies of P (Callery et al., 2016; Lalley et al., 2015), fluoride (Brunson and Sabatini, 2014; Wu et al., 2018), paracetamol (García-Mateos et al., 2015), and varying species of arsenic (Pantoja et al., 2014; Tresintsi et al., 2014).

As P adsorption tests on bauxite residues have been commonly conducted using batch-scale studies, which may have many shortcomings as detailed above, the objectives of this study were to use rapid, small-scale column studies to (1) to assess the potential of bauxite residue as a low-cost adsorbent for DRP removal from two types of an agricultural water (dairy soiled water (DSW)) and forest run-off (2) compare the composition of the bauxite residue media before and after use in the column tests (3) investigate the

speciation of P adsorption onto the bauxite residue, and (4) identify any potential trace metal mobilisation from the bauxite residue during the study.

5.2. Materials and Methods

5.2.1 Sample Collection

Bauxite residue was obtained from a European refinery. Residue was sampled to a depth of 30 cm below the surface of the BRDA, returned to the laboratory and dried at 105˚C for 24 hr. Once dry, the samples were pulverised using a mortar and pestle and sieved to a particle size < 0.5 mm. The pH and electrical conductivity (EC) were measured (n=3) using 5 g of sample in an aqueous extract, using a 1:5 ratio (solid:liquid) (Courtney and Harrington, 2010). Dairy soiled water (milk parlour washings composed of cow faeces and urine, milk and detergents; Minogue et al., 2015) was collected from Teagasc Agricultural Research Centre, Moorepark, Co. Cork, Ireland [52° 9' 48.114" N, 8° 15' 34.6464" W] and forest run-off was collected from Kilmoon, Co. Clare, Ireland [53° 2' 48.0372" N, 9° 16' 21.1368" W]. The DSW and forest run-off were transferred directly to a temperature-controlled room (11°C) prior to commencement of testing. The DRP was measured using filtered (0.45 µm) subsamples using a nutrient analyser (Konelab20, Thermo Clinical Lab systems, Finland) and the pH was measured using a Eutech Instruments pH 700 (Thermo Scientific, USA).

5.2.1.1 Media Characterisation

The bauxite residue media was characterised before and after the experiment. Mineralogical detection was carried out on 1 g powdered samples using X-ray diffraction (XRD) on a Philips X'Pert PRO MPD® (California, USA) at 40 kV, 40 mA, 25 °C by Cu X-ray tube (Kα-radiation). The patterns were collected in the angular range from 5 to 80 º (2ɵ) with a step-size of 0.008 º (2ɵ) (Castaldi et al., 2011). The surface morphology and elemental detection were carried out using scanning electron microscopy (SEM) and energy-dispersive X-ray spectroscopy (EDS) on a Hitachi SU-70 (Berkshire, UK). X-ray fluorescence (XRF) analysis was carried out onsite at the refinery using a Panalytical Axios XRF.

5.2.2 Rapid Small Scale Column Study

Small bore adsorption columns were prepared after Callery et al., (2016) using polycarbonate tubes, with an internal diameter of 0.94 cm and lengths of 20, 30 and 40

cm. The tubes were packed with a mixture of bauxite residue. The bauxite residue was held in place within each column using acid-washed glass wool and plastic syringes with an internal diameter equal to outside diameter of the polycarbonate tube, placed at the top and bottom of each of the polycarbonate tube columns. To each end of the polycarbonate tube column, flexible silicone tubing was attached to the syringe ends in order to provide lines for the influent and effluent. The columns were secured on a metal frame, allowing for a stable, vertical orientation to be maintained, as seen in Figure 5.1. A Masterflex® L/S Variable-Speed Drive peristaltic pump (Gelsenkirchen, Germany) with a variable speed motor was used to pump the influent, DSW and forest run-off, into the base of each column at an estimated flow rate of 30.49 ± 0.85 mL hr^{-1} (equivalent to a hydraulic loading rate used in a P removal system for wastewater treatment on a poultry farm; Penn et al., 2014). The pump was operated in 12 hr on/off cycles (to allow the filter media to replenish some of its adsorption sites) to achieve loading periods of 24 – 36 hr, in order to obtain enough data points for the determination of the adsorption model coefficients. Every 2 hr, aliquots of the filtered effluent were collected using an auto-sampler and measured for volume, pH and DRP.

Figure 5.1 Image of the rapid small-scale column tests (RSSCT) set-up used in this study.

The adsorption performance of the media was evaluated using a model developed by Callery and Healy (2017), wherein the column effluent (C_e) is taken as a function of the volume of influent treated (V) and breakthrough concentrations (BTCs) formed by plotting V (x-axis) against C_e (y-axis). The breakthrough of the column media was taken to be when the column effluent is approximately 5% of the influent concentration (Chen et al., 2003).

The overall bauxite residue media service time or longevity of the bauxite residue media can be found by first determining the volume treated, using Eqn. 1, where q_t is the time dependent sorbate concentration per unit mass of adsorbent (mg g^{-1}), M is the mass of the adsorbent (g), B is a constant of system heterogeneity, C_o is the sorbate concentration of

the influent (mg L^{-1}) and C_t is the solution adsorbate concentration at any filter depth (mg L^{-1}), by dividing the volume treated, V (in L) by the loading rate (L min^{-1}).

$$V = \frac{q_t \, M}{B \, (C_o - C_t)}$$

(1)

The q_t used in Eqn. 1 was calculated using Eqn. 2:

$$q_t = AV_B^{\left(\frac{1}{B}\right)} \Big| \frac{t}{t+a^{**}}$$

(2)

Where A is a constant of proportionality (mg L^{-1}), t is the service time/operating time of the filter bed at the end of the rapid small-scale column test (min), and a** is a time constant.

5.2.3 Speciation of P Adsorbed

Fourier transform infrared (FT-IR) analysis was carried out using a Perkin Elmer Spectrum 100 (PerkinElmer, USA). The FT-IR spectra were recorded in the 4000 to 650 cm^{-1} range and were collected after 256 scans at 4 cm^{-1} resolution (Castaldi et al., 2010).

5.2.4 Trace Metal Analysis

Every 2 hr, 10 mL of the aliquot collected from the columns, was preserved in nitric acid (HNO$_3$), to a pH <2 and refrigerated before elemental analysis was carried out using an Agilent Technologies 5100 Inductively Coupled Plasma Optical Emission Spectrometer (ICP-OES). In order to carry out the ICP-OES analysis, a calibration curve was created using standardised solutions comprised of 100, 50, 10, 5 and 1 g L^{-1} multi element standard (Inorganic Ventures, Ireland) and 1M HNO$_3$. The analytical lines (in nm) used for the calculations of each element were as follows: Al 237.312, 396.152; calcium (Ca) 396.847, 422.673; cadmium (Cd) 214.439, 226.502, 228.802; chromium (Cr) 205.560, 267.716, 357.868; copper (Cu) 213.598, 324.754, 327.395; Fe 234.350, 238.204, 259.940; gallium (Ga) 287.423, 294.363, 417.204; mercury (Hg) 184.887, 194.164; magnesium (Mg) 279.553, 280.270, 285.213; manganese (Mn) 257.610, 259.372, 260.568; molybdenum (Mo) 202.032, 203.846, 204.598; sodium (Na) 589.592; nickel (Ni) 216.555, 221.648, 231.604; lead (Pb) 220.353, 283.305; selenium (Se) 196.026, 203.985; silicon (Si) 250.690, 251.611, 288.158; vanadium (V) 268.796, 292.401,

309.310; zinc (Zn) 202.548, 206.200, 213.857 (Bridger and Knowles, 2010). The XRF analysis performed on the bauxite residue was carried out using a Panalytical Axios XRF (Malvern Panalytical Ltd., United Kingdom).

5.3 Results and Discussion

5.3.1 Media Characterisation Before and After the Experiments

Bauxite residue typically comprises Fe, Al, Ti, Si, Na and Ca, mainly in the form of oxides (Gräfe et al., 2009). The presence of Fe and Al oxides, which can range from 5 to 60 and 5 to 30 %, respectively (Evans 2016), and Ti oxides, which are typically in the range of 0.3 to 15 % (Evans 2016), mean that bauxite residue is a potential adsorbent for both cations and anions from aqueous solutions (Arco-Lázaro et al., 2018; Atasoy and Bilgic 2018; Bhatnagar et al., 2011; Cusack et al., 2018). This is why numerous studies have investigated the potential of P removal from aqueous solution (Table 5.1).

The main mineralogical composition of the bauxite residue used in this study comprised mainly iron and aluminium oxides (Fe_2O and Al_2O_3) (Table 5.2). SEM-EDS analysis also indicated the dominance of Fe and Al (Figure D1 in Appendix D). Titanium, Si, Ca and Na were also detected in the main composition. Prior to use in the column, there was a mineralogical dominance of the iron oxide hematite (as represented by H in Figure 5.2), detected at positions 33.153 and 35.612°2Θ, respectively (Figure 5.2). Rutile (TiO_2) was also detected at position 27.459 °2Θ. Following the column trials, XRD analysis was carried out on the spent media from both the DSW and forest run-off columns. New peaks were identified in the XRD patterns, as seen in Figure 5.2, which show the presence of P-based minerals, which were not present in the raw media. The new peaks detected in both the spent media following treatment of the DSW and forest run-off include calcium hydrogenphosphate (III) hydrate ($CaHPO_4.3H_2O$) at positions 19.120 and 30.001 °2Θ in the spent media following the treatment of the DSW. The presence of this mineral in the spent media indicates P retention within the bauxite residue after treatment.

Table 5.2 Main mineralogical composition (%) of the bauxite residue determined by XRF.

Mineral oxide	%
Aluminum oxide, Al_2O_3	14.8 ± 1.5
Iron oxide, Fe_2O	47.5 ± 2.0
Titanium oxide, TiO_2	10.3 ± 0.95
Silicon oxide, SiO_2	7.20 ± 1.0
Calcium oxide, CaO	6.1 ± 1.0
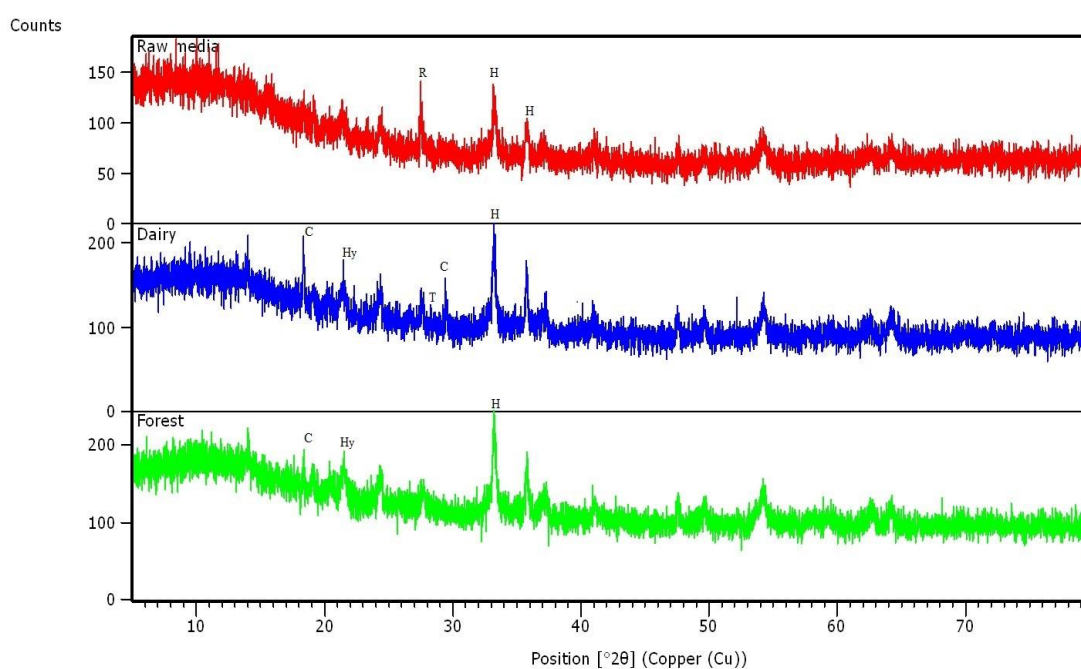
Figure 5.2 XRD pattern as determined for the column media before ('Raw media', top) and after the loading period with DSW ('Dairy', middle) and forest run-off ('Forest', bottom). Hematite (H; Fe_2O_3), detected at position 33.153 and 35.612°2Θ and rutile (R; TiO_2), detected at position 27.459 °2Θ were present in the raw bauxite residue media. Calcium hydrogenphosphate (III) hydrate (C; $CaHPO_4.3H_2O$), detected at positions 19.120 and 30.001 °2Θ was present in both the spent media following treatment of the DSW and forest run-off.

5.3.2 Influent and Effluent Water Characterisation and Rapid Small-scale Column Study

The forest run-off had a pH of 7.57 and a DRP concentration of 1.10 mg P L^{-1}. The total phosphorus (TP) concentration of forest run-off is usually around 1 mg L^{-1} (Finnegan et al., 2012), whereas DSW has a TP concentration of 20 to 100 mg L^{-1} and a total nitrogen (TN) concentration of 70 to 500 mg L^{-1} (Minogue et al., 2015). The DSW used in this study had a pH of 7.79 and a DRP concentration of 10.64 mg P L^{-1}.

The BTC approached saturation much quicker for the DSW than for the forest run-off water (Figure 5.3(a) and 5.3(b)). Similar to the findings of Vuković et al., (2011), the breakthrough time and exhaustion time increased with bed depth. As a result of its composition, there are other anions such as nitrates (NO$_3^-$) and nitrites (NO$_2^-$) present in the DSW (Ruane et al., 2011), and therefore there is greater competiveness for available adsorption sites and interferences between the adsorbent surface and the ions present in the aqueous solution. This may explain why the DSW-treating columns generated a BTC approaching saturation much faster than the bauxite residue columns treating forest run-off. When treating the forest run-off, the bauxite residue media had a service time of approximately 22.80 min, based on the largest column before the initial breakthrough time of the bauxite residue media occurred. However, when treating the DSW, it had a shorter service time of 5.80 min, as noted for the largest column before the initial breakthrough occurred. Taking into account the amount of bauxite residue media used in the largest columns (21.16 and 20.78 g), this gives an estimated service time of 1.08 min g^{-1} bauxite residue and 0.28 min g^{-1} bauxite residue when treating forest run-off and DSW, respectively, before initial breakthrough (5%) would occur.

The modelled qt value, which is the sorbate concentration per unit mass of the bauxite residue, was 0.27 mg P g^{-1} media and 0.045 mg P g^{-1} media when treating the DSW and forest run-off, respectively. This overall P adsorption rate is lower than that recorded by Despland et al. (2011), who reported values of between 2.85 and 8.74 mg P g^{-1} for Bauxsol (neutralised bauxite residue using synthetic brine water based on a seawater neutralisation technique) media used when treating secondary effluent and by Herron et al., (2016), who, in their column trials found an adsorption rate of 25 mg P g^{-1} as estimated using the Langmuir adsorption isotherm when treating synthetic water. In general, bauxite residue typically has a low P adsorption rate (Bhatnagar et al., 2011),

however once amended through the application of treatments such as acid (Ye et al., 2014) and heat (Liu et al., 2007), the P adsorption capacity increases as noted in the studies previously mentioned.

When comparing the bauxite residue media used in this study to other studies which have trialled the incorporation of other possible low-cost adsorbents such as zeolites and granular ceramics, it was found that bauxite residue media had a higher P adsorbency rate, when compared to a P adsorption rate of 0.01 mg P g^{-1} for zeolite (Grace et al., 2015) and a P adsorbent rate of 0.9 mg g^{-1} for the granular ceramics (Chen et al., 2012). However, the bauxite residue media used in this study did show a lower P adsorption rate when compared to crushed concrete, which had a P adsorbent rate of 19.6 mg P g^{-1} (Egemose et al., 2012) and untreated biochar, which had a P adsorption rate of 32 mg P g^{-1} (Wang et al., 2015).

Although the values reported in this study are lower other studies using bauxite residue (treated) and other potential low-cost adsorbents such as biochar and crushed concrete, it is important to note that full saturation of the bauxite residue was not reached and the type of wastewaters used had an impact on the P adsorption capacity with interferences and competion for adsorption sites highlighted when using 'real' wastewater types such as DSW, due to containing other ions and contaminants in addition to the phosphate ions.
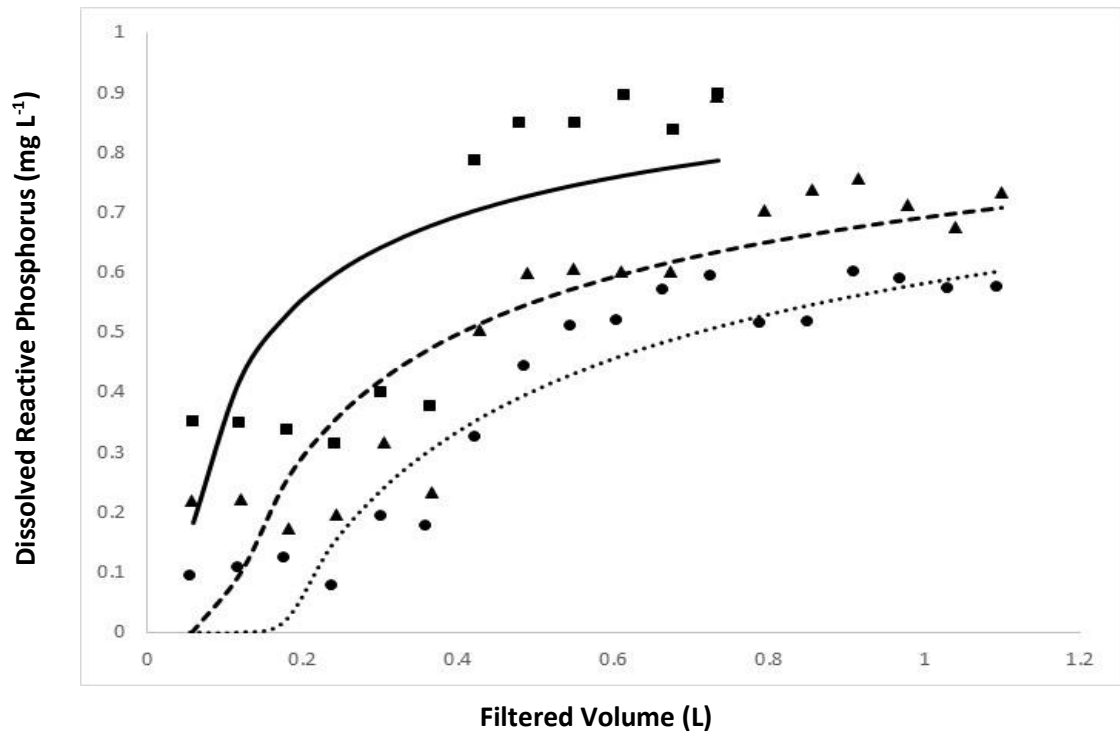
Figure 5.3(a) The breakthrough curves for the effluent dissolved reactive phosphorus concentration versus loading time for forest run-off using experimental and modelled data.
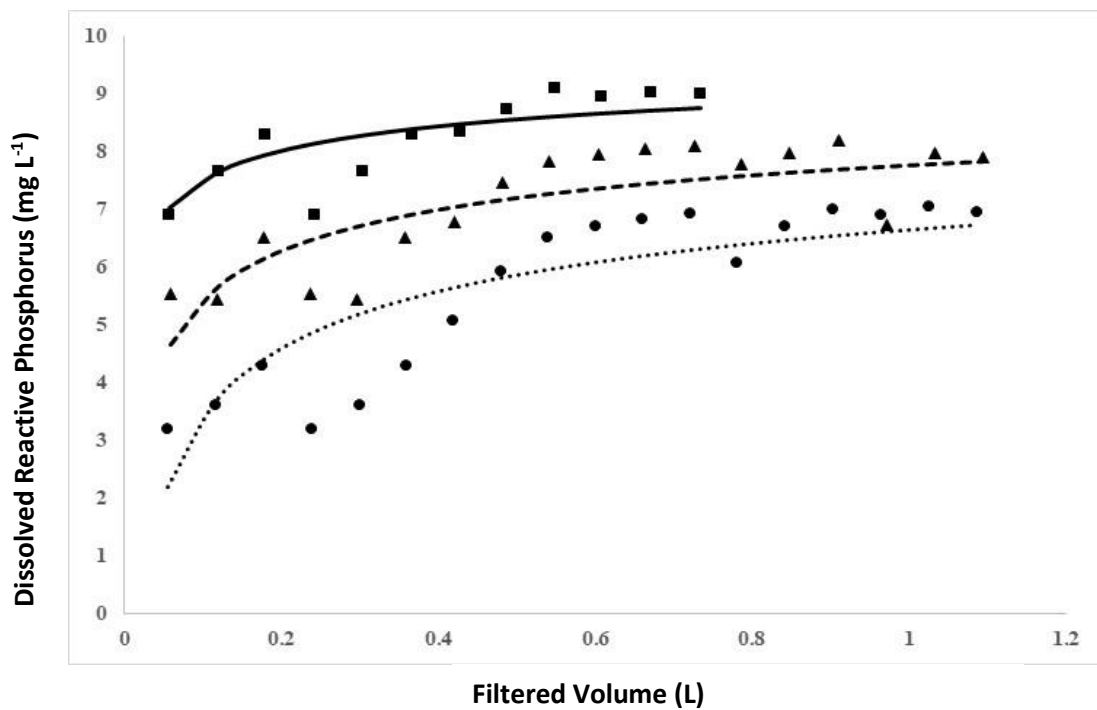
Figure 5.3(b) The breakthrough curves for the effluent dissolved reactive phosphorus concentration versus loading time for dairy soiled water using experimental and modelled data.

5.3.3 Speciation of P Adsorbed

The adsorption of phosphate ions onto an adsorbent is measured by the decrease for phosphate in the influent after a certain amount of time (Loganathan et al., 2014). Typically, the main mechanism of phosphate adsorption (and other anions and cations) onto the surface of iron and aluminium oxides may be separated into two processes: specific and non-specific adsorption (Stumm, 1992; Cornell and Schwertmann, 2003). Specific adsorption takes place through the process of ligand exchange (Jacukowicz-Sobala et al., 2015). A phosphate ion exchanges with one or more hydroxyl groups, with the release of OH_2 and/or OH^- back into the surrounding solution, contributing to the alkalisation of the surrounding environment (Cornell and Schwertmann, 2003), as shown in the following equations:

$$\equiv FeOH + An^- \leftrightarrow \equiv FeAn + OH^- \tag{3}$$
$$\equiv Fe(OH)_2 + An^- \leftrightarrow \equiv Fe_2 + An^+ + 2OH^- \tag{4}$$

Non-specific adsorption, which was the main mechanism evident in this study, is inclusive of electrostatic interactions and surface precipitation (Loganathan et al., 2014) between the surface of the sorbent and the phosphate ion (Jacukowicz-Sobala et al., 2015). The electrostatic interactions occur between the electric charge carried on the surface of the sorbent and type of ion present in the surrounding solution. Phosphate ions, which are of anionic nature, carry a negative charge, which interacts with the positive charge as carried by Ca, a cation (Loganathan et al., 2014). Surface precipitation involves the formation of complexes/precipitates on the surface of the sorbent such as $CaHPO_4^{3-}$ as a result of these ion interactions (Loganathan et al., 2014). The adsorption of the phosphate ions is greatest in a low pH environment due to the abundance of positively charged sites (Jacukowicz-Sobala et al., 2015).

X-ray diffraction and SEM analysis have been used in previous studies to show evidence of the presence of newly formed surface precipitates following the P adsorption process (Bowden et al., 2009). The XRD data obtained in this study (Figure 1) show that the main interactions and complexes formed by the phosphate ions present in the wastewater (negative charge) were with Ca (positive charge) present in the bauxite residue, as evidenced by the presence of new peaks of $CaHPO_4^{3-}$ in the XRD patterns following the

treatment of both the DSW and forest run-off. Depending on the pH of the solution, the species of P found in aqueous solution are H_3PO_4 (pH < 4), $H_2PO_4^-$ (pH ~ 0-9), HPO_4^{2-} (pH ~ 5-11) and PO_4^{3-} (pH >10) (Karageorgiou et al., 2007; Despland et al., 2011).

The FT-IR analysis of the bauxite residue media before and after treatment of both the DSW and forest run-off (Figures 5.4 and 5.5) indicated that similar changes occurred in the media following treatment of both wastewaters. Two distinct broad bands were detected between wavelength 600 to 900 cm^{-1} and again at 1000 to 1400 cm^{-1}. This was evident for both the DSW and forest run-off spent media. Intensive IR absorption bands are typically in the range of 560 to 600 cm^{-1} and 1000 to 1100 cm^{-1} for P species (Tejedor-Tejedor and Anderson, 1990; Berzina-Cimdina and Borodajenko, 2012). However, it was not possible to identify specific P species due to some interferences, which are most likely due to the presence of many other ions present in each of the wastewater sources used.
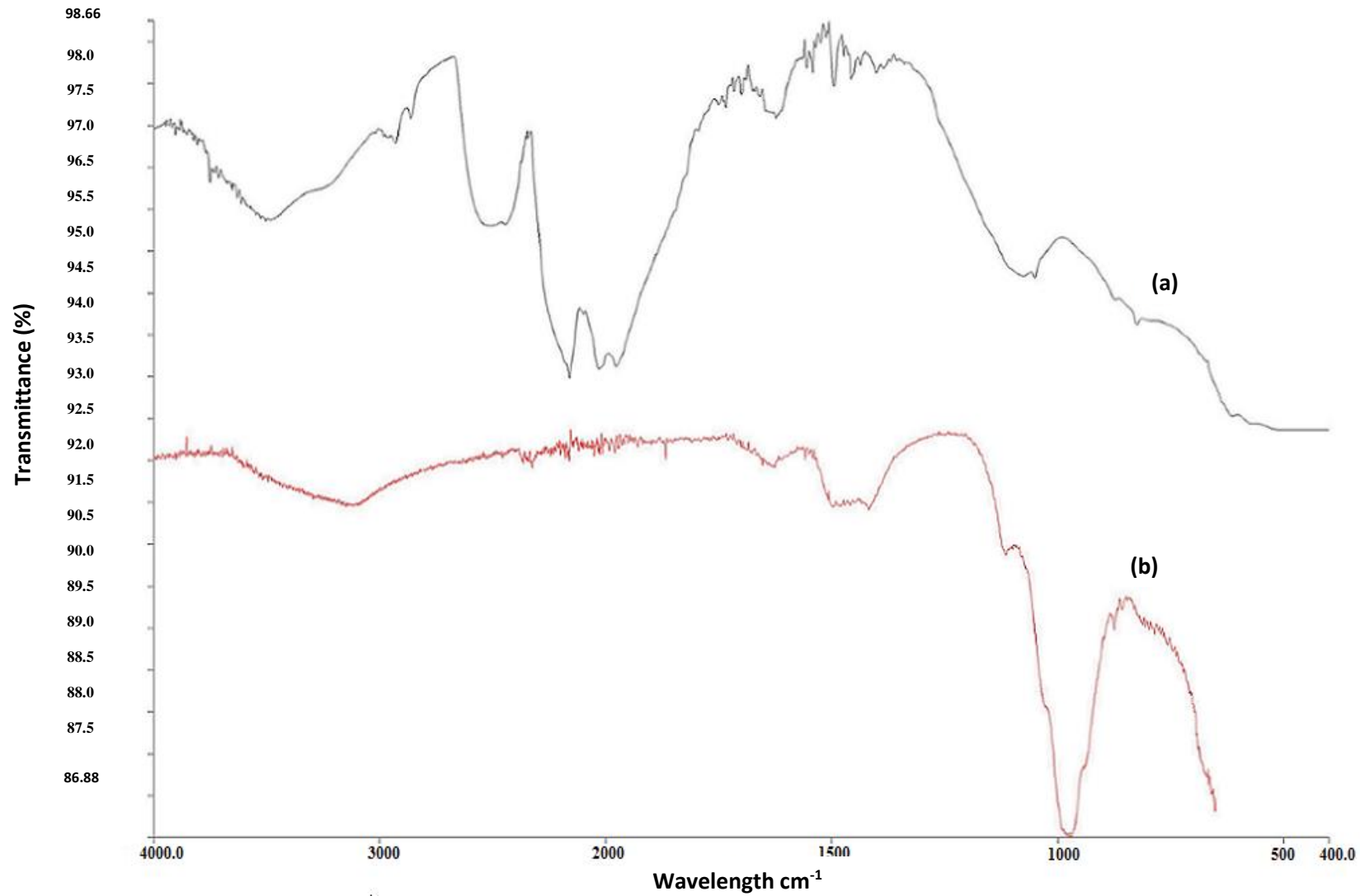
Figure 5.4 FT-IR analysis of the bauxite residue media before (a) and after use in the column treating DSW (b).
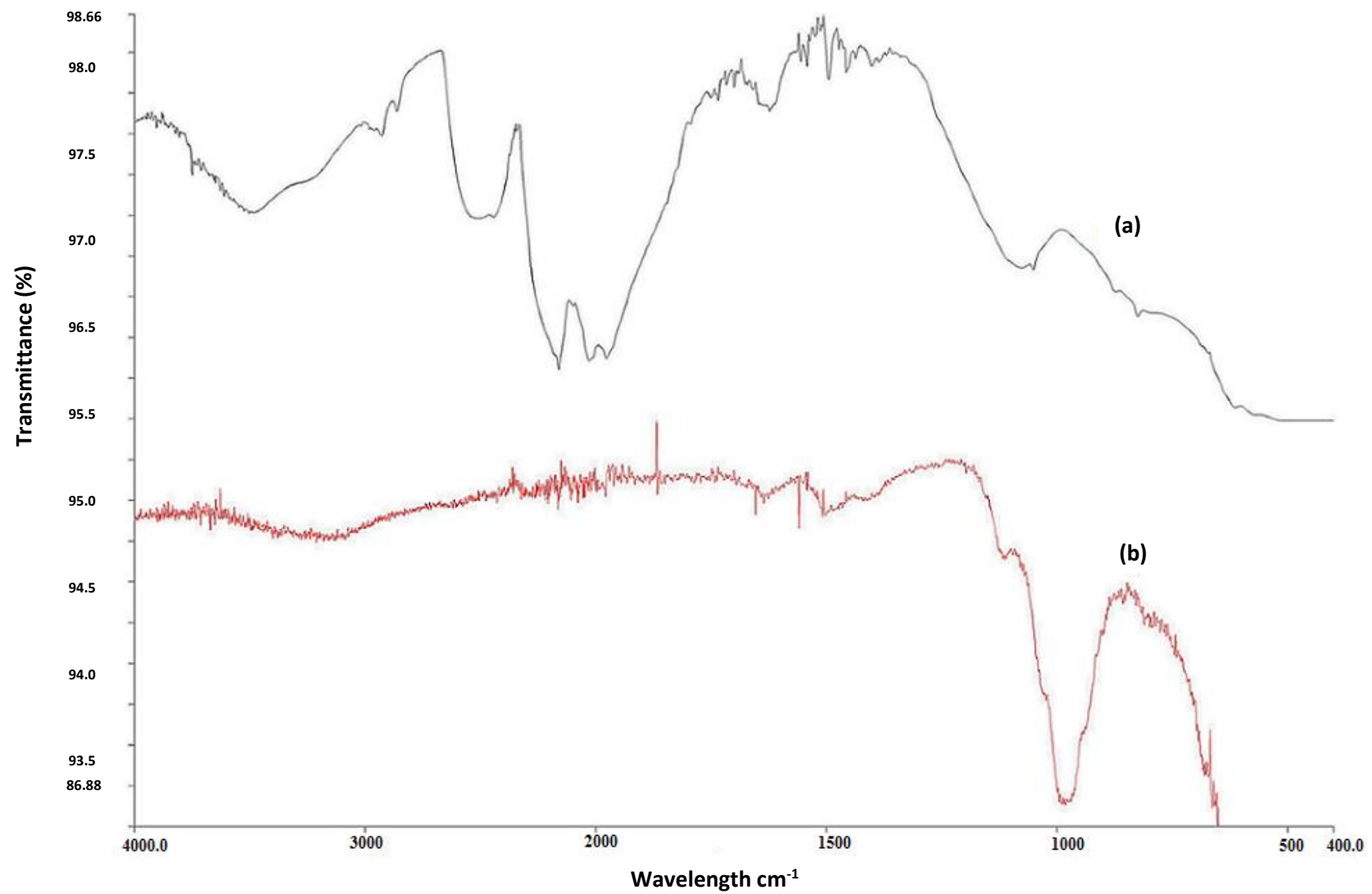
Figure 5.5 FT-IR analysis of the bauxite residue media before **(a)** and after use in the column treating forest run-off **(b)**.
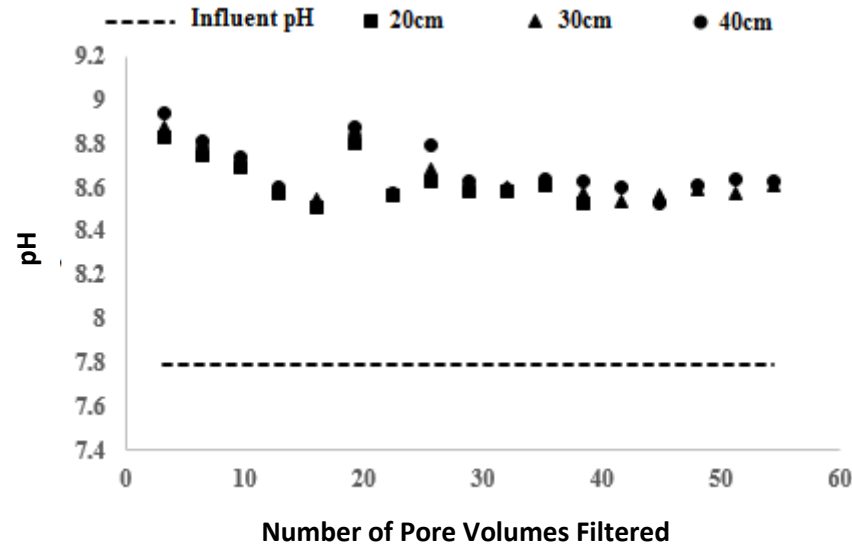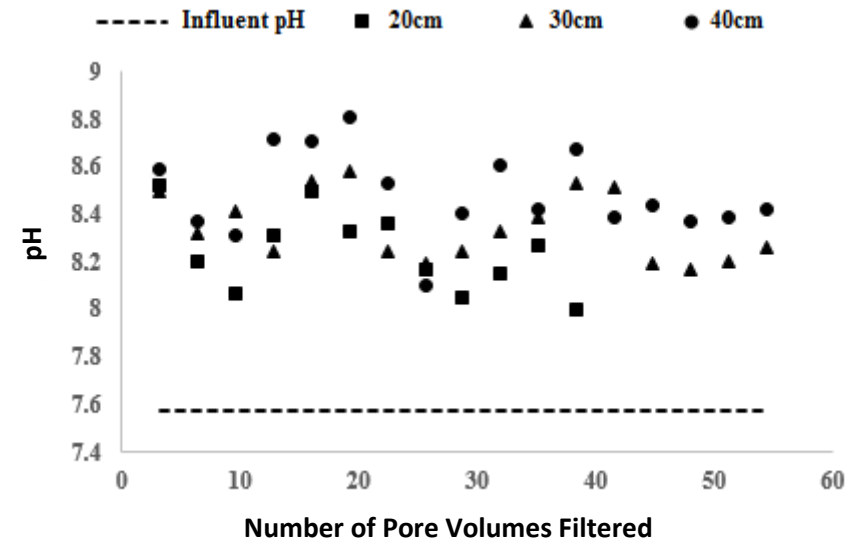
Figure 5.6 The pH values of (a) the dairy soiled water and (b) forest run-off effluent from the columns over the 24 – 36 hr loading period, showing that there was an overall increase in the pH of the effluent treated.

There was an increase in the pH in the effluent for both the DSW and forest run-off treated wastewater (Figure 5.6). The influent pH of the DSW was 7.79, which increased to 8.94 in the 40 cm column at t = 2 hr. The influent pH of the forest run-off was 7.57 and increased to 8.81 at t = 12 hr in the 40 cm column. According to the Drinking Water Directive (98/83/EC), the pH value should be in the range of ≥ 6.5 and ≤ 9.5. The values recorded in this study show that the pH values in the effluent are within this range, highlighting no potential risk to the surrounding environment.

5.3.4 Trace Metal and Elemental Analysis

Due to the complex nature of bauxite residue and its composition, there is potential for trace metal leaching to the surrounding environment (Despland et al., 2011; Evans 2016). Pollution from metals can have an adverse and detrimental effect on the surrounding environment, affecting plant and animal life (Gomes et al., 2016; Olszewska et al., 2017). In addition, the majority of metals that are in a soil environment are non-degradable (Guo et al., 2006).

The influent and effluent metal concentrations from the columns treating DSW and forest run-off, along with the parametric values, as mandated by the Irish EPA (2014), are displayed in Figures 5.7 and 5.8. In this study, the dominant species present in both effluents were Al and Fe, which were above the parametric values (0.2 mg L^{-1} for both Al and Fe). Copper was released in both effluents, but did decrease with loading time when treating the DSW and the level of Cu reduced to below the parametric value of 2 mg L^{-1}. The level of Mn was lower in the effluent compared to the influent for all columns, showing a retention capacity within the column media, but it was higher than the parametric value of 0.05 mg L^{-1}. Magnesium, Ga, V and Zn were also present in increased amounts in the effluent, due to leaching from the bauxite residue media. However, the Mg and Zn did decrease with increasing loading time. There are currently no parametric values or EPA guideline values for drinking water parameters for Mg, Ga, V and Zn, although previous studies have highlighted that bauxite residue is inclusive of oxyanionic-forming elements, which are soluble at high pH range; these include Al, As, Cr, Mo and V (Mayes et al., 2016). The main species of V present in bauxite residue is in the pentavalent form (Burke et al., 2012, 2013), which may be problematic due to its toxicity (Burke et al., 2012). Whilst V may be a potential issue (depending on the source of bauxite ore), it is also the focus of critical raw material (CRM) recovery studies (Gomes

et al., 2016; Zhu et al., 2018), which suggests the potential and need for further studies investigating the adsorbent potential of bauxite residue following the removal and recovery of CRMs such as V.

Previous work by Lopez et al. (1998) highlighted the ability of bauxite residue to retain Ni, Cu and Zn. Despland et al. (2014) showed that Bauxsol™ (neutralised bauxite residue produced using the Basecon™ procedure) had the ability to remove trace amounts of As, lead (Pb), Cd, Cr, Cu, Ni, Se, Zn, Mn and Al. This highlights the potential of bauxite residue in the removal of both cations and anions from aqueous solution. However, the composition and concentration of elements in bauxite will vary depending on the type of ore (Mayes et al., 2011).

Although there was overall evidence of mobilisation of some trace elements while treating the wastewater, one suggestion would be to include a rinse/wash period prior to packing the columns. This would reduce and/or eliminate the potential leaching of metals at the initial loading period and avoid further release as the loading period increases. Another option would be to apply a seawater treatment to the bauxite residue, which has been proven to lower the pH and therefore reduce the leaching of metal(loid) species (Cusack et al., 2018; Johnston et al., 2010).

Figure 5.7 Comparison of the composition of (a) Al, (b) Fe, (c) Na (d) Cu (e) Mn (f) Mg (g) Ga (h) V and (i) Zn in both the influent and effluent in the columns treating DSW over the 24 -36 hr loading period. EPA indicator parameter or EPA chemical parameter included for each element.
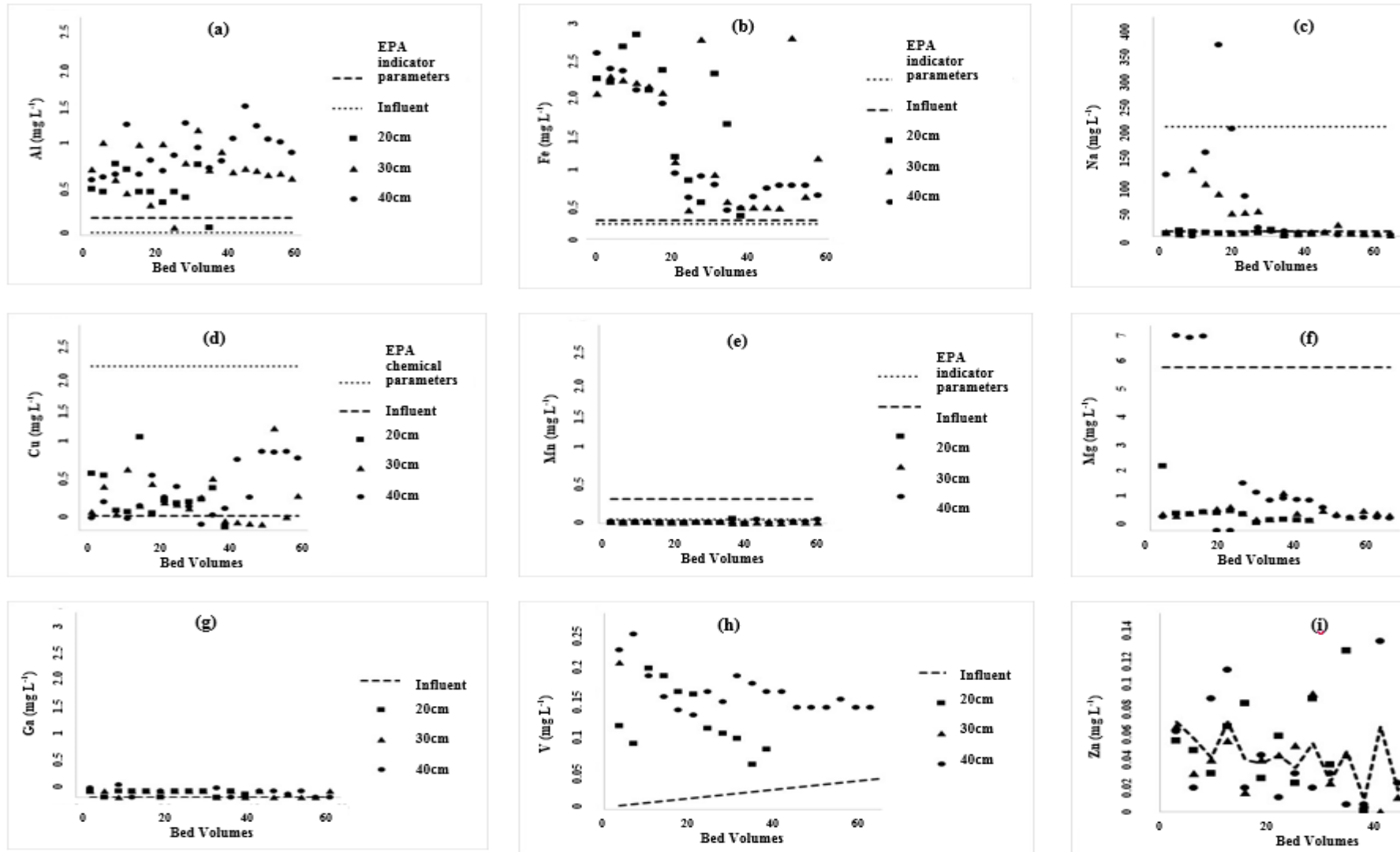
Figure 5.8 Comparison of the composition of (a) Al, (b) Fe, (c) Na (d) Cu (e) Mn (f) Mg (g) Ga (h) V and (i) Zn in both the influent and effluent in the columns treating forest run-off over the 24 -36 hr loading period. EPA indicator parameter or EPA chemical parameter included for each element.

140

5.4 Conclusions

Several studies have focussed on the use of low-cost adsorbents in the removal of contaminants such as P from contaminated waters due to possible cost savings and to reutilise by-products from various sectors. This study demonstrated that bauxite residue has P (particularly dissolved reactive phosphorus) removal capabilities in both low (forest run-off) and high (dairy soiled water) range P-concentrated waters. The estimated service time of the column media before initial breakthrough, based on the performance of the largest columns, was 1.08 min g^{-1} media for the forest run-off and 0.28 min g^{-1} media for the dairy soiled water. Due to the composition of the bauxite residue, potential for metal(loid) leaching is a concern. Aluminium and iron were the dominant metals released in the treated effluent, but this may be eliminated by a preventative step such as introducing a washing period or a seawater neutralisation step prior to packing the bauxite residue into the columns.

5.5 References

Acelas, N.Y., Martin, B.D., López, D. and Jefferson, B., 2015. Selective removal of phosphate from wastewater using hydrated metal oxides dispersed within anionic exchange media. *Chemosphere. 119*, pp.1353-1360.

ÁdÁm, K., Sovik, A.K., Krogstad, T. and Heistad, A., 2007. Phosphorous removal by the filter materials light-weight aggregates and shellsand-a review of processes and experimental set-ups for improved design of filter systems for wastewater treatment. *Vatten. 63*(3), p.245.

Akay, G., Keskinler, B., Cakici, A. and Danis, U., 1998. Phosphate removal from water by red mud using crossflow microfiltration. *Water. Res. 32*(3), pp.717-726.

Akhurst, D.J., Jones, G.B., Clark, M. and McConchie, D., 2006. Phosphate removal from aqueous solutions using neutralised bauxite refinery residues (Bauxsol™). *Environ. Chem. 3*(1), pp.65-74.

Arco-Lázaro, E., Pardo, T., Clemente, R. and Bernal, M.P., 2018. Arsenic adsorption and plant availability in an agricultural soil irrigated with As-rich water: Effects of Fe-rich amendments and organic and inorganic fertilisers. *J. Environ. Manage.* 209, pp.262-272.

Atasoy, A.D. and Bilgic, B., 2018. Adsorption of Copper and Zinc Ions from Aqueous Solutions Using Montmorillonite and Bauxite as Low-Cost Adsorbents. *Mine. Water. Environ. 37*(1), pp.205-210.

Barca, C., Gérente, C., Meyer, D., Chazarenc, F. and Andrès, Y., 2012. Phosphate removal from synthetic and real wastewater using steel slags produced in Europe. *Water. Res. 46*(7), pp.2376-2384.

Berzina-Cimdina, L. and Borodajenko, N., 2012. Research of calcium phosphates using Fourier transform infrared spectroscopy. In *Infrared Spectroscopy-Materials Science, Engineering and Technology.* InTech. Available: http://scholar.google.com/scholar_url?url=https%3A%2F%2Fwww.intechopen.com%2

Fdownload%2Fpdf%2F36171&hl=en&sa=T&oi=ggp&ct=res&cd=0&d=18760135324 13993455&ei=JQ5fW6ODB4SQmwHoq7O4BA&scisig=AAGBfm0zcrG1iAsbV5Fv1k KQs9aPk9QMNA&nossl=1&ws=1440x845 [accessed 30.07.2018].

Bhatnagar, A. and Sillanpää, M., 2010. Utilization of agro-industrial and municipal waste materials as potential adsorbents for water treatment—a review. *Chem. Eng. J. 157*(2-3), pp.277-296.

Bhatnagar, A., Vilar, V.J., Botelho, C.M. and Boaventura, R.A., 2011. A review of the use of red mud as adsorbent for the removal of toxic pollutants from water and wastewater. *Environ. Technol.* 32(3), pp.231-249.

Blackall, L.L., Crocetti, G.R., Saunders, A.M. and Bond, P.L., 2002. A review and update of the microbiology of enhanced biological phosphorus removal in wastewater treatment plants. *Antonie Van Leeuwenhoek*, *81*(1-4), pp.681-691.

Bolster, C.H., Forsberg, A., Mittelstet, A., Radcliffe, D.E., Storm, D., Ramirez-Avila, J., Sharpley, A.N. and Osmond, D., 2017. Comparing an Annual and a Daily Time-Step Model for Predicting Field-Scale Phosphorus Loss. *J. Environ. Qual. 46*(6), pp.1314-1322.

Brennan, R.B., Wall, D., Fenton, O., Grant, J., Sharpley, A.N., Healy, M.G., 2014. The impact of chemical amendment of dairy cattle slurry before land application on soil phosphorus dynamics. *Communications. Soil. Sci. Plant Analysis.* 45(16): 2215 – 2233.

Bridger, S. and Knowles, M., 2000. A complete method for environmental samples by simultaneous axially viewed ICP-AES following USEPA guidelines. Varian ICP-OES At Work (29) Available: https://www.agilent.com/cs/library/applications/ICPES-29.pdf [accessed 24.05.2018].

Brunson, L.R. and Sabatini, D.A., 2014. Practical considerations, column studies and natural organic material competition for fluoride removal with bone char and aluminum amended materials in the Main Ethiopian Rift Valley. *Sci. Total. Environ. 488*, pp.580-587.

Burke, I.T., Mayes, W.M., Peacock, C.L., Brown, A.P., Jarvis, A.P. and Gruiz, K., 2012. Speciation of arsenic, chromium, and vanadium in red mud samples from the Ajka spill site, Hungary. *Environ. Sci. Technol. 46*(6), pp.3085-3092.

Burke, I.T., Peacock, C.L., Lockwood, C.L., Stewart, D.I., Mortimer, R.J., Ward, M.B., Renforth, P., Gruiz, K. and Mayes, W.M., 2013. Behavior of aluminum, arsenic, and vanadium during the neutralization of red mud leachate by HCl, gypsum, or seawater. *Environ. Sci. Technol.* 47(12), pp.6527-6535.

Callery, O., Brennan, R.B., Healy, M.G., 2015. Use of amendments in a peat soil to reduce phosphorus losses from forestry operations. *Eco. Eng.* 85: 193 – 200.

Callery, O., Healy, M.G., Rognard, F., Barthelemy, L. and Brennan, R.B., 2016. Evaluating the long-term performance of low-cost adsorbents using small-scale adsorption column experiments. *Water. Res. 101*, pp.429-440.

Callery, O. and Healy, M.G., 2017. Predicting the propagation of concentration and saturation fronts in fixed-bed filters. *Water. Res. 123*, pp.556-568.

Castaldi, P., Silvetti, M., Enzo, S. and Melis, P., 2010. Study of sorption processes and FT-IR analysis of arsenate sorbed onto red muds (a bauxite ore processing waste). *J. Hazard. Mater. 175*(1-3), pp.172-178.

Castaldi, P., Silvetti, M., Enzo, S. and Deiana, S., 2011. X-ray diffraction and thermal analysis of bauxite ore-processing waste (red mud) exchanged with arsenate and phosphate. *Clays. Clay. Min.* 59(2), pp.189-199.

Chen, J.P., Yoon, J.T. and Yiacoumi, S., 2003. Effects of chemical and physical properties of influent on copper sorption onto activated carbon fixed-bed columns. *Carbon*. 41(8), pp.1635-1644.

Claveau-Mallet, D., Wallace, S. and Comeau, Y., 2013. Removal of phosphorus, fluoride and metals from a gypsum mining leachate using steel slag filters. *Water. Res. 47*(4), pp.1512-1520.

Cordell, D. and White, S., 2011. Peak phosphorus: clarifying the key issues of a vigorous debate about long-term phosphorus security. *Sustainability. 3*(10), pp.2027-2049.

Cornell, R.M. and Schwertmann, U., 2003. *The iron oxides: structure, properties, reactions, occurrences and uses*. John Wiley & Sons. Available: https://books.google.ie/books?hl=en&lr=&id=dlMuE3_klW4C&oi=fnd&pg=PA1&dq= Cornell,+R.M.+and+Schwertmann,+U.,+2003.+The+iron+oxides:+structure,+properties ,+reactions,+occurrences+and+uses.+John+Wiley+%26+Sons.&ots=l0jQWg_4gN&sig =kNxeJyUHBF3-UemiW- s_EvlaeCs&redir_esc=y#v=onepage&q=Cornell%2C%20R.M.%20and%20Schwertma nn%2C%20U.%2C%202003.%20The%20iron%20oxides%3A%20structure%2C%20pr operties%2C%20reactions%2C%20occurrences%20and%20uses.%20John%20Wiley% 20%26%20Sons.&f=false [accessed 11.09.2018].

Courtney, R. and Harrington, T., 2010. Assessment of plant-available phosphorus in a fine textured sodic substrate. *Eco. Eng.* 36(4), pp.542-547.

Cusack, P.B., Healy, M.G., Ryan, P.C., Burke, I.T., O'Donoghue, L.M., Ujaczki, É. and Courtney, R., 2018. Enhancement of bauxite residue as a low-cost adsorbent for phosphorus in aqueous solution, using seawater and gypsum treatments. *J. Clean. Prod. 179*, pp.217-224.

De, D., Aniya, V. and Satyavathi, B., 2018. Application of an agro-industrial waste for the removal of As (III) in a counter-current multiphase fluidized bed. *Int. J. Environ. Sci. Technol.* pp.1-16.

De Gisi, S., Lofrano, G., Grassi, M. and Notarnicola, M., 2016. Characteristics and adsorption capacities of low-cost sorbents for wastewater treatment: a review. *Sustain. Mater. Technol. 9*, pp.10-40.

Desmidt, E., Ghyselbrecht, K., Zhang, Y., Pinoy, L., Van der Bruggen, B., Verstraete, W., Rabaey, K. and Meesschaert, B., 2015. Global phosphorus scarcity and full-scale P-recovery techniques: a review. *Critical. Reviews. Environ. Sci. Technol. 45*(4), pp.336-384.

Despland, L.M., Clark, M.W., Vancov, T., Erler, D. and Aragno, M., 2011. Nutrient and trace-metal removal by Bauxsol pellets in wastewater treatment. *Environ. Sci. Technol. 45*(13), pp.5746-5753.

Despland, L.M., Clark, M.W., Vancov, T. and Aragno, M., 2014. Nutrient removal and microbial communities' development in a young unplanted constructed wetland using Bauxsol™ pellets to treat wastewater. *Sci. Total. Environ. 484*, pp.167-175.

Drizo, A., Comeau, Y., Forget, C. and Chapuis, R.P., 2002. Phosphorus saturation potential: a parameter for estimating the longevity of constructed wetland systems. *Environ. Sci. Technol. 36*(21), pp.4642-4648.

EPA, 2014. Drinking Water Parameters Microbiological, Chemical and Indicator Parameters in the 2014 Drinking Water Regulations. Available: www.epa.ie/pubs/advice/drinkingwater/2015_04_21_ParametersStandaloneDoc.pdf [accessed 29.05.2018].

European Drinking Water Directive (Council Directive 98/83/EC of 3 November 1998 on the quality of water intended for human consumption), 1998. Available: https://eur-lex.europa.eu/legal-content/EN/TXT/PDF/?uri=CELEX:31998L0083&from=EN [accessed 20.07.208].

Evans, K., 2016. The history, challenges, and new developments in the management and use of bauxite residue. *J. Sustain. Metall.* 2(4), pp.316-331.

Fenton, O., Healy, M.G., Rodgers, M., 2009. Use of ochre from an abandoned metal mine in the south east of Ireland for phosphorus sequestration from dairy dirty water. *J. Environ. Qual.* 38: 1120 – 1125.

Finnegan, J., Regan, J.T., De Eyto, E., Ryder, E., Tiernan, D. and Healy, M.G., 2012. Nutrient dynamics in a peatland forest riparian buffer zone and implications for the establishment of planted saplings. *Ecol. Eng. 47*, pp.155-164.

García-Mateos, F.J., Ruiz-Rosas, R., Marqués, M.D., Cotoruelo, L.M., Rodríguez-Mirasol, J. and Cordero, T., 2015. Removal of paracetamol on biomass-derived activated carbon: modeling the fixed bed breakthrough curves using batch adsorption experiments. *Chem. Eng. J. 279*, pp.18-30.

Ge, H., Batstone, D.J. and Keller, J., 2015. Biological phosphorus removal from abattoir wastewater at very short sludge ages mediated by novel PAO clade Comamonadaceae. *Water. Res. 69*, pp.173-182.

Gomes, H.I., Mayes, W.M., Rogerson, M., Stewart, D.I. and Burke, I.T., 2016. Alkaline residues and the environment: a review of impacts, management practices and opportunities. *J. Clean. Prod.* 112, pp.3571-3582.

Gomes, H.I., Jones, A., Rogerson, M., Burke, I.T. and Mayes, W.M., 2016. Vanadium removal and recovery from bauxite residue leachates by ion exchange. *Env. Sci. Poll. Res. 23*(22), pp.23034-23042.

Grace, M.A., Healy, M.G. and Clifford, E., 2015. Use of industrial by-products and natural media to adsorb nutrients, metals and organic carbon from drinking water. *Sci. Total. Environ. 518*, pp.491-497.

Grace, M.A., Clifford, E. and Healy, M.G., 2016. The potential for the use of waste products from a variety of sectors in water treatment processes. *J. Clean. Prod. 137*, pp.788-802.

Gräfe, M., Power, G. and Klauber, C., 2011. Bauxite residue issues: III. Alkalinity and associated chemistry. *Hydrometallurgy*, *108*(1-2), pp.60-79.

Guo, G., Zhou, Q. and Ma, L.Q., 2006. Availability and assessment of fixing additives for the in situ remediation of heavy metal contaminated soils: a review. *Environ. Monitoring. Assessment. 116*(1-3), pp.513-528.

Hauduc, H., Takács, I., Smith, S., Szabo, A., Murthy, S., Daigger, G.T. and Spérandio, M., 2015. A dynamic physicochemical model for chemical phosphorus removal. *Water. Res. 73*, pp.157-170.

Herron, S.L., Sharpley, A.N., Brye, K.R. and Miller, D.M., 2016. Optimizing Hydraulic and Chemical Properties of Iron and Aluminum Byproducts for Use in On-Farm Containment Structures for Phosphorus Removal. *J. Environ. Protection. 7*(12), p.1835.

Huang, W., Wang, S., Zhu, Z., Li, L., Yao, X., Rudolph, V. and Haghseresht, F., 2008. Phosphate removal from wastewater using red mud. *J. Hazard. Mater. 158*(1), pp.35-42.

Jacukowicz-Sobala, I., Ociński, D. and Kociołek-Balawejder, E., 2015. Iron and aluminium oxides containing industrial wastes as adsorbents of heavy metals: Application possibilities and limitations. *Waste. Manage. Res. 33*(7), pp.612-629.

Johnston, M., Clark, M.W., McMahon, P. and Ward, N., 2010. Alkalinity conversion of bauxite refinery residues by neutralization. *J. Hazard. Mater.* 182(1-3), pp.710-715.

Karageorgiou, K., Paschalis, M. and Anastassakis, G.N., 2007. Removal of phosphate species from solution by adsorption onto calcite used as natural adsorbent. *J. Hazard. Mater. 139*(3), pp.447-452.

Kong, X., Li, M., Xue, S., Hartley, W., Chen, C., Wu, C., Li, X. and Li, Y., 2017. Acid transformation of bauxite residue: conversion of its alkaline characteristics. *J. Hazard. Mater. 324*, pp.382-390.

Lalley, J., Han, C., Mohan, G.R., Dionysiou, D.D., Speth, T.F., Garland, J. and Nadagouda, M.N., 2015. Phosphate removal using modified Bayoxide® E33 adsorption media. *Environ. Sci. Water. Res. Technol. 1*(1), pp.96-107.

Langmuir, D., 1997. *Aqueous Environ.* Prentice Hall: Upper Saddle River, NJ.

Liu, Y., Lin, C., Wu, Y., 2007. Characterization of red mud derived from a combined Bayer Process and bauxite calcination method. *J. Hazard. Mater.* 146, 255-261.

Lombi, E., Zhao, F.J., Zhang, G., Sun, B., Fitz, W., Zhang, H. and McGrath, S.P., 2002. In situ fixation of metals in soils using bauxite residue: chemical assessment. *Environ. Poll. 118*(3), pp.435-443.

Lopez, E., Soto, B., Arias, M., Nunez, A., Rubinos, D., Barral, M.T., 1998. Adsorbent properties of red mud and its use for wastewater treatment. *Water. Res.* 32, 1314-1322.

Mayes, W.M., Jarvis, A.P., Burke, I.T., Walton, M., Feigl, V., Klebercz, O. and Gruiz, K., 2011. Dispersal and attenuation of trace contaminants downstream of the Ajka bauxite residue (red mud) depository failure, Hungary. *Environ. Sci. Technol. 45*(12), pp.5147-5155.

Mayes, W.M., Burke, I.T., Gomes, H.I., Anton, Á.D., Molnár, M., Feigl, V. and Ujaczki, É., 2016. Advances in understanding environmental risks of red mud after the Ajka spill, Hungary. *J. Sustain. Metall. 2*(4), pp.332-343.

McConchie, D., Clark, M., Davies-McConchie, F., 2001. Processes and Compositions for Water Treatment, Neauveau Technology Investments, Australian, p. 28.

Minogue, D., French, P., Bolger, T. and Murphy, P.N.C., 2015. Characterisation of dairy soiled water in a survey of 60 Irish dairy farms. *Irish. J. Agri. Food Res. 54*(1), pp.1-16.

Murnane, J.G., Brennan, R.B., Fenton, O., Healy, M.G., 2016a. Zeolite combined with alum and aluminium chloride mixed with agricultural slurries reduces carbon losses in runoff from grassed soil boxes. *J. Environ. Qual.* 44(5): 1674 – 1683.

Murnane, J.G., Brennan, R.B., Healy, M.G. and Fenton, O., 2016b. Assessment of intermittently loaded woodchip and sand filters to treat dairy soiled water. *Water. Res. 103*, pp.408-415.

Nowak, B., Aschenbrenner, P. and Winter, F., 2013. Heavy metal removal from sewage sludge ash and municipal solid waste fly ash—a comparison. *Fuel. Processing. Technol. 105*, pp.195-201.

O'Flynn, C.J., Fenton, O., Wall, D., Brennan, R.B., McLaughlin, M.J. and Healy, M.G., 2018. Influence of soil phosphorus status, texture, pH and metal content on the efficacy of amendments to pig slurry in reducing phosphorus losses. *Soil. Use. Manage. 34*(1), pp.1-8.

Oguz, E., 2004. Removal of phosphate from aqueous solution with blast furnace slag. *J. Hazard. Mater. 114*(1-3), pp.131-137.

Olszewska, J.P., Heal, K.V., Winfield, I.J., Eades, L.J. and Spears, B.M., 2017. Assessing the role of bed sediments in the persistence of red mud pollution in a shallow lake (Kinghorn Loch, UK). *Water. Res. 123*, pp.569-577.

Pan, G., Lyu, T. and Mortimer, R., 2018. Comment: Closing phosphorus cycle from natural waters: re-capturing phosphorus through an integrated water-energy-food strategy. *J. Environ. Sci.* 65, 375-376.

Pantoja, M.L., Jones, H., Garelick, H., Mohamedbakr, H.G. and Burkitbayev, M., 2014. The removal of arsenate from water using iron-modified diatomite (D-Fe): isotherm and column experiments. *Environ. Sci. Poll. Res. 21*(1), pp.495-506.

Penn, C., McGrath, J., Bowen, J. and Wilson, S., 2014. Phosphorus removal structures: A management option for legacy phosphorus. *J. Soil. Water. Conservation*, *69*(2), pp.51A-56A.

Pratt, C., Parsons, S.A., Soares, A. and Martin, B.D., 2012. Biologically and chemically mediated adsorption and precipitation of phosphorus from wastewater. *Current. Opinion. Biotechnol. 23*(6), pp.890-896.

Pretty, J. and Bharucha, Z.P., 2014. Sustainable intensification in agricultural systems. *Annals. Botany. 114*(8), pp.1571-1596.

Ruane, E.M., Murphy, P.N., Healy, M.G., French, P. and Rodgers, M., 2011. On-farm treatment of dairy soiled water using aerobic woodchip filters. *Water. Res. 45*(20), pp.6668-6676.

Ruttenberg, K.C. and Sulak, D.J., 2011. Sorption and desorption of dissolved organic phosphorus onto iron (oxyhydr) oxides in seawater. *Geochimica et Cosmochimica Acta*, *75*(15), pp.4095-4112.

Schindler, D.W., Carpenter, S.R., Chapra, S.C., Hecky, R.E. and Orihel, D.M., 2016. Reducing phosphorus to curb lake eutrophication is a success. Available: https://pubs.acs.org/doi/abs/10.1021/acs.est.6b02204 [accessed 06.06.2018].

Sharpley, A., 2016. Managing agricultural phosphorus to minimize water quality impacts. *Scientia Agricola. 73*(1), pp.1-8.

Smith, D.R., King, K.W. and Williams, M.R., 2015. What is causing the harmful algal blooms in Lake Erie?. *J. Soil. Water. Conserv. 70*(2), pp.27A-29A.

Søvik, A.K. and Kløve, B., 2005. Phosphorus retention processes in shell sand filter systems treating municipal wastewater. *Ecol. Eng. 25*(2), pp.168-182.

Stumm, W., 1992. *Chemistry of the solid-water interface: processes at the mineral-water and particle-water interface in natural systems*. John Wiley & Son Inc..

Sukačová, K., Trtílek, M. and Rataj, T., 2015. Phosphorus removal using a microalgal biofilm in a new biofilm photobioreactor for tertiary wastewater treatment. *Water. Res. 71*, pp.55-63.

Taneez, M., Hurel, C., Marmier, N. and Lefèvre, G., 2017. Adsorption of inorganic pollutants on bauxite residues: An example of methodology to simulate adsorption in complex solids mixtures. *Applied. Geochem.* 78, pp.272-278.

Tejedor-Tejedor, M.I. and Anderson, M.A., 1990. The protonation of phosphate on the surface of goethite as studied by CIR-FTIR and electrophoretic mobility. *Langmuir. 6*(3), pp.602-611.

Tresintsi, S., Simeonidis, K., Katsikini, M., Paloura, E.C., Bantsis, G. and Mitrakas, M., 2014. A novel approach for arsenic adsorbents regeneration using MgO. *J. Hazard. Mater. 265*, pp.217-225.

Ujaczki, É., Feigl, V., Molnár, M., Cusack, P., Curtin, T., Courtney, R., O'Donoghue, L., Davris, P., Hugi, C., Evangelou, M.W. and Balomenos, E., 2018. Re-using bauxite residues: benefits beyond (critical raw) material recovery. *J. Chem. Technol. Biotechnol. 93*(9), pp.2498-2510.

United Nations. 2015. Transforming our world: the 2030 agenda for sustainable development. Available: http://www.un.org/en/development/desa/population/migration/generalassembly/docs/globalcompact/A_RES_70_1_E.pdf [accessed 18.07.2018].

Vohla, C., Alas, R., Nurk, K., Baatz, S. and Mander, Ü., 2007. Dynamics of phosphorus, nitrogen and carbon removal in a horizontal subsurface flow constructed wetland. *Sci. Total. Environ. 380*(1-3), pp.66-74.

Vohla, C., Kõiv, M., Bavor, H.J., Chazarenc, F. and Mander, Ü., 2011. Filter materials for phosphorus removal from wastewater in treatment wetlands—A review. *Ecol. Eng. 37*(1), pp.70-89.

Vuković, G.D., Marinković, A.D., Škapin, S.D., Ristić, M.Đ., Aleksić, R., Perić-Grujić, A.A. and Uskoković, P.S., 2011. Removal of lead from water by amino modified multi-walled carbon nanotubes. *Chem. Eng. J. 173*(3), pp.855-865.

Wang, X.X., Wu, Y.H., Zhang, T.Y., Xu, X.Q., Dao, G.H. and Hu, H.Y., 2016. Simultaneous nitrogen, phosphorous, and hardness removal from reverse osmosis concentrate by microalgae cultivation. *Water. Res. 94*, pp.215-224.

Weissert, C. and Kehr, J., 2018. Macronutrient sensing and signaling in plants. In *Plant Macronutrient Use Efficiency* (pp. 45-64).

Wilkie, M.P. and Wood, C.M., 1996. The adaptations of fish to extremely alkaline environments. *Comparative Biochem. Physiology Part B: Biochem. Molecular Bio. 113*(4), pp.665-673.

Wu, K., Chen, Y., Ouyang, Y., Lei, H. and Liu, T., 2018. Adsorptive removal of fluoride from water by granular zirconium–aluminum hybrid adsorbent: performance and mechanisms. *Environ. Sci. Poll. Res.* 25(16), pp.15390-15403.

Ye, J., Zhang, P., Hoffmann, E., Zeng, G., Tang, Y., Dresely, J., Liu, Y., 2014. Comparison of response surface methodology and artificial neural network in optimization and prediction of acid activation of Bauxsol for phosphorus adsorption. *Water. Air. Soil. Poll*. 225(12), 2225.

Zhou, Z., Hu, D., Ren, W., Zhao, Y., Jiang, L.M. and Wang, L., 2015. Effect of humic substances on phosphorus removal by struvite precipitation. *Chemosphere. 141*, pp.94-99.

Zhou, B., Xu, Y., Vogt, R.D., Lu, X., Li, X., Deng, X., Yue, A. and Zhu, L., 2016. Effects of land use change on phosphorus levels in surface waters—a case study of a watershed strongly influenced by agriculture. *Water. Air. Soil. Poll. 227*(5), p.160.

Zhu, F., Li, Y., Xue, S., Hartley, W. and Wu, H., 2016. Effects of iron-aluminium oxides and organic carbon on aggregate stability of bauxite residues. *Environ. Sci. Poll. Res. 23*(9), pp.9073-9081.

Zhu, X., Li, W., Zhang, Q., Zhang, C. and Chen, L., 2018. Separation characteristics of vanadium from leach liquor of red mud by ion exchange with different resins. *Hydrometallurgy. 176*, pp.42-48.

Chapter 6

An Investigation into the Growth of *Lolium perenne* L. and Soil Properties such as Phosphorus Availability, pH and Electrical Conductivity following the use of Spent Bauxite Residue Column Media as a Nutrient Source.

Overview

The aim of this chapter was to compare the effects of using phosphorus (P) saturated bauxite residue media as opposed to a conventional P fertiliser on a P deficient soil by comparing soil quality properties and plant growth in perennial ryegrass (*Lolium perenne* L.). The design of this study incorporated the use of spent P saturated bauxite residue media taken from the rapid small-scale column test study (Chapter 6) and the implementation of the RHIZOtest™ procedure (ISO 16198:2015) to carry out a short growth trial. The overall aim was to include analysis on the P and trace metal uptake within the plant biomass following the plant growth trial, however issues arose with the limited biomass in terms of dilutions required for the ICP-OES analysis.

6.1 Introduction

Phosphorus (P) is essential in the successful production and maintenance of food supply (Elser et al., 2007; Wilfert et al., 2015) and is found in two main allotropes, white phosphorus and red phosphorus (Desmidt et al., 2015). The P required for the production of food is applied in the form of fertilisers developed from phosphoric acid produced from the digestion of phosphate rock/ore in sulphuric acid (H_2SO_4) (Cánovas et al., 2017). Phosphorus is rarely found in its elemental form, and is referred to as P pentoxide (which contains $\sim$ 44% P) within the mining and fertiliser industries (Cordell et al., 2009). With an increasing population, further demand is being placed on food supply and, consequently, phosphate rock, which is a non-renewable resource (Achat et al., 2014). Currently, 95% of the global P production is being utilised for the food production sector, with the remaining 5% being used in industrial applications such as in the production of

154

detergents (Desmidt et al., 2015). Ironically, P is also one of the key nutrients resulting in the eutrophication of water bodies (Baker et al., 2015). These two issues have been referred to as the *P paradox* (Baker et al., 2015; Sharpley 2015).

Between 2010 to 2014, 88 % of phosphate rock and 100 % of P (in the form of white P) was imported into the European Union (EU), and mainly originated from China (EC, 2017). The dependence of the EU for materials such as phosphate rock from outside of Europe has highlighted its vulnerability. As a result, in 2017 the European Commission (EC) included both phosphate rock and white P in a list of critical raw materials (CRMs) that have potential supply risk to the EU (EC 2017). This highlights the need to establish a potential secondary source within Europe for these materials.

Several approaches have been used to recover P from municipal and industrial wastewater (Desmidt et al., 2015) and include the recycling of P from effluents and sewage sludge at wastewater treatment plants using processes such as chemical crystallisation in which struvite (magnesium-ammonium-phosphate; $NH_4MgPO.6H_2O$) is the end product (Antonini et al., 2012; Moerman et al., 2009). As it is slightly soluble in aqueous and soil solutions, struvite is considered to be an effective source of P, nitrogen (N) and magnesium (Mg) for plants (Ryu et al., 2012). Similarly, treated sludge produced following wastewater treatment, may be applied to agricultural land as a source of P (SEPA 2015), and in countries like the Republic of Ireland, up to 80% of treated municipal sludge is currently applied to land (Healy et al., 2017). However, the recycling of P using biological or chemical methods, or combinations of both, is expensive and often requires the use of large amounts of chemicals (Zhou et al., 2016). Recently, the potential of industrial wastes as low-cost P adsorbents (De Gisi et al., 2016; De et al., 2018; Grace et al., 2016) has been explored. Also, there has been little focus on the recovery and recycling of P from an agricultural wastewater such as dairy soiled water (DSW) and also forest run-off, both key sources of P run-off leading to poor water quality within an Irish setting (EPA, 2017).

Numerous studies have investigated the potential re-use of bauxite residue (Grace et al., 2015; 2016; Ye et al., 2014), as well as other potential industrial by-products (Callery et al., 2017; Grace et al., 2015), as an adsorbent in wastewater treatment, in particular for P removal. Bauxite residue (red mud), the by-product produced in the alumina industry, is

being produced at an annual global rate of 150 Mt (Evans, 2016). The current re-use rate of bauxite residue is ~ 2 %, the remainder of which is being disposed of into bauxite residue disposal areas (BRDAs) (Evans, 2016; Ujaczki et al., 2018). Bauxite residue in its unamended form, is highly alkaline, sodic, generally composed of trace metals and is typically nutrient deficient (Courtney and Harrington, 2010), and is therefore an unsuitable growth medium. However, if treatments are applied such as gypsum (Lopez et al., 1998), acid (Huang et al., 2008), heat (Liu et al., 2007) and seawater (Hanahan et al., 2004), it has been shown to enhance its P retention capacity and potential as a P adsorbent. Once any medium reaches P saturation, the point at which it ceases to adsorb any further P, an obvious final pathway is to become a nutrient source (i.e. a fertiliser). To date, little to no work has investigated the re-use of P-saturated bauxite residue as a potential nutrient source. Additionally and due to the alkaline, sodic and saline nature of bauxite residue, further investigations to assess for potential phytotoxic effects to both plant and animal life are necessary when considering the application of the P-saturated bauxite residue to land as a nutrient source.

Therefore, the aims of this laboratory study were to (1) compare the efficacy of P-saturated bauxite residue, following use in the treatment of forest run-off and DSW, as a fertiliser with conventional superphosphate fertiliser in terms of biomass yield in the growth of perennial ryegrass (*Lolium perenne* L.) (2) investigate any changes in soil chemical properties following bauxite addition (3) identify any phytotoxic effects on the germination of seeds and root growth, and (4) assess land application impact on soil fauna using *Eisenia fetida* L. choice tests.

6.2 Materials and Methods
6.2.1 Nutrient Source and Soil Composition
In a previous study, rapid small-scale column tests (RSSCTs) were used to predict the dissolved reactive phosphorus (DRP) removal capacity of bauxite residue when treating two waters of low (forest run-off) and high (dairy soiled water; DSW) P content (Chapter 5). The columns were considered to be P-saturated, and therefore of no further use in the removal of DRP, when the DRP concentration in the outlet water was equal to that of the inlet. The bauxite residue was then removed from the columns and oven dried at 105°C for 24 hr. Once dry, the samples were pulverised using a mortar and pestle, and sieved to a particle size < 2 mm. The superphosphate fertiliser used in the study had a P content

of 16% and was applied to all containers (except the control) at a rate of 30 t P ha^{-1}. The bauxite residue media was also applied at a rate of 30 t P ha^{-1}, in order to compare its ability to perform as a nutrient source/fertiliser The number of treatments investigated are detailed in Table 6.1.

Table 6.1 Description of the treatments used for the plant growth trials.

Treatment	Description
Control	No P source applied (control treatment)
Bauxite residue + gypsum	Gypsum treated and P saturated bauxite residue media application
Bauxite residue	P saturated bauxite residue media application
Superphosphate fertiliser	Superphosphate fertiliser (16 % P) application

The RHIZOtest™ procedure (ISO 16198:2015) was used for the plant growth trial. The RHIZOtest™ procedure is an innovative tool in the assessment of soils and phytoavailability for elements, and allows for the replication of larger scale experiments on a much smaller scale (Lemal et al., 2017). Therefore, it was an obvious choice, considering the small volumes of spent bauxite residue media generated in the RSSCT (Chapter 5).

In this procedure, seeds (*L. perenne* L.) were sterilised by immersing for 10 min in 6 % hydrogen peroxide (H_2O_2), before placing 40 seeds on the polyamide mesh in each of the plant pots (n = 5). The soil used for the study was a P-deficient mineral soil, with a Morgan's P index of 1, obtained from an ungrazed field which had received no fertiliser treatment in previous years, (supplied from Lufa-Speyer, Germany), and was packed to a density of 1.2 g cm^{-3} on each soil-receiving plate (after ISO 16198:2015).

Soil pH and electrical conductivity (EC) were measured using a 5 g sample in an aqueous extract, using a 1:5 ratio (solid: liquid) (Courtney and Harrington, 2010). X-ray fluorescence (XRF) analysis of the bauxite residue was with a Panalytical Axios XRF.

6.2.2 Plant Growth Trial
Lolium perenne L. (perennial ryegrass) seeds which were chosen due to their prevalence in agricultural grassland, were germinated for 4 days in the dark at $20 \pm 2°C$ in an aerated

solution (Figure 6.1 (a)) containing 600 µmol dm^{-3} CaCl$_2$ and 2 µmol dm^{-3} H$_2$BO$_3$ (following the RHIZOtest™ procedure, ISO 16198:2015), using a Betta AP – 4500 Air Pumps (U.K.). Once germinated, the seedlings were placed in a glasshouse and exposed to a pre-culture period in a hydroponic solution (Figure 6.1 (b)), containing 500 µmol dm^{-3} KH$_2$PO$_4$, 2000 µmol dm^{-3} KNO$_3$, 2000 µmol dm^{-3} Ca(NO$_3$)$_2$, 1000 µmol dm^{-3} MgSO$_4$, 0.2 µmol dm^{-3} CuCl$_2$, 10 µmol dm^{-3} H$_3$BO$_2$, 2 µmol dm^{-3} MnCl$_2$, 1 µmol dm^{-3} ZnSO$_4$, 0.05 µmol dm^{-3} Na$_2$MoO$_4$ and 100 µmol dm^{-3} NaFe(III)EDTA (ISO 16198:2015), and the seedlings were allowed to develop a dense and planar mat of roots for 7 to 10 days. The conditions for this preculture period required 16/8 hr light/dark, 25/20 ± 3°C, 65-70% relative humidity and a light intensity of 200-400 µmol m^{-2} s^{-1}, and the solution was changed every three days.

Once established, the seedlings were transferred to individual plant pots containing P-deficient soil (Figure 6.1 (c) and Figure 6.2) and amended with one of the four treatments listed in Table 6.1 (n = 5 per treatment) for the growth trial.

| (a) | (b) | (c) |
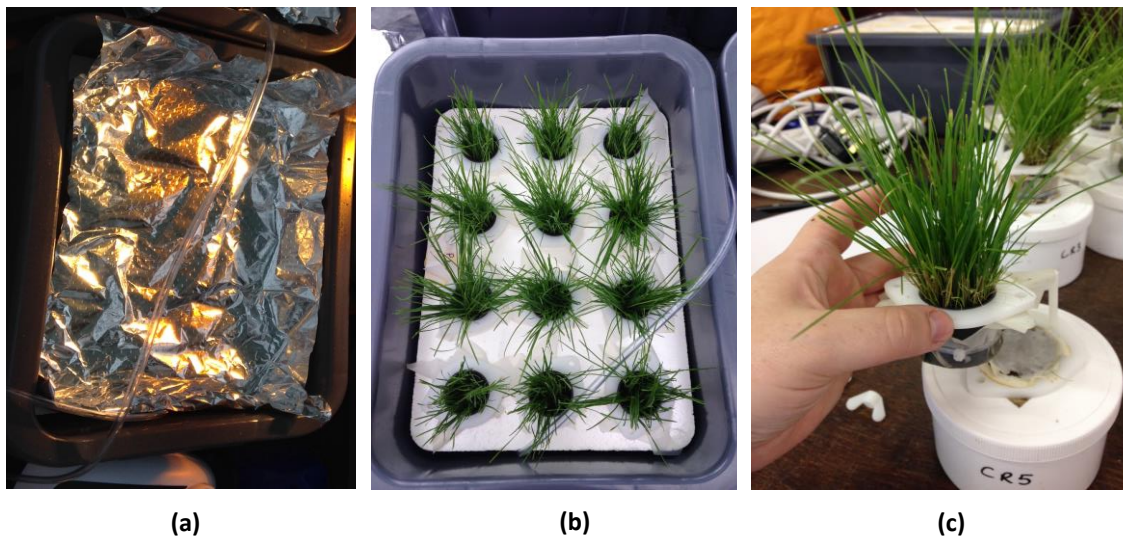
Figure 6.1 (a) Germination of seeds in the dark at 20 ± 2°C in an aerated solution **(b)** Pre-culture period in a hydroponic solution and **(c)** Growth trial using individual plant pots containing P-deficient soil.
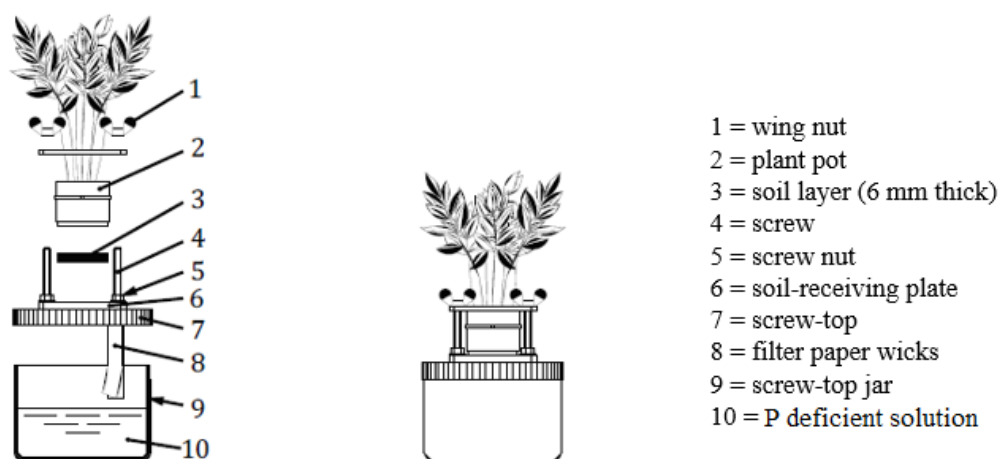
Figure 6.2 RHIZOtest™ set-up for the plant growth trial as taken from ISO 16198:2015.

A filter paper wick at the base of the soil-receiving plate was immersed in a P-deficient solution (changed every two days) (Figure 6.2), containing 2000 µmol dm^{-3} KNO$_3$, 2000 µmol dm^{-3} Ca(NO$_3$)$_2$ and 1000 µmol dm^{-3} MgSO$_4$. The growth trial was carried out over 14 days, under the same growing conditions as the preculture period. After the growth trial period of 14 days, the plant biomass was harvested and the dry weight measurements of the total biomass was determined. The plant material was then placed in an oven at 60°C for 72 hr.

6.2.3 Soil P Extracts

Soil P extracts were performed on the dried and sieved (< 2 mm) soil samples. Water extractable P was detemined using 1 g of soil with 20 mL deionised water and shaking for 1 hr at 180 rpm on a reciprocal shaker (Tessier et al., 1979). Morgan's P analysis was carried out using 0.54 M CH$_3$COOH and 0.7 M NaCH$_3$COO at pH 4.8 in a ratio of 6 mL: 30 mL.   This was then placed on a reciprocal shaker for 30 min at 180 rpm (Peech and English, 1944).

Olsen P analysis was conducted using 0.5 M NaHCO$_3$ at pH 8.5 in a ratio of 1g: 20 ml, followed by shaking on a reciprocating shaker for 30 min at 180 rpm (Olsen et al., 1954). The soil samples were also externally analysed by spectrophotometry following digestion for total P (TP) and total nitrogen (TN) content (HACH DR3900, APHA 4500-N and APHA 4500-P, Southern Scientific Services Ltd., Kerry, Ireland).

6.2.4 Phytotoxicity Tests

6.2.4.1 Seed Germination and Root Elongation Tests

Seed germination and root elongation tests were carried out after Courtney and Mullen (2009). The tests (n = 3) were performed using water extracts prepared by shaking the soil and their corresponding treatment, i.e. control, bauxite residue + gypsum, bauxite residue and super phosphate fertiliser, with deionized water using a 1:2 (soil/residue: water) ratio on a reciprocal shaker for 1 hr at 180 rpm, followed by centrifugation at 3,000 rpm, and then filtration through 0.45 μm syringe filters. Ten seeds (*L. perenne* L.) were placed in 100 × 15 mm plastic petri dish containing 6 mL of the prepared soil treatment extract. Deionised water was the control treatment used and the petri dishes were germinated at 25 °C. The number of seeds germinated were counted, and the length of the roots were measured at 2, 4 and 7 days. Germination was defined as a primary root of ≥ 5 mm and the test was terminated when the control seed had developed roots of at least 20 mm long (USEPA 1992).

Seedling performance was assessed using the relative seed germination (RSG) (Eqn. 1), which calculates the % of seeds germinated in the extracted water solution from the soil and individual treatment applied compared to the number of seeds germinated in the control soil water extract.

$$Relative\ seed\ germination\ (RSG)(\%) = \frac{number\ of\ seeds\ germinated\ in\ residue\ extract}{number\ of\ seeds\ germinated\ in\ control}$$
$$\times\ 100$$

Eqn. 1

Relative root growth (RRG) (Eqn. 2) compares the % root growth of seeds exposed to the water extract of the various treatments applied to the soil to the % root growth of seeds present in the water extract of the control soil.

$$Relative\ root\ growth\ (RRG)(\%) = \frac{mean\ root\ length\ in\ residue\ extract}{mean\ root\ length\ in\ control} \times 100$$

Eqn. 2

The germination index (GI) test (Eqn. 3) gives an overall percentage based on the RSG and RRG calculated (Tiquia et al., 1996).

160

$$Germination\ index\ (GI)(\%) = \frac{RSG \times RRG}{100}$$
Eqn. 3

6.2.4.2 Choice Test

Earthworms such as the species *E. fetida* L. are commonly used in soil ecotoxicological tests (Udovic and Lestan 2010) due to their increased sensitivity to their surrounding environment as a result of the many chemoreceptors found in their bodies (Curry and Schmidt 2007). Choice (avoidance) tests allow for the easy identification of any avoidance behaviour as favoured by the *E. fetida* L. (Amorim et al., 2008).

The preference behaviour of the earthworm *Eisinea fetida* L. *(E. fetida* L.*)* (locally sourced) was examined after Finnegan et al. (2018) using a six-sectioned preference chamber (n = 3) in accordance with ISO 17512-2 (2008), depicted in Figure 6.3, and as described by McShane et al. (2012). Each of the six-interconnected chambered stainless steel avoidance ring segments were filled with approximately 700 cm^{-3} of soil and the corresponding treatment applied (control, bauxite residue + gypsum, bauxite residue, superphosphate fertiliser) as described in Table 6.1. Twenty-five *E. fetida* L. individuals were gently rinsed using deionised water and patted dry with muslin cloth, and placed into the central cavity of each ring, which was then sealed for 72 hr. After the 72 hr period, the seal was removed and each of the inter-chamber openings were temporarily sealed with cardboard. The number of *E. fetida* L. in each chamber was then recorded, and the results were expressed as a percentage of the total population.
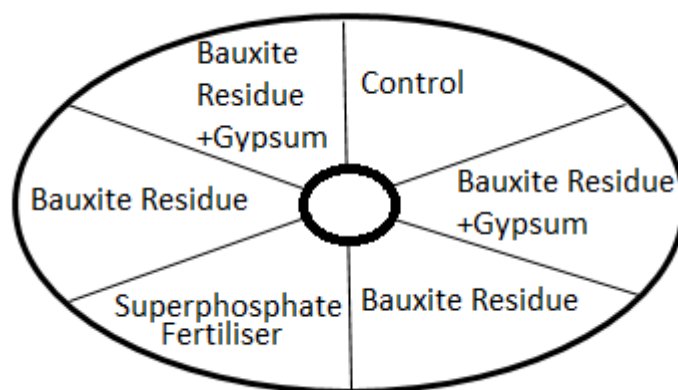
Figure 6.3 Six sectioned preference chamber (ISO 17512-2) used in the Choice Test with *E. fetida* L.

6.2.5 Statistical Analysis

Differences between soil properties and plant growth parameters in the different treatments was performed using Duncan's post hoc tests on one-way ANOVA using SPSS Version 21.

6.3 Results and Discussion

6.3.1 Nutrient Source and Soil Composition

The mineralogical composition of the spent bauxite residue (Table 6.2) predominantly comprised of iron and aluminium oxides (Fe_2O and Al_2O_3). Titanium, silicon and calcium oxides (TiO_2, SiO_2 and CaO) were also detected (Table 6.2). These were consistent with previous descriptions of the mineralogical composition of bauxite residue (Gräfe et al., 2011).

The mineral soil as provided by Lufa-Speyer (Germany) had a loamy sand texture and had a Morgan's P value of 0.64 ± 0.08 mg L^{-1} (Table 6.3). Soils with a Morgan's P value ranging from 0 to 3 mg L^{-1} are referred to as having a P index of 1, which is the lowest value possible in the index table (Coulter et al., 2008), indicating that the soil is very deficient in P (Coulter et al, 2008) and will have a definite response to fertilisers applied (Lalor et al., 2013).

Table 6.2 Main mineralogical composition (%) of the bauxite residue used, as determined from XRF analysis onsite at the alumina refinery.

Mineral Oxide	%
Al_2O_3	14.8 ± 1.5
Fe_2O	47.5 ± 2.0
SiO_2	7.20 ± 1.0
TiO_2	10.3 ± 0.95
CaO	6.1 ± 1.0

Table 6.3 The main composition of the P deficient (P1 index) mineral soil used in this study, as provided by Lufa-Speyer (Germany) who supplied the soil used in this study.

Soil Parameter	Value
Organic carbon (% C)	1.73 ± 0.27
Organic matter (% OM)	3.46
Nitrogen (% N)	0.19 ± 0.03
pH (0.01 M $CaCl_2$)	5.6 ± 0.4
Cation exchange capacity (meq 100 g^{-1})	9.8 ± 0.5
Particle Size (%)	
<0.002 mm	8.3 ± 1.8
0.002 – 0.05 mm	14.9 ± 3.0
0.05 – 2.0 mm	76.8 ± 4.0
Morgan's P (mg L^{-1})	0.64 ± 0.08 (P index 1)

6.3.2 Plant Growth Trial and Impact on Selected Soil Properties

Following the RHIZOtest™ growth trial period of 14 days (Figure 6.4), growth was evident for all the treatments applied. There was no significant difference ($p > 0.05$) in total plant biomass yield between the treatments applied (Figure 6.5). The lowest biomass content was measured in the control (1.25 ± 0.39 g DW), whereas the highest biomass harvested was observed for the plants grown on the soil receiving superphosphate fertiliser – 1.66 ± 0.33 g DW (Figure 6.5).
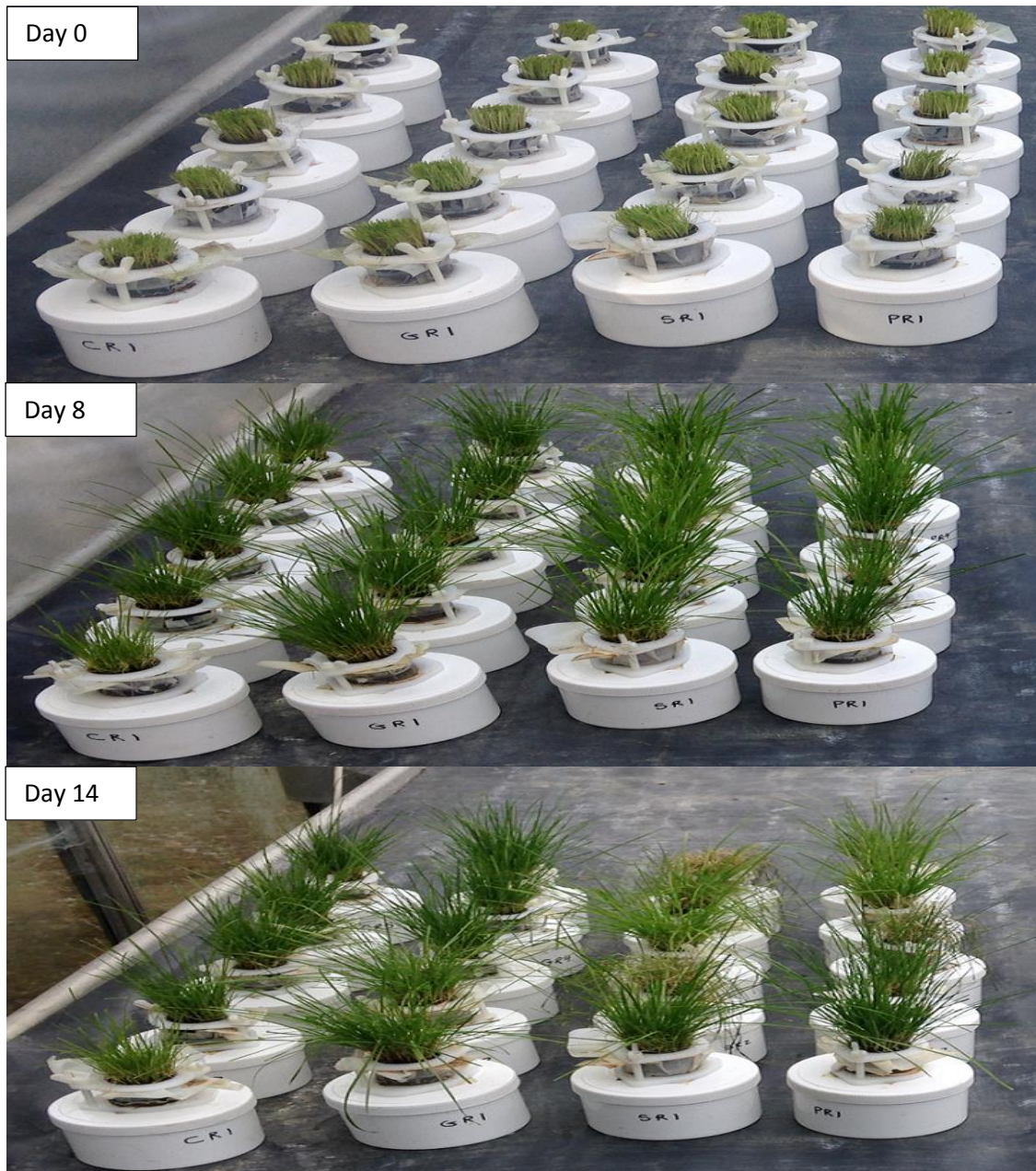
Figure 6.4 Time lapse of the plant growth trial using the RHIZOtest™.
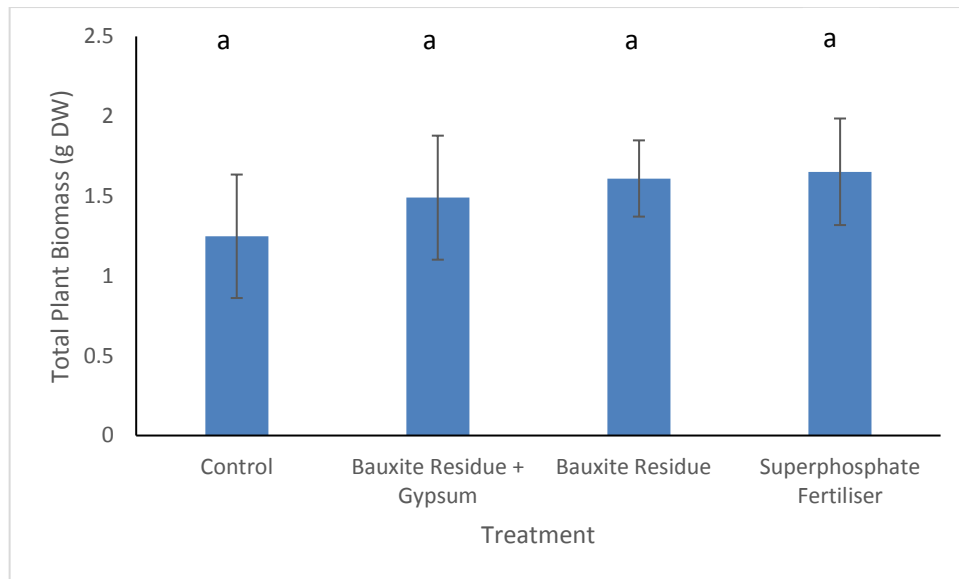
Figure 6.5 Total plant biomass following harvest of *L. perenne* L. content following growth on each of the soil treatments. Means followed by the same letter are not significantly different at $P \leq 0.05$.

Bauxite residue is generally nutrient deficient, lacking in N, P and K (Xue et al., 2016). No significant difference (p>0.05) was detected between TP and treatments applied (Figure 6.6). However, there was a significant difference (p<0.05) in the TN content and treatment applied between the study control and the treatments, with the bauxite residue performing best amongst treatments (Figure 6.7).
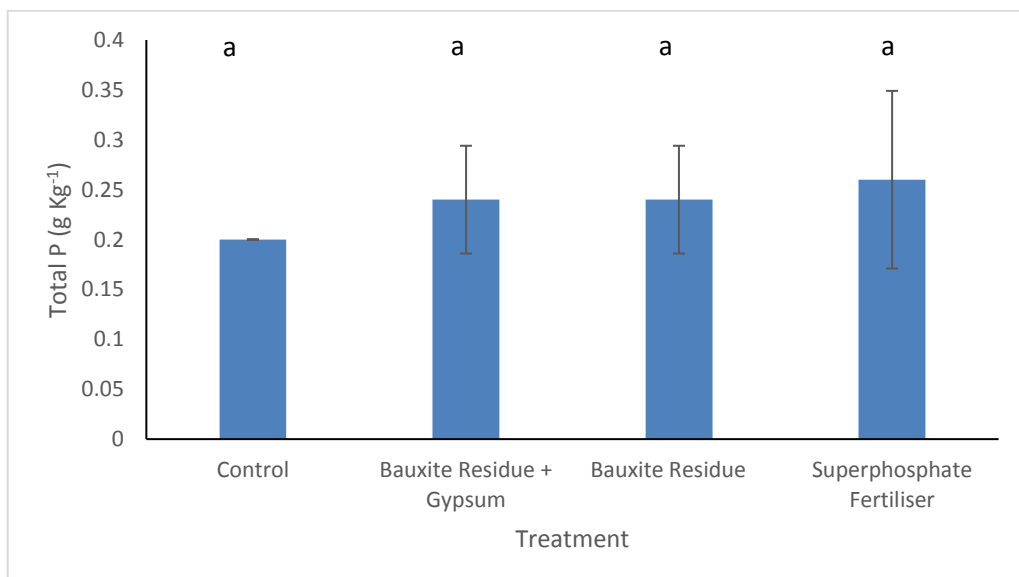
Figure 6.6 The total P content measured in the soil for all treatments following the harvest of *L. perenne* L. Means followed by the same letter are not significantly different at $P \leq 0.05$.
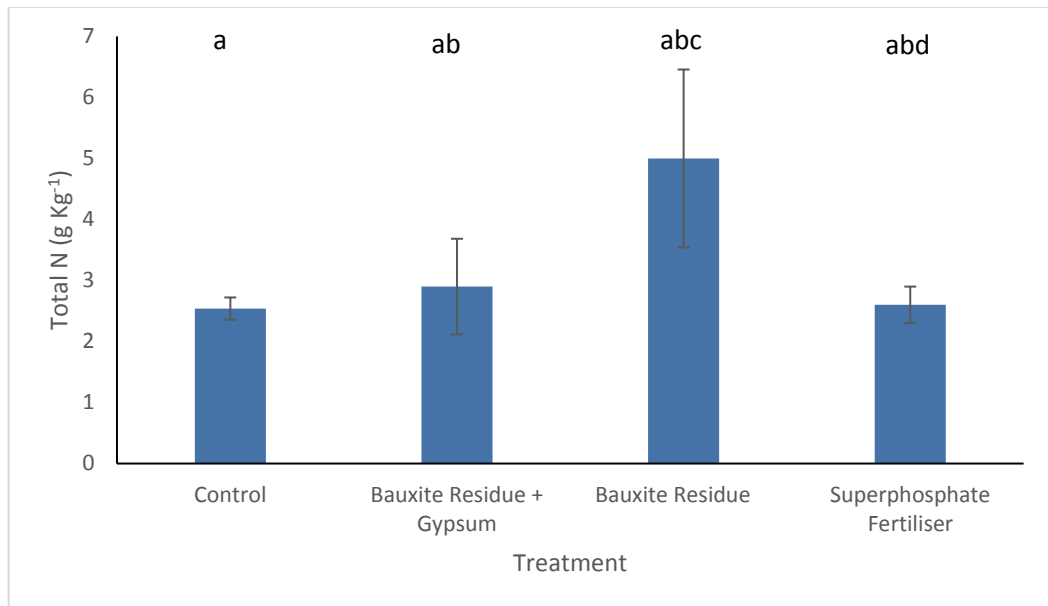
Figure 6.7 The total N content measured in the soil for all treatments following the harvest of *L. perenne* L. Means followed by the same letter are not significantly different at $P \leq 0.05$.

There was no significance (p>0.05) detected between soil pH values and treatments applied (Figure 6.8). This was unsurprising, given the short timeframe of the study. The pH ranged from 6.4 ± 0.1 to 6.62 ± 0.11 and fit in the desirable pH range for plant growth, which is between pH 5.5 and 9 (Mendez and Maier, 2007). A previous 8-week pot trial study carried out by Summers et al. (2000), who applied bauxite residue coated superphosphate fertiliser at a rate of 20 t ha^{-1} found that there was an increase in pH from 3.9 to 6.2. Similarly, Ruyters et al. (2011) found that the pH of soil increased from 6.8 to 8.3 after 3 weeks of plant growth following the addition of bauxite residue at a rate of 16.5%.
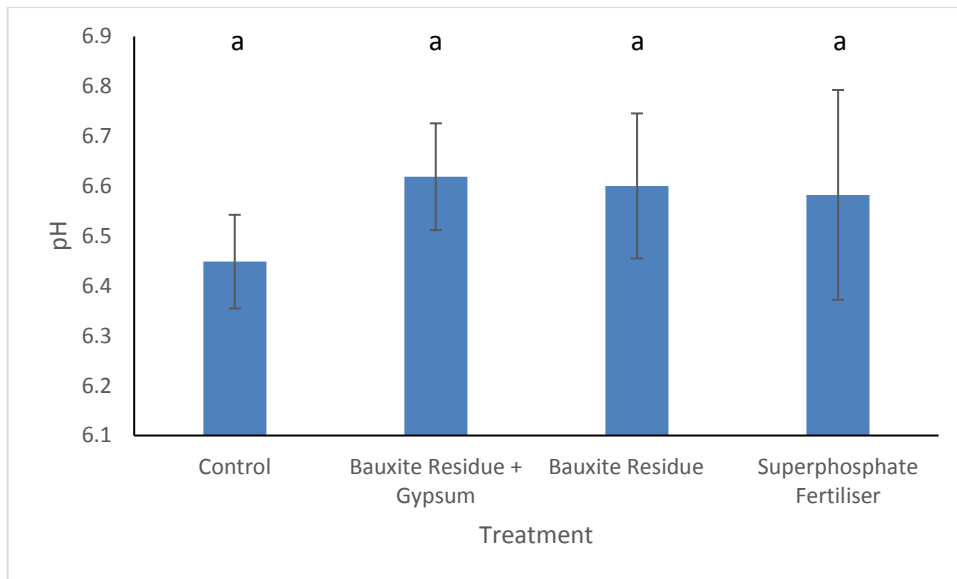
Figure 6.8 Measurement of the soil pH. Means followed by the same letter are not significantly different at $P \leq 0.05$.

A significant difference was detected in the salinity, as measured by the EC between the control and the soil receiving the gypsum-treated bauxite residue (Figure 6.9). Significant differences were also noted in the salinity between the gypsum-treated bauxite residue and the bauxite residue treatment. There was an increase in the EC, which varied from $147.06 \pm 19.6 \, \mu S \, cm^{-1}$ in the bauxite residue to $235.2 \pm 24.4 \, \mu S \, cm^{-1}$ in the gypsum-treated bauxite residue (Figure 6.9). Plant growth is optimal at an EC of 4 mS cm^{-1} (Li et al., 2006). The EC measured for the soil following application of the treatment in this study were below this value (Figure 6.9).
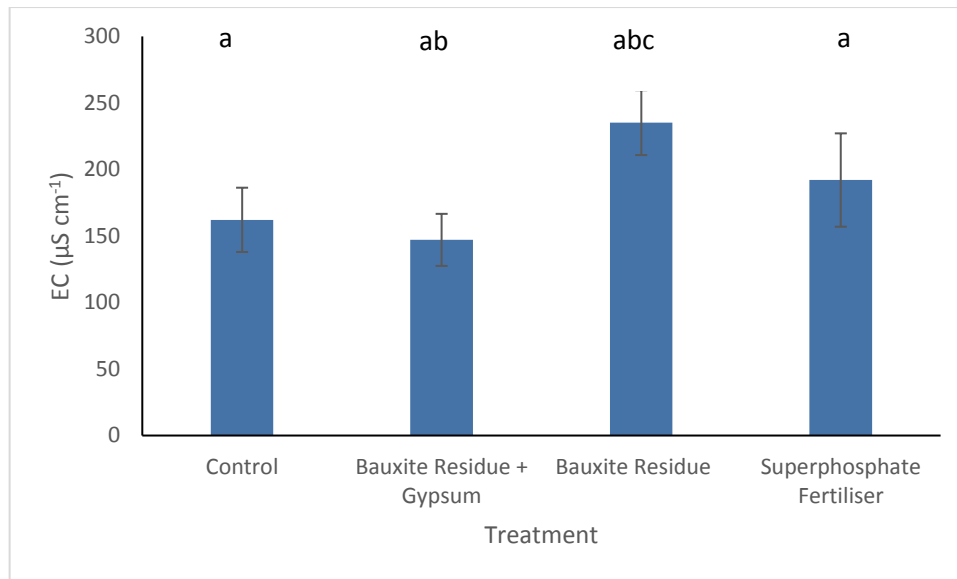
Figure 6.9 Measurement of the soil EC. Means followed by the same letter are not significantly different at $P \leq 0.05$.

Bauxite residue is often an undesirable growth media for plants due to its generally high alkalinity, sodicity and salinity (Jones and Haynes 2011). Previous studies have highlighted the positive effects of treatments such as gypsum in the improvement of the physico-chemical properties of bauxite residue (Courtney et al., 2009). In addition to this, previous work has investigated the use of bauxite residue as a potential amendment to a coarse textured sandy soil prone to P loss/leaching based on its recognised P adsorption capabilities (Summers et al., 2000; 2001). Summers et al. (1993) found that bauxite residue (neutralised with phosphogypsum), used as a soil amendment to reduce P leaching from a catchment area, resulted in a 70 % decrease in P loss – 13.8 kg ha^{-1} on the untreated catchment area to 4.2 kg ha^{-1} on the treated catchment area containing the bauxite residue. In a similar study by Summers et al. (1996), bauxite residue was added at a rate of 40 t ha^{-1} to a sandy soil prone to P loss and consequently, an increase in production of 24% was noted as a result of its P retention capacity. However, Summers et al. (1996) found that as a result in the rise of pH following bauxite residue application, manganese became deficient in plants. This highlights the necessity to monitor other key nutrients such as copper, zine and molybdenum, which are sensitive to pH. Indeed, one area of concern in the application of bauxite residue is potential metal mobilisation. Ruyters et al. (2011) found that although the addition of the bauxite residue increased levels of Cu, Cr, Fe and Ni concentrations in shoot biomass, they did not exceed maximum allowable limits for these elements. However, due to the insufficient amount of plant biomass obtained in

this short study for the dilutions required for the ICP-OES, metal analysis could not be carried out.

6.3.3 Soil P Extracts

Soil test phosphorus (STP) measurements such as Morgan's and Olsen are used to give an estimated value for soil P available for vegetative growth (Neyroud and Lischer 2003). There were significant differences in the Morgan's P content between the study control and all three treatments (Figure 6.10). A significant difference ($p<0.05$) was also noted between the superphosphate fertiliser and both the gypsum-treated bauxite residue and the bauxite residue treatments.
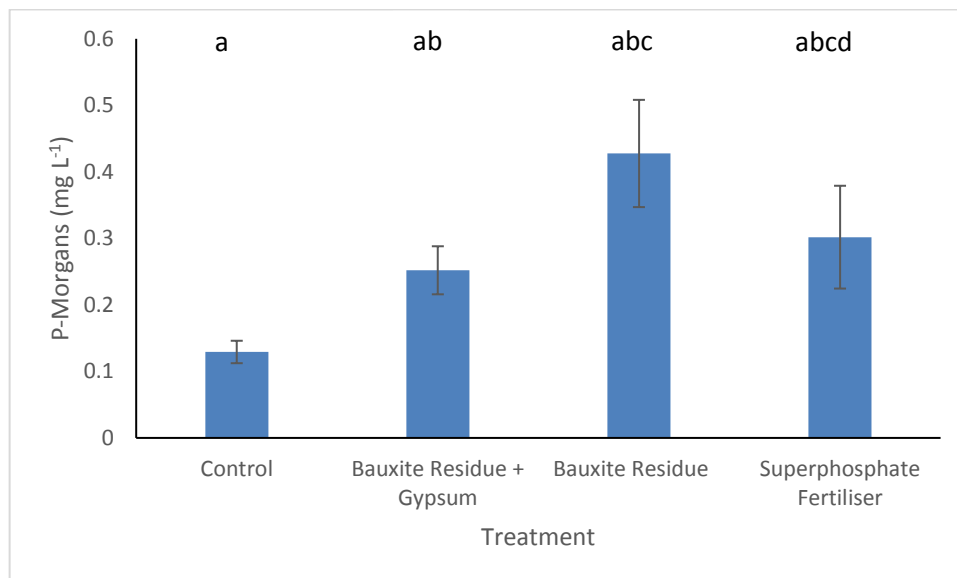
Figure 6.10 Morgan's P content measured in each of the soil treatments. Means followed by the same letter are not significantly different at $P \leq 0.05$.

The Morgan's extracted P varied from 0.13 ± 0.02 in the control to 0.43 ± 0.08 mg P L^{-1} in the soil receiving the bauxite residue. Overall, the soil was characterised as P deficient with a P1 index, as the original Morgan's P value for the soil used in the study was 0.64 ± 0.08 mg P L^{-1} (Table 6.3), which indicates that there was P uptake from soil P pool even when treatments were applied. This emphasises the importance of building up and managing soil P in very P-deficient soils such as those used in this study.

There was a significant difference ($p<0.05$) between the water extractable P in the control compared to all three treatments. Water extractable P varied from within the four

treatments, with the lowest amount observed for the control (0.04 ± 0.003 mg P L^{-1}) and the highest observed for the soil treated with the superphosphate fertiliser (0.10 ± 0.02 mg P L^{-1}) (Figure 6.11). Olsen (CaCl$_2$) extractable P was below detection limits (<0.02 mg L^{-1}) in all soils.
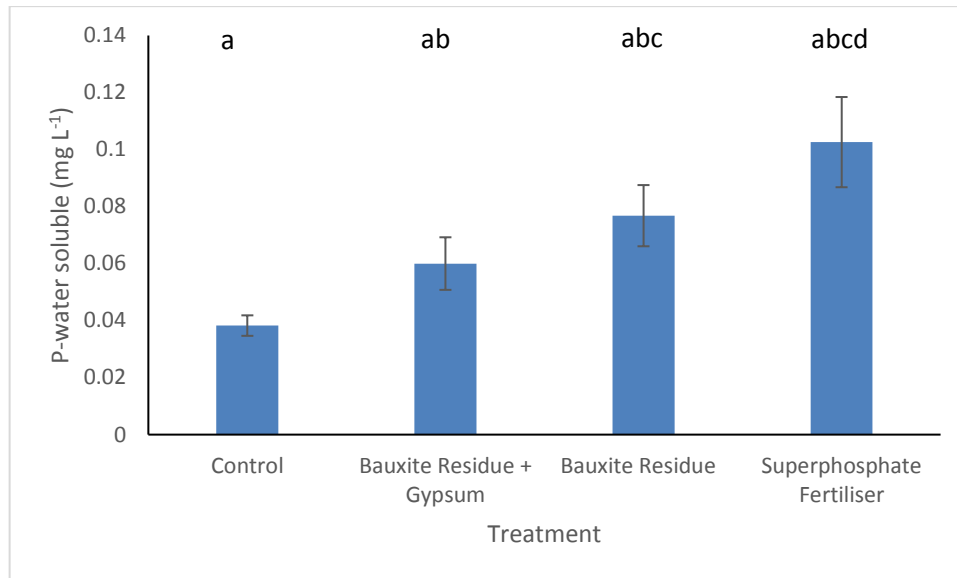
Figure 6.11 Water-extractable P content measured in each of the soil treatments. Means followed by the same letter are not significantly different at $P \leq 0.05$.

6.3.4 Phytotoxicity Tests

6.3.4.1 Seed Germination and Root Elongation Tests

The *L. perenne* L. germinated in all treatments (Figure 6.12), with a RSG > 73.1 % observed in all four treatments. The rate of germination is a factor in the establishment of vegetative growth (Harris 1996) and is reduced by environmental conditions such as a highly saline growth media (Rashid et al., 2006).
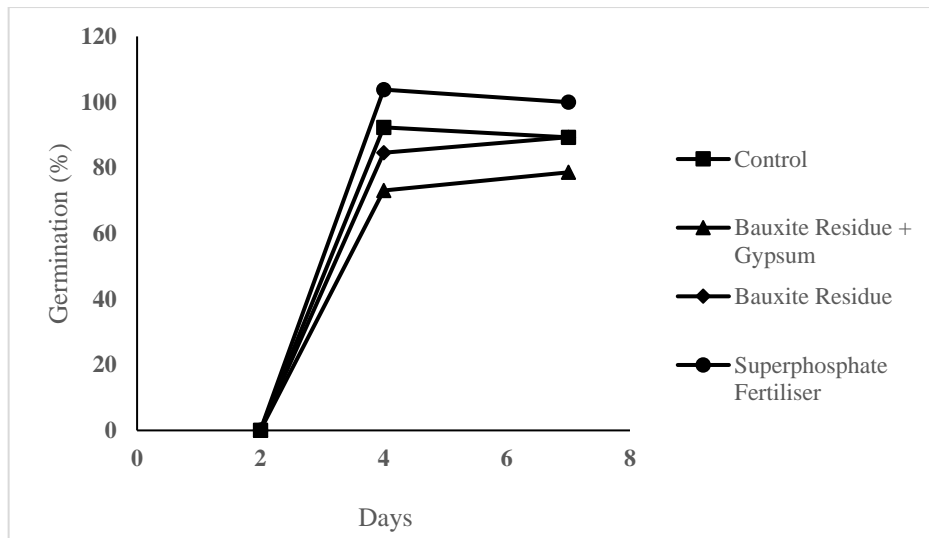
Figure 6.12 Relative seed germination (RSG) percentages of four bauxite residue extracts and one control using the species *L. perenne* L.

No significant difference was detected between the EC and the final root length. The RRG (Figure 6.13) was observed to decrease in all four treatments from day 4 to day 7. These values were observed for the gypsum-treated bauxite residue and bauxite residue treatments. Similar observations have been previously made when using bauxite residue, due to its high salinity and sodic nature (Jones and Haynes 2011). The GI (Figure 6.14) percentages were higher than 80%, with the exception of the gypsum-treated bauxite residue which was 78.2 % on day 7. Zucconi et al. (1982) state that no phytotoxic effects are present when the GI values are greater than 80 %.
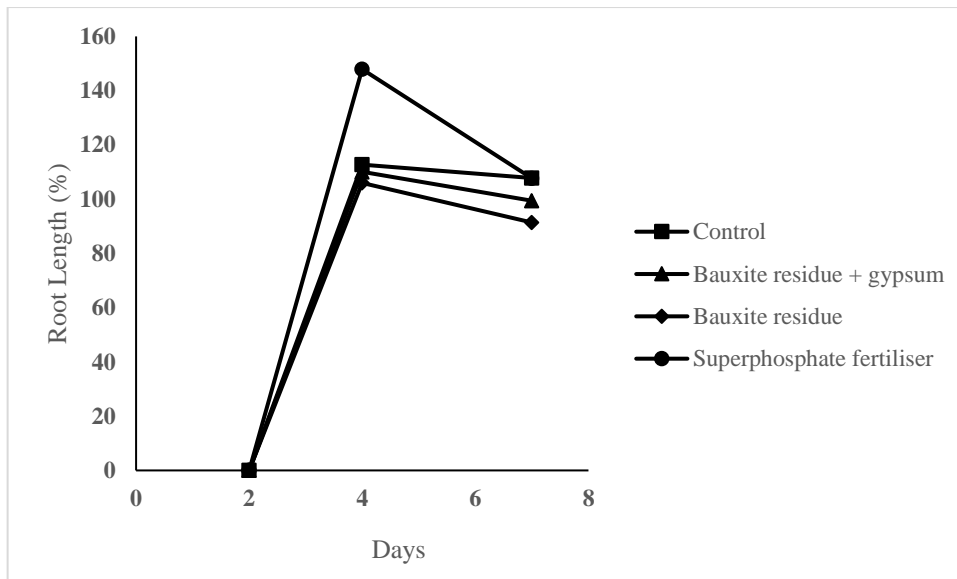
Figure 6.13 Relative root growth (RRG) percentages of four bauxite residue extracts and one control using the species *L. perenne* L.
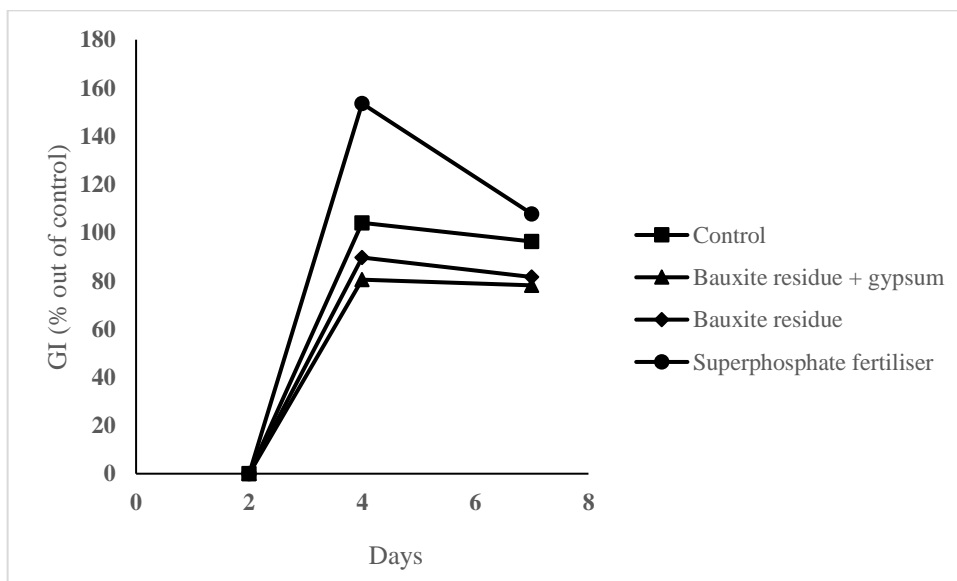
Figure 6.14 Germination indices (GI) percentages of four bauxite residue extracts and one control using the species *L. perenne* L.

6.3.4.2 Choice Test

In this study, there was a significant difference detected between the *E. fetida* L.'s choice of soils and the treatment applied (Figure 6.15). The largest percentage (57.7 ± 2.1 %) of *E. fetida* L. favoured the control soil (Figure 6.15). *E. fetida* L. were distributed amongst the other treatments (Figure 6.15), with the lowest population of *E. fetida* L. (12.2 ± 2.7

%) found in the soil containing the superphosphate application, which may suggest a sensitivity to the chemical composition of the superphosphate fertiliser (Figure 6.15).
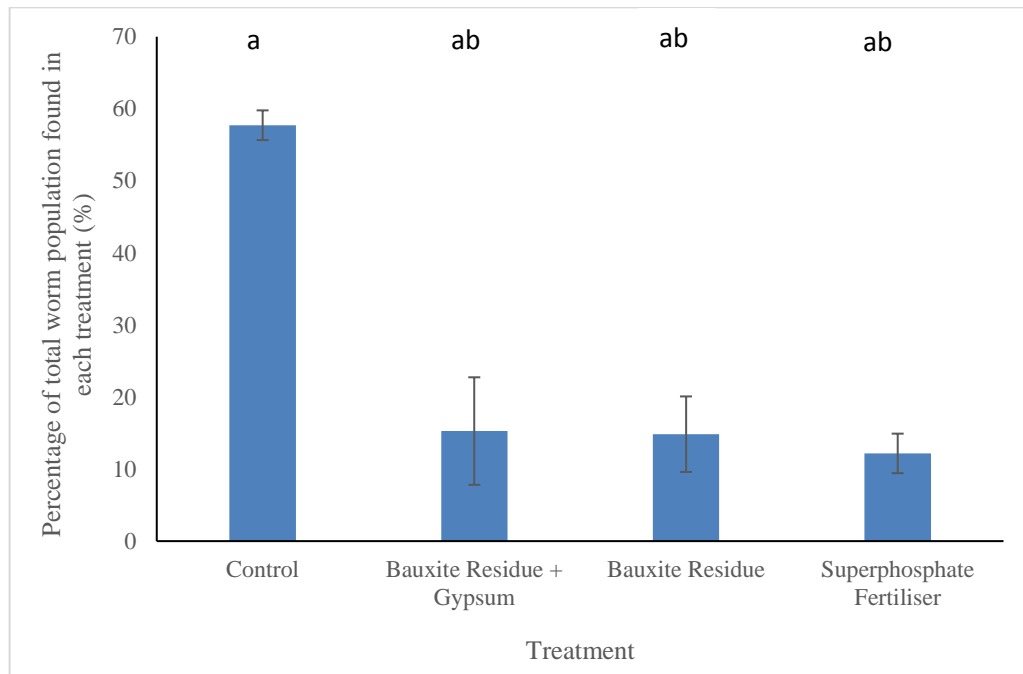
Figure 6.15 Preference of *E. fetida* L. expressed as the percentage of the total population recovered from each treatment sample at the end of the test period. Values are representative of the mean (n = 3) ± SD. Means followed by the same letter are not significantly different at $P \leq 0.05$.

6.5 Conclusions

This study investigated the efficacy of bauxite residue as a nutrient source on the growth of *Lolium perenne* L. and its impact on soil chemical properties, and compared its impact to a conventional superphosphate fertiliser. Although the results indicate a comparative biomass yield in the treatments using the application of the bauxite residue nutrient source, there was no significant difference detected between biomass yield and treatments detected. There were significant differences in the Morgan's P and the water extractable P between the control and the three treatments. Choice tests indicated that *E. fetida* L. preferred the control soil over the soils receiving the bauxite residue and the superphosphate treatments.

Implications of using bauxite residue as a nutrient source include the potential for metal mobilisation and uptake within the plant vegetation, which was not addressed in this study (due to insufficient plant biomass) but which needs to be assessed prior to using bauxite residue as a nutrient source. Phosphorus uptake and P supply within the plant vegetation may also be limited as bauxite residue - known for its high P adsorption rate - may hinder the potential mobilisation of P to plant.

6.6 References

Achat, D.L., Sperandio, M., Daumer, M.L., Santellani, A.C., Prud'Homme, L., Akhtar, M. and Morel, C., 2014. Plant-availability of phosphorus recycled from pig manures and dairy effluents as assessed by isotopic labeling techniques. *Geoderma*. *232*, pp.24-33.

Amorim, M.J., Novais, S., Römbke, J. and Soares, A.M., 2008. Avoidance test with Enchytraeus albidus (Enchytraeidae): Effects of different exposure time and soil properties. *Environ. Poll.* 155(1), pp.112-116.

Antonini, S., Arias, M.A., Eichert, T. and Clemens, J., 2012. Greenhouse evaluation and environmental impact assessment of different urine-derived struvite fertilizers as phosphorus sources for plants. *Chemosphere*. *89*(10), pp.1202-1210.

Baker, A., Ceasar, S.A., Palmer, A.J., Paterson, J.B., Qi, W., Muench, S.P. and Baldwin, S.A., 2015. Replace, re-use, recycle: improving the sustainable use of phosphorus by plants. *J. Experiment. Botany.* *66*(12), pp.3523-3540.

Cabeza, R., Steingrobe, B., Römer, W. and Claassen, N., 2011. Effectiveness of recycled P products as P fertilizers, as evaluated in pot experiments. *Nutrient. Cycling. Agroecosystems. 91*(2), p.173.

Callery, O. and Healy, M.G., 2017. Predicting the propagation of concentration and saturation fronts in fixed-bed filters. *Water. Res. 123*, pp.556-568.

Cánovas, C.R., Pérez-López, R., Macías, F., Chapron, S., Nieto, J.M. and Pellet-Rostaing, S., 2017. Exploration of fertilizer industry wastes as potential source of critical raw materials. *J. Clean. Prod. 143*, pp.497-505.

Castaldi, P., Silvetti, M., Enzo, S. and Melis, P., 2010. Study of sorption processes and FT-IR analysis of arsenate sorbed onto red muds (a bauxite ore processing waste). *J. Hazard. Mater. 175*(1-3), pp.172-178.

Cordell, D., Drangert, J.O. and White, S., 2009. The story of phosphorus: global food security and food for thought. *Global. Environ. Change*. *19*(2), pp.292-305.

Coulter, S., Lalor, S., Alex, C.S., Black, A., Bol, A., Burke, J., Carton, O.T., Coulter, B.S., Culleton, N., Dillon, P. and Humphreys, J., 2008. Major and micro nutrient advice for productive agricultural crops. Available: http://citeseerx.ist.psu.edu/viewdoc/summary?doi=10.1.1.608.6186 [accessed 01.05.2019].

Courtney, R. and Mullen, G., 2009. Use of germination and seedling performance bioassays for assessing revegetation strategies on bauxite residue. *Water. Air. Soil. Poll. 197*(1-4), pp.15-22.

Courtney, R.G., Jordan, S.N. and Harrington, T., 2009. Physico-chemical changes in bauxite residue following application of spent mushroom compost and gypsum. *Land. Degrad. Develop.* 20(5), pp.572-581.

Courtney, R. and Harrington, T., 2010. Assessment of plant-available phosphorus in a fine textured sodic substrate. *Ecol. Eng. 36*(4), pp.542-547.

Curry, J.P. and Schmidt, O., 2007. The feeding ecology of earthworms–a review. *Pedobiologia,* 50(6), pp.463-477.

Cusack, P.B., Healy, M.G., Ryan, P.C., Burke, I.T., O'Donoghue, L.M., Ujaczki, É. and Courtney, R., 2018. Enhancement of bauxite residue as a low-cost adsorbent for phosphorus in aqueous solution, using seawater and gypsum treatments. *J. Clean. Prod. 179*, pp.217-224.

De, D., Aniya, V. and Satyavathi, B., 2018. Application of an agro-industrial waste for the removal of As (III) in a counter-current multiphase fluidized bed. *Int. J. Environ. Sci. Technol.* pp.1-16.

De Gisi, S., Lofrano, G., Grassi, M. and Notarnicola, M., 2016. Characteristics and adsorption capacities of low-cost sorbents for wastewater treatment: a review. *Sustain. Mater. Technol. 9*, pp.10-40.

DEFRA, 2011. Anaerobic Digestion Strategy and Action Plan Department for Environment Food and Rural Affairs, London UK.

Despland, L.M., Clark, M.W., Vancov, T., Erler, D. and Aragno, M., 2011. Nutrient and trace-metal removal by Bauxsol pellets in wastewater treatment. *Environ. Sci. Technol. 45*(13), pp.5746-5753.

Desmidt, E., Ghyselbrecht, K., Zhang, Y., Pinoy, L., Van der Bruggen, B., Verstraete, W., Rabaey, K. and Meesschaert, B., 2015. Global phosphorus scarcity and full-scale P-recovery techniques: a review. *Critical. Reviews. Environ. Sci. Technol. 45*(4), pp.336-384.

Elser, J.J., Bracken, M.E., Cleland, E.E., Gruner, D.S., Harpole, W.S., Hillebrand, H., Ngai, J.T., Seabloom, E.W., Shurin, J.B. and Smith, J.E., 2007. Global analysis of nitrogen and phosphorus limitation of primary producers in freshwater, marine and terrestrial ecosystems. *Ecol. Letters. 10*(12), pp.1135-1142.

EPA, 2017. Water Quality in 2017, An Indicators Report. Available: https://www.epa.ie/pubs/reports/water/waterqua/Water%20Quality%20in%202017%20-%20an%20indicators%20report.pdf [accessed 23.04.2019].

European Commission. Communication from the Commission to the European Parliament, the Council, the European Economic and Social Committee and the Committee of the Regions on the 2017 list of critical raw materials for the EU, 2017. Available: https://eur-lex.europa.eu/legal-content/EN/TXT/?uri=CELEX:52017DC0490 [accessed 08.08.2018].

Evans, K., 2016. The history, challenges, and new developments in the management and use of bauxite residue. *J. Sustain. Metall.* 2(4), pp.316-331.

Finngean, G., O'Grady, A. and Courtney, R., 2018. Plant assays and avoidance tests with collembola and earthworms demonstrate rehabilitation success in bauxite residue. *Environ. Sci. Poll. Res. 25*(3), pp.2157-2166.

Friesl, W., Horak, O. and Wenzel, W.W., 2004. Immobilization of heavy metals in soils by the application of bauxite residues: pot experiments under field conditions. *J. Plant. Nutrition. Soil. Sci.* 167(1), pp.54-59.

Grace, M.A., Healy, M.G. and Clifford, E., 2015. Use of industrial by-products and natural media to adsorb nutrients, metals and organic carbon from drinking water. *Sci. Total. Environ. 518*, pp.491-497.

Grace, M.A., Clifford, E. and Healy, M.G., 2016. The potential for the use of waste products from a variety of sectors in water treatment processes. *J. Clean. Prod. 137*, pp.788-802.

Gräfe, M., Power, G. and Klauber, C., 2011. Bauxite residue issues: III. Alkalinity and associated chemistry. *Hydrometallurgy.* 108(1-2), pp.60-79.

Gray, C.W., Dunham, S.J., Dennis, P.G., Zhao, F.J. and McGrath, S.P., 2006. Field evaluation of in situ remediation of a heavy metal contaminated soil using lime and red-mud. *Environ. Poll.* 142(3), pp.530-539.

Harris, D., 1996. The effects of manure, genotype, seed priming, depth and date of sowing on the emergence and early growth of Sorghum bicolor (L.) Moench in semi-arid Botswana. *Soil. Tillage. Res.* 40(1-2), pp.73-88.

Healy, M.G., Fenton, O., Cormican, M., Peyton, D.P., Ordsmith, N., Kimber, K., Morrison, L., 2017. Antimicrobial compounds (triclosan and triclocarban) in sewage sludges, and their presence in runoff following land application. *Ecotoxicity. Environ. Safety.* 142: 448 – 453.

ISO, 2007. Soil quality-Avoidance test for determining the quality of soils and effects of chemicals on behaviour-Part 2: Test with collembolans (Folsomia candida). ISO/CD 17512-2.

Jones, B.E. and Haynes, R.J., 2011. Bauxite processing residue: a critical review of its formation, properties, storage, and revegetation. *Critical. Reviews. Environ. Sci. Technol.* 41(3), pp.271-315.

Jordan, P., Melland, A.R., Mellander, P.E., Shortle, G. and Wall, D., 2012. The seasonality of phosphorus transfers from land to water: implications for trophic impacts and policy evaluation. *Sci. Total. Environ.* 434, pp.101-109.

Lalor, S., Wall, D. and Plunkett, M., 2013. Maintaining optimum soil fertility – focus on offtake. The Fertiliser Association of Ireland, Proceedings of Spring Scientific Meeting 2013. Available: https://www.fertilizer-assoc.ie/wp-content/uploads/2014/10/FAI-2013-Proceedings-No-481.pdf [accessed 27.11.2018].

Lemal, L., Valmier, M. and Bravin, M., 2017. RHIZOtest: an innovative tool for phytoavailability assessment and risk management in polluted soils. Deltares.

Li, H., Huang, G., Meng, Q., Ma, L., Yuan, L., Wang, F., Zhang, W., Cui, Z., Shen, J., Chen, X. and Jiang, R., 2011. Integrated soil and plant phosphorus management for crop and environment in China. *A review. Plant. Soil.* 349(1-2), pp.157-167.

McShane, H., Sarrazin, M., Whalen, J.K., Hendershot, W.H. and Sunahara, G.I., 2012. Reproductive and behavioral responses of earthworms exposed to nano-sized titanium dioxide in soil. *Environ. Toxicol. Chem. 31*(1), pp.184-193.

Mendez MO, Maier RM., 2007. Phytostabilization of mine tailings in arid and semiarid environments—an emerging remediation technology. *Environ. Health. Perspect.* 116:278–283.

Moerman, W., Carballa, M., Vandekerckhove, A., Derycke, D. and Verstraete, W., 2009. Phosphate removal in agro-industry: pilot-and full-scale operational considerations of struvite crystallization. *Water. Res. 43*(7), pp.1887-1892.

Neyroud, J.A. and Lischer, P., 2003. Do different methods used to estimate soil phosphorus availability across Europe give comparable results?. *J. Plant. Nutrition. Soil. Sci.* 166(4), pp.422-431.

Olsen, S.R., 1954. *Estimation of available phosphorus in soils by extraction with sodium bicarbonate*. United States Department Of Agriculture; Washington.

Parsons, S.A. and Smith, J.A., 2008. Phosphorus removal and recovery from municipal wastewaters. *Elements. 4*(2), pp.109-112.

Peech, M. and English, L., 1944. Rapid microchemical soil tests. *Soil. Sci. 57*(3), pp.167-196.

Ruyters, S., Mertens, J., Vassilieva, E., Dehandschutter, B., Poffijn, A. and Smolders, E., 2011. The red mud accident in Ajka (Hungary): plant toxicity and trace metal bioavailability in red mud contaminated soil. *Environ. Sci. Technol.* 45(4), pp.1616-1622.

Ryu, H.D., Lim, C.S., Kang, M.K. and Lee, S.I., 2012. Evaluation of struvite obtained from semiconductor wastewater as a fertilizer in cultivating Chinese cabbage. *J. Hazard. Mater. 221*, pp.248-255.

SEPA, 2015. SEPA Briefing for the Scottish Parliament's Public Petitions Committee: Oral Evidence Session on Use of Sewage Sludge on Land – 23 June 2015 Edinburgh.

Sharpley, A.N., 2015. The Phosphorus Paradox: Productive Agricultural and Water Quality.   Available: https://scholar.uwindsor.ca/cgi/viewcontent.cgi?article=1018&context=icei2015 [accessed 08.08.2018].

Shepherd, J.G., Sohi, S.P. and Heal, K.V., 2016. Optimising the recovery and re-use of phosphorus from wastewater effluent for sustainable fertiliser development. *Water. Res. 94*, pp.155-165.

Summers, R.N., Guise, N.R. and Smirk, D.D., 1993. Bauxite residue (red mud) increases phosphorus retention in sandy soil catchments in Western Australia. *Fert. Res.* 34(1), pp.85-94.

Summers, R.N., Guise, N.R., Smirk, D.D. and Summers, K.J., 1996. Bauxite residue (red mud) improves pasture growth on sandy soils in Western Australia. *Soil. Res.* 34(4), pp.569-581.

Summers, R., Clarke, M., Pope, T. and O'Dea, T., 2000. Comparison of single superphosphate and superphosphate coated with bauxite residue for subterranean clover production on phosphorus-leaching soils. *Soil. Res.* 38(3), pp.735-744.

Summers, R.N., Bolland, M.D.A. and Clarke, M.F., 2001. Effect of application of bauxite residue (red mud) to very sandy soils on subterranean clover yield and P response. *Soil. Res.* 39(5), pp.979-990.

Tessier, A., Campbell, P.G. and Bisson, M., 1979. Sequential extraction procedure for the speciation of particulate trace metals. *Analytical. Chem. 51*(7), pp.844-851.

Tiquia, S.M., Tam, N.F.Y. and Hodgkiss, I.J., 1996. Effects of composting on phytotoxicity of spent pig-manure sawdust litter. *Environ. Poll. 93*(3), pp.249-256.

Udovic, M. and Lestan, D., 2010. Eisenia fetida avoidance behavior as a tool for assessing the efficiency of remediation of Pb, Zn and Cd polluted soil. *Environ. Poll.* 158(8), pp.2766-2772.

Ujaczki, É., Feigl, V., Molnár, M., Cusack, P., Curtin, T., Courtney, R., O'Donoghue, L., Davris, P., Hugi, C., Evangelou, M.W. and Balomenos, E., 2018. Re-using bauxite residues: benefits beyond (critical raw) material recovery. *J. Chem. Technol. Biotechnol.* 93(9), pp.2498-2510.

USEPA, 1992. Seed germination/ root elongation toxicity test. Washington: EG-12, Office of Toxic Substances, U. S. Environmental Protection Agency.

Wilfert, P., Kumar, P.S., Korving, L., Witkamp, G.J. and van Loosdrecht, M.C., 2015. The relevance of phosphorus and iron chemistry to the recovery of phosphorus from wastewater: a review. *Environ. Sci. Technol. 49*(16), pp.9400-9414.

Xue, S., Zhu, F., Kong, X., Wu, C., Huang, L., Huang, N. and Hartley, W., 2016. A review of the characterization and revegetation of bauxite residues (Red mud). *Environ. Sci. Poll. Res.* 23(2), pp.1120-1132.

Ye, J., Zhang, P., Hoffmann, E., Zeng, G., Tang, Y., Dresely, J., Liu, Y., 2014. Comparison of response surface methodology and artificial neural network in optimization and prediction of acid activation of Bauxsol for phosphorus adsorption. *Water. Air. Soil. Poll.* 225(12), 2225.

Zhou, K., Barjenbruch, M., Kabbe, C., Inial, G. and Remy, C., 2017. Phosphorus recovery from municipal and fertilizer wastewater: China's potential and perspective. *J. Environ. Sci. 52*, pp.151-159.

Zucconi, F., Pera, A., Forte, M. and De Bertoldi, M., 1982. Evaluating toxicity of immature compost [Phytotoxicity].

Chapter 7

Conclusions and Recommendations

7.1 General Discussion

As the European Commission (EC) advocates for the re-use of waste/by-products in the creation of a "circular economy" (EC 2015), several studies have investigated the use of such materials as potential low-cost adsorbents (Ahmed and Ahmaruzzaman 2016; Grace et al., 2016). One by-product that has shown great potential for re-use as a low-cost adsorbent for P is bauxite residue, which is currently being produced at a rate of 150 Mt per annum (Evans 2016) and has a utilisation rate of ~ 2 % (Ujaczki et al., 2018), with the remaining amount being placed in carefully managed bauxite residue disposal areas (BRDAs) (Burke et al., 2013). The overall aim of this study was to focus on the P adsorption capacity of bauxite residue, in raw or treated form, and to assess its ability as a medium for the retention of P from water and wastewater, and its fertiliser replacement potential.

Bauxite residue, which is generally characterised as being highly alkaline, saline, sodic and composed of very fine particles (Snars and Gilkes, 2009), has been previously investigated to determine potential avenues of re-use (Klauber et al., 2011). Such re-use possibilities have included applications in the construction industry (Pontikes and Angelopoulos 2013), the production of polymers (Hertel et al., 2016), and re-use as an adsorbent in wastewater treatment (Arco- Lázaro et al., 2018). In recent years, several studies have been conducted to investigate its potential for re-use as a secondary source for critical raw materials (CRMs) (Borra et al., 2016; Ujaczki et al., 2018). However, due to its general composition, there have been a number of barriers and limitations identified. These have included issues surrounding the transport of bauxite residue as a result of its high alkalinity and low solid percentage, and potential leaching of metal(loids) (Evans, 2016). Although the composition of bauxite residue can be generalised, there are variations in bauxite residue generated within different and sometimes the same

refineries, due to the differences in bauxite ore type and parameters used in the extraction of alumina (Gräfe et al., 2011).

To date, no detailed study has investigated the potential variation in bauxite residue within a BRDA in terms of its general composition and CRM content. Assessment of bauxite residue over a 12-year period (**Objective 1**) showed that there was little variation in its general composition. However, pH and EC did show some variation, with pH ranging from 10 ± 0.1 to 12.0 ± 0.02 and EC ranging from 0.4 ± 0.01 to 3.3 ± 0.2 mS cm^{-1}. There was no significant variation in the concentration of CRMs over time in storage. This highlights the potential of bauxite residue as a source of CRMs in one particular BRDA. However, it should be noted that variation may be present within other BRDAs.

A lot of emphasis has been placed on the use of bauxite residue as a potential low-cost adsorbent, in particular for the removal of P, due to its high abundance of both Al and Fe oxides (Jacukowicz-Sobala et al., 2015) present within the bauxite residue. Aluminium and Fe oxides can range from 10 to 22 % and 20 to 45 %, respectively (IAI, 2015), and are essential in the adsorption of P from aqueous solutions using the mechanism of ligand exchange (Jacukowicz-Sobala et al., 2015). Several studies have reported P adsorption rates ranging from 0.2 mg P g^{-1} (Grace et al., 2015) to 202.9 mg P g^{-1} (Liu et al., 2007), with the higher adsorption rates reported for bauxite residue which has undergone treatment with acid (Huang et al., 2008), heat (Liu et al., 2007), seawater (Akhurst et al., 2006), and gypsum (Lopez et al., 1998). Whilst these treatments prove effective in the enhancement of bauxite residue's adsorption capacity, they are often expensive in terms of the volumes of acid and energy required (Xue et al., 2016). No study was found in the literature, which investigated the P adsorption capacities of both fractions of bauxite residue, nor the impact on P adsorption of less energy intensive enhancement treatments such as gypsum and seawater.

To address this knowledge gap, this study investigated the P adsorption capacity (using batch studies and synthetic water) of bauxite residue produced in one alumina refinery, which did not operate a separation technique, and compared it to a fine and coarse fraction bauxite residue generated within an alumina refinery who did operate a separation technique. Seawater and gypsum treatments were applied to the different bauxite residue samples, and the effects of both treatments on the mineralogical, elemental, physico-

chemical and P adsorption capabilities (**Objective 2**) of the different bauxite residue samples were examined. The main findings of this study showed that both the seawater and gypsum treatments reduced the pH and increased the P adsorption capacities of all the bauxite residue samples examined. The P adsorption capacities of each of the bauxite residue samples examined were determined by fitting the data obtained from the batch studies to a Langmuir adsorption isotherm, giving an approximate P adsorption range of 0.345 to 2.73 mg P per g of bauxite residue. The gypsum treatment had the greatest effect on enhancing the P adsorption capacity. The conclusion of this part of the study was that bauxite residue, once treated with seawater or gypsum, has potential in the removal of P from aqueous solutions.

Although the P adsorption capacity of bauxite residue has been investigated in several studies incorporating treatments such as acid (Huang et al., 2008) and seawater to enhance its P adsorption capability, the majority of these studies involved the use of P synthetic water and batch studies (Grace et al., 2015; Ye et al., 2014). Batch studies do not predict true adsorption values for an adsorbent due to the incorporation of shaking of samples and unrealistic ratios of the adsorbent to the solution being treated (ÁdÁm et al., 2007). Pratt et al., (2012) identified the need of continuous flow/column studies to determine the true adsorption potential and longevity of an adsorbent material. In addition to investigating the potential of bauxite residue in the adsorption of P from synthetic water using batch studies, the current study also examined the P adsorption performance of the bauxite residue using small-scale laboratory filter columns, with two real wastewaters (**Objective 3**): forest run-off, which typically has a total phosphorus (TP) concentration in the range of 1 mg P L^{-1} (Finnegan et al., 2012), and dairy soiled water (DSW), which has a higher TP concentration ranging from 20 to 100 mg L^{-1} (Minogue et al., 2015). The bauxite residue performed best in the adsorption of P from the forest run-off. The approximate "service time" (time to operate effectively), determined from mathematical modelling of the performance of the filter columns, was 1.08 min g^{-1} media for the forest run-off and 0.28 min g^{-1} media for the DSW, before initial breakthrough time (which was taken as the time when the final effluent attained 5% of the influence concentration) occurred. Due to the composition of the bauxite residue, the effluent from the columns was analysed for the presence of metals. Analysis using ICP-OES identified that Al and Fe were the dominant metals present and were above the EPA parametric values − 0.2

mg L^{-1}. This would suggest the need to develop a rinse/wash cycle prior to operation of the columns.

The final part of the study examined the potential recycling of the bauxite residue media taken from the filter columns, once fully P-saturated, and investigated its potential as a nutrient source of plant growth using the RHIZOtest™ procedure. Due to the emergence of the CRMs list and the inclusion of both phosphate rock and phosphorus (EC 2017), there are several studies which have focussed on the potential of P to be recycled from wastewater sludge (Desmidt et al., 2015) such as the precipitation of struvite (Antonini et al., 2012). Struvite has been of particular interest as a potential fertiliser replacement due to its water solubility and therefore availability of elements such as Mg, N and P, which are key in the successful growth and sustenance of plants (Ryu et al., 2012).

Bauxite residue has previously been applied to soils, in particular sandy soils that are prone to leaching (Summers et al., 1993), to help prevent further P loss and leaching (Summers et al., 1996). The results from these studies are promising, showing the capabilities of bauxite residue application in the prevention of P loss due to its high P retention capacity (Summers et al., 2001). With this in mind, the final part of this study focussed on comparing the use of the P-saturated bauxite residue to a conventional superphosphate fertiliser in terms of impact on soil properties, plant growth, and P uptake in ryegrass (*Lolium perenne* L.) (**Objective 4**).

The plant biomass of the *L. perenne* L. growing in pots amended with both bauxite residue treatments (1.49 ± 0.39 to 1.61 ± 0.24 g DW) was comparable to the biomass in the pots amended with superphosphate fertiliser (1.65 ± 0.33 g DW). Regarding the potential ecotoxicological effects on fauna, "choice tests" indicated that *Eisenia fetida* L. preferred the control soil over the soils amended with either bauxite or superphosphate.

7.2 Conclusions

The main conclusions of this study are:

1. Bauxite residue, ranging from one to twelve years in storage, had little variation in terms of the mineralogical, elemental and general composition, with the exception of the pH and EC. There were no significant differences detected in the

186

CRM content over time in storage. This is a promising result for this particular BRDA in highlighting a potential untapped resource for CRMs if future supply risks increase within Europe, but the results obtained may not apply to other BRDAs.

2. Both seawater and gypsum treatments applied to coarse and fine fractions of bauxite residue, and also applied to bauxite residue which had not undergone separation into its separate fractions, were successful in reducing the pH of all the bauxite residue samples examined. The P adsorption capacity of the bauxite residue samples ranged from 0.345 to 2.73 mg P g^{-1}, with the highest P adsorption noted in the bauxite residue, which had not been separated into the different fractions, followed by the fine fraction bauxite residue. This highlights potential re-use for bauxite residue as an adsorbent, particularly for the fine fraction, ~ 98 % of which is currently placed in storage. Gypsum was the most effective amendment and depending on the location of the alumina refinery, this suggests potential re-use of gypsum material recycled from the construction industry. However, depending on the location of the alumina refinery, it may not be feasible to incorporate the use of seawater treatments.

3. The fine fraction bauxite residue media was effective in the removal of P from both a low P concentration wastewater (forest run-off) and a high P concentration wastewater (DSW), with the greatest performance observed when treating the forest run-off. The longevity of the bauxite residue was estimated to be 1.08 min g^{-1} for the forest run-off and 0.28 min g^{-1} for DSW. The difference in performance of the bauxite residue is a reflection on the type of wastewater and the greater number of contaminants present in the DSW (such as nitrates) which show competitive behaviour for the adsorption sites present on the surface of the bauxite residue. Aluminium and Fe were the dominant metals present in the effluent from the filters, which highlights the need to develop a wash/rinse cycle prior to the packing of columns with the bauxite residue.

4. Phosphorus-saturated bauxite residue from a column was examined and compared as a nutrient source to a conventional superphosphate fertiliser in the growth of ryegrass. The bauxite residue was comparable to the superphosphate fertiliser in

terms of the biomass yield obtained and changes to the soil P. In addition, there was no evidence to suggest phtotoxic effects on the growth of ryegrass, nor any effects on the *E. fetida* L. present in the soil.

7.3 Recommendations for Future Research

Recommendations for future work following this research include:

1. With emphasis being placed on the assurance of a CRM supply within Europe and the identification of vast CRM content present within by-products such as bauxite residue, which is underutilised and predominantly put in BRDA following generation, future studies should include the development of a new technology which would use reduced volumes of acid (which are currently used in leaching technologies) to recover CRMs from bauxite residue. Currently, the technologies used to recover CRMs from bauxite residue are heavily reliant on large volumes of acids and energy inputs such as heat. However, there are variations in CRM content of bauxite residue due to differences in bauxite ore used and differences in parameters used within alumina refineries.

2. Utilising by-products such as bauxite residue as a potential low-cost adsorbent for P from aqueous solutions, further research should focus on the development of a bauxite residue product, which would incorporate the use of wash/rinse cycles, to help alleviate potential risks to water treatment such as the leaching of trace metals.

3. Future studies should focus on the capability of bauxite residue as a potential reactive barrier in the active treatment and removal of other contaminants particularly from agricultural wastewaters. A life cycle assessment is necessary to fully assess the potential of bauxite residue as an adsorbent and to identify any potential problems, which may arise in its use in different environmental conditions.

4. Taking cognisance of the mineralogical and elemental composition of untreated bauxite residue, analysis on metal mobilisation/uptake in plant vegetation is also

necessary to determine any potential risks that may arise from using a treated bauxite residue as a fertiliser replacement.

7.4 References

ÁdÁm, K., Sovik, A.K., Krogstad, T. and Heistad, A., 2007. Phosphorous removal by the filter materials light-weight aggregates and shellsand-a review of processes and experimental set-ups for improved design of filter systems for wastewater treatment. *Vatten.* 63(3), 245.

Ahmed, M.J.K. and Ahmaruzzaman, M., 2016. A review on potential usage of industrial waste materials for binding heavy metal ions from aqueous solutions. *J.Water. Process Eng.* 10, pp.39-47.

Akhurst, D.J., Jones, G.B., Clark, M., McConchie, D., 2006. Phosphate removal from aqueous solutions using neutralised bauxite refinery residues (Bauxsol™). *Environ. Chem.* 3, 65-74.

Antonini, S., Arias, M.A., Eichert, T. and Clemens, J., 2012. Greenhouse evaluation and environmental impact assessment of different urine-derived struvite fertilizers as phosphorus sources for plants. *Chemosphere.* 89(10), pp.1202-1210.

Arco-Lázaro, E., Pardo, T., Clemente, R. and Bernal, M.P., 2018. Arsenic adsorption and plant availability in an agricultural soil irrigated with As-rich water: effects of Fe-rich amendments and organic and inorganic fertilisers. *J. Environ. Manage*. 209, 262-272.

Borra, C.R., Blanpain, B., Pontikes, Y., Binnemans, K. and Van Gerven, T., 2016. Recovery of rare earths and other valuable metals from bauxite residue (red mud): a review. *J. Sustain. Metallurgy*. 2(4), pp.365-386.

Burke, I.T., Peacock, C.L., Lockwood, C.L., Stewart, D.I., Mortimer, R.J., Ward, M.B., Renforth, P., Gruiz, K. and Mayes, W.M., 2013. Behavior of aluminum, arsenic, and vanadium during the neutralization of red mud leachate by HCl, gypsum, or seawater. *Environ. Sci. Technol.* 47, 6527-6535.

Cusack, P.B., Healy, M.G., Ryan, P.C., Burke, I.T., O'Donoghue, L.M., Ujaczki, É. and Courtney, R., 2018. Enhancement of bauxite residue as a low-cost adsorbent for

phosphorus in aqueous solution, using seawater and gypsum treatments. *J. Clean. Prod.* 179, 217-224.

Desmidt, E., Ghyselbrecht, K., Zhang, Y., Pinoy, L., Van der Bruggen, B., Verstraete, W., Rabaey, K. and Meesschaert, B., 2015. Global phosphorus scarcity and full-scale P-recovery techniques: a review. *Crit. Rev. Env. Sci. Tec.* 45(4), pp.336-384.

Eastham J, Morald T, Aylmore P., 2006. Effective nutrient sources for plant growth on bauxite residue. *Water. Air. Soil. Poll.* 176(1–4),5–19

European Commission, 2015. COM 2015. 614 Communication from the commission to the European Parliament, the Council, the European Economic and Social Committee and the Committee of the regions - Closing the loop - An EU action plan for the circular economy. Brussels.

European Commission, 2017. Communication from the Commission to the European Parliament, the Council, the European Economic and Social Committee and the Committee of the Regions on the 2017 list of critical raw materials for the EU, 2017. Available: https://eur-lex.europa.eu/legal-content/EN/TXT/?uri=CELEX:52017DC0490 [accessed 08.08.2018].

Evans, K., 2016. The history, challenges, and new developments in the management and use of bauxite residue. *J. Sustain. Metall.* 2, 316-331.

Finnegan, J., Regan, J.T., De Eyto, E., Ryder, E., Tiernan, D. and Healy, M.G., 2012. Nutrient dynamics in a peatland forest riparian buffer zone and implications for the establishment of planted saplings. *Ecol. Eng.* 47, 155-164.

Grace, M.A., Healy, M.G., Clifford, E., 2015. Use of industrial by-products and natural media to adsorb nutrients, metals and organic carbon from drinking water. *Sci. Total. Environ.* 518, 491-497.

Huang, W., Wang, S., Zhu, Z., Li, L., Yao, X., Rudolph, V., Haghseresht, F., 2008. Phosphate removal from wastewater using red mud. *J. Hazard. Mater.* 158, 35-42.

IAI, 2015. Bauxite Residue Management: Best Practice. http://www.world-aluminium.org/media/filer_public/2015/10/15/bauxite_residue_management_-_best_practice_english_oct15edit.pdf. [accessed 14.10.2017].

Jacukowicz-Sobala, I., Ociński, D. and Kociołek-Balawejder, E., 2015. Iron and aluminium oxides containing industrial wastes as adsorbents of heavy metals: Application possibilities and limitations. *Waste. Manage. Res.* 33(7), pp.612-629.

Jones, B.E., Haynes, R.J., Phillips, I.R., 2012. Addition of an organic amendment and/or residue mud to bauxite residue sand in order to improve its properties as a growth medium. *J. Environ. Manage.* 95, 29-38.

Klauber, C., Gräfe, M. and Power, G., 2011. Bauxite residue issues: II. options for residue utilization. *Hydrometallurgy.* 108(1-2), pp.11-32.

Liu, Y., Lin, C., Wu, Y., 2007. Characterization of red mud derived from a combined Bayer Process and bauxite calcination method. *J. Hazard. Mater.* 146, 255-261.

Lopez, E., Soto, B., Arias, M., Nunez, A., Rubinos, D., Barral, M.T., 1998. Adsorbent properties of red mud and its use for wastewater treatment. *Water. Re*s. 32, 1314-1322.

Minogue, D., French, P., Bolger, T. and Murphy, P.N.C., 2015. Characterisation of dairy soiled water in a survey of 60 Irish dairy farms. *Irish J. Agri. Food. Res.* 54(1), 1-16.

Pontikes, Y., Rathossi, C., Nikolopoulos, P., Angelopoulos, G.N., Jayaseelan, D.D. and Lee, W.E., 2009. Effect of firing temperature and atmosphere on sintering of ceramics made from Bayer process bauxite residue. *Ceramics. Internat.* 35, 401-407.

Pratt, C., Parsons, S.A., Soares, A. and Martin, B.D., 2012. Biologically and chemically mediated adsorption and precipitation of phosphorus from wastewater. *Curr. Opin. Biotechnol.* 23(6), 890-896.

Ryu, H.D., Lim, C.S., Kang, M.K. and Lee, S.I., 2012. Evaluation of struvite obtained from semiconductor wastewater as a fertilizer in cultivating Chinese cabbage. *J. Hazard. Mat.* 221, pp.248-255.

Snars, K. and Gilkes, R.J., 2009. Evaluation of bauxite residues (red muds) of different origins for environmental applications. *Applied Clay Science,* 46(1), pp.13-20.

Summers, R.N., Guise, N.R. and Smirk, D.D., 1993. Bauxite residue (red mud) increases phosphorus retention in sandy soil catchments in Western Australia. *Fert. Res.* 34(1), pp.85-94.

Summers, R.N., Guise, N.R., Smirk, D.D. and Summers, K.J., 1996. Bauxite residue (red mud) improves pasture growth on sandy soils in Western Australia. *Soil. Res.* 34(4), pp.569-581.

Summers, R.N., Bolland, M.D.A. and Clarke, M.F., 2001. Effect of application of bauxite residue (red mud) to very sandy soils on subterranean clover yield and P response. *Soil. Res.* 39(5), pp.979-990.

Udovic, M. and Lestan, D., 2010. Eisenia fetida avoidance behavior as a tool for assessing the efficiency of remediation of Pb, Zn and Cd polluted soil. *Environ. Pollut.* 158(8), pp.2766-2772.

Ujaczki, É., Feigl, V., Molnár, M., Cusack, P., Curtin, T., Courtney, R., O'Donoghue, L., Davris, P., Hugi, C., Evangelou, M.W. and Balomenos, E., 2018. Re-using bauxite residues: benefits beyond (critical raw) material recovery. *J. Chem. Technol. Biotech* 93, 2498-2510.

Xue, S., Zhu, F., Kong, X., Wu, C., Huang, L., Huang, N., Hartley, W., 2016. A review of the characterization and revegetation of bauxite residues (Red mud). *Environ. Sci. Poll. Res.* 23, 1120-1132.

Ye, J., Zhang, P., Hoffmann, E., Zeng, G., Tang, Y., Dresely, J., Liu, Y., 2014. Comparison of response surface methodology and artificial neural network in

optimization and prediction of acid activation of Bauxsol for phosphorus adsorption. *Water. Air. Soil. Pollut.* 225(12), 2225.

Appendix A

An Evaluation of the General Composition and Critical Raw Material Content of Bauxite Residue in a Storage Area over a Twelve-year Period

Patricia B. Cusack, Ronan Courtney, Mark G. Healy, Lisa M. T. O' Donoghue, Éva Ujaczki[*]

Article associated with Chapter 3.

An evaluation of the general composition and critical raw material content of bauxite residue in a storage area over a twelve-year period

Patricia B. Cusack [a, b], Ronan Courtney [a, b], Mark G. Healy [c], Lisa M.T. O' Donoghue [d], Éva Ujaczki [b, d, e, *]

[a] Department of Biological Sciences, University of Limerick, Castletroy, Co. Limerick, Ireland
[b] The Bernal Institute, University of Limerick, Castletroy, Co. Limerick, Ireland
[c] Civil Engineering, National University of Ireland, Galway, Ireland
[d] School of Engineering, University of Limerick, Castletroy, Co. Limerick, Ireland
[e] Department of Applied Biotechnology and Food Science, Faculty of Chemical Technology and Biotechnology, Budapest University of Technology and Economics, Müegyetem rkp. 3, 1111 Budapest, Hungary

ARTICLE INFO

ABSTRACT

Bauxite residue, the by-product produced in the alumina industry, is being produced at an estimated global rate of approximately 150 million tonnes per annum. Currently, the reuse of bauxite residue is low (~2%), due to limitations associated with its alkalinity, salinity, low solid content, fine particle size and potential leaching of metal(loid)s. It has been identified as a potential secondary source for critical raw materials such as vanadium, gallium and scandium, which currently have an associated supply risk and high economic cost within Europe. However, there is an uncertainty regarding the possible variation in these and other physico-chemical, elemental and mineralogical parameters within bauxite residue disposal areas. This paper aimed to address this knowledge gap by examining the variation of these parameters in a bauxite residue disposal area (BRDA) over a twelve-year period. The general composition did not vary greatly within the bauxite residue examined, with the exception of pH and electrical conductivity, which ranged from 10 ± 0.1 to 12.0 ± 0.02 and from 0.4 ± 0.01 to 3.3 ± 0.2 mS cm^{-1}, respectively. The bauxite residue contained critical raw materials, of which the amount of vanadium, gallium and scandium did not vary significantly over time. The vanadium and gallium were present in larger amounts compared to other European bauxite residues. On average the vanadium, gallium and scandium content measured in the bauxite residue samples were 510 ± 77.8, 107 ± 7.3 and 51.4 ± 5.4 mg kg^{-1}, respectively. This shows promise for the potential reuse of bauxite residue as a secondary source for critical raw materials and also indicates that BRDAs may be potential mines for critical raw material extraction.

© 2018 Elsevier Ltd. All rights reserved.

1. Introduction

Bauxite residue (red mud) is the by-product generated during the extraction of alumina from bauxite ore using the Bayer Process (Kirwan et al. 2013), and is currently being produced at a global rate of 150 Mt per annum, adding to the 3 Bt already in storage worldwide (Evans, 2016). Currently, less than 2% of the bauxite residue generated annually is being reused (Ujaczki et al. 2018), with the remaining ~98% going into bauxite residue disposal areas (BRDAs) (Burke et al. 2013). The average cost of disposing and managing of bauxite residue in storage is 1—2% of the alumina price for the alumina refinery (Tsakiridis et al. 2004).

Current best practice guidelines for the storage of bauxite residue is to use dry-stacking, a method which involves the thickening of the bauxite residue slurry from the Bayer process, using a filter press or vacuum filtration (depending on the refinery), before being spread in layers in the BRDA (Power et al. 2011; Evans, 2016). Depending on the nature of the bauxite ore used, some refineries operate a separation technique (Evans, 2016), which allows the bauxite residue to be separated into two main size fractions: a fine fraction (particle size <100 μm) and a coarse fraction (particle size > 150 μm) (IAI, 2015; Jones et al. 2012). Bauxite residue is typically characterised as being highly alkaline, saline and composed of mainly fine particles comprised of a wide range of metal(loid)s and minerals (Gräfe et al. 2011). This poses challenges in the long-term management of BRDAs in terms of protecting the

Nomenclature

Al	aluminium
AlO(OH)	boehmite
Al(OH)$_3$	aluminium hydroxide hydrate
Al$_2$O$_3$	aluminium oxide
As	arsenic
BRDA(s)	bauxite residue disposal area(s)
Bt	billion tonnes
CaO	calcium oxide
Ca(OH)$_2$	slaked lime
CaTiO$_3$	perovskite
Cd	cadmium
Ce	cerium
Co	cobalt
CO$_2$	carbon dioxide
CRM(s)	critical raw material(s) (mg kg^{-1})
Cr	chromium
Cu	copper
DSC	differential scanning calorimetry (mW)
Dy	dysprodium
EC	electrical conductivity (mS cm^{-1})
EDS	energy-dispersive x-ray spectroscopy (weight %)
Er	erbium
Eu	europium
EU	European Union
Fe	iron
FeO(OH)	goethite
Fe$_2$O$_3$	iron oxide
Ga	gallium
Gd	gadolinium
HCl	hydrochloric acid
HNO$_3$	nitric acid
Ho	holmium
ICP-OES	inductively coupled plasma optical emission spectrometer
In	indium
Kα	k alpha
kV	kilovolt
La	lanthanum
Lu	lutetium
1M	1 M
mA	milliamp
Mo	molybdenum
MPa	megapascal
Mt	million tonnes
N	nitrogen
NaOH	sodium hydroxide
Nd	neodymium
Ni	nickel
P	phosphorus
ρ$_b$	bulk density (g cm^{-3})
PGM	platinum group metals
PVDF	polyvinylidene difluoride
pH	pH(pH unit)
Pr	praseodymium
PSA	particle size analysis (μm and in % of the total particle distribution)
REE(s)	rare earth element(s) (mg kg^{-1})
REO(s)	rare earth oxide(s)
Sc	scandium
SEM	scanning electron microscope (μm)
SiO$_2$	silicon oxide
Sm	samarium
Tb	terbium
TGA	thermogravimetric analysis (mg)
Ti	titanium
TiO$_2$	titanium oxide
Tm	thulium
Tn	terbium
V	vanadium
XRD	x-ray diffraction (°2θ)
XRF	x-ray fluorescence (%)
Y	yttrium
Yb	ytterbium

surrounding environment (Higgins et al. 2017; Kong et al. 2017a; b), due to the high alkalinity, increased risk of dust pollution (due to the fine particles), and leaching of trace elements (Wang et al. 2015; Kong et al. 2017a,b). The disposal conditions and management of residue in a BRDA is dependent on many factors such as location, climate, engagement with local communities and stakeholders (IAI, 2015) and involves licencing permits from regulatory authorities (such as the Environmental Protection Agency). For example, European operators must meet the requirements according to the European List of Waste and Directive (EU Communities, 1999,2000). As a result of this, some refineries implement neutralisation techniques prior to disposal, such as carbon dioxide (CO$_2$) sparging of residues (Cooling, 2007) or post disposal through the use of atmospheric carbonation (mud farming) with amphirolling (Evans, 2016) in the BRDA, which helps in the neutralisation, dewatering and compaction of the bauxite residue (Evans, 2016; Gomes et al. 2016; Higgins et al. 2016; Zhu et al. 2016a; b), reducing both alkalinity and moisture content, which are two limitations to the re-use of bauxite (Evans, 2016).

Traditionally, the reuse of bauxite residue has focussed on construction applications such as cementitious application (Pontikes and Angelopoulos, 2013; Nikbin et al. 2018). Some other reuse options for bauxite residue have included polymers (Hertel et al. 2016), ceramics (Pontikes et al. 2009) and catalysts (Wang et al. 2008); adsorbents for wastewater treatment (Bhatnagar et al. 2011), particularly for the removal of arsenic (As) (Arco-Lázaro et al. 2018), chromium (Cr) (Dursun et al. 2008), nickel (Ni) (Hannachi et al. 2010), copper (Cu) (Atasoy and Bilgic, 2018), cadmium (Cd) (Ha et al. 2017) and phosphorus (P) (Cusack et al. 2018), as well as applications as potential soil ameliorants (Ujaczki et al. 2015). More recently and due to the demand of critical raw materials (CRMs), particularly the rare earth elements (REEs), studies have examined the potential of bauxite residue as a secondary source of these materials and their potential economic value (Gomes et al. 2016; Xue et al. 2016; Ujaczki et al. 2017).

Within the European Union (EU), the 'Raw Materials Initiative' ensures that Europe secures and sustains an affordable supply of CRMs which are identified as being of high economic importance and having a risk to their supply (EU COM/2017/0490). The list of 27 CRMs features elemental groups and single elements, including platinum group metals (PGM) and REEs (EU COM/2017/0490). The REEs are divided into light REE [lanthanum (La), cerium (Ce), praseodymium (Pr), neodymium (Nd), samarium (Sm), europium (Eu)] and heavy REE [gadolinium (Gd), terbium (Tb), dysprodium (Dy), holmium (Ho), erbium (Er), thulium (Tm), ytterbium (Yb), lutetium (Lu), including yttrium (Y)] (Xu et al. 2017) plus scandium (Sc)

(Binnemans et al. 2018). Depending on the origin of the bauxite residue generated, it may be a potentially valuable source of CRM and other elements e.g. REEs, Sc, V, Ga, and titanium (Ti) (Liu and Naidu, 2014). Also included in the 2017 CRM list is P and phosphate rock, which are also of particular interest, as bauxite residue has been previously identified as having a high P retention capacity (Grace et al. 2015, 2016; Cusack et al. 2018) due to its high aluminium (Al) and iron (Fe) oxide content (IAI, 2015), making it a possible resource in the removal and recovery of P from aqueous solutions (Grace et al. 2015; Cusack et al. 2018).

Although bauxite residues are typically similar in composition, properties can vary between refineries and this is attributed to the type of ore used, as well as different process parameters, such as temperature, pressure and concentrations of caustic soda (NaOH), slaked lime (Ca(OH)$_2$) and other additives used in the Bayer process (Gräfe et al. 2011). This indicates that re-use options should be refinery-specific (Balomenos et al. 2017). A further potential limitation, is that bauxite residue composition, such as pH and bulk density, may change over time in storage (Kong et al. 2017a; Zhu et al. (2016a,b), which greatly influences the possibility of reusing bauxite residue.

To date, no study has investigated the CRM content variability in bauxite residue stored within one specific BRDA. Therefore, the objectives of this study were to: (1) characterise the physico-chemical, elemental and mineralogical composition of the dominant fraction (fine fraction) bauxite residue in storage over a twelve-year period, and to determine if there is any variation over the time spent in storage, which could affect possible reuse of the bauxite residue (2) create an inventory of economically interesting elements in bauxite residue over the storage period, and (3) calculate the financial value of economically interesting elements present in the bauxite residue.

2. Materials and methods

2.1. Site description and sample collection

Bauxite residue was obtained from a European refinery, who operated a separation technique to isolate the fine (particle sizes <100 μm) and coarse (particle sizes >150 μm) fractions of bauxite residue before disposal (IAI, 2015), in an approximate ratio of 9:1 (fine: coarse). Bauxite residue was sampled to a depth of 30 cm and the bulk samples were stored in 1 L containers, returned to the laboratory, and dried at 105 °C for 24 h. Once dry, the samples were pulverised using a mortar and pestle and sieved to a particle size <2 mm. In this paper, the age of the samples will be described (Table 1) relative to the sample collection time (2016).

Table 1
Sample information regarding the year of production for each of the bauxite residue samples over a twelve-year period. The sample code for each bauxite residue sample is also included in the table.

Sample Code	Sample Description	Year of Disposal
BR 12	Bauxite Residue	2004
BR 11	Bauxite Residue	2005
BR 10	Bauxite Residue	2006
BR 9	Bauxite Residue	2007
BR 8	Bauxite Residue	2008
BR 7	Bauxite Residue	2009
BR 6	Bauxite Residue	2010
BR 5	Bauxite Residue	2011
BR 4	Bauxite Residue	2012
BR 3	Bauxite Residue	2013
BR 2	Bauxite Residue	2014
BR 1	Bauxite Residue	2015

2.2. Characterisation study

2.2.1. Physico-chemical composition

The bauxite residue samples were characterised (n = 3) for their physical, chemical, elemental and mineralogical properties (Fig. 1). The pH and electrical conductivity (EC) were measured using a 5 g sample in an aqueous extract, using a 1:5 ratio (solid: liquid) (Courtney and Harrington, 2010). The bulk density (ρ_b) was determined after Blake (1965), the effective particle size analysis (PSA) was determined on particle sizes < 53 μm using optical laser diffraction on a Malvern Zetasizer 3000HS® (Malvern, United Kingdom) with online autotitrator and a Horiba LA-920, and reported at specific cumulative % (10, 50 and 90%). Thermogravimetric analysis (TGA) was carried out to identify any change in mass over time with temperature, and change in heat flow over time with temperature was analysed using differential scanning calorimetry (DSC). TGA and DSC were carried out using a Labsys TG (DSC/TGA 1600) in a nitrogen (N) atmosphere at a temperature range of 30 °C—1000 °C at a heating rate of 10 °C min^{-1} (Borra et al. 2015). Due to cost limitations, only six samples were analysed (BR12, BR10, BR8, BR6, BR4 and BR2).

2.2.2. Mineralogical composition

Mineralogical detection was carried out on 1 g powdered samples using X-ray diffraction (XRD) on a Philips X'Pert PRO MPD® (California, USA) at 40 kV, 40 mA, 25 °C by Cu X-ray tube (Kα-radiation). The patterns were collected in the angular range from 5 to 80° (2θ) with a step-size of 0.008° (2θ) (Castaldi et al. 2011), whilst surface morphology and elemental detection were carried out using scanning electron microscopy (SEM) and energy-dispersive X-ray spectroscopy (EDS) on a Hitachi SU-70 (Berkshire, UK). X-ray fluorescence (XRF) analysis was carried out onsite at the refinery using a Panalytical Axios XRF (Malvern, UK).

2.2.3. Elemental composition

Chemical analysis of minor elements was performed after aqua regia digestion (HCl: HNO$_3$) with a solid to liquid ration of 1:10 in a Multiwave 3000 (Rotor 8XF100) type microwave digestion system at 200 °C 1.25 MPa. After digestion, the solutions were filtered through 0.45 μm PVDF syringe filters and diluted in 1 M HNO$_3$ for the analysis (Ujaczki et al. 2017). The metal analysis was carried out using an Agilent Technologies 5100 inductively coupled plasma optical emission spectrometer (ICP-OES). The calibration curve was constructed using standard solutions of 100, 50, 10, 5 and 1 g L^{-1} multi-element standard (Inorganic Ventures, Ireland) and 5, 2.5, 0.5, 0.25 and 0.05 g L^{-1} REE standard (Inorganic Ventures, Ireland). The 1M HNO$_3$ solution was also used for the dilutions of the standard solutions and as a calibration blank. For the ICP-OES analysis, the following analytical lines (in nm) were used for the calculations of each of the elements: Ce 418.659, 446.021; cobalt (Co) 228.615, 230.786; Dy 353.171; Er 349.910, 369.265; Eu 397.197, 412.972, 420.504; Ga 294.363; Gd 335.048, 336.224; Ho 339.895, 345.600, 389.094; indium (In) 230.606, 352.609; La 333.749, 379.477, 408.671; Lu 261.541, 307.760; molybdenum (Mo) 202.032, 203.846, 204.598; Nd 401.224, 406.108, 410.945; Pr 390.843, 417.939; Sc 335.372, 361.383, 363.074; Sm 359.259, 360.949; Tb 350.914,367.636; Tm 313.125, 342.508; Y 360.074, 371.029, 377.433; Yb 289.138, 328.937, 369.419; V 268.796, 292.401, 311.070 (Bridger and Knowles, 2000).

2.3. Statistical analysis

Pearson's correlation coefficients were used to determine any relationships between age of sample and sample properties (pH, EC, bulk density, particle size, mineralogical composition and
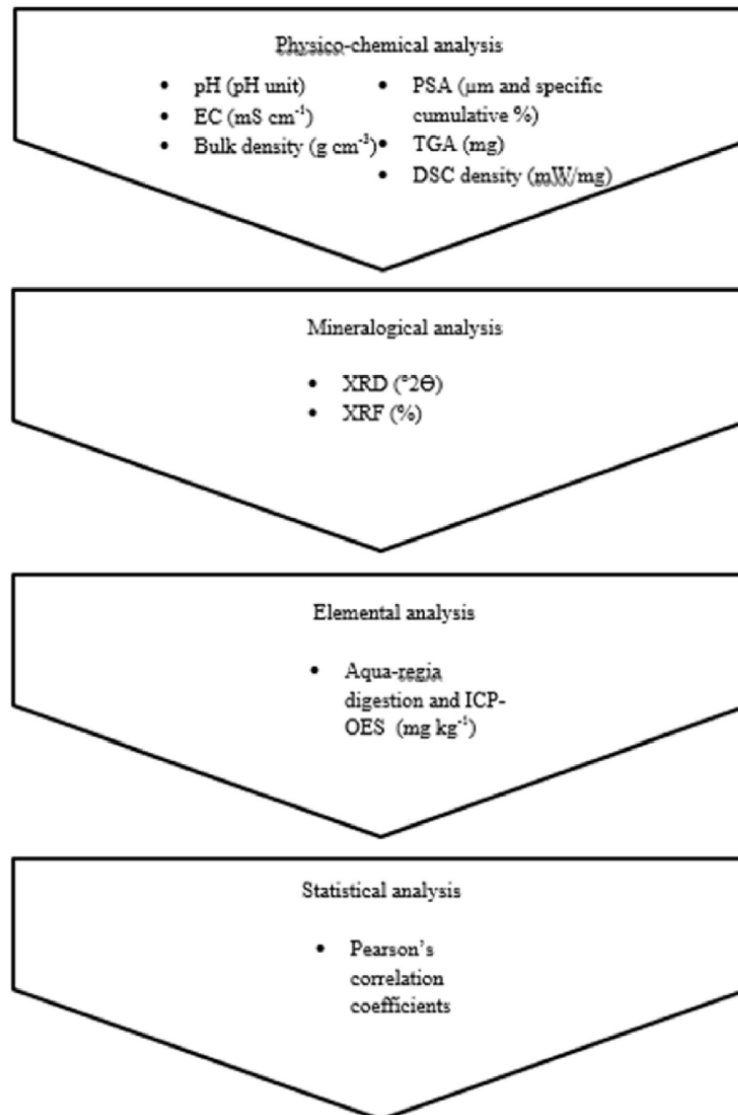
Fig. 1. Flow chart illustrating the experimental analysis carried out on the bauxite residue samples obtained. Once obtained from the BRDA, the bauxite residue was analysed for its main physico-chemical analysis (pH, EC, bulk density, PSA, TGA and DSC), mineralogical analysis (XRD and XRF), and elemental analysis (measure using ICP-OES following aqua-regia digestion). Once all data was obtained, statistical analysis was carried out using Pearson's correlation coefficients.

elemental composition), using IBM SPSS Statistics 24.

3. Results

3.1. Physico-chemical composition

The pH of the bauxite residue (Table 2) ranged from 10.0 ± 0.1 to 12.0 ± 0.02 over the twelve-year period, with the ten-year-old sample (BR10) having the highest value. The EC (Table 2) of the bauxite residue ranged from 0.4 ± 0.01 to 3.3 ± 0.2 mS cm^{-1}, with again, the highest being for BR10. Small variation in the moisture

content (Table 2) for the each of the bauxite residues was recorded. The bulk density (Table 2) for the bauxite residue ranged from 1.2 ± 0.1 to 1.5 ± 0.02 g cm^{-3}.

The bauxite residue had a high composition of fine particles, which ranged from 0.6 ± 0.01 to 12.7 ± 2.3 μm (Table 2). There was some agglomerate formation evident in all samples, as seen in the accumulation of finer particles in the images captured by SEM (Figs. S1, S2, S3 in the Supplementary Information). The medium value, d_{50}, of the particle size distribution for bauxite residues ranged from 2.2 ± 0.1 μm (BR1) to 4.3 ± 0.4 μm (BR9). Ninety percent of the distribution (d_{90}) was under 12.7 ± 2.7 μm and 10%

Table 2
Physico-chemical composition of the bauxite residue mud over a twelve-year storage period, inclusive of pH, EC, moisture content, bulk density and particle size distribution.

Sample	pH	EC (mS cm^{-1})	Moisture content (%)	Bulk density (g cm^{-3})	d_{10} (µm)[a]	d_{50} (µm)[b]	d_{90} (µm)[c]
BR 12	11.6 ± 0.02	1.0 ± 0.01	26.8 ± 0.7	1.4 ± 0.04	0.7 ± 0.1	2.6 ± 0.1	7.0 ± 1.2
BR 11	10.8 ± 0.1	0.4 ± 0.02	28.2 ± 0.7	1.3 ± 0.03	0.9 ± 0.1	3.5 ± 0.5	9.6 ± 0.5
BR 10	12.0 ± 0.02	3.3 ± 0.2	26.8 ± 0.1	1.4 ± 0.1	1.4 ± 0.1	4.0 ± 0.3	12.3 ± 1.6
BR 9	10.0 ± 0.1	0.4 ± 0.01	24.3 ± 0.3	1.1 ± 0.1	1.0 ± 0.1	4.3 ± 0.4	12.4 ± 1.0
BR 8	11.4 ± 0.1	1.0 ± 0.1	27.2 ± 0.3	1.4 ± 0.1	0.8 ± 0.1	2.6 ± 0.1	6.8 ± 0.2
BR 7	10.4 ± 0.02	0.5 ± 0.01	22.3 ± 0.6	1.4 ± 0.04	0.9 ± 0.2	3.2 ± 0.5	12.7 ± 2.7
BR 6	10.7 ± 0.03	0.5 ± 0.03	25.8 ± 1.0	1.3 ± 0.04	0.7 ± 0.1	2.6 ± 0.01	6.7 ± 0.2
BR 5	10.3 ± 0.1	0.4 ± 0.03	22.0 ± 0.5	1.2 ± 0.1	0.6 ± 0.01	2.4 ± 0.04	7.9 ± 1.1
BR 4	11.5 ± 0.1	0.9 ± 0.02	31.1 ± 0.5	1.3 ± 0.1	1.2 ± 0.1	3.8 ± 0.6	12.70 ± 2.3
BR 3	10.6 ± 0.02	0.5 ± 0.01	23.8 ± 0.3	1.3 ± 0.03	0.8 ± 0.2	2.6 ± 0.3	8.3 ± 1.6
BR 2	11.2 ± 0.01	0.9 ± 0.02	28.1 ± 1.9	1.3 ± 0.1	1.1 ± 0.02	3.2 ± 0.02	9.7 ± 0.9
BR 1	10.3 ± 0.1	0.7 ± 0.03	25.0 ± 2.7	1.5 ± 0.02	0.5 ± 0.01	2.2 ± 0.1	6.7 ± 0.6

[a] d_{10} (µm) = the size of particles at 10% of the total particle distribution.
[b] d_{50} (µm) = the median; the size of particles at 50% of the total particle distribution.
[c] d_{90} (µm) = the size of particles at 90% of the total particle distribution.

(d_{10}) was under 0.5 ± 0.01 µm (Table 2). Iron, Al, sodium (Na), calcium (Ca), titanium (Ti), and silicon (Si) were the main elements present in all the bauxite residue samples (Fig. S4). TGA curves showed weight loss between 300 and 975 °C for all the bauxite residues (Fig. 2 and S5). However, sample BR12 (from 2014) had a larger temperature range over which weight loss occurred (between 150 and 975 °C).

3.1.1. Mineralogical composition

The main mineralogical composition of the bauxite residue detected by XRD included haematite (Fe_2O_3), goethite (FeO(OH)), perovskite ($CaTiO_3$), rutile (TiO_2), gibbsite Al(OH)$_3$, sodalite ($Na_8(Al_6Si_6O_{24})Cl_2$) and cancrinite ($Na_6Ca_2(CO_3)$) (Figs. S6 and S7). Sample BR9 had an extra rutile peak at position 27.459 °2θ and no sodalite peak at position 14 °2θ; samples BR1 to BR6 had similar patterns, but with less intense peaks and sodalite peaks at position 14 °2θ (Fig. S6). Sample BR1 had one peak of boehmite (AlO(OH)) at position 13.9 °2θ and gibbsite at position 18.5 °2θ (Fig. S6). Sample BR1 also had an unidentified peak at position 47 °2θ (Fig. S6).

XRF analysis carried out on the bauxite residue samples (Table 3) reflected the main mineralogical composition detected by XRD analysis. The dominant oxides found were Fe$_2$O (ranging from 40.1 ± 1.40 to 47.5 ± 2.0%) and Al_2O_3 (14.8 ± 1.5 to 17.8 ± 0.73%). SiO_2 (7.20 ± 1.0 to 10.9 ± 0.47%), TiO_2 (8.62 ± 0.71 to 10.3 ± 0.95%) and CaO (5.70 ± 0.66 to 6.1 ± 1.0%) were also present (Table 3).

3.1.2. Elements of economic importance in bauxite residue

An extensive inventory of CRMs and further elements of economic importance were developed using microwave-assisted aqua

Table 3
Main mineralogical composition (%) of the bauxite residue samples taken from the BRDA ranging from one to twelve years old, as determined by XRF.

Code	Al$_2$O$_3$	Fe$_2$O	SiO$_2$	TiO$_2$	CaO
BR 11	17.0 ± 0.61	42.0 ± 1.20	9.82 ± 0.32	9.41 ± 0.34	6.03 ± 0.79
BR 10	17.1 ± 0.4	41.5 ± 0.96	10.2 ± 0.56	9.52 ± 0.6	6.03 ± 0.49
BR 9	17.8 ± 0.73	40.1 ± 1.40	10.9 ± 0.47	8.97 ± 0.51	6.04 ± 0.4
BR 8	16.8 ± 0.58	41.8 ± 1.40	9.89 ± 0.39	9.41 ± 0.61	5.97 ± 0.49
BR 7	14.8 ± 1.5	47.5 ± 2.0	7.20 ± 1.0	10.3 ± 0.95	6.1 ± 1.0
BR 6	16.2 ± 0.54	45.9 ± 2.10	8.0 ± 0.57	9.54 ± 0.78	5.70 ± 0.66
BR 5	16.2 ± 0.66	44.4 ± 1.30	9.35 ± 0.60	8.62 ± 0.71	5.75 ± 0.53
BR 4	16.5 ± 0.65	43.3 ± 1.20	9.38 ± 0.53	8.91 ± 0.53	6.21 ± 0.35
BR 3	15.8 ± 0.45	44.3 ± 1.90	8.85 ± 0.47	9.18 ± 0.62	6.34 ± 0.35
BR 2	16.0 ± 0.71	46.6 ± 1.80	8.95 ± 0.70	8.21 ± 0.38	5.0 ± 0.40
BR 1	16.2 ± 0.6	46.8 ± 1.61	8.76 ± 0.48	8.33 ± 0.56	4.69 ± 0.43

regia digestion, with subsequent ICP-OES analysis (Table 4). Overall, no trend was noted in the elemental content between the oldest and newest bauxite residue in the BRDA. However, In, Mo, Ce, Nd, Dy and Er were present in smaller amounts in the oldest samples compared to the fresh sample. Terbium (Tb), Tm and Ho were not detected in the bauxite residue.

4. Discussion

4.1. Characterisation of bauxite residue

Bauxite residue typically has a pH > 10 (Goloran et al. 2013) and an EC ranging from 1.4 to 28.4 mS cm^{-1} (Gräfe et al. 2011). The high
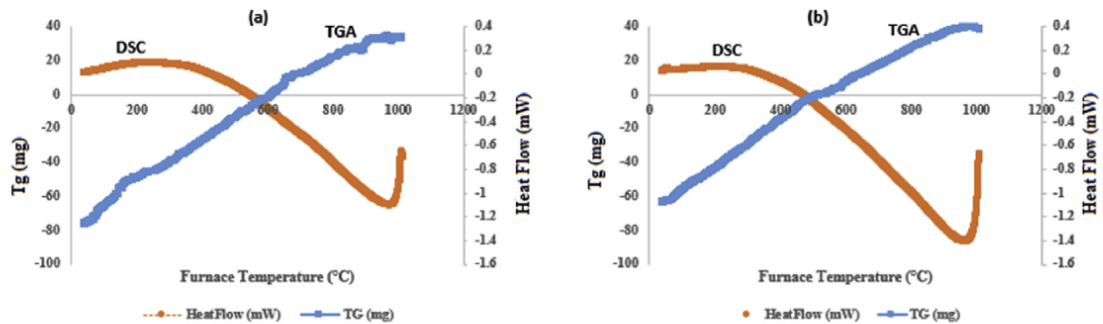
Fig. 2. TGA (descending)/DSC (ascending) curve obtained for bauxite residue (a) BR12 (2004) and (b) BR2 (2014). Remaining TGA/DSC graphs found in Fig. S4. The TGA curves showed weight loss between 300 and 975 °C for all the bauxite residues examined.

Table 4

CRM composition (in mg kg^{-1}) of the bauxite residue samples, taken from the BRDA, as detected on ICP-OES following aqua regia digestion.

Element	BR 12	BR 11	BR 10	BR 9	BR 8	BR 7	BR 6	BR 5	BR 4	BR 3	BR 2
Dy	3.6 ± 0.02	5.4 ± 0.01	7.19 ± 0.01	5.39 ± 0.001	5.4 ± 0.04	5.39 ± 0.01	5.4 ± 0.01	5.38 ± 0.02	4.51 ± 1.3	7.2 ± 0.002	5.4 ± 0.02
Er	4.8 ± 0.5	5.4 ± 0.01	5.7 ± 0.5	4.94 ± 0.6	5.4 ± 0.04	5.39 ± 0.01	4.49 ± 0.01	5.38 ± 0.01	4.05 ± 0.6	5.4 ± 0.001	5.4 ± 0.02
Lu	8.39 ± 0.5	7.8 ± 0.5	8.09 ± 0.01	7.49 ± 0.5	8.1 ± 0.05	7.63 ± 0.6	8.1 ± 0.02	8.37 ± 0.5	7.66 ± 0.7	8.1 ± 0.002	8.09 ± 0.03
Y	35.6 ± 3.2	39.8 ± 1.2	44.4 ± 1.5	41.9 ± 1.5	42 ± 0.4	39.5 ± 0.04	33.4 ± 0.4	41 ± 2.0	36.9 ± 1.4	47.4 ± 1.2	39.3 ± 0.5
Yb	8.39 ± 0.6	8.8 ± 0.3	9.39 ± 0.3	8.79 ± 0.7	9.4 ± 0.3	8.68 ± 0.4	8.2 ± 0.4	8.97 ± 0.9	8.11 ± 0.4	9.6 ± 0.002	8.71 ± 0.4
Ce	126 ± 10.1	126 ± 3.5	156 ± 2.2	136 ± 7.6	157 ± 2.2	128 ± 3.3	146 ± 6.7	200 ± 8.4	102 ± 3.5	147 ± 4.2	139 ± 6.8
Eu	2.40 ± 0.01	2.40 ± 0.01	2.40 ± 0.005	2.40 ± 0.01	2.40 ± 0.02	2.39 ± 0.003	2.40 ± 0.01	3.59 ± 0.01	2.40 ± 0.001	2.40 ± 0.01	2.40 ± 0.005
Gd	6.75 ± 0.6	6.60 ± 0.5	7.64 ± 0.6	7.63 ± 0.6	9.30 ± 0.6	7.18 ± 1.3	6.75 ± 0.6	8.98 ± 0.02	5.41 ± 0.02	9 ± 0.002	6.73 ± 0.6
La	91.3 ± 8.6	88.2 ± 3.2	108 ± 2.3	94.1 ± 2.7	106.4 ± 1.0	89.2 ± 0.9	104 ± 3.5	134 ± 4.4	68.8 ± 4.0	98.2 ± 2.1	91 ± 2.4
Nd	80.1 ± 7.4	77.2 ± 5.3	93.9 ± 6.5	72.5 ± 3.1	98 ± 5.3	85.6 ± 8.6	88.9 ± 8.6	118 ± 4.4	64.6 ± 4.0	93 ± 2.2	94.3 ± 11.3
Pr	41.1 ± 3.5	42.9 ± 4.2	47.7 ± 3.3	42.5 ± 3.1	50.1 ± 1.6	40.8 ± 1.9	45 ± 2.7	56.2 ± 5.3	34.7 ± 3.3	45 ± 0.9	42.3 ± 1.1
Sc	50.2 ± 4.1	50.4 ± 1.6	60.2 ± 2.2	56.1 ± 2.7	54.2 ± 0.9	55.7 ± 1.3	45.4 ± 0.2	56 ± 4.2	42.9 ± 2.3	49 ± 1.3	45.6 ± 4.3
Sm	19.3 ± 0.7	20.7 ± 1.8	21 ± 2.2	21.6 ± 0.9	21.6 ± 0.8	18.4 ± 1.9	21.6 ± 0.9	25.1 ± 0.05	18 ± 1.2	21 ± 1.0	20.3 ± 2.0
Co	8.69 ± 0.5	7.64 ± 0.6	7.79 ± 0.5	6.73 ± 0.6	8.10 ± 0.05	7.63 ± 0.6	6.6 ± 0.5	8.67 ± 0.5	7.21 ± 0.02	8.4 ± 0.5	7.49 ± 0.6
Ga	107 ± 8.5	112 ± 2.3	102 ± 0.7	114 ± 5.2	98.6 ± 0.2	113 ± 3.8	106 ± 2.7	114 ± 5.1	99.5 ± 1.8	114 ± 1.9	94.4 ± 2.7
In	30.1 ± 1.8	34.6 ± 0.7	31.5 ± 1.5	32.1 ± 2.7	36.9 ± 0.9	30.5 ± 1.3	29.2 ± 2	33.6 ± 0.7	28.4 ± 0.7	34.5 ± 7.2	36.4 ± 4.3
Mo	3.14 ± 0.6	4.49 ± 0.01	4.04 ± 0.6	4.95 ± 0.6	4.48 ± 0.004	4.95 ± 0.6	4.49 ± 0.01	4.48 ± 0.01	4.94 ± 1.9	4.8 ± 0.5	4.48 ± 0.01
V	593 ± 60.6	419 ± 8.2	596 ± 19.8	439 ± 41.1	491 ± 20.3	445 ± 41.2	484 ± 48.2	600 ± 24.3	401 ± 41.2	571 ± 13.3	573 ± 41.1

pH is attributed to the presence of alkaline anions such as hydroxides (OH$^-$), carbonate or bicarbonates (CO$_3^{2-}$/HCO$_3^-$), aluminates or aluminium hydroxides (Al(OH)$_4^-$/Al(OH)$_3$), and di/trihydrogen orthosilicates (H$_2$SiO$_4^{2-}$/H$_3$SiO$_4^-$) introduced and formed during the Bayer process (Gräfe et al. 2011). At the end of the Bayer process, prior to disposal, residue undergoes a repeated washing stage. However, the bauxite residue remains highly alkaline due to the alkalinity being in the form of slow dissolving solid phases (Gräfe et al. 2011).

Depending on the refinery and the advances in residue management steps employed, the pH may be further reduced through practices such as atmospheric carbonation (mud farming) (Clohessy, 2015; Evans, 2016), seawater disposal (Menzies et al. 2009), application of spent acid (Kirwan et al. 2013), phosphogypsum (Xue et al. 2018), or by the addition of an acidic gas such as CO$_2$ or SO$_2$ (Xue et al. 2016). Consequently, surface pH values for residues may vary between refineries and within BRDAs.

The bauxite residue examined in this study showed variation in terms of both the pH and the EC (p < 0.01) (Table 2). Whilst the pH and EC did decrease across all the bauxite residue samples examined in this study (Table 2), this was attributed to different causes. The reduced pH value of the fresh bauxite residue examined (BR1) in this study (Table 2) is as a result of the atmospheric carbonation technique, mud farming, which can effectively decrease alkalinity (Clohessy, 2015; McMahon, 2017). This helps in removing the alkalinity limitation/barrier to the reutilisation of the bauxite residue (Evans, 2016) and has been shown to successfully decrease the pH of fresh bauxite residue (~13.5) to below < 11.5 within seven days (Clohessy, 2015). The mud farming technique sequesters CO$_2$ from the atmosphere, allowing for the accelerated carbonation of the bauxite residue (IAI, 2015; Evans, 2016). Due to this process, the free OH$^-$ present in the bauxite residue is neutralised due to the carbonation of the CO$_2$ present in the surrounding atmosphere (air), resulting in the formation of carbonates, therefore creating a buffering effect, which results in a drop in pH (Han et al. 2017).

Natural weathering processes may play an important role in the improvement of the physico-chemical composition of bauxite residue in storage (Zhu et al. 2018). The reduction observed in the pH of the older samples (Table 2) is as a result of the natural ageing and weathering of the bauxite residue in storage. Evidence of the natural weathering decreasing the pH was shown by Khaitan et al. (2010), who reported a pH of 10.5 for 14-year-old bauxite residue and 9.5 for 35-year-old bauxite residue, with the decreases attributed to the slow carbonation from atmospheric CO$_2$. Zhu et al.

(2016a,b) also measured a decrease in residue pH from 10.98 to 9.45 in stored bauxite residue exposed to natural weathering processes. Similar to pH, EC usually decreases with time in the storage area due to weathering (Zhu et al. 2016a; b; Kong et al. 2017a). Rainfall events allow the soluble alkaline minerals such as sodalite and calcite, which result in a buffering effect for both pH and salinity (EC) (Santini and Fey, 2013).

The thermal analysis (TGA/DSC) indicated an overall weight loss occurring between 300 and 975 °C for all the bauxite residue samples examined. Previous work has shown weight loss between temperature ranges of 300 and 600 °C (attributed to the decomposition of hydroxides in different stages), 300 and 400 °C (as a result of the decomposition of diaspora), and between 600 and 800 °C (due to the decomposition of calcium carbonate) (Agatzini-Leonardou et al. 2008), all dominant minerals in bauxite residue. There were numerous endothermic peaks observed on the DSC curve for the six samples examined, particularly in the region above 800 °C. Endothermic peaks above this temperature are indicative of the decomposition of sodalite phases and also the decomposition of quartz, which occurs between 550 and 1000 °C (Atasoy, 2005). Small endothermic peaks throughout the DSC curve may be attributed to loss of physically held water (Atasoy, 2005), which was notable in all the bauxite residue samples examined.

The mineralogical composition of bauxite residue typically comprises Al$_2$O$_3$ and Fe$_2$O$_3$ in the range of 20–45% and 10–22%, respectively (IAI, 2015). This composition is reflected in the XRF and XRD analysis, which showed the dominant presence of Fe$_2$O$_3$, FeO(OH), and Al(OH)$_3$. CaTiO$_3$, AlO(OH) and TiO$_2$ were also detected in all samples, which is common amongst bauxite residue (Gräfe et al. 2011). Sodalite (Na$_8$(Al$_6$Si$_6$O$_{24}$)Cl$_2$) was also present in the bauxite residue, and is one of the most common desilication products formed during the pre-desilication stage during the Bayer process, along with CaTiO$_3$ which is often found as a result of the lime added (Gräfe et al. 2011).

4.2. Economic value of bauxite and potential for reuse

In recent years, several studies have been conducted to investigate the potential use of industrial residues such as phosphogypsum, mine tailings, slags and bauxite residue as a possible source for CRMs and REEs (Binnemans et al. 2015). Currently, the global production rate of REEs, which is typically expressed in tons of rare earth oxides (REOs) is 130,000 to 140,000 tons, of which 95% is produced in China (Binnemans et al. 2018). Five of the REEs (Nd,

Table 5
Associated financial value of economically interesting elements in the bauxite residue (average over a twelve-year period, n = 11).

Element	Average aqua regia extracted content (mg kg^{-1})	Price[a] (US $ t^{-1})	Economic value of the bauxite residue in this study[c] (US $ t^{-1})
Ga	107 ± 7.3	400,000	42.73
Sc	51.4 ± 5.4	4,600,000	236.44
In	32.5 ± 2.9	240,000	7.81
V	510 ± 77.8	6889	3.51
Nd	89.0 ± 13.6	39,500	3.51
Dy	5.48 ± 1.0	184,500	1.01
Pr	44.4 ± 5.6	5,500[b]	0.24
Y	40.1 ± 3.9	35,500	1.42
Ce	142 ± 24.9	2000	0.28
Sm	20.8 ± 1.9	12,500[b]	0.26
Co	7.72 ± 0.7	26,444	0.20
La	97.5 ± 16.3	2000	0.19
Eu	2.51 ± 0.4	66,000	0.16
Yb	8.82 ± 0.5	5,500[b]	0.04
Lu	7.99 ± 0.3	5,500[b]	0.04
Gd	7.45 ± 1.2	5,500[b]	0.04
Mo	4.48 ± 0.5	14,500	0.06
Er	5.12 ± 0.5	5,500[b]	0.03

[a] Values from USGS (2016).
[b] Average value for mischmetals of REE/expected higher individual prices.
[c] Economic value of the bauxite residue in this study, determined using current price (US $ t^{-1}) and the average content in the bauxite residue studied.

Eu, Tb, Dy, Y) are now described as being of a high supply risk within Europe, Japan and the USA (Binnemans et al. 2018). Such CRMs and REEs are necessary for the production of magnets, lighting, lasers, batteries, catalysts, and alloys in aerospace (Weng et al. 2015).

While this study did show differences in the bauxite residue over the twelve-year period, in terms of decreased pH and EC, there were no significant changes in the CRM content of the bauxite residue (Table 4). This indicates that some BRDAs may be a potential resource for the reprocessing and recovery of CRMs and REEs. However, this is not certain for all BRDAs, as variation can and does occur within BRDAs and refineries due to differences in bauxite ore type, parameters used within the Bayer Process, as well as varying disposal and neutralisation techniques.

The Sc, Ga and V content of the bauxite residue in the current study are of particular interest, due to their high economic value (Table 5) and supply risk. Scandium, a trace constituent of igneous rocks (European Commission, 2017), is used in the production of aluminium alloys (Ricketts and Duyvesteyn, 2018), and V, present in minor amounts in the Earth's crust and seawater and the majority of which is sourced as a by-product of the steel industry (European Commission, 2017), is used in electrodes (Morel et al. 2016). Gallium is primarily sourced from bauxite ore and bauxite residue, as it found naturally as a trace element dispersed in minerals, which also includes coal (Qin et al. 2015), and is used in the production of catalysts (Qin and Schneider, 2016). The Sc in this study (Table 4) was lower than values found in fresh Hungarian (Ujaczki et al. 2017), Greek (Borra et al. 2015), Russian (Petrakova et al. 2015) and Australian (Wang et al. 2013) bauxite residues. However, the Ga content (Table 4) was higher than that found by Ujaczki et al. (2017) in Hungarian bauxite residue, as well as in Australian (Wang et al. 2013), Indian (Mohapatra et al. 2012) and Turkish (Abdulvaliyev et al. 2015) bauxite residues. Finally, the V content was present in higher amounts compared to Hungarian (Ujaczki et al. 2017), Indian (Mohapatra et al. 2012) and Turkish (Abdulvaliyev et al. 2015) bauxite residues. This is indicative of the variation of CRM content in residues between refineries. In addition to Sc, Ga and V, there is now a focus on further valuable element extraction (Jowitt et al. 2018) and recovery of REE due to the overproduction of REEs such as La and Ce, which is leading to an imbalance in the supply of REEs produced and a demand for Nd and Dy (Binnemans and Jones, 2015; Binnemans et al. 2018), both of

which were found in the bauxite residue in this study.

The typical methods of CRM recovery from bauxite residue include direct leaching using mineral acids such as HNO$_3$, sulphuric acid (H$_2$SO$_4$) or hydrochloric acid (HCl), or leaching following pyrometallurgical applications such as roasting (Ujaczki et al. 2018). Although there are high recovery rates of CRMs from bauxite residue reported (Abdulvaliyev et al. 2015; Borra et al. 2015), so too are the associated costs for acids and energy required in these processes, which questions the justification of extracting CRMs from by-products such as bauxite residue. Recent studies have also highlighted the need to develop new technologies to optimise the efficiency of CRM recovery from bauxite residue to ensure cost-effectiveness (Gomes et al. 2016; Akcil et al. 2018). Ujaczki et al. (2018) in their review on the reuse of bauxite residue as a source of CRMs, highlighted the extent of the benefits following CRM recovery from a wider perspective in terms of the technological (development of more efficient technologies), social (such as improvements to health), economic (mainly reduction in refinery disposal costs), and environmental factors such as reduced emissions and loss of habitable land.

4.3. The findings of this study from an industrial perspective on potential re-use of bauxite residue

This study found that there was very little variation in the CRM content of bauxite residue in a BRDA over a twelve-year period. This shows promise for the potential reuse of bauxite residue as a secondary source of CRMs. Finding a suitable and long-term use for bauxite residue may be hampered by several barriers and limitations (Klauber et al. 2011; Evans, 2016), such as high alkalinity and salinity which were shown by this study to be reduced by weathering and mud farming. However, limitations to the reuse of bauxite residue may be overcome through management strategies involving its partial neutralisation and increased solids content (Klauber et al. 2011).

5. Conclusions

This study showed that there was a reduction in both the pH and the EC (p < 0.01) of bauxite residue in a BRDA over a twelve-year period. There was little variation in the CRM content of the bauxite residue sampled. The CRMs of particular interest were V, Ga

and Sc due their potential supply risk and associated economic value. The V, Ga and Sc content of the bauxite residue samples were 510 ± 77.8, 107 ± 7.3 and 51.4 ± 5.4 mg kg^{-1}, respectively, giving current economic values of 3.51, 42.73 and 236.44 US \$ t^{-1}. From a European and global context, this highlights a potential resource for CRMs in the event of a scarcity of these materials. However, the general composition and CRM content of bauxite residue varies greatly due to the bauxite ore and parameters used in the Bayer Process, as well as the disposal and neutralisation methods implemented by refineries. Depending on the history of the refinery and BRDA, there may be little variation over time, making BRDAs possible sources for the extraction of CRMs. There are currently high-costs associated with the extraction of CRMs from bauxite residue due to the large amount of reagent and/or energy required in the process, before purifying the CRMs recovered for reuse. However, these need to be set against the overall benefits of recovering CRMs in terms of the environmental, economic and social factors. Further research is necessary to investigate the cost and environmental implications and limitations of extraction of CRMs from BRDAs, as opposed to conventional extraction techniques from mines, in terms of emissions produced, machinery required, fuel needed and human resources required.

Acknowledgements

Appendix A. Supplementary data

Supplementary data to this article can be found online at https://doi.org/10.1016/j.jclepro.2018.10.083.

References

Abdulvaliyev, R.A., Akcil, A., Gladyshev, S.V., Tastanov, E.A., Beisembekova, K.O., Akhmadiyeva, N.K., Deveci, H., 2015. Gallium and vanadium extraction from red mud of Turkish alumina refinery plant: hydrogarnet process. Hydrometallurgy 157, 72–77.

Agatzini-Leonardou, S., Oustadakis, P., Tsakiridis, P.E., Markopoulos, C., 2008. Titanium leaching from red mud by diluted sulfuric acid at atmospheric pressure. J. Hazard Mater. 157, 579–586.

Akcil, A., Akhmadiyeva, N., Abdulvaliyev, R., Abhilash, Meshram, P., 2018. Overview on extraction and separation of rare earth elements from red mud: focus on scandium. Miner. Process. Extr. Metall. Rev. 39, 145–151.

Arco-Lázaro, E., Pardo, T., Clemente, R., Bernal, M.P., 2018. Arsenic adsorption and plant availability in an agricultural soil irrigated with As-rich water: effects of Fe-rich amendments and organic and inorganic fertilisers. J. Environ. Manag. 209, 262–272.

Atasoy, A., 2005. An investigation on characterization and thermal analysis of the Aughinish red mud. J. Therm. Anal. Calorim. 81, 357–361.

Atasoy, A.D., Bilgic, B., 2018. Adsorption of copper and zinc ions from aqueous solutions using montmorillonite and bauxite as low-cost adsorbents. Mine Water Environ. 37, 205–210.

Balomenos, E., Davris, P., Pontikes, Y., Panias, D., 2017. Mud2Metal: lessons learned on the path for complete utilization of bauxite residue through industrial symbiosis. J. Sustain. Metall. 3, 551–560.

Bhatnagar, A., Vilar, V.J., Botelho, C.M., Boaventura, R.A., 2011. A review of the use of red mud as adsorbent for the removal of toxic pollutants from water and wastewater. Environ. Technol. 32, 231–249.

Binnemans, K., Jones, P.T., 2015. Rare earths and the balance problem. J. Sustain. Metall. 1, 29–38.

Binnemans, K., Jones, P.T., Blanpain, B., Van Gerven, T., Pontikes, Y., 2015. Towards zero-waste valorisation of rare-earth-containing industrial process residues: a critical review. J. Clean. Prod. 99, 17–38.

Binnemans, K., Jones, P.T., Müller, T., Yurramendi, L., 2018. Rare earths and the balance problem: how to deal with changing markets? J. Sustain. Metall. 4, 1–21.

Blake, G.R., 1965. Bulk Density 1. Methods of Soil Analysis. Part 1. Physical and Mineralogical Properties, Including Statistics of Measurement and Sampling, (Methodsofsoilana), pp. 374–390. Available: https://dl.sciencesocieties.org/publications/books/tocs/agronomymonogra/methodsofsoilana. (Accessed 24 May 2018).

Borra, C.R., Pontikes, Y., Binnemans, K., Van Gerven, T., 2015. Leaching of rare earths from bauxite residue (red mud). Miner. Eng. 76, 20–27.

Bridger, S., Knowles, M., 2000. A Complete Method for Environmental Samples by Simultaneous Axially Viewed ICP-AES Following USEPA Guidelines. Varian ICP-OES at Work (29). Available: https://www.agilent.com/cs/library/applications/ICPES-29.pdf. (Accessed 24 May 2018).

Burke, I.T., Peacock, C.L., Lockwood, C.L., Stewart, D.I., Mortimer, R.J., Ward, M.B., Renforth, P., Gruiz, K., Mayes, W.M., 2013. Behavior of aluminum, arsenic, and vanadium during the neutralization of red mud leachate by HCl, gypsum, or seawater. Environ. Sci. Technol. 47, 6527–6535.

Castaldi, P., Silvetti, M., Enzo, S., Deiana, S., 2011. X-ray diffraction and thermal analysis of bauxite ore-processing waste (red mud) exchanged with arsenate and phosphate. Clay Clay Miner. 59, 189–199.

Clohessy, J., 2015. Closure and rehabilitation of rusal aughinish BRDA, presented at the residue closure and rehabilitation workshop. In: In 10th Alumina Quality Workshop, Perth, Western Australia. Available: http://aqw.com.au/2015papers.html. (Accessed 18 April 2018).

Cooling, D.J., 2007. Improving the Sustainability of Residue Management Practices-Alcoa World Alumina Australia. Paste and Thickened Tailings: a Guide, p. 316. Available: http://citeseerx.ist.psu.edu/viewdoc/download?doi=10.1.1.629.1067&rep=rep1&type=pdf. (Accessed 24 May 2018).

Courtney, R., Harrington, T., 2010. Assessment of plant-available phosphorus in a fine textured sodic substrate. Ecol. Eng. 36, 542–547.

Cusack, P.B., Healy, M.G., Ryan, P.C., Burke, I.T., O'Donoghue, L.M., Ujaczki, É., Courtney, R., 2018. Enhancement of bauxite residue as a low-cost adsorbent for phosphorus in aqueous solution, using seawater and gypsum treatments. J. Clean. Prod. 179, 217–224.

Dursun, S., Guclu, D., Berktay, A., Guner, T., 2008. Removal of chromate from aqueous system by activated red-mud. Asian J. Chem. 20, 6473–6478.

EU, 2000. Communities Commission Decision 2000/532/EC, OJ L 226, 06.09, pp. 3–24. Available online: http://eur-lex.europa.eu/legal-content/EN/TXT/PDF/?uri=CELEX:22002D0009&from=EN. (Accessed 27 September 2018).

EU, 1999. Communities Council Directive 1999/31/EC on the Landfill of Waste, OJ L 182, 16.07, pp. 1–19. Available online:http://eur-lex.europa.eu/legal-content/EN/TXT/PDF/?uri=CELEX:31999L0031&from=EN. (Accessed 27 September 2018).

European Commission, 2017. Study on the Review of the List of Critical Raw Materials. Critical Raw Materials Factsheets. Catalogue number ET-04-15-307-EN-N. Available: https://publications.europa.eu/en/publication-detail/-/publication/7345e3e8-98fc-11e7-b92d-01aa75ed71a1/language-en. (Accessed 15 May 2018).

Evans, K., 2016. The history, challenges, and new developments in the management and use of bauxite residue. J. Sustain. Metall. 2, 316–331.

Goloran, J.B., Chen, C.R., Phillips, I.R., Xu, Z.H., Condron, L.M., 2013. Selecting a nitrogen availability index for understanding plant nutrient dynamics in rehabilitated bauxite-processing residue sand. Ecol. Eng. 58, 228–237.

Gomes, H.I., Jones, A., Rogerson, M., Burke, I.T., Mayes, W.M., 2016. Vanadium removal and recovery from bauxite residue leachates by ion exchange. Environ. Sci. Pollut. Res. 23, 23034–23042.

Grace, M.A., Healy, M.G., Clifford, E., 2015. Use of industrial by-products and natural media to adsorb nutrients, metals and organic carbon from drinking water. Sci. Total Environ. 518, 491–497.

Grace, M.A., Clifford, E., Healy, M.G., 2016. The potential for the use of waste products from a variety of sectors in water treatment processes. J. Clean. Prod. 137, 788–802.

Gräfe, M., Power, G., Klauber, C., 2011. Bauxite residue issues: III. Alkalinity and associated chemistry. Hydrometallurgy 108, 60–79.

Ha, X.L., Hoang, N.H., Nguyen, T.T.N., Nguyen, T.T., Nguyen, T.H., Dang, V.T., Nguyen, N.H., 2017. October. Removal of Cd (II) from aqueous solutions using red mud/graphene composite. In: Congrès International de Géotechnique–Ouvrages–Structures. Springer, Singapore, pp. 1044–1052.

Han, Y.S., Ji, S., Lee, P.K., Oh, C., 2017. Bauxite residue neutralization with simultaneous mineral carbonation using atmospheric CO2. J. Hazard Mater. 326, 87–93.

Hannachi, Y., Shapovalov, N.A., Hannachi, A., 2010. Adsorption of nickel from aqueous solution by the use of low-cost adsorbents. Kor. J. Chem. Eng. 27, 152–158.

Hertel, T., Blanpain, B., Pontikes, Y., 2016. A proposal for a 100% use of bauxite residue towards inorganic polymer mortar. J. Sustain. Metall. 2, 394–404.

Higgins, D., Curtin, T., Pawlett, M., Courtney, R., 2016. The potential for constructed wetlands to treat alkaline bauxite-residue leachate: phragmites australis growth. Environ. Sci. Pollut. Res. 23, 24305–24315.

Higgins, D., Curtin, T., Courtney, R., 2017. Effectiveness of a constructed wetland for treating alkaline bauxite residue leachate: a 1-year field study. Environ. Sci. Pollut. Res. 24, 8516–8524.

IAI, 2015. Bauxite Residue Management: Best Practice. http://www.world-aluminium.org/media/filer_public/2015/10/15/bauxite_residue_management_-_best_practice_english_oct15edit.pdf. (Accessed 14 October 2017).

Jones, B.E., Haynes, R.J., Phillips, I.R., 2012. Addition of an organic amendment and/or residue mud to bauxite residue sand in order to improve its properties as a growth medium. J. Environ. Manag. 95, 29–38.

Jowitt, S.M., Werner, T.T., Weng, Z., Mudd, G.M., 2018. Recycling of the rare Earth elements. Curr. Opin. Green. Sustain. Chem. 13, 1–7.

Khaitan, S., Dzombak, D.A., Swallow, P., Schmidt, K., Fu, J., Lowry, G.V., 2010. Field evaluation of bauxite residue neutralization by carbon dioxide, vegetation, and organic amendments. J. Environ. Eng. 136, 1045–1053.

Kirwan, L.J., Hartshorn, A., McMonagle, J.B., Fleming, L., Funnell, D., 2013. Chemistry of bauxite residue neutralisation and aspects to implementation. Int. J. Miner. Process. 119, 40–50.

Klauber, C., Gräfe, M., Power, G., 2011. Bauxite residue issues: II. Options for residue utilization. Hydrometallurgy 108, 11–32.

Kong, X., Guo, Y., Xue, S., Hartley, W., Wu, C., Ye, Y., Cheng, Q., 2017a. Natural evolution of alkaline characteristics in bauxite residue. J. Clean. Prod. 143, 224–230.

Kong, X., Li, M., Xue, S., Hartley, W., Chen, C., Wu, C., Li, X., Li, Y., 2017b. Acid transformation of bauxite residue: conversion of its alkaline characteristics. J. Hazard Mater. 324, 382–390.

Liu, Y., Naidu, R., 2014. Hidden values in bauxite residue (red mud): recovery of metals. Waste Manag. 34, 2662–2673.

Menzies, N.W., Fulton, I.M., Kopittke, R.A., Kopittke, P.M., 2009. Fresh water leaching of alkaline bauxite residue after sea water neutralization. J. Environ. Qual. 38, 2050–2057.

McMahon, K., 2017. Bauxite residue disposal area rehabilitation. In: ISCOBA Conference November 2017, Hamburg, 02-05 Oct, Hamburg, Germany. Available: http://icsoba.org/sites/default/files/2017papers/Bauxite%20Residue%20Papers/BR01%20-%20Bauxite%20Residue%20Disposal%20Area%20Rehabilitation.pdf. (Accessed 21 February 2018).

Mohapatra, B.K., Mishra, B.K., Mishra, C.R., 2012. Studies on metal flow from khondalite to bauxite to alumina and rejects from an alumina refinery, India. In: Light Metals 2012. Springer, Cham, pp. 87–91.

Morel, A., Borjon-Piron, Y., Porto, R.L., Brousse, T., Bélanger, D., 2016. Suitable conditions for the use of vanadium nitride as an electrode for electrochemical capacitor. J. Electrochem. Soc. 163, A1077–A1082.

Nikbin, I.M., Aliaghazadeh, M., Charkhtab, S., Fathollahpour, A., 2018. Environmental impacts and mechanical properties of lightweight concrete containing bauxite residue (red mud). J. Clean. Prod. 172, 2683–2694.

Petrakova, O.V., Panov, A.V., Gorbachev, S.N., Klimentenok, G.N., Perestoronin, A.V., Vishnyakov, S.E., Anashkin, V.S., 2015. Improved efficiency of red mud processing through scandium oxide recovery. In: Light Metals 2015. Springer, Cham, pp. 93–96.

Pontikes, Y., Rathossi, C., Nikolopoulos, P., Angelopoulos, G.N., Jayaseelan, D.D., Lee, W.E., 2009. Effect of firing temperature and atmosphere on sintering of ceramics made from Bayer process bauxite residue. Ceram. Int. 35, 401–407.

Pontikes, Y., Angelopoulos, G.N., 2013. Bauxite residue in cement and cementitious applications: current status and a possible way forward. Resour. Conserv. Recycl. 73, 53–63.

Power, G., Gräfe, M., Klauber, C., 2011. Bauxite residue issues: I. current management, disposal and storage practices. Hydrometallurgy 108, 33–45.

Qin, S., Sun, Y., Li, Y., Wang, J., Zhao, C., Gao, K., 2015. Coal deposits as promising alternative sources for gallium. Earth Sci. Rev. 150, 95–101.

Qin, B., Schneider, U., 2016. Catalytic use of elemental gallium for carbon–carbon bond formation. J. Am. Chem. Soc. 138, 13119–13122.

Ricketts, N.J., Duyvesteyn, W.P., 2018. March. Scandium recovery from the Nyngan laterite project in NSW. In: TMS Annual Meeting & Exhibition. Springer, Cham, pp. 1539–1543.

Santini, T.C., Fey, M.V., 2013. Spontaneous vegetation encroachment upon bauxite residue (red mud) as an indicator and facilitator of in situ remediation

processes. Environ. Sci. Technol. 47, 12089–12096.

Tsakiridis, P.E., Agatzini-Leonardou, S., Oustadakis, P., 2004. Red mud addition in the raw meal for the production of Portland cement clinker. J. Hazard Mater. 116, 103–110.

Ujaczki, É., Klebercz, O., Feigl, V., Molnár, M., Magyar, Á., Uzinger, N., Gruiz, K., 2015. Environmental toxicity assessment of the spilled Ajka red mud in soil microcosms for its potential utilisation as soil ameliorant. Period. Polytech. - Chem. Eng. 59, 253.

Ujaczki, É., Zimmermann, Y., Gasser, C., Molnár, M., Feigl, V., Lenz, M., 2017. Red mud as secondary source for critical raw materials–purification of rare earth elements by liquid/liquid extraction. J. Chem. Technol. Biotechnol. 92, 2835–2844.

Ujaczki, É., Feigl, V., Molnár, M., Cusack, P., Curtin, T., Courtney, R., O'Donoghue, L., Davris, P., Hugi, C., Evangelou, M.W., Balomenos, E., 2018. Re-using bauxite residues: benefits beyond (critical raw) material recovery. J. Chem. Technol. Biotechnol. 93, 2498–2510.

United States Geological Survey Website (USGS), 2016. Commodity Statistics and Information. Available: http://minerals.usgs.gov/minerals/pubs/commodity/. (Accessed 30 January 2018).

Wang, S., Ang, H.M., Tade, M.O., 2008. Novel applications of red mud as coagulant, adsorbent and catalyst for environmentally benign processes. Chemosphere 72, 1621–1635.

Wang, W., Pranolo, Y., Cheng, C.Y., 2013. Recovery of scandium from synthetic red mud leach solutions by solvent extraction with D2EHPA. Sep. Purif. Technol. 108, 96–102.

Wang, X., Zhang, Y., Lv, F., An, Q., Lu, R., Hu, P., Jiang, S., 2015. Removal of alkali in the red mud by SO2 and simulated flue gas under mild conditions. Environ. Prog. Sustain. Energy 34, 81–87.

Weng, Z., Jowitt, S.M., Mudd, G.M., Haque, N., 2015. A detailed assessment of global rare earth element resources: opportunities and challenges. Econ. Geol. 110, 1925–1952.

Xu, C., Kynický, J., Smith, M.P., Kopriva, A., Brtnický, M., Urubek, T., Yang, Y., Zhao, Z., He, C., Song, W., 2017. Origin of heavy rare earth mineralization in South China. Nat. Commun. 8, 14598.

Xue, S., Kong, X., Zhu, F., Hartley, W., Li, X., Li, Y., 2016. Proposal for management and alkalinity transformation of bauxite residue in China. Environ. Sci. Pollut. Res. 23, 12822–12834.

Xue, S., Li, M., Jiang, J., Millar, G.J., Li, C., Kong, X., 2018. Phosphogypsum stabilization of bauxite residue: conversion of its alkaline characteristics. J. Environ. Sci. https://doi.org/10.1016/j.jes.2018.05.016.

Zhu, F., Liao, J., Xue, S., Hartley, W., Zou, Q., Wu, H., 2016a. Evaluation of aggregate microstructures following natural regeneration in bauxite residue as characterized by synchrotron-based X-ray micro-computed tomography. Sci. Total Environ. 573, 155–163.

Zhu, F., Xue, S., Hartley, W., Huang, L., Wu, C., Li, X., 2016b. Novel predictors of soil genesis following natural weathering processes of bauxite residues. Environ. Sci. Pollut. Res. 23, 2856–2863.

Zhu, F., Cheng, Q., Xue, S., Li, C., Hartley, W., Wu, C., Tian, T., 2018. Influence of natural regeneration on fractal features of residue microaggregates in bauxite residue disposal areas. Land Degrad. Dev. 29, 138–149.

Enhancement of Bauxite Residue as a Low-cost Adsorbent for Phosphorus in Aqueous Solution, using Seawater and Gypsum Treatments.

Patricia B. Cusack, Mark G. Healy, Paraic C. Ryan, Ian T. Burke, Lisa M. T. O' Donoghue, Éva Ujaczki, Ronan Courtney[*]

Article associated with Chapter 4.
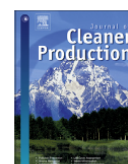
Enhancement of bauxite residue as a low-cost adsorbent for phosphorus in aqueous solution, using seawater and gypsum treatments

Patricia B. Cusack [a, b, c], Mark G. Healy [b, *], Paraic C. Ryan [g], Ian T. Burke [d], Lisa M.T. O' Donoghue [e], Éva Ujaczki [c, e, f], Ronan Courtney [a, c]

[a] Department of Biological Sciences, University of Limerick, Castletroy, Co. Limerick, Ireland
[b] Civil Engineering, National University of Ireland, Galway, Ireland
[c] The Bernal Institute, University of Limerick, Castletroy, Co. Limerick, Ireland
[d] School of Earth and Environment, University of Leeds, Leeds, LS2 9JT, United Kingdom
[e] Design and Manufacturing Technology, University of Limerick, Castletroy, Co. Limerick, Ireland
[f] Department of Applied Biotechnology and Food Science, Faculty of Chemical Technology and Biotechnology, Budapest University of Technology and Economics, Müegyetem rkp. 3, 1111, Budapest, Hungary
[g] Discipline of Civil, Structural and Environmental Engineering, School of Engineering, University College Cork, Ireland

ARTICLE INFO

ABSTRACT

Bauxite residue (red mud), the by-product produced in the alumina industry, is being produced at an estimated global rate of approximately 150 Mt per annum. Due to its highly alkaline nature, many refineries use neutralisation techniques such as mud farming (atmospheric carbonation), direct carbonation using carbon dioxide or reactions with seawater, to treat the bauxite residue and reduce its alkalinity prior to disposal in the BRDA (bauxite residue disposal area). Applying a treatment can render the bauxite residue non-hazardous and may also prepare the bauxite residue for reuse, particularly as an adsorbent. In this study, gypsum and seawater treatments were applied to the various bauxite residue samples obtained and the effects on its mineral, elemental and physiochemical properties were examined, as well as the effect on its phosphorus (P) adsorption capacity. It was found that in addition to reducing the alkalinity of all bauxite residue samples used, the P adsorption capacity was also enhanced following amendment with seawater or gypsum, particularly with gypsum. A positive correlation was detected between P adsorption and both Ca and CaO. A negative correlation was detected between the P adsorption and pH of the media. Fitting the data obtained from a batch adsorption experiment to the Langmuir adsorption isotherm, the maximum adsorption capacity was estimated to range from 0.345 to 2.73 mg P per g bauxite residue, highlighting the re-use potential for bauxite residue as an adsorbent for P.

© 2018 Elsevier Ltd. All rights reserved.

1. Introduction

During the extraction of alumina from bauxite ore using the Bayer process, a by-product called bauxite residue (red mud) (Kirwan et al., 2013; Liu et al., 2014) is produced. The global inventory for bauxite residue is approximately 3 billion tonnes, with an estimated annual production rate of 150 million tonnes (Evans, 2016; Mayes et al., 2016). Bauxite residue is highly alkaline

(pH > 10) (Goloran et al., 2013), with a high salinity and sodicity (Gräfe et al., 2009). Current best practice within this industry includes careful planning and management of highly engineered bauxite residue disposal areas (BRDAs), avoiding contamination of the surrounding environment (Prajapati et al., 2016). In addition, some refineries use neutralisation techniques for the bauxite residue before disposal into the BRDAs (Klauber et al., 2011; IAI, 2015; Evans, 2016). These techniques include (1) direct carbonation, whereby the residue slurry is treated with either carbon dioxide, sulfur dioxide gas, or undergoes intensive mud farming using amphirollers (atmospheric carbonation) (Cooling, 2007; Fois et al., 2007; Dilmore et al., 2009; Evans, 2016) (2) addition of spent acids

and/or gypsum ($CaSO_4.2H_2O$) (Kirwan et al., 2013), or (3) reaction of residues with seawater (Hanahan et al., 2004; Palmer and Frost, 2009; Couperthwaite et al., 2014).

Bauxite residues typically comprise very fine particles, ranging from 0.01 μm to 200 μm (Pradhan et al., 1996). Depending on the type of bauxite ore used, in some refineries the bauxite residue undergoes a separation technique during processing (Evans, 2016), which allows it to be separated into two main fractions: a fine fraction with a particle size <100 μm and a coarse fraction with a particle size >150 μm (Eastham et al., 2006; Jones et al., 2012). The coarse fraction mainly consists of quartz (SiO_2), whereas the fine fraction is dominated by iron (Fe) oxides (Snars and Gilkes, 2009). The ratio of the fine to coarse fraction produced is dependent on the bauxite ore used and the Bayer process employed (Li, 2001). Refineries which carry out the separation technique, have found use for the coarse fraction to create roadways to the BRDA and/or storage embankments (Evans, 2016). However, finding appropriate options for the re-use of the fine fraction bauxite residue remains elusive (Power et al., 2011; IAI, 2015).

Fine fraction bauxite residue comprises Fe oxides (20–45%) and aluminium (Al) oxides (10–22%) (IAI, 2015), which make it suitable as a medium to adsorb phosphorus (P). The European Commission (EC) has identified waste management as an important aspect of the "circular economy" (European Commission, 2015), so in recent years, emphasis has been placed on investigating alternative methods of P recovery from wastewater (Grace et al., 2015, 2016). A move from the more conventional methods of P recovery such as biological removal and chemical precipitation (Wang et al., 2008), to the use of low-cost adsorbents from industrial solid wastes, such as bauxite residue, have been examined. In comparison to standard P removal by sand, bauxite residue has a high P retention capacity (Vohla et al., 2007). However, its P removal potential is enhanced following treatment by heat, acid or gypsum (Table 1). Of the methods employed, acid and heat treatment have proved most successful in increasing the P adsorption capacity of the bauxite residue, with maximum adsorption capacities of up to 203 mg P g^{-1} bauxite being achieved (Liu et al., 2007) compared to untreated residue (0.20 mg P g^{-1}; Grace et al., 2015) (Table 1). However, whilst acid and heat treatments have proven to be very successful in increasing the adsorption capacity of bauxite residue, they are expensive, energy consuming (using high temperatures up to 700 °C) (Xue et al., 2016), and, without further treatment, do not allow for the easy reuse of the bauxite residue (e.g. as a possible media for plant growth) (Xue et al., 2016).

Treatments such as seawater or gypsum provide relatively inexpensive, alternative treatments, which may not only enhance the P adsorption capacity of the bauxite residue media, but may also help to improve its physicochemical characteristics. Seawater treatment improves bauxite's physical structure, due to the addition of magnesium (Mg) and calcium (Ca) which behave as flocculating agents, allowing many of the fine particles in bauxite residue to form more stable aggregates (Jones and Haynes, 2011), and a partial decrease in sodium (Na) due to ion exchange with Mg, Ca and potassium (K) (Hanahan et al., 2004). Seawater-treated bauxite residues also allow adsorbed P to become bio-available, unlike the metal cations which are unavailable, highlighting the P and metal retention capabilities (Fergusson, 2009). Revegetation of bauxite residue using gypsum has also improved plant growth by reducing its alkalinity and salinity, and improving the structure of the residue (Courtney et al., 2009; Courtney and Kirwan, 2012). In addition to this, modern alumina refineries are often located close to deep water ports, to allow for the bulk shipment of incoming bauxite (sometimes from multiple sources) to the refinery and/or for bulk shipment of alumina to aluminium smelters situated elsewhere. Therefore, there is ample scope for the increasing use of seawater neutralization technology for pre-treatment of residues in refineries not already employing treatments previously mentioned, prior to their deposition in the BRDA.

To the best of the authors' knowledge, no study has previously compared the use of raw seawater or gypsum treatments on the separate fractions of bauxite residue as a method of neutralisation and preparation for the re-use of bauxite residue in its separated and unseparated fractions as low-cost adsorbents and a potential source of P. The objectives of this study were to (1) characterise bauxite residue from two different sources, before and after treatment with seawater and gypsum, and to investigate their potential to release trace elements (2) investigate the effect of the treated bauxite residue on P adsorption (3) assess the impact of particle size, mineral and elemental (particularly Ca and Mg) composition of the bauxite residue on the adsorption of P.

2. Materials and methods

2.1. Sample preparation

A 1 kg sample of fresh bauxite residue was obtained from Alteo Gardanne [Gardanne, France (4327′9″N, 527′41″ E)], who operate a co-disposal method for fine and coarse fractions of bauxite. This sample will be referred to hereafter as UFR. One kilogram of mud-farmed bauxite residue samples (treated by atmospheric

Table 1
Phosphorus (P) adsorption studies that have been carried out using bauxite residues, untreated and treated residues, and their recovery efficiencies.

	P recovery technique	Factors investigated	Type of water	Initial P concentration of the water	P recovered	Reference
Untreated bauxite residue	Batch adsorption experiment	Kinetics, pH and temperature	Synthetic water	5-100 mg P L^{-1}	0.20 mg P g^{-1}	Grace et al., 2015
Gypsum Treated	Batch adsorption experiment	Contact time (3, 6, 24, 48hr)	Synthetic water	20-400 mg P L^{-1}	7.03 mg P g^{-1}	Lopez et al., 1998
Brine treated bauxite residue (Bauxsol™)	Batch adsorption experiment	pH, ionic strength, time	Synthetic water	0.5–2 mg P L^{-1}	6.5–14.9 mg P g^{-1}	Akhurst et al., 2006
Acid and brine treated bauxite residue (Bauxsol™ [a])	Batch adsorption experiment	Kinetics and isotherms	Synthetic water	200 mg P L^{-1}	55.72 mg P g^{-1}	Ye et al., 2014
Heat treated bauxite residue	Batch adsorption experiment	Time, pH and initial concentration	Synthetic water	155 mg P L^{-1}	155.2 mg P g^{-1}	Liu et al., 2007
Acid and heat treated bauxite residue	Batch adsorption experiment	Time, pH and initial concentration	Synthetic water	155 mg P L^{-1}	202.9 mg P g^{-1}	Liu et al., 2007
Acid treated bauxite residue	Batch adsorption experiment	Acid type, pH	Synthetic water	1 mg P L^{-1}	1.1 mg P g^{-1}	Huang et al., 2008

[a] Bauxsol™ = neutralised bauxite residue produced using the Basecon™ procedure, which uses brines high in Ca^{2+} and Mg^{2+} (McConchie et al., 2001).

carbonation and therefore non-hazardous), were also obtained from Rusal Aughinish Alumina [Limerick, Ireland (5237′06″N, 904′19″W)], who separate the fine (particle sizes <100 μm) and coarse (particle sizes >150 μm) fraction of bauxite residue before disposal (IAI, 2015) in a ratio of 9:1 (fine: coarse). The fine and coarse fractions will be referred to hereafter as UF (untreated fine) and UC (untreated coarse).

Before any analysis or experiments were conducted, all bauxite residue samples were dried at 105 °C for 24 h. Once dry, the samples were pulverised using a mortar and pestle and sieved to a particle size <2 mm. 0.3 kg of each sample were then treated with either seawater (S) or laboratory-grade gypsum (G) (Lennox, Ireland), so two treatments were applied to each source of bauxite residue. S or G, placed after the above abbreviations, indicates the treatment applied. Gypsum was applied to the 0.3 kg bauxite residue samples at a ratio of 8% (w/w) (Lopez et al., 1998) and leached for 72 h in accordance with standard methods (British Standard Institution, 2002). Seawater amendment involved mixing with 0.3 kg bauxite at a ratio of 5:1 (v/w) (after Johnston et al., 2010), for 1 h, followed by a 12 h settlement period overnight. The bauxite residue and seawater mixture was then filtered through a 0.45 μm membrane using a vacuum pump. The treated bauxite residue samples were then oven dried for 24 h, pulverised with a mortar and pestle, and sieved to <2 mm in size.

2.2. Characterisation study

Untreated and treated bauxite samples were characterised (n = 3) for their physical, chemical, elemental and mineralogical properties. Soil pH and electrical conductivity (EC) were measured in an aqueous extract, using 5 g of bauxite residue sample in a 1:5 ratio (solid: liquid) (Courtney and Harrington, 2010). The bulk density (ρ_b) was determined after Blake (1965) and the particle density (ρ_p) after Blake and Hartge (1986) using 10 g of bauxite residue samples. Total pore space (S_t) was calculated using the values obtained for the bulk and particle densities (Danielson and Sutherland, 1986). The effective particle size analysis (PSA) was determined on particle sizes <53 μm using optical laser diffraction on the Malvern Zetasizer 3000HS® (Malvern, United Kingdom) with online autotitrator and a Horiba LA-920, and reported at specific cumulative % (10, 50 and 90%). Mineralogical detection was carried out using X-ray diffraction (XRD) on 1 g samples using a Philips X'Pert PRO MPD® (California, USA), whilst surface morphology and elemental detection were carried out using scanning electron microscopy (SEM) and energy-dispersive X-ray spectroscopy (EDS) on a Hitachi SU-70 (Berkshire, UK), using approximately 1 g samples. Quantification of the elemental content was carried out on 1 g samples by Brookside Laboratories (OH, USA) after digestion (EPA, 1996) using Inductively Coupled Plasma Atomic Emission Spectroscopy (ICP-AES) and elemental composition quantified using X-ray fluorescence (XRF). Measurement of the point of zero charge (PZCpH) was after Vakros et al. (2002) using 1 g samples, and cation exchange capacity (CEC) was determined using the K saturation technique (Thomas, 1982), using 5 g samples. Brunauer-Emmett-Teller specific surface area (SSA) and pore volume analysis were conducted on 1 g samples, which were degassed at 120 °C for 3 h prior to analysis carried out by Glantreo Laboratories (Cork, Ireland).

2.3. Phosphorus adsorption batch study

The P adsorption capacity of nine bauxite samples (untreated and gypsum/seawater treated samples) were examined in a bench-scale experiment. To conduct a P adsorption isotherm test, ortho-phosphorus (PO_4^{3-}-P) solutions were made up to known concentrations using potassium dihydrogen phosphate (K_2HPO_4) in distilled water. One gram of each of the sieved media was placed into a series of 50 ml-capacity containers and was overlain with 25 ml of the solutions. Each sample was then shaken in a reciprocal shaker at 250 rpm for 24 h. At t = 24 h, the supernatant water from each sample container was filtered using 0.45 μm filters and analysed immediately using a nutrient analyser (Konelab 20, Thermo Clinical Labsystems, Finland). The data obtained from the P adsorption batch studies were modelled using the Langmuir adsorption isotherm (McBride, 2000), which assumes monolayer adsorption on adsorption sites and allows for the estimation of the maximum P adsorption capacity (q_{max}) of the media:

$$q_i = q_{max}\left(\frac{k_a C_e}{1 + k_a C_e}\right) \qquad (1)$$

where q_i is the quantity of the contaminant adsorbed per gram of media (g g^{-1}), C_e is the equilibrium contaminant concentration in the water (g m^{-3}), k_a is a measure of the affinity of the contaminant for the media (m^3 g^{-1}), and q_{max} is the maximum amount of the contaminant that can be adsorbed onto the media (g g^{-1}).

2.3.1. Mobilization of metals

To determine whether the residue media released trace elements, 25 ml of water was mixed with 1 g of media for 24 h and the supernatant was analysed by ICP-MS. The elements selected for detection were Al, arsenic (As), barium (Ba), beryllium (Be), boron (B), cadmium (Cd), Ca, chromium (Cr), copper (Cu), Fe, gallium (Ga), K, lead (Pb), Mg, manganese (Mn), mercury (Hg), molybdenum (Mo), Na, nickel (Ni), P, selenium (Se), silicon (Si), titanium (Ti), vanadium (V), and zinc (Zn).

2.4. Statistical analysis

Linear regression analysis was utilised to examine the extent of correlation between the individual characteristic parameters of the bauxite residue samples and bauxite adsorption, using Minitab. A Pearson correlation coefficient and a correlation p-value were determined to quantify correlation. The p-value represents the probability that the correlation between the bauxite residue characteristic in question and the response variable (adsorption) is zero i.e. the probability that there is no relationship between the two.

3. Results and discussion

3.1. Characterisation of bauxite residue

3.1.1. Effect of treatments on elemental and mineralogical composition

The mineral and total elemental composition of the three untreated bauxite residues [UF (untreated fine fraction), UC (untreated coarse fraction), and UFR (untreated co-disposed)] are shown in Tables 2 and 3. Bauxite residues are typically high in Fe and Al oxides (Liu et al., 2007), which was found to be the case in this study. The mineralogical composition present for all untreated samples was dominated by Fe_2O_3, Al_2O_3, SiO_2 and CaO. A decrease in Al_2O_3 was noted following treatment with the gypsum and the seawater in all samples, with an increase in CaO content noted in samples treated with gypsum.

XRD analysis showed that the main crystalline phases present in UF were haematite (Fe_2O_3), goethite (FeO(OH)), perovskite (CaTiO₃), boehmite (AlO(OH)), rutile (TiO₂), gibbsite Al(OH)₃ and sodalite Na₈(Al₆Si₆O₂₄)Cl₂ (Figure S1 in the Supplementary Material). Similarly, the main minerals in UFR were haematite (Fe_2O_3),

Table 2
Mineralogical composition of the bauxite residues, untreated and treated.

Parameter	Untreated Fine (UF)	Fine + gypsum (UFG)	Fine + seawater (UFS)	Untreated Coarse (UC)	Coarse + gypsum (UCG)	Coarse + seawater (UCS)	Untreated French (UFR)	French + gypsum (UFRG)	French + seawater (UFRS)
Fe_2O_3 (%)	43.9 ± 1.1	40.6 ± 0.6	41.8 ± 1.2	64.0 ± 5.1	61.4 ± 3.0	69.9 ± 3.8	43.9 ± 0.6	47.9 ± 0.5	53.3 ± 5.8
Al_2O_3 (%)	12.7 ± 0.6	11.3 ± 1.0	11.1 ± 2.5	19.4 ± 1.8	11.1 ± 0.6	7.4 ± 0.7	14.0 ± 1.0	11.2 ± 0.3	11.4 ± 2.2
CaO (%)	5.9 ± 0.2	8.2 ± 0.5	4.4 ± 0.3	1.1 ± 0.2	7.6 ± 0.4	1.2 ± 0.1	5.6 ± 0.1	7.7 ± 0.3	3.2 ± 0.5
MgO (%)	3.6 ± 1.3	3.5 ± 0.8	3.1 ± 1.0	4.7 ± 1.8	3.6 ± 0.8	2.6 ± 0.6	4.1 ± 0.6	3.8 ± 0.9	3.2 ± 1.6
SiO_2 (%)	8.6 ± 0.7	8.5 ± 0.9	8.6 ± 1.7	2.6 ± 0.3	1.3 ± 0.2	1.4 ± 0.2	9.4 ± 0.5	5.1 ± 0.4	4.3 ± 0.3
TiO_2 (%)	2.4 ± 0.3	2.1 ± 0.6	2.7 ± 0.1	0.9 ± 0.1	1.0 ± 0.1	2.1 ± 0.6	2.5 ± 0.02	2.3 ± 0.1	2.3 ± 0.5
P_2O_5 (%)	0.6 ± 0.04	0.4 ± 0.02	0.4 ± 0.1	0.3 ± 0.02	0.2 ± 0.02	0.2 ± 0.06	0.5 ± 0.01	0.5 ± 0.02	0.5 ± 0.01

Table 3
Elemental composition of the bauxite residues, untreated and treated.

Parameter	Untreated Fine (UF)	Fine + gypsum (UFG)	Fine + seawater (UFS)	Untreated Coarse (UC)	Coarse + gypsum (UCG)	Coarse + seawater (UCS)	Untreated French (UFR)	French + gypsum (UFRG)	French + seawater (UFRS)
B (mg kg^{-1})	470 ± 8.81	425 ± 29	448 ± 13	615 ± 13.3	622 ± 29	722 ± 32.1	566 ± 18.9	539 ± 25	483.8 ± 31
Al (mg kg^{-1})	72538 ± 1390	81095 ± 1219	80608 ± 3090	45854 ± 2769	48851 ± 2336	45917 ± 2080	67295 ± 3343	65389 ± 1326	64189 ± 595
As (mg kg^{-1})	21.9 ± 1.73	9.7 ± 0.4	<LOD[a]	<LOD[a]	<LOD[a]	<LOD[a]	8.1 ± 0.2	9.75 ± 0.6	6.51 ± 0.43
Ba (mg kg^{-1})	43.8 ± 1.19	29.4 ± 5	33.3 ± 0.7	13.9 ± 1.01	18.3 ± 3.4	12.7 ± 2.8	45.7 ± 1.5	41.4 ± 1.4	49.4 ± 3.8
Cd (mg kg^{-1})	8.033 ± 0.16	7.02 ± 0.3	7.33 ± 0.19	10.7 ± 0.18	10.8 ± 0.5	11.8 ± 0.59	9.31 ± 0.2	8.87 ± 0.3	8.21 ± 0.3
Cr (mg kg^{-1})	1698 ± 37.2	933 ± 44	1170 ± 12.9	880 ± 3.8	817 ± 13	803 ± 21.3	1184 ± 15.9	1090 ± 9	1159 ± 31.2
Fe (mg kg^{-1})	338571 ± 3057	289459 ± 1859	298282 ± 4937	434739 ± 9980	460078 ± 23043	471204 ± 25753	353392 ± 10003	328114 ± 4498	332251 ± 3435
Pb (mg kg^{-1})	34.88 ± 0.54	27.8 ± 2.8	36.9 ± 0.8	29.56 ± 3.03	24.6 ± 3	22.06 ± 2.47	34.5 ± 0.9	32.3 ± 0.8	37.4 ± 2.1
Mg (mg kg^{-1})	122.28 ± 4.96	163 ± 37	1047 ± 25.6	18.32 ± 4.78	8.5 ± 2.21	511.6 ± 25.4	109 ± 3.9	150 ± 9	2203.8 ± 134
Mn (mg kg^{-1})	163 ± 2.63	140 ± 6.1	167 ± 6.8	187 ± 15.5	223 ± 99	185 ± 31.1	134 ± 0.9	139 ± 1.9	142.9 ± 4.2
Ni (mg kg^{-1})	18.6 ± 0.89	<LOD[a]	2.25 ± 0.2	3.54 ± 0.27	3.15 ± 0.5	4.18 ± 0.22	1.1 ± 0.1	1.24 ± 0.2	1.23 ± 0.3
K (mg kg^{-1})	391 ± 13.68	454 ± 29	1108 ± 41	255 ± 38	195 ± 23	556.99 ± 67.38	399 ± 13	359 ± 11	1048 ± 63.2
Si (mg kg^{-1})	223.5 ± 46.1	256 ± 92	245.7 ± 35	213 ± 6.6	234 ± 34	194.46 ± 10.58	276 ± 20	285 ± 34	258.5 ± 11.7
Na (mg kg^{-1})	28347 ± 553	38180 ± 352	41864 ± 2012	8804 ± 666	5935 ± 114	11101.55 ± 1121.8	25514 ± 317	23703 ± 499	31974 ± 1087
Ti (mg kg^{-1})	1395 ± 196	1309 ± 100	1265 ± 22	<LOD[a]	<LOD[a]	<LOD[a]	1382 ± 38	1288 ± 120	1233 ± 46
V (mg kg^{-1})	1050 ± 21.6	781 ± 29	777 ± 8	786 ± 23.6	731 ± 20	731.04 ± 23	1036 ± 12	920 ± 7	983 ± 21
Zn (mg kg^{-1})	50.7 ± 0.71	40.6 ± 1.2	42.6 ± 1.3	86.7 ± 1.7	82 ± 5.4	84.68 ± 4.2	55.8 ± 0.5	55.6 ± 1.17	57.3 ± 0.9
Ga (mg kg^{-1})	78.9 ± 2.02	81.2 ± 0.53	73.9 ± 0.6	71.8 ± 1.03	69.3 ± 2.3	73.5 ± 1.6	86.8 ± 1.3	78.6 ± 2	78.8 ± 0.9
Ca (mg kg^{-1})	46657 ± 832	51641 ± 485	17159 ± 413	4152 ± 490	12771 ± 823	4089.42 ± 588.32	15084 ± 358	42703 ± 2383	14820 ± 926
P (mg kg^{-1})	955 ± 0.57	962 ± 99	1018 ± 15	1040 ± 23	1011 ± 59	1039.6 ± 23	1298 ± 26	1220 ± 10	1320 ± 53.8
Be (mg kg^{-1})	<LOD[a]	<LOD[a]	<LOD[a]	<LOD[a]	<LOD[a]	<LOD[a]	<LOD[a]	<LOD[a]	<LOD[a]
Cu (mg kg^{-1})	<LOD[a]	<LOD[a]	<LOD[a]	<LOD[a]	<LOD[a]	<LOD[a]	<LOD[a]	<LOD[a]	<LOD[a]
Hg (mg kg^{-1})	<LOD[a]	<LOD[a]	<LOD[a]	<LOD[a]	<LOD[a]	<LOD[a]	<LOD[a]	<LOD[a]	<LOD[a]
Mo (mg kg^{-1})	<LOD[a]	<LOD[a]	<LOD[a]	<LOD[a]	<LOD[a]	<LOD[a]	<LOD[a]	<LOD[a]	<LOD[a]
Se (mg kg^{-1})	<LOD[a]	<LOD[a]	<LOD[a]	<LOD[a]	<LOD[a]	<LOD[a]	<LOD[a]	<LOD[a]	<LOD[a]

[a] <LOD = below the limits of detection.

goethite (FeO(OH)), boehmite (AlO(OH)), rutile (TiO_2), gibbsite Al(OH)$_3$ and sodalite $Na_8(Al_6Si_6O_{24})Cl_2$ (Figure S2). Boehmite (AlO(OH)), rutile (TiO_2), gibbsite Al(OH)$_3$ haematite (Fe_2O_3) were the predominant minerals present in UC (Figure S3). Following treatment with seawater and gypsum, a change in mineral phase in UFG, UFS, UFRS and UFRG occurred (Figure S4, S5, S6, S7). After treatment with gypsum, a higher presence of the calcium carbonate, calcite ($CaCO_3$), was detected in UFRG and UCG (Figure S7 and S8), and post seawater treatment, small peaks representing brucite (Mg(OH)$_2$) were detected in UFS and UCS (S5 and S9).

These findings are similar to previous studies that examined various neutralization techniques for bauxite residue (Gräfe et al., 2009). When seawater is added to bauxite residue, a reaction occurs where the hydroxide, carbonate and aluminate ions are eliminated due to a reaction involving Mg^{2+} and Ca^{2+} (from the seawater) (Gräfe et al., 2009; Palmer and Frost, 2009). This results in the formation of alkaline solids such as the calcium carbonates, calcite and brucite, which cause a buffering effect, evidenced in a shift of pH to between 8 and 9 (Power et al., 2011). The addition of gypsum ($CaSO_4$) results in a drop in the pH (approximately 8.6) due to the precipitation of excess hydroxides (OH−), aluminium hydroxides (Al(OH)$_4^-$), carbonates (CO_3^{2-}) to form calcium hydroxide/lime (Ca(OH)), tri-calcium aluminate (TCA), hydrocalumite and calcium carbonate ($CaCO_3$), which behave as buffers and maintain pH (Gräfe et al., 2009). The addition of Ca also flocculates and helps with the formation of more stable aggregates (Jones and Haynes, 2011).

An analysis of water samples (Table S1) to examine mobilisation of metals showed that As, Al and Cr were present in the leachate from the UFR sample, but decreased following gypsum and seawater treatments. Arsenic, Fe and Al were mobilised from the UF sample, but these concentrations were reduced following treatment with gypsum and seawater. Aluminium was mobilised from the UC. The reduction in Fe and Al following treatment with either gypsum or seawater is in line with previous studies, which have shown that water soluble Fe and Al decrease following gypsum application (Courtney and Timpson, 2005). Overall, Al still remained above the maximum allowable concentration (MAC) of 0.2 mg L^{-1} (200 µg L^{-1}) (EPA, 2014) for Al for drinking water. Sodium was still at a high level following gypsum and seawater treatments, ranging from 139.3 ± 3.2 to 153 ± 24.8 mg L^{-1} and 241.3 ± 26 to 388.7 ± 18.6 mg L^{-1}, respectively. The MAC for Na in drinking water is 200 mg L^{-1} (EPA, 2014).

3.1.2. Effect of treatments on physicochemical properties

The untreated bauxite residues had high pH (10.8 ± 0.12 to 11.9 ± 0.06) and EC (704 ± 90.8 to 1184 ± 48.8 µS cm^{-1}) (Table 4). Following treatment with gypsum and seawater, pH decreased and

Table 4
Physical and chemical characterisation of the bauxite residues, untreated and treated.

Parameter	Untreated Fine (UF)	Fine + gypsum (UFG)	Fine + seawater (UFS)	Untreated Coarse (UC)	Coarse + gypsum (UCG)	Coarse + seawater (UCS)	Untreated French (UFR)	French + gypsum (UFRG)	French + seawater (UFRS)
pH	10.8 ± 0.12	8.7 ± 0.04	9.02 ± 0.07	11.4 ± 0.29	6.79 ± 0.08	7.95 ± 0.16	11.9 ± 0.06	9.17 ± 0.02	9.49 ± 0.01
EC (μS cm^{-1})	704 ± 90.8	1338 ± 3.5	3080 ± 17.3	856 ± 1.53	909 ± 2	916 ± 1.53	1184 ± 48.8	1219 ± 7.21	5323 ± 172
% Water	23.5 ± 0.65	28.9 ± 0.6	32.1 ± 1.72	0.39 ± 0.2	0.82 ± 0.18	3.13 ± 0.72	28 ± 0.54	35.3 ± 1.32	36.5 ± 0.16
d_{10} (μm)[a]	0.6 ± 0.09	1.37 ± 0.23	1.26 ± 0.06	1.27 ± 0.47	1.11 ± 0.23	1.66 ± 0.83	1.3 ± 0.04	1.49 ± 0.06	1.08 ± 0.74
d_{50} (μm)[b]	2.43 ± 0.29	3.56 ± 0.59	3.52 ± 0.11	5.13 ± 0.63	3.69 ± 0.49	3.68 ± 0.4	3.7 ± 0.12	4.11 ± 0.39	3.47 ± 0.98
d_{90} (μm)[c]	6.02 ± 0.86	7.12 ± 1.98	7.69 ± 1.97	12.04 ± 1.27	9.51 ± 0.25	7.0 ± 0.13	10.11 ± 2.37	9.81 ± 2.68	7.17 ± 3.25
Total Pore Space (%)[d]	50.03 ± 2.25	50.73 ± 9.04	50.03 ± 1.75	9.63 ± 6.46	10.82 ± 1.09	7.65 ± 5.26	61.77 ± 1.16	53.6 ± 1.95	53.87 ± 0.78
Bulk Density (g cm^{-3})[e]	1.5 ± 0.02	1.5 ± 0.01	1.49 ± 0.01	2.53 ± 0.01	2.48 ± 0.03	2.55 ± 0.01	1.31 ± 0.03	1.32 ± 0.03	1.31 ± 0.02
Particle Size Density (g cm^{-3})[f]	2.99 ± 0.1	3.11 ± 0.5	2.94 ± 0.12	2.81 ± 0.21	2.65 ± 0.4	2.7 ± 0.14	3.41 ± 0.07	2.85 ± 0.08	2.85 ± 0.07
PZCpH[g]	6.96 ± 1.21	3.43 ± 0.73	6.28 ± 0.98	6.89 ± 0.09	3.11 ± 0.12	6.39 ± 0.51	6.16 ± 0.21	6.32 ± 0.51	4.43 ± 0.09
CEC (K)(cmol kg^{-1})[h]	63.3 ± 2.56	64.1 ± 3.41	60.1 ± 2.96	N/A[k]	N/A[k]	N/A[k]	57.5 ± 2.13	56.4 ± 3.49	48.9 ± 13.7
Total Pore Volume (cm^{-3} g^{-1})[i]	0.03	0.03	0.03	0.02	0.02	0.03	0.03	0.04	0.03
BET SSA (m^2 g^{-1})[j]	11.73	12.77	13.82	12.58	13.19	15.37	15.24	17.57	17.57

[a] d_{10} (μm) = the size of particles at 10% of the total particle distribution, expressed in μm.
[b] d_{50} (μm) = the median; the size of particles at 50% of the total particle distribution, expressed in μm.
[c] d_{90} (μm) = the size of particles at 90% of the total particle distribution, expressed in μm.
[d] Total Pore Space = the total pore space which may be calculated from particle density and bulk density.
[e] Bulk density = the mass of soil per unit volume, expressed as g cm^{-3}.
[f] Particle size density = the density of the solid particles, excluding pore spaces between them, expressed as g cm^{-3}.
[g] PZCpH = the pH at which the point of zero charge is occurring.
[h] CEC = the cation exchange capacity, expressed as cmol kg^{-1}.
[i] BET SSA = specific surface area analysed using Brunauer-Emmett-Teller isotherm and expressed as m^2 g^{-1}.
[j] Total Pore Volume = measurement of total pore volume expressed as cm^{-3} g^{-1}.
[k] N/A = not available.

EC increased. Changes for pH after treatment with either seawater or gypsum are due to precipitation of calcium carbonates such calcite, brucite and aragonite, which behave as buffers and maintain a reduced pH (Menzies et al., 2004), while the increase in EC is attributed to the introduction of excess Na$^+$ and Ca^{2+} (Gräfe et al., 2009). The pH of bauxite residue is normally within the range of 11–13 (Newson et al., 2006), but varies due to the type of bauxite ore, Bayer process, and neutralisation techniques used in the refinery. Both seawater (Menzies et al., 2004; Johnston et al., 2010) and gypsum applications (Jones and Haynes, 2011; Courtney and Kirwan, 2012; Lehoux et al., 2013) are recognised methods of reducing the alkalinity of bauxite residues.

No change was observed in the particle size or particle size density following the addition of the gypsum and seawater treatments to the various bauxite residue samples (Table 4). Similarly, the addition of gypsum or seawater did not have any impact on bulk density (Table 4).

The surface morphology of bauxite residues typically comprises 30% amorphous and 70% crystalline phase (Gräfe et al., 2009). However, in this study SEM imaging suggests that the bauxite residue samples were not present in strong crystalline form (Fig. 1), in particular for samples UF and UFR, as no distinctive crystalline structure to the bauxite residue samples was observed. Liu et al. (2007) examined the effect of age on stored bauxite residue, and found that fresh bauxite residue particles are present in poorly formed crystallised or amorphous form in comparison to older bauxite residue (10 years), which has a stronger crystalline formation, indicating that crystallisation occurs in some of the minerals over time. As the bauxite residue used in this study was fresh, this would explain why there was not a strong distinction between amorphous or crystalline forms, similar to the findings of Liu et al. (2007). The composition of fine particles and larger particles in the coarse fraction (UC) were noticeable from the SEM (Fig. 1).

Improved aggregate formation was noticeable in the gypsum and seawater-treated bauxite residues (Fig. 1), due to the addition of Ca^{2+}, which results in flocculation (Zhu et al., 2016). Changes in the surface morphology were also evident in the gypsum and seawater-treated residues in comparison to the untreated residues, which appeared to have a much smoother surface (Fig. 1). This change in surface morphology following the treatments was attributed to the changes in mineral phase (Huang et al., 2008).

3.2. Phosphorus adsorption study

3.2.1. Effect of seawater and gypsum treatment on P adsorption

All nine bauxite residue samples in this study were successful in removing P from aqueous solution (Table 5). Bauxite residue has been shown in numerous P adsorption studies to have a high P retention capacity, particularly following treatment or modification (Ye et al., 2014; Grace et al., 2015). In this study, gypsum or seawater treatment had a positive impact on P removal, with the gypsum-treated bauxite residue performing best (Table 5).

Following seawater treatment, the P adsorption capacity of the bauxite residues increased to q_{max} values of 0.48, 0.66 and 1.92 mg P g^{-1} media for UFS, UCS and UFRS, respectively. In previous studies, following treatment with seawater, bauxite residue had a higher adsorption capacity for P. Akhurst et al. (2006) reported a maximum adsorption of 6.5 mg P g^{-1} when using a bauxite residue treated with brine (Bauxsol™). This relatively high adsorption may be attributed to the higher concentrations of Ca^{2+} and Mg^{2+} in the brines (or products such as Bauxsol™, developed by Basecon™), in comparison to raw seawater (0.41, 1.29 and 10.77 g kg^{-1} of Ca^{2+}, Na and Mg^{2+}, respectively) used in this study (Gräfe et al., 2009). The gypsum-treated bauxite residues had the highest q_{max} values — 2.46, 1.39 and 2.73 mg P g^{-1} media for UFG, UCG and UFRG, respectively. However, these values were lower than a P adsorption study carried out by Lopez et al. (1998), who used the same application rate of gypsum to the bauxite residue samples and reported a q_{max} of 7.03 mg P g^{-1}. The lower rate observed in the current study may be attributed to the 72 h leaching process that the gypsum-treated bauxite residue underwent before use in the adsorption study, which may have allowed

UF
UC
UFR

Untreated　　　　Gypsum Treated　　　　Seawater Treated
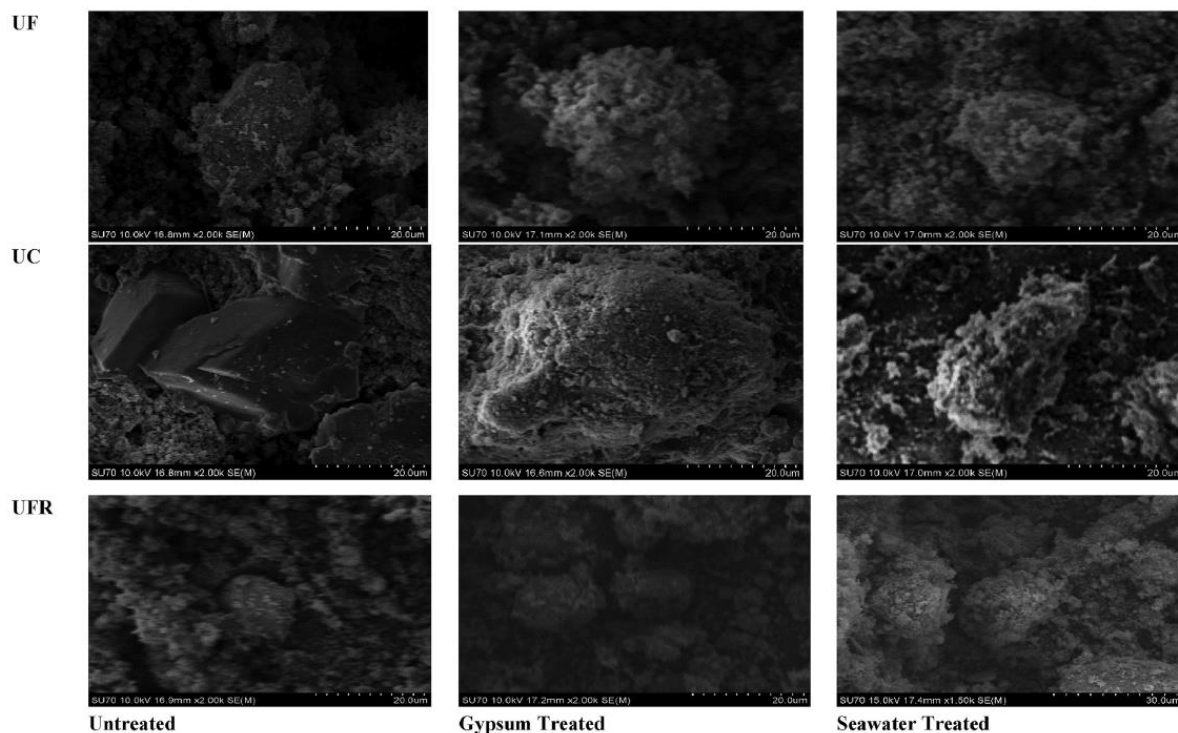
Fig. 1. SEM (10 kV; magnification ×2,000; working distance 16.8 mm) imaging for the three untreated bauxite residue pre and post treatment with either gypsum or seawater.

Table 5
Maximum adsorbency (mg P g^{-1} media) of P using each of the bauxite residue samples, untreated and treated (level of fit of the data, R^2, to Langmuir isotherm is included in brackets).

Media	Treatment method employed		
	Untreated	Gypsum	Seawater
	mg P g^{-1} media		
UFR	1 (0.99)	2.73 (0.99)	1.92 (0.99)
UF	0.38 (0.99)	2.46 (0.97)	0.48 (0.99)
UC	0.35 (0.98)	1.39 (0.99)	0.66 (0.99)

for further exchange and removal of Ca^{2+} following the leaching process.

Overall, the bauxite residue in the current study had a higher P adsorbency than in other studies for zeolite (0.01 mg P g^{-1}, Grace et al., 2015) and granular ceramics (0.9 mg g^{-1}; Chen et al., 2012), but lower than fly ash, granular blast furnace slag and pyritic fill (6.48, 3.61 and 0.88 mg P g^{-1}, respectively; Grace et al., 2015), crushed concrete (19.6 mg P g^{-1}; Egemose et al., 2012), untreated biochar (32 mg P g^{-1}; Wang et al., 2015), and NaOH-modified co-conut shell powder (200 mg P g^{-1}; de Lima et al., 2012).

3.2.2. Factors affecting P adsorption

The adsorption of P onto media is influenced by many factors which include particle size, pH, component and surface character-istics (Wang et al., 2016). Numerous studies have investigated the effect of parameters such as kinetics of P adsorption (Akhurst et al., 2006; Liu et al., 2007; Ye et al., 2014; Grace et al., 2015), ionic so-lution (Akhurst et al., 2006), pH (Liu et al., 2007; Huang et al., 2008;

Grace et al., 2015) on the adsorption of P from aqueous solution. While all bauxite residue samples in this study did remove P from aqueous solution, it is clear that the application of treatments, such as gypsum or seawater, has an effect on the adsorption capability, and that the rate of adsorption will vary as a result of the source of bauxite residue and treatments used (Wang et al., 2008).

The parameters which showed a statistically significant positive correlation of medium strength with P adsorption in this study were Ca (correlation coefficient = 0.47, p = .01, Degrees of Freedom (DoF) = 25) and CaO (correlation coefficient = 0.39, p = .04, DoF = 25). A statistically significant negative correlation of medium strength was also detected between pH and P adsorption (corre-lation coefficient = - 0.38, p = .05, DoF = 25). pH was a contributing factor to the adsorption process with the amount of phosphate adsorbed increasing with a decrease in pH in the media following treatments, UFRG > UFRS > UFR, UFG > UFS > UF, UCG > UCS > UC. This was a similar finding to several studies carried out (Li et al., 2006; Liu et al., 2007; Huang et al., 2008; Grace et al., 2015). The Ca ions also influenced P adsorption. This is as a result of the high level of Ca^{2+} and Mg^{2+} present in the bauxite residue, particularly after seawater and gypsum treatments, when the majority of PO$_4^{3-}$ is removed from solution due to the formation of magnesium phosphate (Mg$_3$(PO$_4$)$_2$) and calcium phosphate (Ca$_3$(PO$_4$)$_2$) (Akhurst et al., 2006).

The pH at which net charges are neutral on the surface of the adsorbent - the point of zero charge (PZC) - influences the rate of adsorption of P (Jacukowicz-Sobala et al., 2015). Where the pH is higher than the PZCpH, the surface of the adsorbent media be-comes more negative (attracting more cations), as a result of the adsorption of OH$^-$ from the surrounding solution (Prajapati et al.,

2016). The PZCpH ranged from 6.16 ± 0.21 to 6.96 ± 1.21 (Table 4) in the three untreated samples. Following treatment with gypsum and seawater, there were notable changes, but no statistical relevance was detected between the PZCpH and P adsorption in this study. However, as bauxite residue is composed of numerous minerals, each with their own individual PZCpH (which, as noted in the literature, can range from anywhere between pH 2 to pH 9.8 (Gräfe et al., 2009)), this results in the bauxite residue being able to cater for a wide range of pH (Gräfe et al., 2009) and also having the capability of removing both cations and anions from solution.

The SSA analysis carried out on the bauxite residues show an increase in specific surface area in all samples following treatment with either the gypsum or the seawater (Table 4). There was also an increase in pore volume following the addition of either gypsum or seawater (Table 4). This is attributed to the formation of precipitates formed in the neutralisation process of both gypsum and seawater and the effect of the Ca acting as a flocculant with the finer particles present. This increase in surface area also contributes to the increase in P adsorption following treatments. Although particle size affects adsorption onto media, due to the availability of sites for P uptake, no significant correlation was observed in the current study.

3.3. Implications of the findings of this study

The use of gypsum and seawater treatments on bauxite residue improved the overall P adsorption capacity of the bauxite residue samples, but mixing the bauxite residue and treatments with actual wastewater will be necessary to fully understand the total adsorption behaviour of the bauxite residue. In addition to improving the P adsorption, alkalinity was significantly reduced following both treatments; however, the EC was increased. This may limit the growth of plants on the gypsum or seawater-treated bauxite residues; therefore, one option may be to increase the rinsing period of the bauxite residue following treatment to remove the excess Ca^{2+} and Na^+ ions in solution. Lowering the alkalinity, increasing the P, Ca^{2+} and Mg^{2+} content and improving the physical structure, provide the possible re-use option of using the treated bauxite residue as a growth media.

For a refinery, the cost of neutralisation techniques is an obvious consideration when deciding which technique(s) to use. The use of seawater as a neutralisation technique would be a cheap and feasible option for a refinery that is close to the sea. The establishment of a pipeline (if not already in place) would be the dominant capital cost. The use of a Nano filtration system to concentrate the Ca^{2+}, Mg^{2+} and Na^+ ions in the seawater (Couperthwaite et al., 2014) could allow for the reduction in volume of seawater necessary for the neutralisation process, but may add to the cost. Gypsum however may be a more expensive option, requiring machinery such as amphirolls for the mixing and spreading of the gypsum. However, depending on the refinery's location, waste gypsum from construction sites or fossil fuel powered power stations may be used (Jones and Haynes, 2011).

4. Conclusions

This study examined the impact of gypsum and seawater treatments on the mineral, elemental and physiochemical properties of bauxite residue. The untreated bauxite residues were high in Fe and Al oxides and their mineralogical composition was dominated by Fe_2O_3, Al_2O_3, SiO_2 and CaO. Following treatment with gypsum and seawater, the pH decreased and EC increased, but no change was observed in the particle size or density. The SSA and pore volume of the bauxite increased following both treatments,

which contributed to increased P adsorbency. Although the P adsorbency measured in this study was not as high as measured in other studies using different media, it still indicates that reuse in water or wastewater treatment facilities may be an appropriate option for bauxite residue.

Acknowledgements

Appendix A. Supplementary data

Supplementary data related to this article can be found at https://doi.org/10.1016/j.jclepro.2018.01.092.

References

Akhurst, D.J., Jones, G.B., Clark, M., McConchie, D., 2006. Phosphate removal from aqueous solutions using neutralised bauxite refinery residues (Bauxsol™). Environ. Chem. 3, 65—74.

Blake, G.R., 1965. Bulk density. In: Black, C.A. (Ed.), Methods of Soil Analysis. Part 1. Physical and Mineralogical Properties, Including Statistics of Measurement and Sampling. ASA, SSSA, Madison, WI, pp. 374—390.

Blake, G.R., Hartge, K.H., 1986. Particle density. In: Klute, A. (Ed.), Methods of Soil Analysis: Part 1—Physical and Mineralogical Methods. SSSA, ASA, Madison, WI, pp. 377—382.

12457—2 British Standard Institution, 2002. Characterisation of Waste. Leaching. Compliance Test for Leaching of Granular Waste Materials and Sludges. One Stage Batch Test at a Liquid to Solid Ratio of 10 L/kg for Materials with Particle Size below 4 mm (without or with Size Reduction).

Chen, N., Feng, C., Zhang, Z., Liu, R., Gao, Y., Li, M., Sugiura, N., 2012. Preparation and characterization of lanthanum (III) loaded granular ceramic for phosphorus adsorption from aqueous solution. J. Taiwan Inst. Chem. Eng. 43, 783—789.

Cooling, D.J., 2007. Improving the sustainability of residue management practices-Alcoa World Alumina Australia. In: Fouri, A., Jewell, R.J. (Eds.), Paste and Thickened Tailings: a Guide, vol. 316. http://citeseerx.ist.psu.edu/viewdoc/download?doi=10.1.1.629.1067&rep=rep1&type=pdf (accessed 31.10.17).

Couperthwaite, S.J., Johnstone, D.W., Mullett, M.E., Taylor, K.J., Millar, G.J., 2014. Minimization of bauxite residue neutralization products using nanofiltered seawater. Ind. Eng. Chem. Res. 53, 3787—3794.

Courtney, R.G., Timpson, J.P., 2005. Reclamation of fine fraction bauxite processing residue (red mud) amended with coarse fraction residue and gypsum. Water Air Soil Pollut. 164 (1—4), 91—102.

Courtney, R.G., Jordan, S.N., Harrington, T., 2009. Physico-chemical changes in bauxite residue following application of spent mushroom compost and gypsum. Land Degrad. Dev. 20, 572—581.

Courtney, R., Harrington, T., 2010. Assessment of plant-available phosphorus in a fine textured sodic substrate. Ecol. Eng. 36, 542—547.

Courtney, R., Kirwan, L., 2012. Gypsum amendment of alkaline bauxite residue—plant available aluminium and implications for grassland restoration. Ecol. Eng. 42, 279—282.

Danielson, R.E., Sutherland, P.L., 1986. Porosity. In: Klute, A. (Ed.), Methods of Soil Analysis. Part 1. Physical and Mineralogical Methods. SSSA, ASA, Madison, WI, pp. 443—461.

de Lima, A.C.A., Nascimento, R.F., de Sousa, F.F., Josue Filho, M., Oliveira, A.C., 2012. Modified coconut shell fibers: a green and economical sorbent for the removal of anions from aqueous solutions. Chem. Eng. J. 185, 274—284.

Dilmore, R.M., Howard, B.H., Soong, Y., Griffith, C., Hedges, S.W., DeGalbo, A.D., Morreale, B., Baltrus, J.P., Allen, D.E., Fu, J.K., 2009. Sequestration of CO2 in mixtures of caustic byproduct and saline waste water. Environ. Eng. Sci. 26, 1325—1333.

Eastham, J., Morald, T., Aylmore, P., 2006. Effective nutrient sources for plant growth on bauxite residue. Water Air Soil Pollut. 176 (1—4), 5—19.

Egemose, S., Sønderup, M.J., Beinthin, M.V., Reitzel, K., Hoffmann, C.C., Flindt, M.R., 2012. Crushed concrete as a phosphate binding material: a potential new management tool. J. Environ. Qual. 41, 647—653.

EPA, 1996. EPA Method 3050B: Acid Digestion of Sediments, Sludges, and Soils. www.epa.gov/sites/production/files/2015-06/documents/epa-3050b.pdf (accessed 30.10.2, 17).

EPA, 2014. Drinking Water Parameters Microbiological, Chemical and Indicator Parameters in the 2014 Drinking Water Regulations. www.epa.ie/pubs/advice/drinkingwater/2015_04_21_ParametersStandaloneDoc.pdf (accessed 30.10.2017).

European Commission, 2015. COM 2015. 614 Communication from the Commission to the European Parliament, the Council, the European Economic and Social Committee and the Committee of the Regions - Closing the Loop - an EU Action Plan for the Circular Economy. Brussels.

Evans, K., 2016. The history, challenges, and new developments in the management and use of bauxite residue. J. Sustain. Metall. 2, 316–331.

Fergusson, L., 2009. Commercialisation of Environmental Technologies Derived from Alumina Refinery Residues: a Ten-year Case History of Virotec. http://citeseerx.ist.psu.edu/viewdoc/download?doi=10.1.1.458.2073&rep=rep1&type=pdf (accessed 8.12.17).

Fois, E., Lallai, A., Mura, G., 2007. Sulfur dioxide absorption in a bubbling reactor with suspensions of Bayer red mud. Ind. Eng. Chem. Res. 46, 6770–6776.

Grace, M.A., Healy, M.G., Clifford, E., 2015. Use of industrial by-products and natural media to adsorb nutrients, metals and organic carbon from drinking water. Sci. Total Environ. 518, 491–497.

Grace, M.A., Clifford, E., Healy, M.G., 2016. The potential for the use of waste products from a variety of sectors in water treatment processes. J. Clean. Prod. 137, 788–802.

Goloran, J.B., Chen, C.R., Phillips, I.R., Xu, Z.H., Condron, L.M., 2013. Selecting a nitrogen availability index for understanding plant nutrient dynamics in rehabilitated bauxite-processing residue sand. Ecol. Eng. 58, 228–237.

Gräfe, M., Power, G., Klauber, C., 2009. Review of Bauxite Residue Alkalinity and Associated Chemistry. CSIRO, Australia. http://enfo.agt.bme.hu/drupal/sites/default/files/vörösiszpa%20kémia%20és%20lúgosság.pdf (accessed 12.12.17).

Hanahan, C., McConchie, D., Pohl, H., Creelman, R., Clark, M., Stocksiek, C., 2004. Chemistry of seawater neutralization of bauxite refinery residues (red mud). Environ. Eng. Sci. 21, 125–138.

Huang, W., Wang, S., Zhu, Z., Li, L., Yao, X., Rudolph, V., Haghseresht, F., 2008. Phosphate removal from wastewater using red mud. J. Hazard. Mater. 158, 35–42.

IAI, 2015. Bauxite residue Management: Best Practice. http://www.world-aluminium.org/media/filer_public/2015/10/15/bauxite_residue_management_-_best_practice_english_oct15edit.pdf (accessed 14.10.2017).

Jacukowicz-Sobala, I., Ociński, D., Kociołek-Balawejder, E., 2015. Iron and aluminium oxides containing industrial wastes as adsorbents of heavy metals: application possibilities and limitations. Waste Manag. Res. 33, 612–629.

Johnston, M., Clark, M.W., McMahon, P., Ward, N., 2010. Alkalinity conversion of bauxite refinery residues by neutralization. J. Hazard. Mater. 182, 710–715.

Jones, B.E., Haynes, R.J., 2011. Bauxite processing residue: a critical review of its formation, properties, storage, and revegetation. Crit. Rev. Environ. Sci. Technol. 41, 271–315.

Jones, B.E., Haynes, R.J., Phillips, I.R., 2012. Addition of an organic amendment and/or residue mud to bauxite residue sand in order to improve its properties as a growth medium. J. Environ. Manag. 95, 29–38.

Kirwan, L.J., Hartshorn, A., McMonagle, J.B., Fleming, L., Funnell, D., 2013. Chemistry of bauxite residue neutralisation and aspects to implementation. Int. J. Miner. Process. 119, 40–50.

Klauber, C., Gräfe, M., Power, G., 2011. Bauxite residue issues: II. options for residue utilization. Hydrometallurgy 108, 11–32.

Lehoux, A.P., Lockwood, C.L., Mayes, W.M., Stewart, D.I., Mortimer, R.J., Gruiz, K., Burke, I.T., 2013. Gypsum addition to soils contaminated by red mud: implications for aluminium, arsenic, molybdenum and vanadium solubility. Environ. Geochem. Health 35, 643–656.

Li, L.Y., 2001. A study of iron mineral transformation to reduce red mud tailings. Waste Manag. 21, 525–534.

Li, Y., Liu, C., Luan, Z., Peng, X., Zhu, C., Chen, Z., Zhang, Z., Fan, J., Jia, Z., 2006. Phosphate removal from aqueous solutions using raw and activated red mud and fly ash. J. Hazard. Mater. 137, 374–383.

Liu, Y., Lin, C., Wu, Y., 2007. Characterization of red mud derived from a combined Bayer Process and bauxite calcination method. J. Hazard. Mater. 146, 255–261.

Liu, W., Chen, X., Li, W., Yu, Y., Yan, K., 2014. Environmental assessment, management and utilization of red mud in China. J. Clean. Prod. 84, 606–610.

Lopez, E., Soto, B., Arias, M., Nunez, A., Rubinos, D., Barral, M.T., 1998. Adsorbent properties of red mud and its use for wastewater treatment. Water Res. 32, 1314–1322.

Mayes, W.M., Burke, I.T., Gomes, H.I., Anton, A.D., Molnár, M., Feigl, V., Ujaczki, É., 2016. Advances in understanding environmental risks of red mud after the Ajka spill, Hungary. J. Sustain. Metall. 2, 332–343.

Menzies, N.W., Fulton, I.M., Morrell, W.J., 2004. Seawater neutralization of alkaline bauxite residue and implications for revegetation. J. Environ. Qual. 33, 1877–1884.

McBride, M.B., 2000. Chemisorption and Precipitation Reactions. Handbook of Soil Science. CRC Press, Boca Raton, FL, pp. B265–B302.

McConchie, D., Clark, M., Davies-McConchie, F., 2001. Processes and Compositions for Water Treatment. Neauveau Technology Investments, Australian, p. 28.

Newson, T., Dyer, T., Adam, C., Sharp, S., 2006. Effect of structure on the geotechnical properties of bauxite residue. J. Geotech. Geoenviron. 132, 143–151.

Palmer, S.J., Frost, R.L., 2009. Characterisation of bauxite and seawater neutralised bauxite residue using XRD and vibrational spectroscopic techniques. J. Mater. Sci. 44, 55–63.

Power, G., Gräfe, M., Klauber, C., 2011. Bauxite residue issues: I. Current management, disposal and storage practices. Hydrometallurgy 108, 33–45.

Pradhan, J., Das, S.N., Das, J., Rao, S.B., Thakur, R.S., 1996. Characterization of Indian red muds and recovery of their metal values. In: Annual Meeting and Exhibition of the Minerals, Metals and Materials Society, Anaheim, CA, 4 – 8 February 1996.

Prajapati, S.S., Najar, P.A., Tangde, V.M., 2016. Removal of phosphate using red mud: an environmentally hazardous waste by-product of alumina industry. Adv. Phys. Chem. 2016.

Snars, K., Gilkes, R.J., 2009. Evaluation of bauxite residues (red muds) of different origins for environmental applications. Appl. Clay Sci. 46, 13–20.

Thomas, G.W., 1982. Exchangeable Cations. Methods of Soil Analysis. Part 2. Chemical and Microbiological Properties, (Methodsofsoilan2), pp. 159–165.

Vakros, J., Kordulis, C., Lycourghiotis, A., 2002. Potentiometric mass titrations: a quick scan for determining the point of zero charge. Chem. Commun. 17, 1980–1981.

Vohla, C., Alas, R., Nurk, K., Baatz, S., Mander, Ü., 2007. Dynamics of phosphorus, nitrogen and carbon removal in a horizontal subsurface flow constructed wetland. Sci. Total Environ. 380, 66–74.

Wang, S., Ang, H.M., Tadé, M.O., 2008. Novel applications of red mud as coagulant, adsorbent and catalyst for environmentally benign processes. Chemosphere 72, 1621–1635.

Wang, B., Lehmann, J., Hanley, K., Hestrin, R., Enders, A., 2015. Adsorption and desorption of ammonium by maple wood biochar as a function of oxidation and pH. Chemosphere 138, 120–126.

Wang, Z., Shen, D., Shen, F., Li, T., 2016. Phosphate adsorption on lanthanum loaded biochar. Chemosphere 150, 1–7.

Xue, S., Zhu, F., Kong, X., Wu, C., Huang, L., Huang, N., Hartley, W., 2016. A review of the characterization and revegetation of bauxite residues (Red mud). Environ. Sci. Pollut. Res. 23, 1120–1132.

Ye, J., Zhang, P., Hoffmann, E., Zeng, G., Tang, Y., Dresely, J., Liu, Y., 2014. Comparison of response surface methodology and artificial neural network in optimization and prediction of acid activation of Bauxsol for phosphorus adsorption. Water Air Soil Pollut. 225 (12), 2225.

Zhu, F., Li, Y., Xue, S., Hartley, W., Wu, H., 2016. Effects of iron-aluminium oxides and organic carbon on aggregate stability of bauxite residues. Environ. Sci. Pollut. Res. 23, 9073–9081.

A3: Journal of Environmental Management

The Use of Rapid, Small-scale Column Tests to Determine the Efficiency of Bauxite Residue as a Low-cost Adsorbent in the Removal of Dissolved Reactive Phosphorus from Agricultural Waters.

Patricia B. Cusack, Oisín Callery, Ronan Courtney, Éva Ujaczki, Lisa M. T. O' Donoghue, Mark G. Healy.

Article associated with Chapter 5.

Research article

The use of rapid, small-scale column tests to determine the efficiency of bauxite residue as a low-cost adsorbent in the removal of dissolved reactive phosphorus from agricultural waters

Patricia B. Cusack[a,b,c], Oisín Callery[d], Ronan Courtney[a,c], Éva Ujaczki[c,e,f], Lisa M.T. O'Donoghue[f], Mark G. Healy[b,*]

[a] Department of Biological Sciences, University of Limerick, Castletroy, Co. Limerick, Ireland
[b] Civil Engineering, National University of Ireland, Galway, Ireland
[c] The Bernal Institute, University of Limerick, Castletroy, Co. Limerick, Ireland
[d] Earth and Ocean Sciences, National University of Ireland, Galway, Ireland
[e] Department of Applied Biotechnology and Food Science, Faculty of Chemical Technology and Biotechnology, Budapest University of Technology and Economics, Műegyetem rkp. 3, 1111, Budapest, Hungary
[f] School of Engineering, University of Limerick, Castletroy, Co. Limerick, Ireland

ARTICLE INFO

ABSTRACT

Bauxite residue, the by-product produced in the alumina industry, is a potential low-cost adsorbent in the removal of phosphorus (P) from aqueous solution, due to its high composition of residual iron oxides such as hematite. Several studies have investigated the performance of bauxite residue in removing P; however, the majority have involved the use of laboratory "batch" tests, which may not accurately estimate its actual performance in filter systems. This study investigated the use of rapid, small-scale column tests to predict the dissolved reactive phosphorus (DRP) removal capacity of bauxite residue when treating two agricultural waters of low (forest run-off) and high (dairy soiled water) phosphorus content. Bauxite residue was successful in the removal of DRP from both waters, but was more efficient in treating the forest run-off. The estimated service time of the column media, based on the largest column studied, was 1.08 min g^{-1} media for the forest run-off and 0.28 min g^{-1} media for the dairy soiled water, before initial breakthrough time, which was taken to be when the column effluent reached approximately 5% of the influent concentration, occurred. Metal(loid) leaching from the bauxite residue, examined using ICP-OES, indicated that aluminium and iron were the dominant metals present in the treated effluent, both of which were above the EPA parametric values (0.2 mg L^{-1} for both Al and Fe) for drinking water.

1. Introduction

Phosphorus (P) is an essential component of all plant and animal life (Weissert and Kehr, 2018), and is critical in the production and maintenance of food supply (Cordell and White, 2011; Pretty and Bharucha, 2014). Phosphorus is also identified as one of the key nutrients that leads to the eutrophication of water bodies, in which there is an excess production of algal blooms, resulting in detrimental effects to aquatic life (Pan et al., 2018). Agricultural practices, such as the application of slurry and fertiliser, may result in the transport of nutrients in surface runoff (Murnane et al., 2016; Pan et al., 2018) and subsurface flow (O' Flynn et al., 2018; Zhou et al., 2016) to a water body, and have been identified as a major cause of eutrophication (Sharpley, 2016).

The movement of P from soil to water bodies is predominantly in the form of particulate or dissolved reactive P (DRP) (Brennan et al., 2014), the latter being 100% available for aquatic biota and which, therefore, has an immediate effect on the surrounding ecosystems (Penn et al., 2014). Conventional methods of P removal from water have involved the use of enhanced biological removal systems such as polyphosphate accumulating organisms (PAOs) (Ge et al., 2015) and algal biofilms (Sukačová et al., 2015), precipitation methods using hydrous ferric oxides (Hauduc et al., 2015) or struvite (Zhou et al., 2015), the use of adsorbents (Grace et al., 2015; Callery et al., 2016; Callery and Healy, 2017), ion exchange (Acelas et al., 2015), and reverse osmosis

Nomenclature

A	constant of proportionality (mg g^{-1})
a**	a time constant
Al	aluminium
Al$_2$O$_3$	aluminium oxide
As	arsenic
B	constant of system heterogeneity in Eqns. (1) and (2)
BRDA	bauxite residue disposal area
Ca	calcium
Cd	cadmium
C$_t$	solution adsorbate concentration at any filter depth (mg L^{-1})
C$_o$	influent contaminant concentration (mg L^{-1})
Cr	chromium
CRM	critical raw material
Cu	copper
DRP	dissolved reactive phosphorus (mg L^{-1})
DSW	dairy soiled water
EDS	energy-dispersive X-ray spectroscopy
Fe	iron
Fe$_2$O$_3$	iron oxide
Fl	fluoride
FT-IR	Fourier transform infrared
Ga	gallium
Hg	mercury
HNO$_3$	nitric acid
ICP-OES	inductively coupled plasma optical emission spectrometer
M	mass of filter media contained in the filter column (g)
Mg	magnesium
Mn	manganese
Mo	molybdenum
n	the number of containers in which the total volume of effluent is collected
N	nitrogen
Na	sodium
Ni	nickel
P	phosphorus
Pb	lead
pH	pH unit
q$_e$	cumulative mass of contaminant adsorbed per g of filter media (mg g^{-1})
q$_t$	time dependent sorbate concentration per unit mass of adsorbent (mg g^{-1}), RSSCT rapid small-scale column test
Se	selenium
SEM	scanning electron microscopy
t	Empty bed contact time of the column filter bed (min)
V	volume of the influent loaded onto the filter (L)
V	vanadium
V$_B$	number of empty bed volumes of influent/solution filtered
XRD	x-ray diffraction
XRF	x-ray fluorescence
Zn	zinc

(Wang et al., 2016). In recent years, to address the concept of a 'circular economy' (United Nations, 2015), emphasis has been placed on the utilisation of industrial wastes as low-cost adsorbents (De Gisi et al., 2016; Grace et al., 2016). Materials that have been utilised include fly ash (Nowak et al., 2013), steel slags (Claveau-Mallet et al., 2013) and chemical amendments (Callery et al., 2015). Particular focus has been placed on bauxite residue (red mud), the by-product generated in the Bayer Process during the extraction of alumina, as a potential low-cost P adsorbent in aqueous solutions. It is currently being produced at a global rate of 150 Mt per annum (Evans, 2016), but only approximately 2% of the bauxite residue produced is currently re-used (Ujaczki et al., 2018), with the remaining ~ 98% being disposed of into bauxite residue disposal areas (BRDAs) (Burke et al., 2013; Kong et al., 2017). The general composition of bauxite residue comprises high amounts of iron (Fe) and aluminium (Al) oxides (Zhu et al., 2016), which are good adsorbents of P. In addition, bauxite residue has a high specific surface area (Gräfe et al., 2011) and therefore has numerous potential adsorption sites, giving it increased capacity for P retention. Previous laboratory studies have shown that bauxite residue has high P adsorption capacity (Table 1).

Traditionally, bench-scale "batch" studies are conducted to evaluate the effectiveness of a material to adsorb P (Table 1). These studies involve placing the material in small containers, overlaying it with solutions of known concentrations, mixing for a period usually of between 24 and 48 h, and then fitting the results obtained to an adsorption isotherm such as the Freundlich or Langmuir, in order to quantify its adsorption potential (Cusack et al., 2018; Grace et al., 2015). However, batch studies have some disadvantages, such as failing to replicate the often passive nature of the adsorption process which exists on site, as well as sometimes using unrealistic ratios of adsorbent to solution, and shaking of the samples (ÁdÁm et al., 2007; Søvik and Kløve, 2005). In addition, concerns have been raised about their accuracy in replicating the actual performance when the adsorbent material is placed in a filter and operated on site (Fenton et al., 2009). Due to the nature of the batch experiment, they also fail to realistically replicate any incidental releases of contaminants, which may occur when some materials are

placed in filters. This may be particularly pertinent in the evaluation of the feasibility of bauxite residue, which contains metals (Cusack et al., 2018). In order to determine the full potential and longevity of an adsorbent, larger scale "column" studies are necessary (Pratt et al., 2012). In these studies, the material is placed in a column, usually operated at laboratory-scale, and water of a known concentration is passed through the material until the effluent concentration is the same as the influent concentration. These continuous flow column studies require vast amounts of influent water, which depending on the type of water utilised, is often difficult to source in the laboratory (Callery and Healy, 2017). On account of this, rapid, small-scale column studies which utilise smaller volumes of media and wastewater have been gaining in popularity, and have been used to successfully model the adsorbancies of P (Callery et al., 2016; Lalley et al., 2015), fluoride (Wu et al., 2018), paracetamol (García-Mateos et al., 2015), and varying species of arsenic (Tresintsi et al., 2014).

As P adsorption tests on bauxite residues have been commonly conducted using batch-scale studies, which may have many short-comings as detailed above, the objectives of this study were to use rapid, small-scale column studies to (1) to assess the potential of bauxite residue as a low-cost adsorbent for DRP removal from two types of agricultural waters (dairy soiled water (DSW) and forest run-off) (2) compare the composition of the bauxite residue before and after use in the column tests (3) investigate the speciation of P adsorption onto the bauxite residue, and (4) identify any potential trace metal mobilisation from the bauxite residue during the study.

2. Materials and methods

2.1. Sample collection

Bauxite residue was obtained from a European refinery. Residue was sampled to a depth of 30 cm below the surface of the BRDA, returned to the laboratory and dried at 105 °C for 24 h. Once dry, the samples were pulverised using a mortar and pestle and sieved to a particle size < 0.5 mm. The pH and electrical conductivity (EC) were

Table 1
Phosphorus (P) adsorption studies that have been carried out using bauxite residue, untreated and treated residues, and their recovery efficiencies (adapted from Cusack et al., 2018).

	P recovery technique	Factors investigated	Type of water	Initial P concentration of the water	P recovered	Reference
Untreated bauxite residue	Batch adsorption experiment	Kinetics, pH and temperature	Synthetic water	5–100 mg P L⁻¹	0.20 mg P g⁻¹	Grace et al. (2015)
Untreated bauxite residue	Column study	Initial concentration, particle size	Synthetic water	60–1000 mg P L⁻¹	25 mg P g⁻¹ᵃ	Herron et al., 2016
Untreated bauxite residue	Batch adsorption experiment	Initial concentration, pH, particle size	Synthetic water	10–150 mg P L⁻¹	0.345–1 mg P g⁻¹	Cusack et al. (2018)
Gypsum Treated	Batch adsorption experiment	Contact time	Synthetic water	20–400 mg P L⁻¹	7.03 mg P g⁻¹	Lopez et al. (1998)
Gypsum Treated	Batch adsorption experiment	Initial concentration, pH, particle size	Synthetic water	10–150 mg P L⁻¹	1.39–2.73 mg P g⁻¹	Cusack et al. (2018)
Seawater Treated	Batch adsorption experiment	Initial concentration, pH, particle size	Synthetic water	10–150 mg P L⁻¹	0.48–1.92 mg P g⁻¹	Cusack et al. (2018)
Brine treated bauxite residue (Bauxsol™ᵇ)	Batch adsorption experiment	pH, ionic strength, time	Synthetic water	0.5–2 mg P L⁻¹	6.5–14.9 mg P g⁻¹	Akhurst et al. (2006)
Brine treated bauxite residue (Bauxsol™ᵇ)	Column study	Kinetics, particle size	Secondary treated effluent	3–9.2 mg P L⁻¹	2.85–8.74 mg P g⁻¹	Despland et al. (2011)
Acid and brine treated bauxite residue (Bauxsol™ᵃᵇ)	Batch adsorption experiment	Kinetics and isotherms	Synthetic water	200 mg P L⁻¹	55.72 mg P g⁻¹	Ye et al. (2014)
Heat treated bauxite residue	Batch adsorption experiment	Time, pH and initial concentration	Synthetic water	155 mg P L⁻¹	155.2 mg P g⁻¹	Liu et al. (2007)
Acid and heat treated bauxite residue	Batch adsorption experiment	Time, pH and initial concentration	Synthetic water	155 mg P L⁻¹	202.9 mg P g⁻¹	Liu et al. (2007)
Acid treated bauxite residue	Batch adsorption experiment	Acid type, pH	Synthetic water	1 mg P L⁻¹	1.1 mg P g⁻¹	Huang et al. (2008)

[a] P_{max} value given i.e. Maximum amount of P adsorbed per g of media, as determined using the Langmuir adsorption isotherm.
[b] Bauxsol™ = neutralised bauxite residue produced using the Basecon™ procedure, which uses brines high in Ca^{2+} and Mg^{2+} (McConchie et al., 2001).

measured (n = 3) using 5 g of sample in an aqueous extract, using a 1:5 ratio (solid:liquid) (Courtney and Harrington, 2010). Dairy soiled water (milk parlour washings composed of cow faeces and urine, milk and detergents; Minogue et al., 2015) was collected from Teagasc Agricultural Research Centre, Moorepark, Co. Cork, Ireland [52° 9′ 48.114″ N, 8° 15′ 34.6464″ W] and forest run-off was collected from Kilmoon, Co. Clare, Ireland [53° 2′ 48.0372″ N, 9° 16′ 21.1368″ W]. The DSW and forest run-off were transferred directly to a temperature-controlled room (11 °C) prior to commencement of testing. The DRP was measured using filtered (0.45 μm) subsamples using a nutrient analyser (Konelab20, Thermo Clinical Lab systems, Finland) and the pH was measured using a Eutech Instruments pH 700 (Thermo Scientific, USA).

2.1.1. Media characterisation

The bauxite residue was characterised before and after the experiment. Mineralogical detection was carried out on 1 g powdered samples using X-ray diffraction (XRD) on a Philips X'Pert PRO MPD* (California, USA) at 40 kV, 40 mA, 25 °C by Cu X-ray tube (Kα-radiation). The patterns were collected in the angular range from 5 to 80° (2ϴ) with a step-size of 0.008° (2ϴ) (Castaldi et al., 2011). The surface morphology and elemental detection were carried out using scanning electron microscopy (SEM) and energy-dispersive X-ray spectroscopy (EDS) on a Hitachi SU-70 (Berkshire, UK). X-ray fluorescence (XRF) analysis was carried out onsite at the refinery using a Panalytical Axios XRF.

2.2. Rapid small scale column study

Small bore adsorption columns were prepared after Callery et al. (2016) using polycarbonate tubes, with an internal diameter of 0.94 cm and lengths of 20, 30 and 40 cm. The tubes were packed with a mixture of bauxite residue. The bauxite residue was held in place within each column using acid-washed glass wool and plastic syringes with an internal diameter equal to outside diameter of the polycarbonate tube, placed at the top and bottom of each of the polycarbonate tube columns. To each end of the polycarbonate tube column, flexible silicone tubing was attached to the syringe ends in order to provide lines for the influent and effluent. The columns were secured on a metal frame, allowing for a stable, vertical orientation to be maintained. A Masterflex® L/S Variable-Speed Drive peristaltic pump (Gelsenkirchen, Germany) with a variable speed motor was used to pump the influent, DSW and forest run-off, into the base of each column at an estimated flow rate of 30.49 ± 0.85 mL h⁻¹ (equivalent to a hydraulic loading rate used in a P removal system for wastewater treatment on a poultry farm; Penn et al., 2014). The pump was operated in 12 h on/off cycles (to allow the filter media to replenish some of its adsorption sites) to achieve loading periods of 24–36 h, in order to obtain enough data points for the determination of the adsorption model coefficients. Every 2 h, aliquots of the filtered effluent were collected using an auto-sampler and measured for volume, pH and DRP.

The adsorption performance of the media was evaluated using a model developed by Callery and Healy (2017), wherein the column effluent (C_e) is taken as a function of the volume of influent treated (V) and breakthrough concentrations (BTCs) formed by plotting V (x-axis) against C_e (y-axis). The breakthrough of the column media was taken to be when the column effluent was approximately 5% of the influent concentration (Chen et al., 2003). This model, which has been successful in the prediction of the performance of a large-scale filter (Callery et al., 2016), was used in the prediction of the longevity of the bauxite residue in the current study.

The overall bauxite residue service time or longevity of the bauxite residue media can be found by first determining the volume treated, using Eqn. (1), where q_t is the time dependent sorbate concentration per unit mass of adsorbent (mg g⁻¹), M is the mass of the adsorbent (g), B is a constant of system heterogeneity, C_o is the sorbate concentration of the influent (mg L⁻¹) and C_t is the solution adsorbate concentration at any filter depth (mg L⁻¹), by dividing the volume treated, V (in L) by

the loading rate (L s^{-1}) and then converting to minutes per g of media.

$$V = \frac{q_{t\,M}}{B\,(C_o - C_t)} \qquad (1)$$

The q$_t$ used in Eqn. (1) was calculated using Eqn. (2):

$$q_t = A V_B^{\left(\frac{1}{B}\right)} \Big|\, \frac{t}{t + a^{**}} \qquad (2)$$

where A is a constant of proportionality (mg L^{-1}), t is the empty bed contact time of the column filter bed (min), V$_B$ is the number of empty bed volumes of influent/solution filtered, and a** is a time constant.

2.3. Speciation of P adsorbed

Fourier transform infrared (FT-IR) analysis was carried out using a PerkinElmer Spectrum 100 (PerkinElmer, USA). The FT-IR spectra were recorded in the 4000 to 650 cm^{-1} range and were collected after 256 scans at 4 cm^{-1} resolution (Castaldi et al., 2010).

2.4. Trace metal analysis

Every 2 h, 10 mL of the aliquot collected from the columns, was preserved in nitric acid (HNO$_3$), to a pH < 2 and refrigerated before elemental analysis was carried out using an Agilent Technologies 5100 Inductively Coupled Plasma Optical Emission Spectrometer (ICP-OES). In order to carry out the ICP-OES analysis, a calibration curve was created using standardised solutions comprised of 100, 50, 10, 5 and 1 g L^{-1} multi element standard (Inorganic Ventures, Ireland) and 1M HNO$_3$. The analytical lines (in nm) used for the calculations of each element were as follows: Al 237.312, 396.152; calcium (Ca) 396.847, 422.673; cadmium (Cd) 214.439, 226.502, 228.802; chromium (Cr) 205.560, 267.716, 357.868; copper (Cu) 213.598, 324.754, 327.395; Fe 234.350, 238.204, 259.940; gallium (Ga) 287.423, 294.363, 417.204; mercury (Hg) 184.887, 194.164; magnesium (Mg) 279.553, 280.270, 285.213; manganese (Mn) 257.610, 259.372, 260.568; molybdenum (Mo) 202.032, 203.846, 204.598; sodium (Na) 589.592; nickel (Ni) 216.555, 221.648, 231.604; lead (Pb) 220.353, 283.305; selenium (Se) 196.026, 203.985; silicon (Si) 250.690, 251.611, 288.158; vanadium (V) 268.796, 292.401, 309.310; zinc (Zn) 202.548, 206.200, 213.857 (Bridger and Knowles, 2000). The XRF analysis performed on the bauxite residue was carried out using a Panalytical Axios XRF (Malvern Panalytical Ltd., United Kingdom).

3. Results and discussion

3.1. Media characterisation before and after the experiments

Bauxite residue typically comprises Fe, Al, Ti, Si, Na and Ca, mainly in the form of oxides (Gräfe et al., 2011). The presence of Fe and Al oxides, which can range from 5 to 60 and 5–30%, respectively (Evans, 2016), and Ti oxides, which are typically in the range of 0.3–15% (Evans, 2016), mean that bauxite residue is a potential adsorbent for both cations and anions from aqueous solutions (Bhatnagar et al., 2011; Cusack et al., 2018). This is why numerous studies have investigated the potential of P removal from aqueous solution (Table 1).

The main mineralogical composition of the bauxite residue used in this study comprised mainly iron and aluminium oxides (Fe$_2$O and Al$_2$O$_3$) (Table 2). SEM-EDS analysis also indicated the dominance of Fe and Al (Fig. S1 in the Supplementary Information). Titanium, Si, Ca and Na were also detected in the main composition. Prior to use in the column, there was a mineralogical dominance of the iron oxide hematite (as represented by H in Fig. 1), detected at positions 33.153 and 35.612°2Θ, respectively (Fig. 1). Rutile (TiO$_2$) was also detected at position 27.459 °2Θ. Following the column trials, XRD analysis was carried out on the spent media from both the DSW and forest run-off columns. New peaks were identified in the XRD patterns, as seen in

Fig. 1, which show the presence of P-based minerals, which were not present in the raw media. The new peaks detected in both the spent media following treatment of the DSW and forest run-off was calcium hydrogenphosphate (III) hydrate (CaHPO$_4$.3H$_2$O) at positions 19.120 and 30.001 °2Θ. The presence of this mineral in the spent media indicates P retention within the bauxite residue after treatment. The particle size analysis (PSA) of the bauxite residue used in this study is shown in Table 3.

3.2. Influent and effluent water characterisation and rapid small-scale column study

The forest run-off had a pH of 7.57 and a DRP concentration of 1.10 mg P L^{-1}. The total phosphorus (TP) concentration of forest run-off is usually around 1 mg L^{-1} (Finnegan et al., 2012), whereas DSW has a TP concentration of 20–100 mg L^{-1} and a total nitrogen (TN) concentration of 70–500 mg L^{-1} (Minogue et al., 2015). The DSW used in this study had a pH of 7.79 and a DRP concentration of 10.64 mg P L^{-1}.

The BTC approached saturation much quicker for the DSW than for the forest run-off water (Fig. 2). Similar to the findings of Vuković et al. (2011), the breakthrough time and exhaustion time increased with bed depth. As a result of its composition, there are other anions such as nitrates (NO$_3^-$) and nitrites (NO$_2^-$) present in the DSW (Ruane et al., 2011), and therefore there is greater competitiveness for available adsorption sites and interferences between the adsorbent surface and the ions present in the aqueous solution. This may explain why the DSW-treating columns generated a BTC approaching saturation much faster than the bauxite residue columns treating forest run-off. When treating the forest run-off, the bauxite residue had a service time of approximately 22.80 min, based on the largest column before the initial breakthrough time of the bauxite residue occurred. However, when treating the DSW, it had a shorter service time of 5.80 min, as noted for the largest column before the initial breakthrough occurred. Taking into account the amount of bauxite residue used in the largest columns (21.16 and 20.78 g), this gives an estimated service time of 1.08 min g^{-1} bauxite residue and 0.28 min g^{-1} bauxite residue when treating forest run-off and DSW, respectively, before initial breakthrough (5%) would occur.

The modelled q$_t$ values were 0.27 mg P g^{-1} media and 0.045 mg P g^{-1} media when treating the DSW and forest run-off, respectively. These were lower than q$_t$ values of between 2.85 and 8.74 mg P g^{-1} for neutralised bauxite residue (Bauxol) used to treat secondary-treated wastewater (Despland et al., 2011) and 25 mg P g^{-1} for untreated bauxite residue used to treat synthetic water (Herron et al., 2016) (Table 1). Compared to other studies that have used low-cost adsorbents such as zeolite (0.01 mg P g^{-1} - Grace et al., 2015) and granular ceramics (0.9 mg g^{-1} - Chen et al., 2012), the bauxite residue in the current study had a higher P adsorbency, but it was lower than crushed concrete (19.6 mg P g^{-1} - Egemose et al., 2012) and untreated biochar (32 mg P g^{-1} - Wang et al., 2015). It is important to note that full saturation of the bauxite residue was not reached in the current study and the wastewaters treated may have had an impact on the P adsorption capacity, as there may have been interferences and competition for adsorption sites due to the presence of other ions and

Table 2
Main mineralogical composition (%) of the bauxite residue determined by XRF.

Mineral oxide	%
Aluminium oxide, Al$_2$O$_3$	14.8 ± 1.5
Iron oxide, Fe$_2$O	47.5 ± 2.0
Titanium oxide, TiO$_2$	10.3 ± 0.95
Silicon oxide, SiO$_2$	7.20 ± 1.0
Calcium oxide, CaO	6.1 ± 1.0
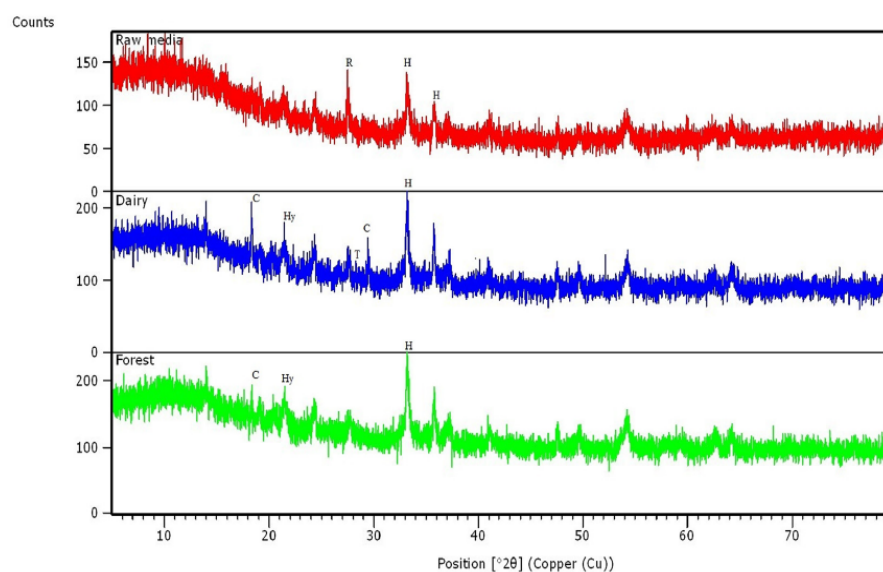
Fig. 1. XRD pattern as determined for the column media before ('Raw media', top) and after the loading period with DSW ('Dairy', middle) and forest run-off ('Forest', bottom). Hematite (H; Fe_2O_3), detected at position 33.153 and 35.612°2Θ and rutile (R; TiO_2), detected at position 27.459 °2Θ were present in the raw bauxite residue media. Calcium hydrogenphosphate (III) hydrate (C; $CaHPO_4.3H_2O$), detected at positions 19.120 and 30.001 °2Θ, was present in both the spent media following treatment of the DSW and forest run-off.

Table 3
Particle size distribution of the bauxite residue used in this study.

d_{10} (µm)[a]	d_{50} (µm)[b]	d_{90} (µm)[c]
0.8 ± 0.1	2.6 ± 0.1	6.8 ± 0.2

[a] d_{10} (µm) = the size of particles at 10% of the total particle distribution.
[b] d_{50} (µm) = the median; the size of particles at 50% of the total particle distribution.
[c] d_{90} (µm) = the size of particles at 90% of the total particle distribution.

contaminants in addition to the phosphate ions.

3.3. Speciation of P adsorbed

The adsorption of phosphate ions onto an adsorbent is measured by the decrease for phosphate in the influent after a certain amount of time (Loganathan et al., 2014). Typically, the main mechanism of phosphate adsorption (and other anions and cations) onto the surface of iron and aluminium oxides may be separated into two processes: specific and non-specific adsorption (Stumm, 1992; Cornell and Schwertmann, 2003). Specific adsorption takes place through the process of ligand exchange (Jacukowicz-Sobala et al., 2015). A phosphate ion exchanges with one or more hydroxyl groups, with the release of OH_2 and/or OH^- back into the surrounding solution, contributing to the alkalisation of the surrounding environment (Cornell and Schwertmann, 2003), as shown in the following equations:

$$\equiv FeOH + An^- \leftrightarrow \equiv FeAn + OH^- \tag{3}$$

$$\equiv Fe(OH)_2 + An^- \leftrightarrow \equiv Fe_2 + An^+ + 2OH^- \tag{4}$$

Non-specific adsorption, which was the main mechanism evident in this study, is inclusive of electrostatic interactions and surface precipitation (Loganathan et al., 2014) between the surface of the sorbent and the phosphate ion (Jacukowicz-Sobala et al., 2015). The electrostatic interactions occur between the electric charge carried on the surface of the sorbent and type of ion present in the surrounding solution. Phosphate ions, which are of anionic nature, carry a negative

charge, which interacts with the positive charge as carried by Ca, a cation (Loganathan et al., 2014). Surface precipitation involves the formation of complexes/precipitates on the surface of the sorbent such as $CaHPO_4^{3-}$ as a result of these ion interactions (Loganathan et al., 2014). The adsorption of the phosphate ions is greatest in a low pH environment due to the abundance of positively charged sites (Jacukowicz-Sobala et al., 2015).

X-ray diffraction and SEM analysis have been used in previous studies to show evidence of the presence of newly formed surface precipitates following the P adsorption process (Bowden et al., 2009). The XRD data obtained in this study (Fig. 1) show that the main interactions and complexes formed by the phosphate ions present in the wastewater (negative charge) were with Ca (positive charge) present in the bauxite residue, as evidenced by the presence of new peaks of $CaHPO_4^{3-}$ in the XRD patterns following the treatment of both the DSW and forest run-off. Depending on the pH of the solution, the species of P found in aqueous solution are H_3PO_4 (pH < 4), $H_2PO_4^-$ (pH ~ 0–9), HPO_4^{2-} (pH ~ 5–11) and PO_4^{3-} (pH > 10) (Karageorgiou et al., 2007; Despland et al., 2011).

The FT-IR analysis of the bauxite residue media before and after treatment of both the DSW and forest run-off (Figs. 3 and 4) indicated that similar changes occurred in the media following treatment of both wastewaters. Two distinct broad bands were detected between wavelength 600 to 900 cm^{-1} and again at 1000 to 1400 cm^{-1}. This was evident for both the DSW and forest run-off spent media. Intensive IR absorption bands are typically in the range of 560–600 cm^{-1} and 1000 to 1100 cm^{-1} for P species (Tejedor-Tejedor and Anderson, 1990; Berzina-Cimdina and Borodajenko, 2012). However, it was not possible to identify specific P species due to some interferences, which are most likely due to the presence of many other ions present in each of the wastewater sources used.

There was an increase in the pH in the effluent for both the DSW and forest run-off treated wastewater (Fig. 5). The influent pH of the DSW was 7.79, which increased to 8.94 in the 40 cm column at t = 2 h. The influent pH of the forest run-off was 7.57 and increased to 8.81 at t = 12 h in the 40 cm column. According to the Drinking Water Directive (98/83/EC), the pH value should be in the range of ≥6.5

277

220
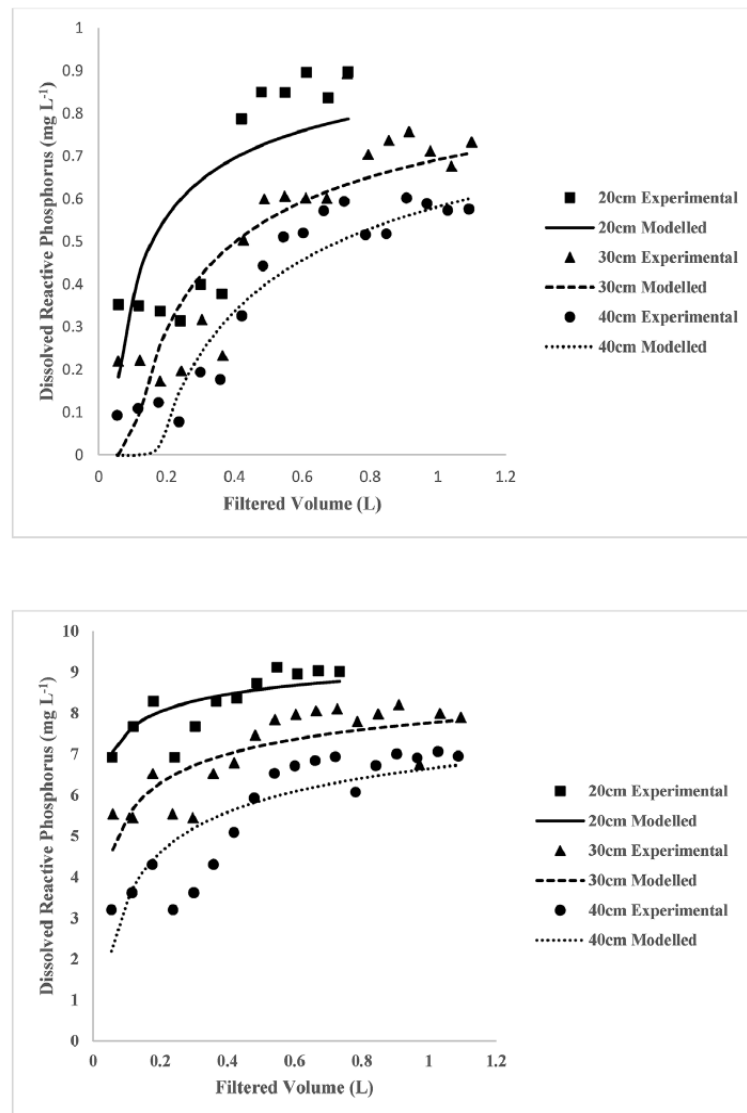
Fig. 2. The breakthrough curves for the effluent dissolved reactive phosphorus concentration versus loading time for forest run-off (top) and dairy soiled water (bottom) using experimental and modelled data.

and ≤ 9.5. The values recorded in this study show that the pH values in the effluent are within this range, highlighting no potential risk to the surrounding environment.

3.4. Trace metal and elemental analysis

Due to the complex nature of bauxite residue and its composition, there is potential for trace metal leaching to the surrounding environment (Despland et al., 2011; Evans, 2016). Pollution from metals can have an adverse and detrimental effect on the surrounding environment, affecting plant and animal life (Gomes et al., 2016a; Olszewska et al., 2017). In addition, the majority of metals that are in a soil environment are non-degradable (Guo et al., 2006).

The influent and effluent metal concentrations from the columns treating DSW and forest run-off, along with the parametric values, as mandated by the Irish EPA (2014), are displayed in Figs. 6 and 7. In this study, the dominant species present in both effluents were Al and Fe, which were above the parametric values ($0.2\,mg\,L^{-1}$ for both Al and Fe). Copper was released in both effluents, but did decrease with loading time when treating the DSW and the level of Cu reduced to below the parametric value of $2\,mg\,L^{-1}$. The level of Mn was lower in the effluent compared to the influent for all columns, showing a retention capacity within the column media, but it was higher than the parametric value of $0.05\,mg\,L^{-1}$. Magnesium, Ga, V and Zn were also present in increased amounts in the effluent, due to leaching from the bauxite residue. However, the Mg and Zn did decrease with increasing loading time. There are currently no parametric values or EPA guideline values for drinking water parameters for Mg, Ga, V and Zn, although previous studies have highlighted that bauxite residue is inclusive of oxyanionic-forming elements, which are soluble at high pH range; these include Al, As, Cr, Mo and V (Mayes et al., 2016). The main species of V present in bauxite residue was in the pentavalent form (Burke et al.,
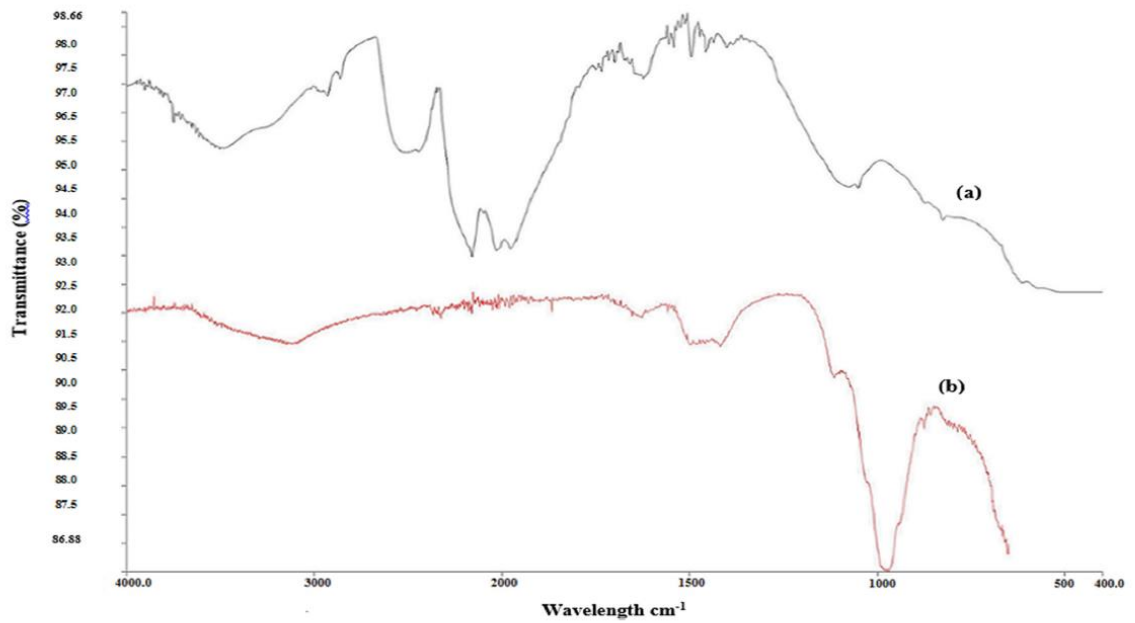
Fig. 3. FT-IR analysis of the bauxite residue media before (a) and after use in the column treating DSW (b).

2012, 2013), which may be problematic due to its toxicity (Burke et al., 2012). Whilst V may be a potential issue (depending on the source of bauxite ore), it is also the focus of critical raw material (CRM) recovery studies (Gomes et al., 2016b; Zhu et al., 2018), which suggests the

potential and need for further studies investigating the adsorbent potential of bauxite residue following the removal and recovery of CRMs such as V.

Previous work by Lopez et al. (1998) highlighted the ability of
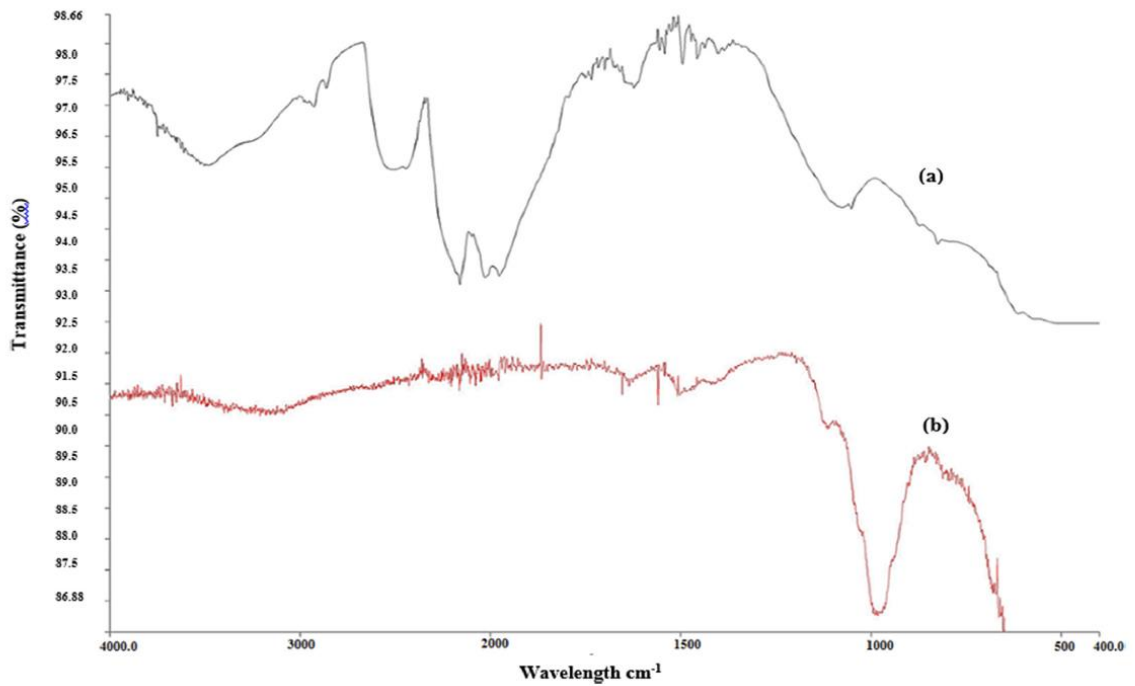
Fig. 4. FT-IR analysis of the bauxite residue media before (a) and after use in the column treating forest run-off (b).

(a)   (b)
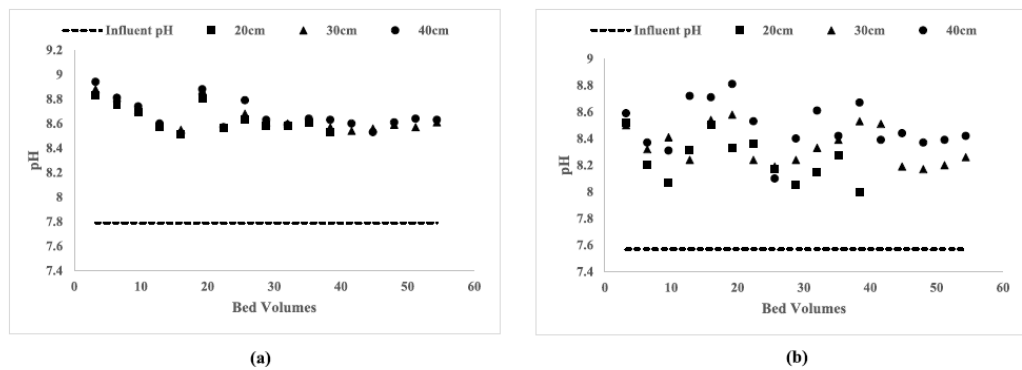
Fig. 5. The pH values of (a) the dairy soiled water and (b) forest run-off effluent from the columns over the 24–36 h loading period, showing that there was an overall increase in the pH of the effluent treated.

bauxite residue to retain Ni, Cu and Zn. Despland et al. (2014) showed that Bauxsol™ (neutralised bauxite residue produced using the Basecon™ procedure) had the ability to remove trace amounts of As, lead (Pb), Cd, Cr, Cu, Ni, Se, Zn, Mn and Al. This highlights the potential of bauxite residue in the removal of both cations and anions from aqueous solution. However, the composition and concentration of elements in bauxite will vary depending on the type of ore (Mayes et al., 2011).

Although there was overall evidence of mobilisation of some trace elements while treating the wastewater, one suggestion would be to include a rinse/wash period prior to packing the columns. This would reduce and/or eliminate the potential leaching of metals at the initial loading period and avoid further release as the loading period increases. Another option would be to apply a seawater treatment to the bauxite residue, which has been proven to lower the pH and therefore reduce

the leaching of metal(loid) species (Cusack et al., 2018; Johnston et al., 2010).

4. Conclusions

Several studies have focussed on the use of low-cost adsorbents in the removal of contaminants such as P from contaminated waters due to possible cost savings and to reutilise by-products from various sectors. This study demonstrated that bauxite residue has P (particularly dissolved reactive phosphorus) removal capabilities in both low (forest run-off) and high (dairy soiled water) range P-concentrated waters. The estimated service time of the column media before initial breakthrough, based on the performance of the largest columns, was $1.08 \, \text{min g}^{-1}$ media for the forest run-off and $0.28 \, \text{min g}^{-1}$ media for the dairy soiled water. Due to the composition of the bauxite residue, potential for

Fig. 6. Comparison of the composition of (a) Al, (b) Fe, (c) Na (d) Cu (e) Mn (f) Mg (g) Ga (h) V and (i) Zn in both the influent and effluent in the columns treating DSW over the 24–36 h loading period. EPA indicator parameter or EPA chemical parameter included for each element.

280
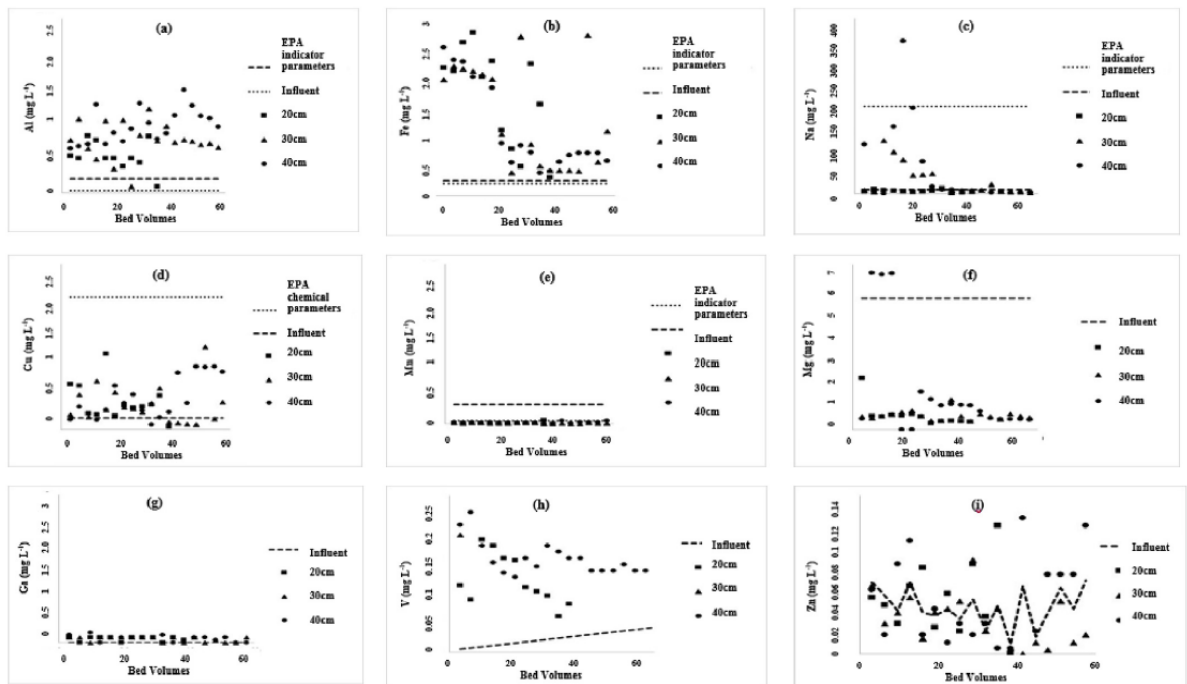
Fig. 7. Comparison of the composition of (a) Al, (b) Fe, (c) Na (d) Cu (e) Mn (f) Mg (g) Ga (h) V and (i) Zn in both the influent and effluent in the columns treating forest run-off over the 24–36 h loading period. EPA indicator parameter or EPA chemical parameter included for each element.

metal(loid) leaching is a concern. Aluminium and iron were the dominant metals released in the treated effluent, but this may be eliminated by a preventative step such as introducing a washing period or a seawater neutralisation step prior to packing the bauxite residue into the columns.

Acknowledgements

Appendix A. Supplementary data

Supplementary data to this article can be found online at https://doi.org/10.1016/j.jenvman.2019.04.042.

References

Acelas, N.Y., Martin, B.D., López, D., Jefferson, B., 2015. Selective removal of phosphate from wastewater using hydrated metal oxides dispersed within anionic exchange media. Chemosphere 119, 1353–1360. DOI Link: https://doi.org/10.1016/j.chemosphere.2014.02.024.

ÁdÁm, K., Sovik, A.K., Krogstad, T., Heistad, A., 2007. Phosphorous removal by the filter materials light-weight aggregates and shells and-a review of processes and experimental set-ups for improved design of filter systems for wastewater treatment. Vatten 63 (3), 245.

Akhurst, D.J., Jones, G.B., Clark, M., McConchie, D., 2006. Phosphate removal from aqueous solutions using neutralised bauxite refinery residues (Bauxsol™). Environ. Chem. 3 (1), 65–74. DOI Link: https://doi.org/10.1071/EN05038.

Berzina-Cimdina, L., Borodajenko, N., 2012. Research of calcium phosphates using Fourier transform infrared spectroscopy. In: Infrared Spectroscopy-Materials Science, Engineering and Technology, InTech. Available. http://scholar.google.com/scholar_url?url=https%3A%2F%2Fwww.intechopen.com%2Fdownload%2Fpdf%2F36171&hl=en&sa=T&oi=ggp&ct=res&cd=0&d=18760135324139934558&ei=JQ5fW6ODB4SQmwHoq7O4BA&scisig=AAGBfm0zcrG1iAsbV5Fv1kKQs9aPk9QMNA&nossl=1&ws=1440x845 [accessed 30.07.2018].

Bhatnagar, A., Vilar, V.J., Botelho, C.M., Boaventura, R.A., 2011. A review of the use of red mud as adsorbent for the removal of toxic pollutants from water and wastewater.

Environ. Technol. 32 (3), 231–249. DOI Link: https://doi.org/10.1080/09593330.2011.560615.

Bowden, L.I., Jarvis, A.P., Younger, P.L., Johnson, K.L., 2009. Phosphorus removal from waste waters using basic oxygen steel slag. Environ. Sci. Technol. 43 (7), 2476–2481.

Brennan, R.B., Wall, D., Fenton, O., Grant, J., Sharpley, A.N., Healy, M.G., 2014. The impact of chemical amendment of dairy cattle slurry before land application on soil phosphorus dynamics. Commun. Soil Sci. Plant Anal. 45 (16), 2215–2233. DOI Link. https://doi.org/10.1080/00103624.2014.912293.

Bridger, S., Knowles, M., 2000. A Complete Method for Environmental Samples by Simultaneous Axially Viewed ICP-AES Following USEPA Guidelines. Varian ICP-OES at Work (29). Available:[24.05.2018]. https://www.agilent.com/cs/library/applications/ICPES-29.pdf.

Burke, I.T., Mayes, W.M., Peacock, C.L., Brown, A.P., Jarvis, A.P., Gruiz, K., 2012. Speciation of arsenic, chromium, and vanadium in red mud samples from the Ajka spill site, Hungary. Environ. Sci. Technol. 46 (6), 3085–3092. https://doi.org/10.1021/es3003475.

Burke, I.T., Peacock, C.L., Lockwood, C.L., Stewart, D.I., Mortimer, R.J., Ward, M.B., Renforth, P., Gruiz, K., Mayes, W.M., 2013. Behavior of aluminum, arsenic, and vanadium during the neutralization of red mud leachate by HCl, gypsum, or seawater. Environ. Sci. Technol. 47 (12), 6527–6535. https://doi.org/10.1021/es4010834.

Callery, O., Brennan, R.B., Healy, M.G., 2015. Use of amendments in a peat soil to reduce phosphorus losses from forestry operations. Ecol. Eng. 85, 193–200. https://doi.org/10.1016/j.ecoleng.2015.10.016.

Callery, O., Healy, M.G., Rognard, F., Barthelemy, L., Brennan, R.B., 2016. Evaluating the long-term performance of low-cost adsorbents using small-scale adsorption column experiments. Water Res. 101, 429–440. https://doi.org/10.1016/j.watres.2016.05.093.

Callery, O., Healy, M.G., 2017. Predicting the propagation of concentration and saturation fronts in fixed-bed filters. Water Res. 123, 556–568. https://doi.org/10.1016/j.watres.2017.07.010.

Castaldi, P., Silvetti, M., Enzo, S., Melis, P., 2010. Study of sorption processes and FT-IR analysis of arsenate sorbed onto red muds (a bauxite ore processing waste). J. Hazard Mater. 175 (1–3), 172–178. https://doi.org/10.1016/j.jhazmat.2009.09.145.

Castaldi, P., Silvetti, M., Enzo, S., Deiana, S., 2011. X-ray diffraction and thermal analysis of bauxite ore-processing waste (red mud) exchanged with arsenate and phosphate. Clay Clay Miner. 59 (2), 189–199. https://doi.org/10.1346/CCMN.2011.0590207.

Chen, J.P., Yoon, J.T., Yiacoumi, S., 2003. Effects of chemical and physical properties of influent on copper sorption onto activated carbon fixed-bed columns. Carbon 41 (8), 1635–1644. https://doi.org/10.1016/S0008-6223(03)00117-9.

Chen, N., Feng, C., Zhang, Z., Liu, R., Gao, Y., Li, M., Sugiura, N., 2012. Preparation and characterization of lanthanum (III) loaded granular ceramic for phosphorus adsorption from aqueous solution. J. Taiwan Inst. Chem. Eng. 43, 783–789. https://doi.org/10.1016/j.jtice.2012.04.003.

Claveau-Mallet, D., Wallace, S., Comeau, Y., 2013. Removal of phosphorus, fluoride and

metals from a gypsum mining leachate using steel slag filters. Water Res. 47 (4), 1512–1520. https://doi.org/10.1016/j.watres.2012.11.048.

Cordell, D., White, S., 2011. Peak phosphorus: clarifying the key issues of a vigorous debate about long-term phosphorus security. Sustainability 3 (10), 2027–2049. https://doi.org/10.3390/su3102027.

Cornell, R.M., Schwertmann, U., 2003. The Iron Oxides: Structure, Properties, Reactions, Occurrences and Uses. John Wiley & Sons. https://books.google.ie/books?hl=en&lr=&id=dlMuE3_klW4C&oi=fnd&pg=PA1&dq=Cornell,+R.M.+and+Schwertmann,+U.,+2003.+The+iron+oxides:+structure,+properties,+reactions,+occurrences+and+uses.+John+Wiley+%26+Sons.&ots=l0jQWg_4gN&sig=kNxeJyUHBF3-UemiW-s_EvlaeCs&redir_esc=y#v=onepage&q=Cornell%2C%20R.M.%20and%20Schwertmann%2C%20U.%2C%202003.%20The%20iron%20oxides%3A%20structure%2C%20properties%2C%20reactions%2C%20occurrences%20and%20uses.%20John%20Wiley%20%26%20Sons.&f=false [accessed 11.09.2018].

Courtney, R., Harrington, T., 2010. Assessment of plant-available phosphorus in a fine textured sodic substrate. Ecol. Eng. 36 (4), 542–547. https://doi.org/10.1016/j.ecoleng.2009.12.001.

Cusack, P.B., Healy, M.G., Ryan, P.C., Burke, I.T., O'Donoghue, L.M., Ujaczki, É., Courtney, R., 2018. Enhancement of bauxite residue as a low-cost adsorbent for phosphorus in aqueous solution, using seawater and gypsum treatments. J. Clean. Prod. 179, 217–224. https://doi.org/10.1016/j.jclepro.2018.01.092.

De Gisi, S., Lofrano, G., Grassi, M., Notarnicola, M., 2016. Characteristics and adsorption capacities of low-cost sorbents for wastewater treatment: a review. Sustain. Mater. Technol. 9, 10–40. https://doi.org/10.1016/j.susmat.2016.06.002.

Despland, L.M., Clark, M.W., Vancov, T., Erler, D., Aragno, M., 2011. Nutrient and trace-metal removal by Bauxsol pellets in wastewater treatment. Environ. Sci. Technol. 45 (13), 5746–5753. https://doi.org/10.1021/es200934y.

Despland, L.M., Clark, M.W., Vancov, T., Aragno, M., 2014. Nutrient removal and microbial communities' development in a young unplanted constructed wetland using Bauxsol™ pellets to treat wastewater. Sci. Total Environ. 484, 167–175. https://doi.org/10.1016/j.scitotenv.2014.03.030.

Egemose, S., Sønderup, M.J., Beinthin, M.V., Reitzel, K., Hoffmann, C.C., Flindt, M.R., 2012. Crushed concrete as a phosphate binding material: a potential new management tool. J. Environ. Qual. 41, 647–653. https://do.org/10.2134/jeq2011.0134.

EPA, 2014. Drinking Water Parameters Microbiological, Chemical and Indicator Parameters in the 2014 Drinking Water Regulations. Available. www.epa.ie/pubs/advice/drinkingwater/2015_04_21_ParametersStandaloneDoc.pdf [accessed 29.05.2018].

Evans, K., 2016. The history, challenges, and new developments in the management and use of bauxite residue. J. Sustain. Metall. 2 (4), 316–331. https://doi.org/10.1007/s40831-016-0060-x.

Fenton, O., Healy, M.G., Rodgers, M., 2009. Use of ochre from an abandoned metal mine in the south east of Ireland for phosphorus sequestration from dairy dirty water. J. Environ. Qual. 38, 1120–1125. https://doi.org/10.2134/jeq2008.0227.

Finnegan, J., Regan, J.T., De Eyto, E., Ryder, E., Tiernan, D., Healy, M.G., 2012. Nutrient dynamics in a peatland forest riparian buffer zone and implications for the establishment of planted saplings. Ecol. Eng. 47, 155–164. https://doi.org/10.1016/j.ecoleng.2012.06.023.

García-Mateos, F.J., Ruiz-Rosas, R., Marqués, M.D., Cotoruelo, L.M., Rodríguez-Mirasol, J., Cordero, T., 2015. Removal of paracetamol on biomass-derived activated carbon: modeling the fixed bed breakthrough curves using batch adsorption experiments. Chem. Eng. J. 279, 18–30. https://doi.org/10.1016/j.cej.2015.04.144.

Ge, H., Batstone, D.J., Keller, J., 2015. Biological phosphorus removal from abattoir wastewater at very short sludge ages mediated by novel PAO clade Comamonadaceae. Water Res. 69, 173–182. https://doi.org/10.1016/j.watres.2014.11.026.

Gomes, H.I., Mayes, W.M., Rogerson, M., Stewart, D.I., Burke, I.T., 2016a. Alkaline residues and the environment: a review of impacts, management practices and opportunities. J. Clean. Prod. 112, 3571–3582. https://doi.org/10.1016/j.jclepro.2015.09.111.

Gomes, H.I., Jones, A., Rogerson, M., Burke, I.T., Mayes, W.M., 2016b. Vanadium removal and recovery from bauxite residue leachates by ion exchange. Environ. Sci. Pollut. Res. 23 (22), 23034–23042. https://doi.org/10.1007/s11356-016-7514-3.

Grace, M.A., Healy, M.G., Clifford, E., 2015. Use of industrial by-products and natural media to adsorb nutrients, metals and organic carbon from drinking water. Sci. Total Environ. 518, 491–497. https://doi.org/10.1016/j.scitotenv.2015.02.075.

Grace, M.A., Clifford, E., Healy, M.G., 2016. The potential for the use of waste products from a variety of sectors in water treatment processes. J. Clean. Prod. 137, 788–802. https://doi.org/10.1016/j.jclepro.2016.07.113.

Gräfe, M., Power, G., Klauber, C., 2011. Bauxite residue issues: III. Alkalinity and associated chemistry. Hydrometallurgy 108 (1–2), 60–79. https://doi.org/10.1016/j.hydromet.2011.02.004.

Guo, G., Zhou, Q., Ma, L.Q., 2006. Availability and assessment of fixing additives for the in situ remediation of heavy metal contaminated soils: a review. Environ. Monit. Assess. 116 (1–3), 513–528. https://doi.org/10.1007/s10661-006-7668-4.

Hauduc, H., Takács, I., Smith, S., Szabo, A., Murthy, S., Daigger, G.T., Spérandio, M., 2015. A dynamic physicochemical model for chemical phosphorus removal. Water Res. 73, 157–170. https://doi.org/10.1016/j.watres.2014.12.053.

Herron, S.L., Sharpley, A.N., Brye, K.R., Miller, D.M., 2016. Optimizing hydraulic and chemical properties of iron and aluminum byproducts for use in on-farm containment structures for phosphorus removal. J. Environ. Prot. 7 (12), 1835. https://doi.org/10.4236/jep.2016.712146.

Huang, W., Wang, S., Zhu, Z., Li, L., Yao, X., Rudolph, V., Haghseresht, F., 2008. Phosphate removal from wastewater using red mud. J. Hazard Mater. 158 (1), 35–42. https://doi.org/10.1016/j.jhazmat.2008.01.061.

Jacukowicz-Sobala, I., Ociński, D., Kociołek-Balawejder, E., 2015. Iron and aluminium oxides containing industrial wastes as adsorbents of heavy metals: application possibilities and limitations. Waste Manag. Res. 33 (7), 612–629. https://doi.org/10.1177/0734242X15584841.

Johnston, M., Clark, M.W., McMahon, P., Ward, N., 2010. Alkalinity conversion of bauxite refinery residues by neutralization. J. Hazard Mater. 182 (1–3), 710–715. https://doi.org/10.1016/j.jhazmat.2010.06.091.

Karageorgiou, K., Paschalis, M., Anastassakis, G.N., 2007. Removal of phosphate species from solution by adsorption onto calcite used as natural adsorbent. J. Hazard Mater. 139 (3), 447–452. https://doi.org/10.1016/j.jhazmat.2006.02.038.

Kong, X., Li, M., Xue, S., Hartley, W., Chen, C., Wu, C., Li, X., Li, Y., 2017. Acid transformation of bauxite residue: conversion of its alkaline characteristics. J. Hazard Mater. 324, 382–390. https://doi.org/10.1016/j.jhazmat.2016.10.073.

Lalley, J., Han, C., Mohan, G.R., Dionysiou, D.D., Speth, T.F., Garland, J., Nadagouda, M.N., 2015. Phosphate removal using modified Bayoxide® E33 adsorption media. Environ. Sci. Water Res. Technol. 1 (1), 96–107. https://doi.org/10.1039/C4EW00020J.

Liu, Y., Lin, C., Wu, Y., 2007. Characterization of red mud derived from a combined Bayer Process and bauxite calcination method. J. Hazard Mater. 146, 255–261. https://doi.org/10.1016/j.jhazmat.2006.12.015.

Loganathan, P., Vigneswaran, S., Kandasamy, J., Bolan, N.S., 2014. Removal and recovery of phosphate from water using sorption. Crit. Rev. Environ. Sci. Technol. 44 (8), 847–907.

Lopez, E., Soto, B., Arias, M., Nunez, A., Rubinos, D., Barral, M.T., 1998. Adsorbent properties of red mud and its use for wastewater treatment. Water Res. 32, 1314–1322. https://doi.org/10.1016/S0043-1354(97)00326-6.

Mayes, W.M., Jarvis, A.P., Burke, I.T., Walton, M., Feigl, V., Klebercz, O., Gruiz, K., 2011. Dispersal and attenuation of trace contaminants downstream of the Ajka bauxite residue (red mud) depository failure, Hungary. Environ. Sci. Technol. 45 (12), 5147–5155. https://doi.org/10.1021/es200850y.

Mayes, W.M., Burke, I.T., Gomes, H.I., Anton, Á.D., Molnár, M., Feigl, V., Ujaczki, É., 2016. Advances in understanding environmental risks of red mud after the Ajka spill, Hungary. J. Sustain. Metall. 2 (4), 332–343. https://doi.org/10.1007/s40831-016-0050-z.

McConchie, D., Clark, M., Davies-McConchie, F., 2001. Processes and Compositions for Water Treatment. Neauveau Technology Investments, Australian, pp. 28.

Minogue, D., French, P., Bolger, T., Murphy, P.N.C., 2015. Characterisation of dairy soiled water in a survey of 60 Irish dairy farms. Ir. J. Agric. Food Res. 54 (1), 1–16. https://doi.org/10.1515/ijafr-2015-0001.

Murnane, J.G., Brennan, R.B., Fenton, O., Healy, M.G., 2016. Zeolite combined with alum and aluminium chloride mixed with agricultural slurries reduces carbon losses in runoff from grassed soil boxes. J. Environ. Qual. 44 (5), 1674–1683. https://doi.org/10.2134/jeq2016.05.0175.

Nowak, B., Aschenbrenner, P., Winter, F., 2013. Heavy metal removal from sewage sludge ash waste fly ash—a comparison. Fuel Process. Technol. 105, 195–201. https://doi.org/10.1016/j.fuproc.2011.06.027.

O'Flynn, C.J., Fenton, O., Wall, D., Brennan, R.B., McLaughlin, M.J., Healy, M.G., 2018. Influence of soil phosphorus status, texture, pH and metal content on the efficacy of amendments to pig slurry in reducing phosphorus losses. Soil Use Manag. 34 (1), 1–8. https://doi.org/10.1111/sum.12391.

Olszewska, J.P., Heal, K.V., Winfield, I.J., Eades, L.J., Spears, B.M., 2017. Assessing the role of bed sediments in the persistence of red mud pollution in a shallow lake (Kinghorn Loch, UK). Water Res. 123, 569–577. https://doi.org/10.1016/j.watres.2017.07.009.

Pan, G., Lyu, T., Mortimer, R., 2018. Comment: Closing Phosphorus Cycle from Natural Waters: Re-capturing Phosphorus through an Integrated Water-Energy-Food Strategy. https://doi.org/10.1016/j.jes.2018.02.018.

Penn, C., McGrath, J., Bowen, J., Wilson, S., 2014. Phosphorus removal structures: a management option for legacy phosphorus. J. Soil Water Conserv. 69 (2), 51A–56A. https://doi.org/10.2489/jswc.69.2.51A.

Pratt, C., Parsons, S.A., Soares, A., Martin, B.D., 2012. Biologically and chemically mediated adsorption and precipitation of phosphorus from wastewater. Curr. Opin. Biotechnol. 23 (6), 890–896. https://doi.org/10.1016/j.copbio.2012.07.003.

Pretty, J., Bharucha, Z.P., 2014. Sustainable intensification in agricultural systems. Ann. Bot. 114 (8), 1571–1596. https://doi.org/10.1093/aob/mcu205.

Ruane, E.M., Murphy, P.N., Healy, M.G., French, P., Rodgers, M., 2011. On-farm treatment of dairy soiled water using aerobic woodchip filters. Water Res. 45 (20), 6668–6676. https://doi.org/10.1016/j.watres.2011.09.055.

Sharpley, A., 2016. Managing agricultural phosphorus to minimize water quality impacts. Sci. Agric. 73 (1), 1–8. https://doi.org/10.1590/0103-9016-2015-0107.

Søvik, A.K., Kløve, B., 2005. Phosphorus retention processes in shell sand filter systems treating municipal wastewater. Ecol. Eng. 25 (2), 168–182. https://doi.org/10.1016/j.ecoleng.2005.04.007.

Stumm, W., 1992. Chemistry of the Solid-Water Interface: Processes at the Mineral-Water and Particle-Water Interface in Natural Systems. John Wiley & Son Inc.

Sukačová, K., Trtílek, M., Rataj, T., 2015. Phosphorus removal using a microalgal biofilm in a new biofilm photobioreactor for tertiary wastewater treatment. Water Res. 71, 55–63. https://doi.org/10.1016/j.watres.2014.12.049.

Tejedor-Tejedor, M.I., Anderson, M.A., 1990. The protonation of phosphate on the surface of goethite as studied by CIR-FTIR and electrophoretic mobility. Langmuir 6 (3), 602–611. https://doi.org/10.1021/0743-7463/90/2406-0602$02.50/0.

Tresintsi, S., Simeonidis, K., Katsikini, M., Paloura, E.C., Bantsis, G., Mitrakas, M., 2014. A novel approach for arsenic adsorbents regeneration using MgO. J. Hazard Mater. 265, 217–225. https://doi.org/10.1016/j.jhazmat.2013.12.003.

Ujaczki, É., Feigl, V., Molnár, M., Cusack, P., Curtin, T., Courtney, R., O'Donoghue, L., Davris, P., Hugi, C., Evangelou, M.W., Balomenos, E., 2018. Re-using bauxite

residues: benefits beyond (critical raw) material recovery. J. Chem. Technol. Biotechnol. 93 (9), 2498–2510. https://doi.org/10.1002/jctb.5687.

United Nations, 2015. Transforming Our World: the 2030 Agenda for Sustainable Development. Available. http://www.un.org/en/development/desa/population/migration/generalassembly/docs/globalcompact/A_RES_70_1_E.pdf, Accessed date: 18 July 2018.

Vuković, G.D., Marinković, A.D., Škapin, S.D., Ristić, M.Ð., Aleksić, R., Perić-Grujić, A.A., Uskoković, P.S., 2011. Removal of lead from water by amino modified multi-walled carbon nanotubes. Chem. Eng. J. 173 (3), 855–865. https://doi.org/10.1016/j.cej.2011.08.036.

Wang, B., Lehmann, J., Hanley, K., Hestrin, R., Enders, A., 2015. Adsorption and desorption of ammonium by maple wood biochar as a function of oxidation and pH. Chemosphere 138, 120–126. https://doi.org/10.1016/j.chemosphere.2015.05.062.

Wang, X.X., Wu, Y.H., Zhang, T.Y., Xu, X.Q., Dao, G.H., Hu, H.Y., 2016. Simultaneous nitrogen, phosphorous, and hardness removal from reverse osmosis concentrate by microalgae cultivation. Water Res. 94, 215–224. https://doi.org/10.1016/j.watres.2016.02.062.

Weissert, C., Kehr, J., 2018. Macronutrient sensing and signaling in plants. In: Plant Macronutrient Use Efficiency, pp. 45–64. https://doi.org/10.1016/B978-0-12-811308-0.00003-X.

Wu, K., Chen, Y., Ouyang, Y., Lei, H., Liu, T., 2018. Adsorptive removal of fluoride from

water by granular zirconium–aluminum hybrid adsorbent: performance and mechanisms. Environ. Sci. Pollut. Res. 25 (16), 15390–15403. https://doi.org/10.1007/s11356-018-1711-1.

Ye, J., Zhang, P., Hoffmann, E., Zeng, G., Tang, Y., Dresely, J., Liu, Y., 2014. Comparison of response surface methodology and artificial neural network in optimization and prediction of acid activation of Bauxsol for phosphorus adsorption. Water, Air, Soil Pollut. 225 (12), 2225. https://doi.org/10.1007/s11270-014-2225-1.

Zhou, Z., Hu, D., Ren, W., Zhao, Y., Jiang, L.M., Wang, L., 2015. Effect of humic substances on phosphorus removal by struvite precipitation. Chemosphere 141, 94–99. https://doi.org/10.1016/j.chemosphere.2015.06.089.

Zhou, B., Xu, Y., Vogt, R.D., Lu, X., Li, X., Deng, X., Yue, A., Zhu, L., 2016. Effects of land use change on phosphorus levels in surface waters—a case study of a watershed strongly influenced by agriculture. Water, Air, Soil Pollut. 227 (5), 160. https://doi.org/10.1007/s11270-016-2855-6.

Zhu, F., Li, Y., Xue, S., Hartley, W., Wu, H., 2016. Effects of iron-aluminium oxides and organic carbon on aggregate stability of bauxite residues. Environ. Sci. Pollut. Res. 23 (9), 9073–9081. https://doi.org/10.1007/s11356-016-6172-9.

Zhu, X., Li, W., Zhang, Q., Zhang, C., Chen, L., 2018. Separation characteristics of vanadium from leach liquor of red mud by ion exchange with different resins. Hydrometallurgy 176, 42–48. https://doi.org/10.1016/j.hydromet.2018.01.009.

Appendix B
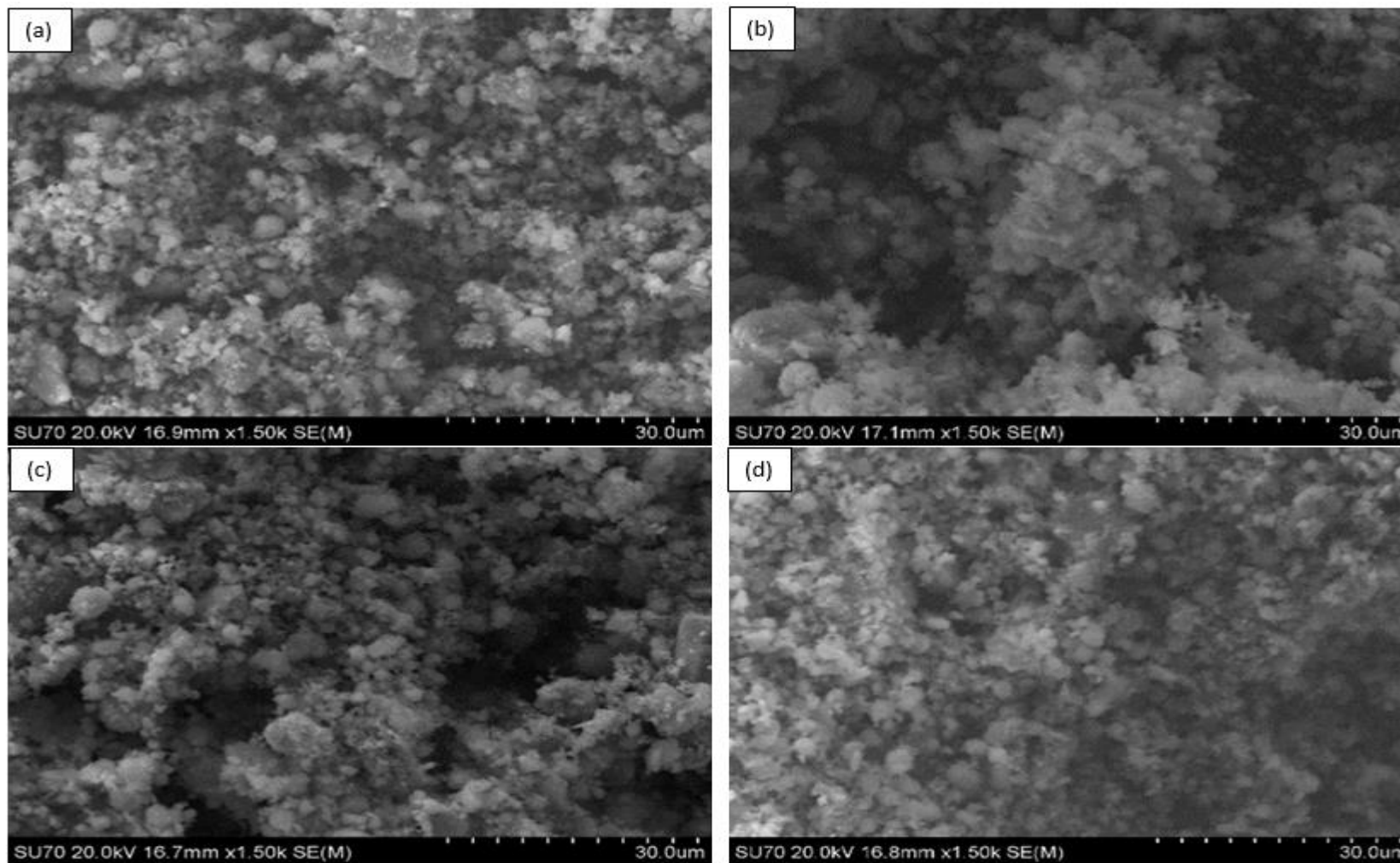
Figure B1 SEM images for each bauxite residue samples in storage over the past twelve years. Sample **(a)** corresponds to the year 2004 **(b)** corresponds to the year 2005 **(c)** corresponds to the year 2006 and **(d)** corresponds to the year 2007.
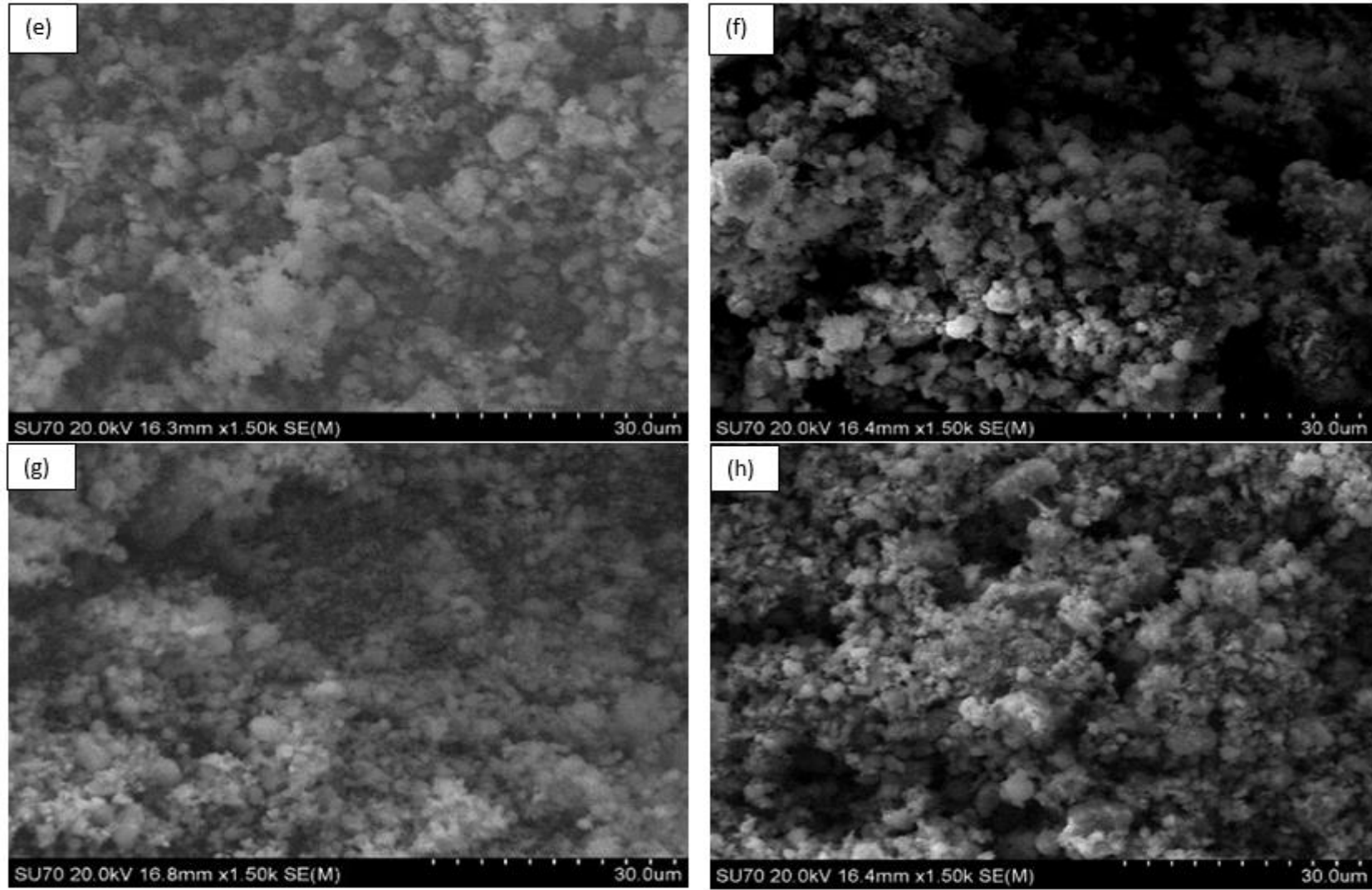
Figure B2 SEM images for each bauxite residue samples in storage over the past twelve years. Sample **(e)** corresponds to the year 2008 **(f)** corresponds to the year 2009 **(g)** corresponds to the year 2010 and **(h)** corresponds to the year 2011.
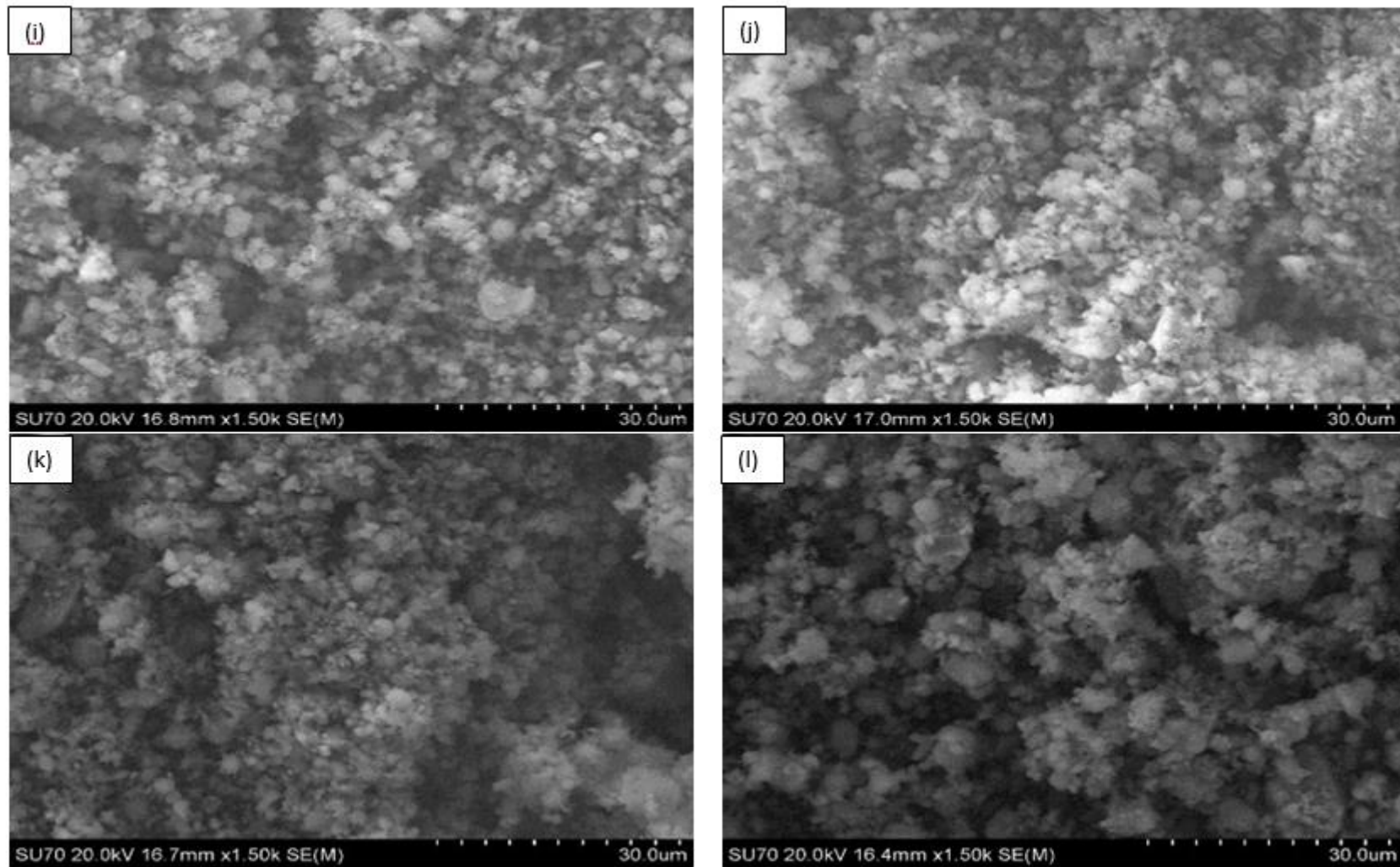
Figure B3 SEM images for each bauxite residue samples in storage over the past twelve years. Sample (**i**) corresponds to the year 2012 (**j**) corresponds to the year 2013 (**k**) corresponds to the year 2014 and (**k**) corresponds to the year 2015.

	Na	Al	Si	Ca	Ti	Fe
2004	11.9	14.0	10.4	8.9	9.2	45.6
2005	7.4	11.7	5.4	5.4	8.9	61.2
2006	11.6	16.0	9.3	9.2	8.7	45.2
2007	3.2	4.7	2.9	6.1	9.1	74.1
2008	13.9	12.9	8.6	7.8	9.6	47.2
2009	10.2	20.1	9.9	8.3	7.9	43.3
2010	11.2	17.8	10.7	7.1	8.3	44.9
2011	8.9	14.5	7.6	6.7	7.7	54.5
2012	9.7	13.4	8.9	7.7	8.4	52.0
2013	8.9	12.7	6.5	4.1	4.6	62.8
2014	9.4	17.3	8.6	8.1	8.8	47.8
2015	15.9	18.9	13.9	5.8	6.2	39.4
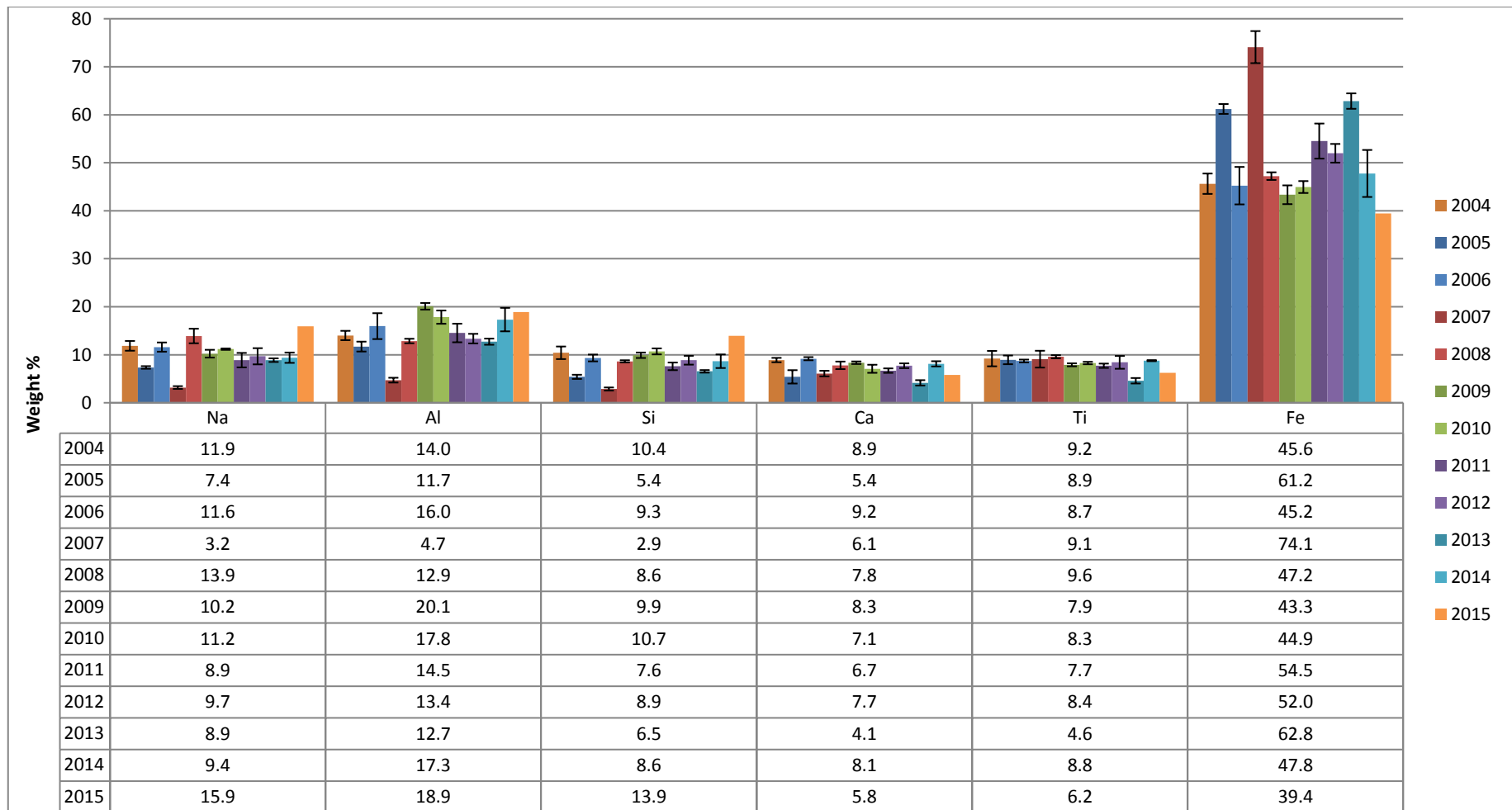
Figure B4 EDS results (in weight %) for the bauxite residue.
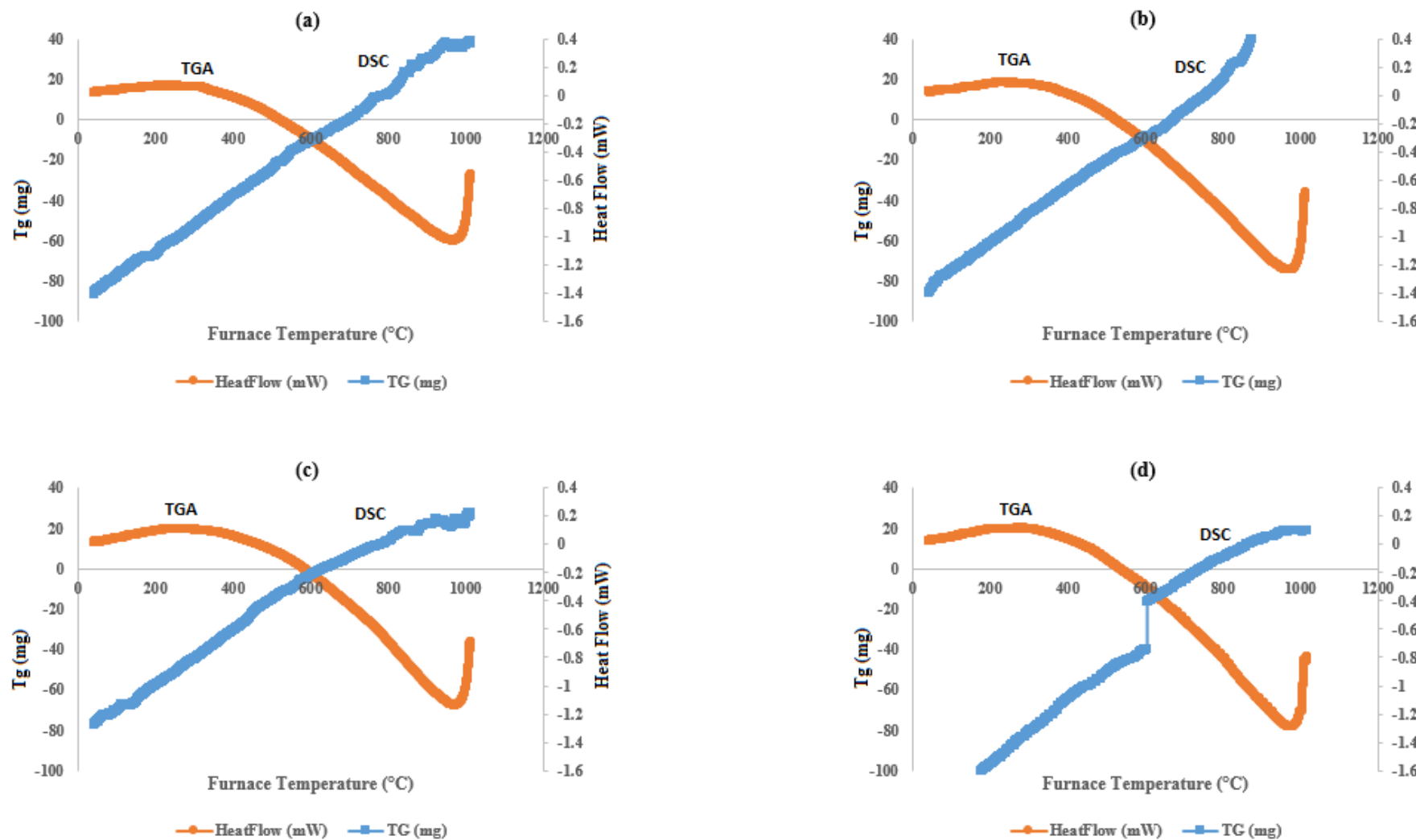
Figure B5 TGA (descending) / DSC (ascending) curve for bauxite residue samples (a) BR10 (2006), (b) BR8 (2008), (c) BR6 (2010), (d) BR4 (2012). The TGA curves showed weight loss between 300 and 975 °C for all the bauxite residues examined.
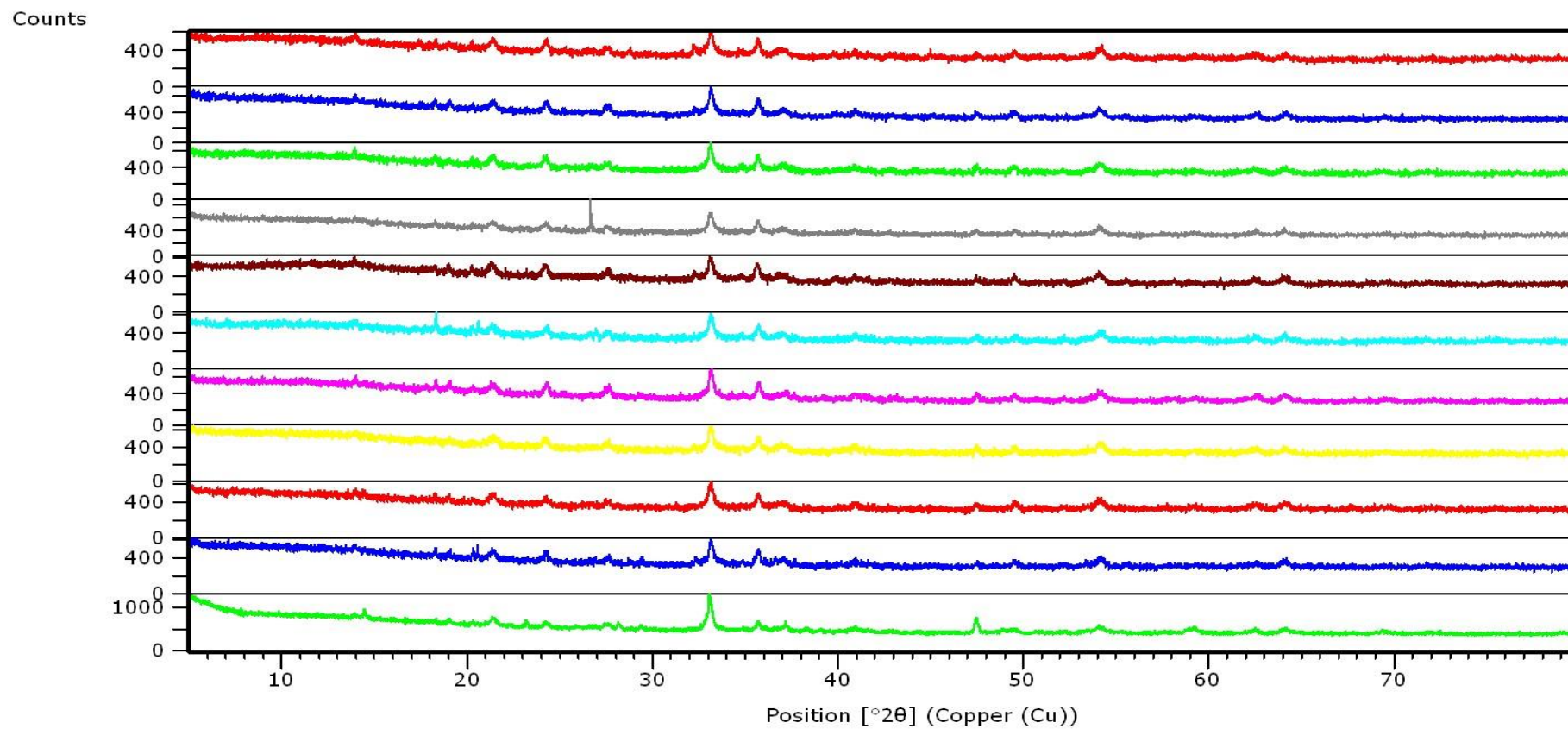
Figure B6 Mineralogical detection using XRD analysis for all 12 bauxite residue samples. From top to bottom: BR12 (2004), BR11 (2005), BR10 (2006), BR9 (2007), BR8 (2008), BR7 (2009), BR6 (2010), BR5 (2011), BR4 (2012), BR3 (2013), BR2 (2014) and BR1 (2015).
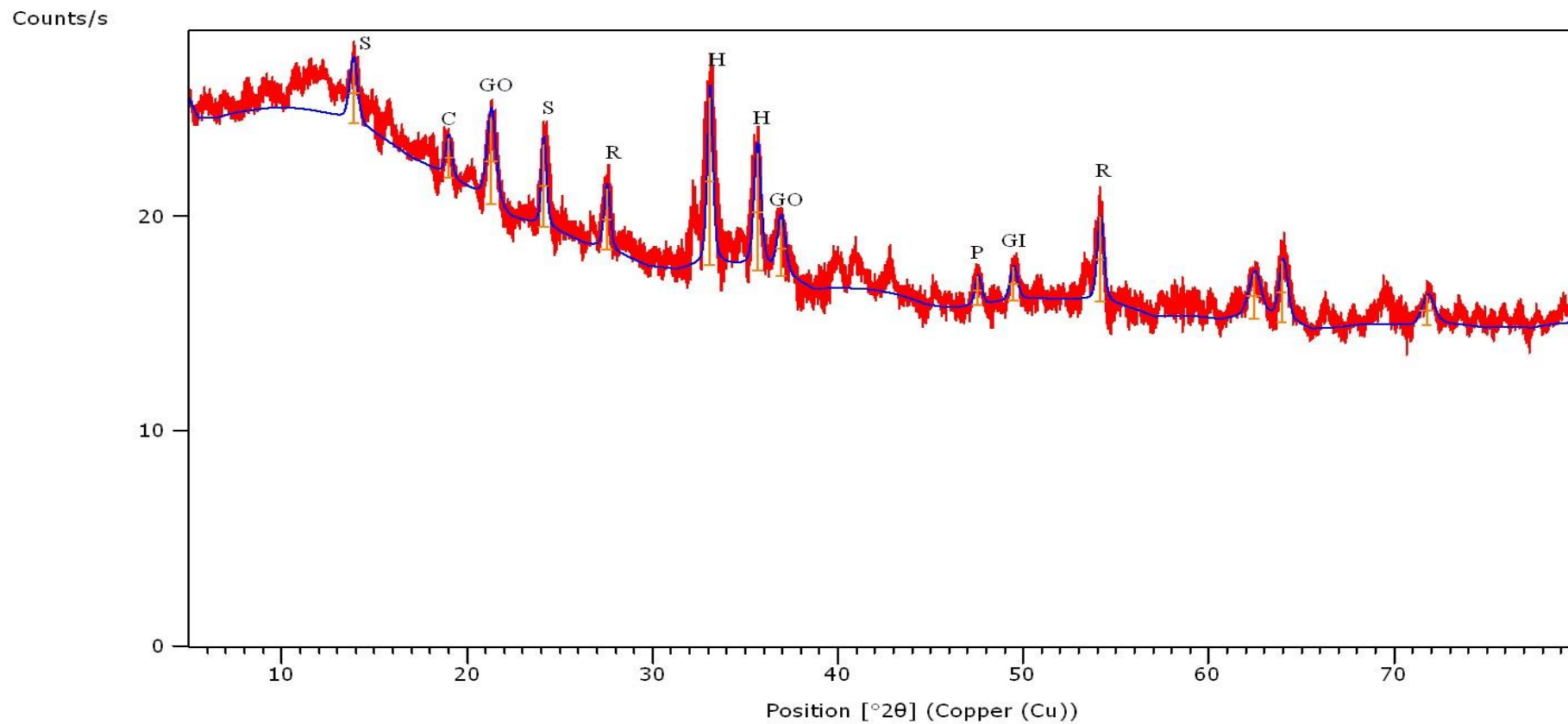
Figure B7 Mineralogical detection of sample BR4 (2012) using XRD analysis, showing the dominant peaks, haematite (H), goethite (GO), perovskite (P), rutile (R), gibbsite (GI), sodalite (S) and cancrinite (C).

Appendix C
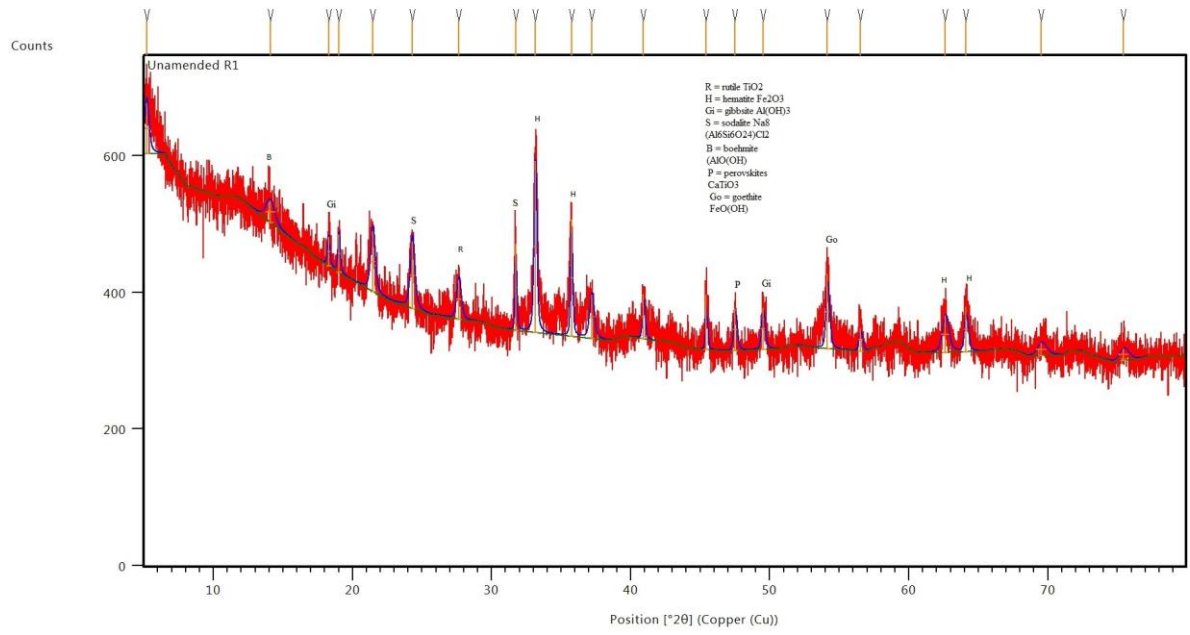
Figure C1 XRD pattern for sample UF.
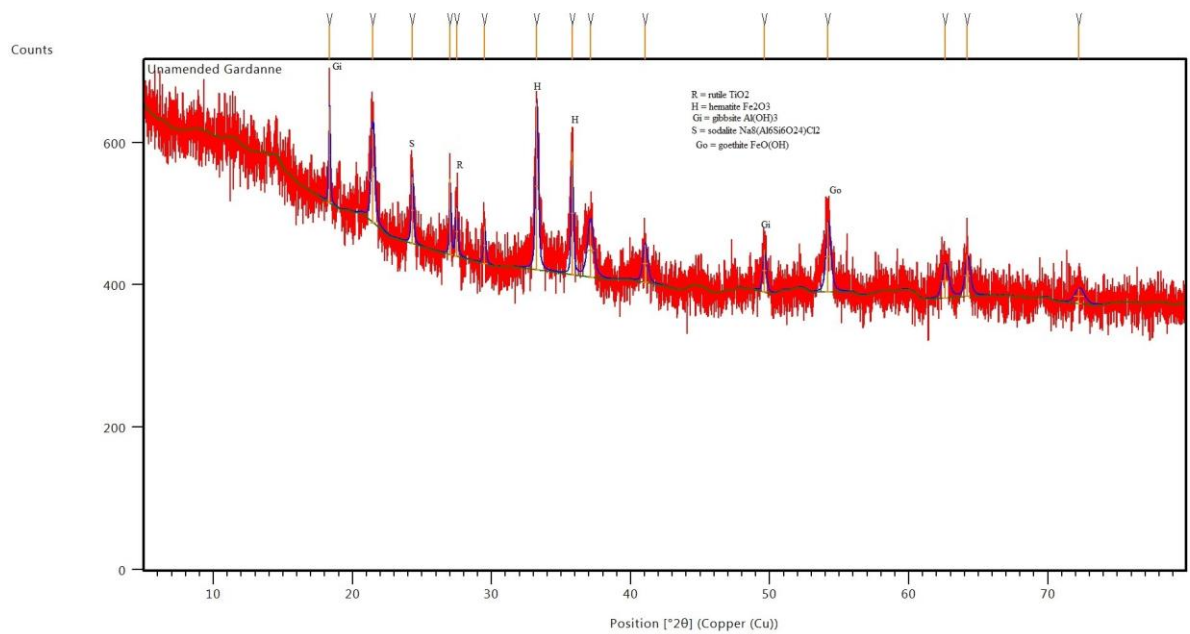
Figure C2 XRD pattern for sample UFR.

236
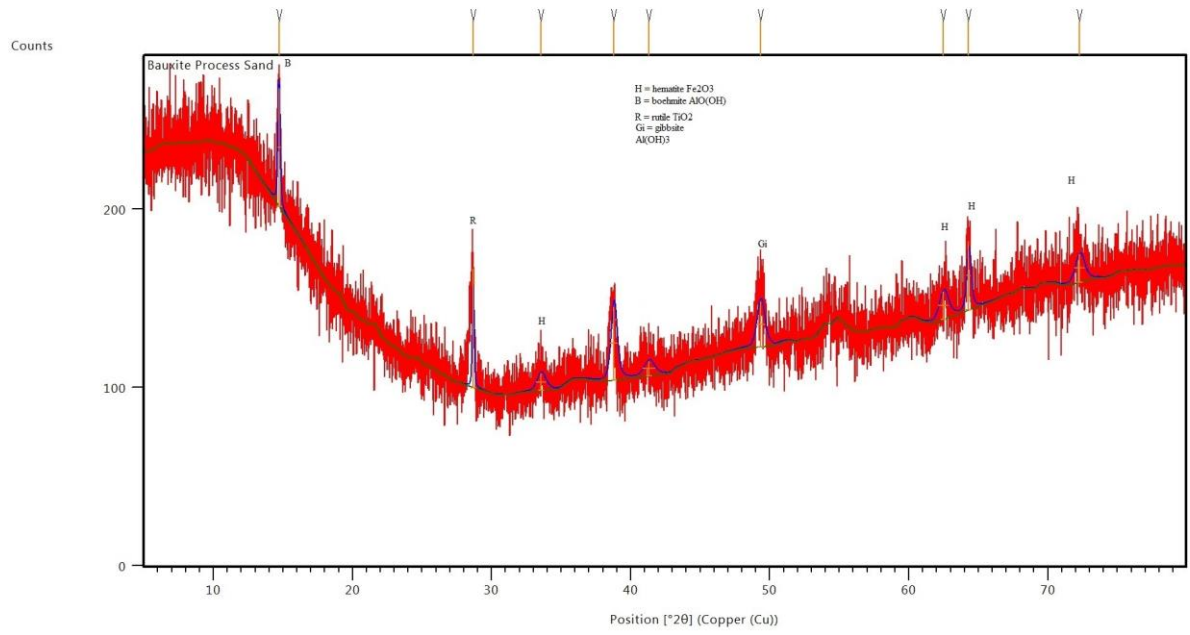
Figure C3 XRD pattern for sample UC.
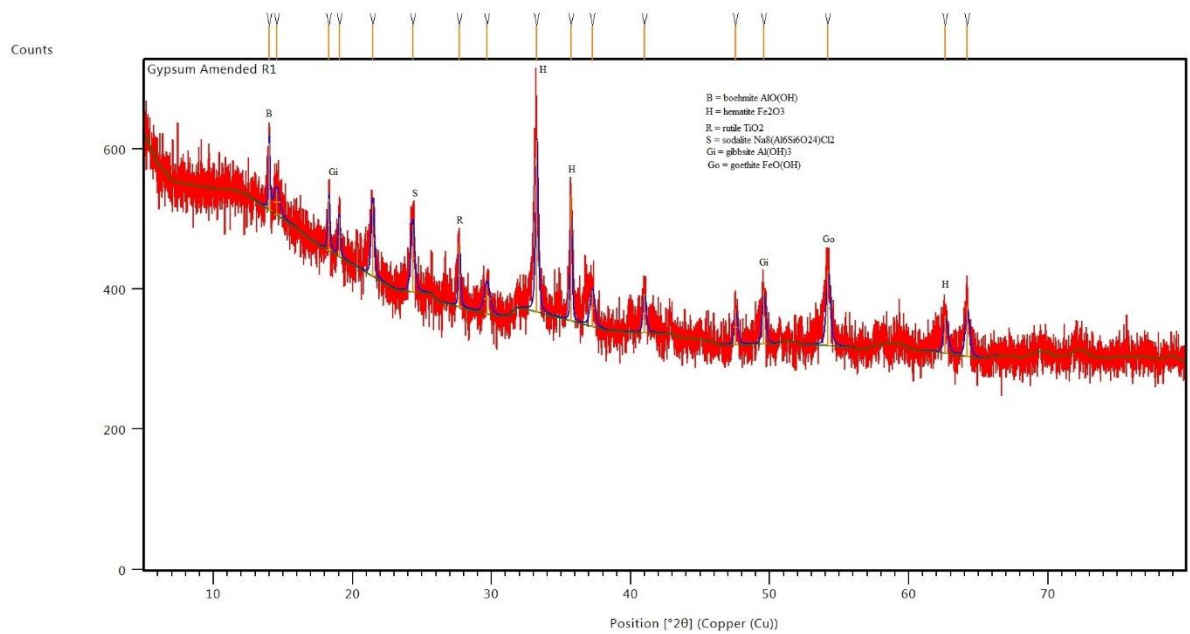
Figure C4 XRD pattern for sample UFG.
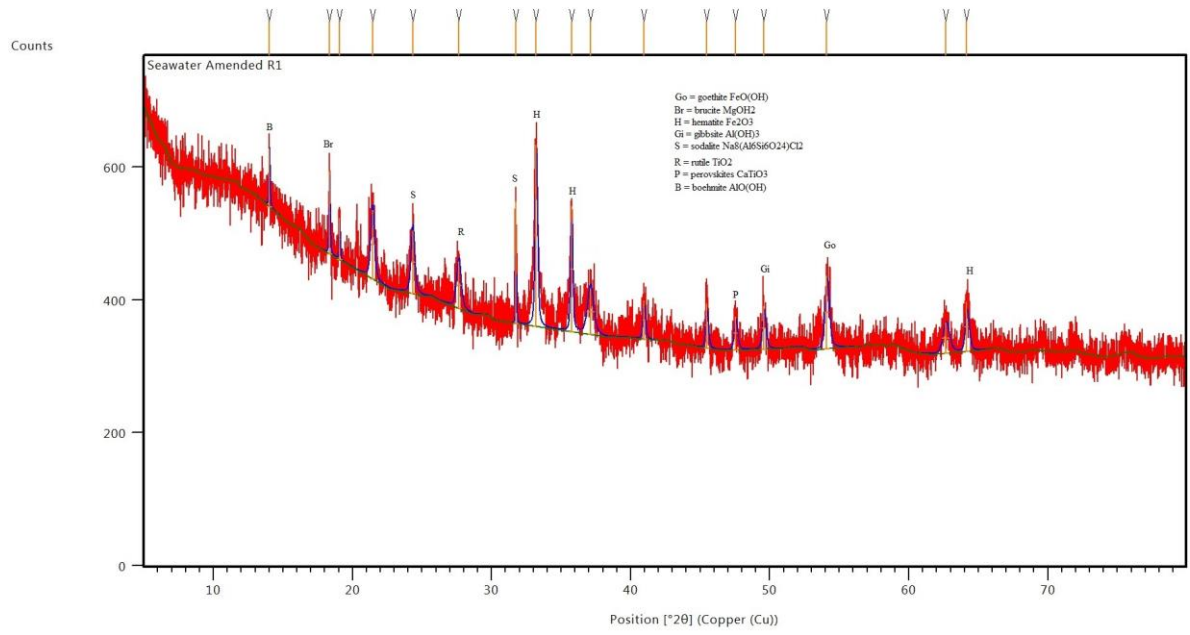
Figure C5 XRD pattern for sample UFS.
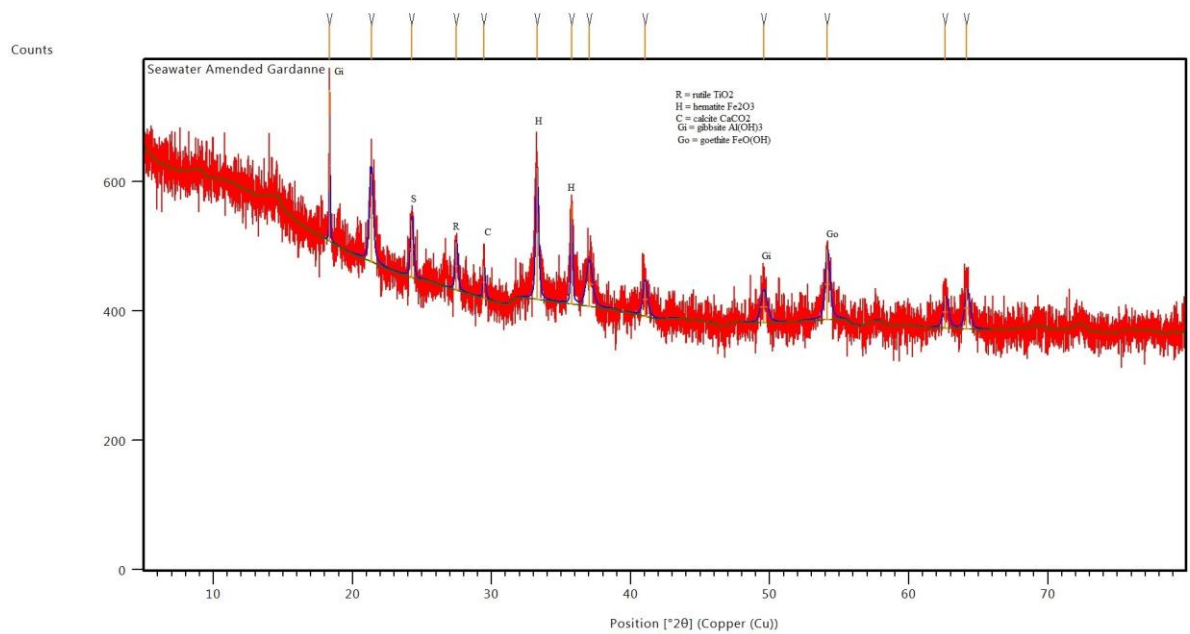
Figure C6 XRD pattern for sample UFRS.
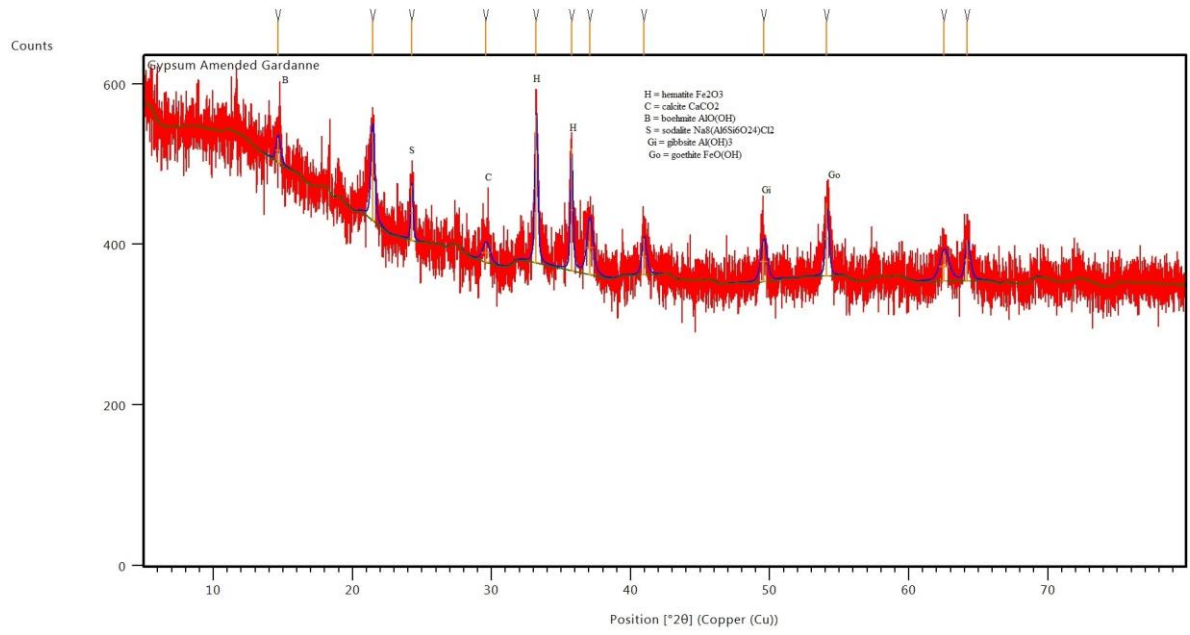
Figure C7 XRD pattern for sample UFRG.
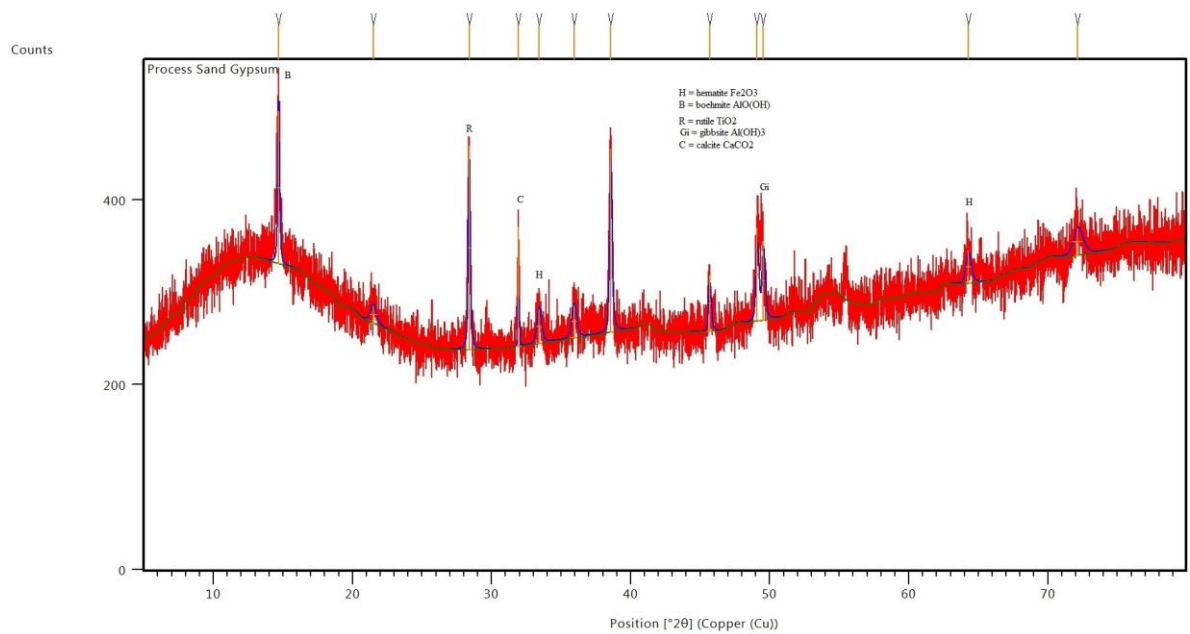
Figure C8 XRD pattern for sample UCG.
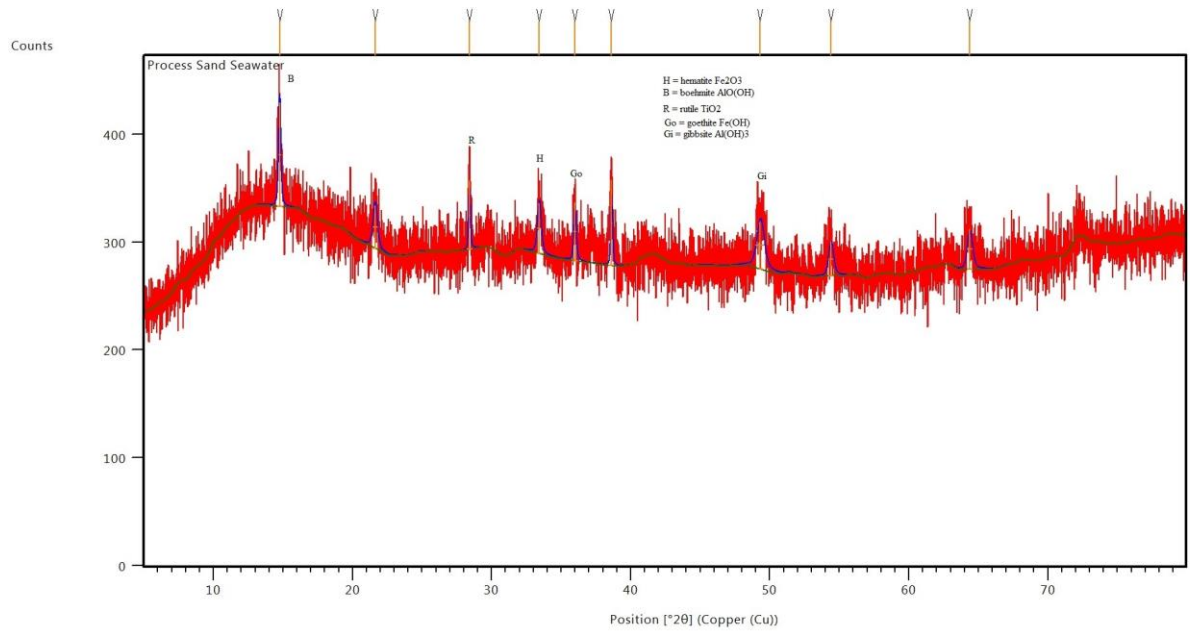
Figure C9 XRD pattern for sample UCS.

Table C1 Results from the metal release analysis carried out on each sample.

Parameter	Untreated Fine (UF)	Fine +gypsum (UFG)	Fine+ seawater (UFS)	Untreated French (UFR)	French+ gypsum (UFRG)	French +seawater (UFRS)	Untreated Coarse (UC)
Al (mg L^{-1})	6.26±0.57	0.065±0.05	0.44±0.4	66.1±6.1	3.2±0.71	9.71±2.7	2.08±0.202
As (mg L^{-1})	0.02±0.0007	0.0003±0.0001	0.001±0.0002	0.045±0.011	0.002±0.0017	0.003±0.0002	0.006±0.00056
Cd (mg L^{-1})	<LOD[j]	0.0006±0.00001	0.000017±0.0005	0.00003±0	0.00001±0	0.00001±0	<LOD[j]
Ca (mg L^{-1})	0.25±0.2	496.0±49.0	404±6.0	715±3	420.0±60.0	39.0±0.3	0.5±4.0
Cr (mg L^{-1})	0.072±0.004	0.0268±0.01	0.00158±0.0001	0.65±0.02	0.38±0.05	0.14±0.01	0.0094±2.9
Cu (mg L^{-1})	0.005±0.03	0.008±0.0057	0.011±0.0002	0.003±0.0002	0.0008±0.005	0.0007±0.0003	0.0105±0.012
Ga (mg L^{-1})	0.026±0.007	0.0045±0.0008	0.0062±0.001	0.11±0.0048	0.012±0.007	0.016±0.003	0.013±0.001
Fe (mg L^{-1})	0.31±0.13	0.0042±0.001	0.001±0.006	0.0016±0.004	0.0023±0.004	0.0014±0.005	0.32±0.422
Mg (mg L^{-1})	<LOD[j]	<LOD[j]	1.77±0.2	<LOD[j]	<LOD[j]	0.31±0	<LOD[j]
Mo (mg L^{-1})	0.0005±0.0005	0.0008±0.02	0.00095±0.05	0.042±0.003	0.013±0.001	0.009±0.001	0.0067±0.002
Hg (mg L^{-1})	<LOD[j]	<LOD[j]	<LOD[j]	0.64±0.02	<LOD[j]	0.08±0.01	<LOD[j]
Na (mg L^{-1})	84.2±2	139.3±3.2	241.3±26	191.3±1	153±24.8	388.7±18.6	83.4±2
V (mg L^{-1})	0.65±0.0040	0.018±0.0014	0.0979±0.0016	2.2±0.001	0.058±0.0023	0.16±0.0065	0.32±0.006

[j]<LOD = below the limits of detection.

Appendix D
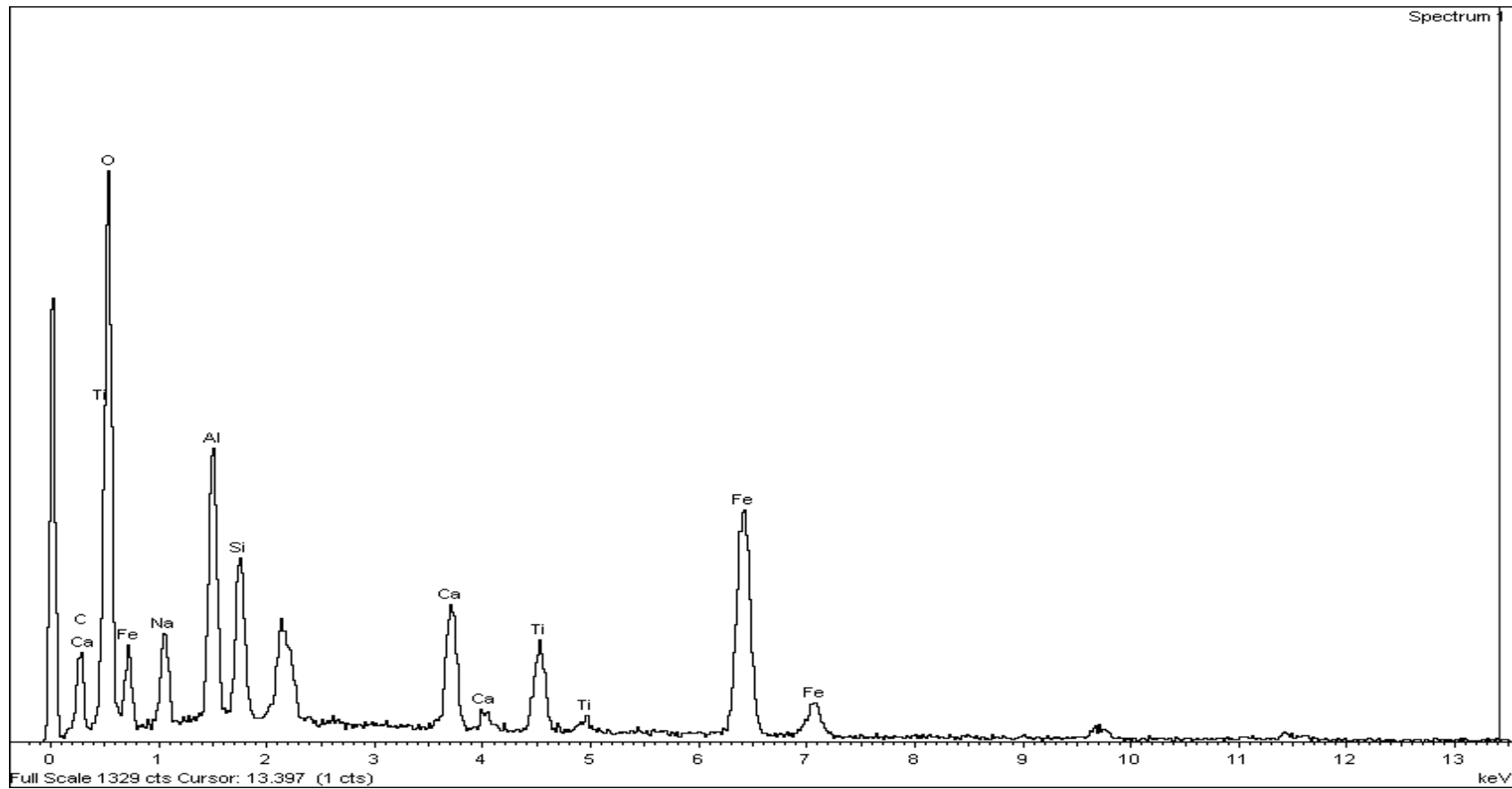
Figure D1 Main mineralogical composition of the bauxite residue mixture before placing in the rapid small-scale column tests, as detected by EDS in conjunction with SEM.